

GRAHAM COOP

POPULATION AND QUANTITATIVE GENETICS

Author: Graham Coop

Author address: Department of Evolution and Ecology & Center for Population Biology,
University of California, Davis.

To whom correspondence should be addressed: gmccoop@ucdavis.edu

This work is licensed under a Creative Commons Attribution 3.0 Unported License.

<http://creativecommons.org/licenses/by/3.0/>

i.e. you are free to reuse and remix this work, but please include an attribution to the original.

Typeset using L^AT_EX and the TUFTE-LATEX book style.

The L^AT_EX code and R code for this book are kept here <https://github.com/cooplab/popgen-notes/> and again are
under a Creative Commons Attribution 3.0 Unported License.

Updated on August 2019

This book was developed from my set of notes for the Population Biology graduate group core class (PBG200A) and Undergraduate Population and Quantitative Genetics class (EVE102) at UC Davis. Thanks to the many students who've read these notes and suggested improvements. Thanks to Simon Aeschbacher, Vince Buffalo, and Erin Calfee who read and extensively edited earlier drafts of these notes. To illustrate these notes I've used old scientific and natural history illustrations, in part because they are out of copyright but mainly because they bring me joy. Many of the old images come from Biodiversity Heritage Library a consortium of natural history institutions that are digitizing their collections and make them freely available online. If you enjoy the images consider donating to the BHL. Many of the data and simulation graphics in the book were prepared in R (2018), the code for each is linked to from the caption of each figure. In many cases data were extracted from old figures using the WebPlotDigitizer tool, as such I advise re-extracting the data if you wish to use it for research purposes.

Contents

1	<i>Introduction</i>	7
2	<i>Allele and Genotype Frequencies</i>	11
3	<i>Genetic Drift and Neutral Diversity</i>	45
4	<i>Phenotypic Variation and the Resemblance Between Relatives</i>	89
5	<i>The Response to Phenotypic Selection</i>	109
6	<i>One-Locus Models of Selection</i>	129
7	<i>The interaction of Selection, Mutation, and Migration.</i>	165
8	<i>The Impact of Genetic Drift on Selected Alleles</i>	181
9	<i>The Effects of Linked Selection.</i>	193
10	<i>Interaction of Multiple Selected Loci</i>	209
11	<i>Bibliography</i>	221

1

2 Introduction

BIOLOGICAL EVOLUTION IS THE CHANGE OVER TIME IN THE
4 GENETIC COMPOSITION OF A POPULATION.¹ Our population is
made up of a set of interbreeding individuals, the genetic composition
6 of which is made up of the genomes that each individual carries. The
genetic composition of the population alters due to the death of indi-
8 viduals or the migration of individuals in or out of the population. If
our individuals vary in the number of children they have, this also al-
10 ters the genetic composition of the population in the next generation.
Every new individual born into the population subtly changes the
12 genetic composition of the population. Their genome is a unique com-
bination of their parents' genomes, having been shuffled by segregation
14 and recombination during meioses, and possibly changed by mutation.
These individual events seem minor at the level of the population, but
16 it is the accumulation of small changes in aggregate across individuals
and generations that is the stuff of evolution. It is the compounding
18 of these small changes over tens, hundreds, and millions of genera-
tions that drives the amazing diversity of life that has emerged on this
20 earth.

Population genetics is the study of the genetic composition of natu-
22 ral populations and its evolutionary causes and consequences. Quantitative genetics is the study of the genetic basis of phenotypic variation
24 and how phenotypic changes evolve over time. Both fields are closely
conceptually aligned as we'll see throughout these notes. They seek to
26 describe how the genetic and phenotypic composition of populations
can be changed over time by the forces of mutation, recombination,
28 selection, migration, and genetic drift. To understand how these forces
interact, it is helpful to develop simple theoretical models to help our
30 intuition. In these notes we will work through these models and sum-
marize the major areas of population- and quantitative-genetic theory.

32 While the models we will develop will seem naïve, and indeed they
are, they are nonetheless incredibly useful and powerful. Throughout

¹ DOBZHANSKY, T., 1951 *Genetics and the Origin of Species* (3rd Ed. ed.), pp. 16

"All models are wrong but some are useful" - Box (1979).

³⁴ the course we will see that these simple models often yield accurate predictions, such that much of our understanding of the process of evolution is built on these models. We will also see how these models are incredibly useful for understanding real patterns we see in the evolution of phenotypes and genomes, such that much of our analysis of evolution, in a range of areas from human medical genetics to conservation, is based on these models. Therefore, population and quantitative genetics are key to understanding various applied questions, from how medical genetics identifies the genes involved in disease to how we preserve species from extinction.

⁴⁴ Population genetics emerged from early efforts to reconcile Mendelian genetics with Darwinian thought. Part of the power of population genetics comes from the fact that the basic rules of transmission genetics are simple and nearly universal. One of the truly remarkable things about population genetics is that many of the important ideas and mathematical models emerged before the 1940s, long before the mechanistic-basis of inheritance (DNA) was discovered, and yet the usefulness of these models has not diminished. This is a testament to the fact that the models are established on a very solid foundation, building from the basic rules of genetic transmission combined with simple mathematical and statistical models.

⁵⁶ Much of this early work traces to the ideas of R.A. Fisher, Sewall Wright, and J.B.S. Haldane, who, along with many others, described the early principals and mathematical models underlying our understanding of the evolution of populations. Building on this conceptual fusion of genetics and evolution, there followed a flourishing of evolutionary thought, the modern evolutionary synthesis, combining these ideas with those from the study of speciation, biodiversity, and paleontology. In total this work showed that both short-term evolutionary change and the long-term evolution of biodiversity could be well understood through the gradual accumulation of evolutionary change within and among populations. This evolutionary synthesis continues to this day, combining new insights from genomics, phylogenetics, ecology, and developmental biology.

⁶⁸ Population and quantitative genetics are a necessary but not sufficient description of evolution; it is only by combining the insights of many fields that a rich and comprehensive picture of evolution emerges. We certainly do not need to know the genes underlying the displays of the birds of paradise to study how the divergence of these displays, due to sexual selection, may drive speciation. Indeed, as we'll see in our discussion of quantitative genetics, we can predict how populations respond to selection, including sexual selection and assortative mating, without any knowledge of the loci involved. Nor do we need to know the precise selection pressures and the ordering of genetic

See PROVINE (2001) for a history of early population genetics.

PROVINE, W. B., 2001 *The origins of theoretical population genetics: with a new afterword.* University of Chicago Press

“DOBZHANSKY (1951)
once defined evolution as ‘a
change in the genetic com-
position of the populations’
an epigram that should not
be mistaken for the claim
that everything worth saying
about evolution is contained
in statements about genes”

— LEWONTIN

78 changes to study the emergence of the tetrapod body plan. We do
not necessarily need to know all the genetic details to appreciate the
80 beauty of these, and many other, evolutionary case studies. However,
every student of biology gains from understanding the basics of pop-
82 ulation and quantitative genetics, allowing them to base their studies
on a solid bedrock of understanding of the processes that underpin all
84 evolutionary change.

2

⁸⁶ Allele and Genotype Frequencies

In this chapter we will work through how the basics of Mendelian
⁸⁸ genetics play out at the population level in sexually reproducing organisms.

⁹⁰ Loci and alleles are the basic currency of population genetics—and indeed of genetics. If all individuals in the population carry the same
⁹² allele, we say that the locus is *monomorphic*; at this locus there is no genetic variability in the population. If there are multiple alleles in
⁹⁴ the population at a locus, we say that this locus is *polymorphic* (this is sometimes referred to as a segregating site).

⁹⁶ Table 2.1 shows a small stretch of orthologous sequence for the ADH locus from samples from *Drosophila melanogaster*, *D. simulans*,
⁹⁸ and *D. yakuba*. *D. melanogaster* and *D. simulans* are sister species and *D. yakuba* is a close outgroup to the two. Each column represents a
¹⁰⁰ single haplotype from an individual (the individuals are diploid but were inbred so they're homozygous for their haplotype). Only sites
¹⁰² that differ among individuals of the three species are shown. Site 834 is an example of a polymorphism; some *D. simulans* individuals carry
¹⁰⁴ a *C* allele while others have a *T*. *Fixed differences* are sites that differ between the species but are monomorphic within the species. Site 781
¹⁰⁶ is an example of a fixed difference between *D. melanogaster* and the other two species.

¹⁰⁸ We can also annotate the alleles and loci in various ways. For example, position 781 is a non-synonymous fixed difference. We call the
¹¹⁰ less common allele at a polymorphism the *minor allele* and the common allele the *major allele*, e.g. at site 1068 the *T* allele is the minor
¹¹² allele in *D. melanogaster*. We call the more evolutionarily recent of the two alleles the *derived allele* and the older of the two the *ancestral allele*.
¹¹⁴ We infer that the *T* allele at site 1068 is the derived allele because the *C* is found in both other species, suggesting that the *T* allele
¹¹⁶ arose via a *C* → *T* mutation.

Question 1. A) How many segregating sites does the sample

A *locus* (plural: *loci*) is a specific spot in the genome. A locus may be an entire gene, or a single nucleotide base pair such as A-T. At each locus, there may be multiple genetic variants segregating in the population—these different genetic variants are known as *alleles*.

pos.	con.	a	b	c	d	e	f	g	h	i	j	k	l	a	b	c	d	e	f	g	h	i	j	k	l	NS/S
781	G	T	T	T	T	T	T	T	T	T	-	-	-	-	-	-	-	-	-	-	-	-	-	-	NS	
789	T	-	-	-	-	-	-	-	-	-	-	-	-	C	C	C	C	C	C	C	C	C	C	C	C	S
808	A	-	-	-	-	-	-	-	-	-	T	T	T	T	T	T	G	G	G	G	G	G	G	G	NS	
816	G	T	T	T	T	-	-	-	-	-	-	-	-	C	C	-	-	-	-	-	-	-	-	-	-	S
834	T	-	-	-	-	-	-	-	-	-	-	-	-	C	-	-	-	-	-	-	-	-	-	-	-	S
859	C	-	-	-	-	-	-	-	-	-	-	-	-	G	G	G	G	G	G	G	G	G	G	G	G	NS
867	C	-	-	-	-	-	-	-	-	-	-	-	-	G	G	G	G	G	A	G	G	G	G	G	G	S
870	C	T	T	T	T	T	T	T	T	T	-	-	-	-	-	-	-	-	-	-	-	-	-	-	S	
950	G	-	-	-	-	-	-	-	-	-	-	-	-	A	-	-	-	-	-	-	-	-	-	-	-	S
974	G	-	-	-	-	-	-	-	-	-	T	-	T	T	T	T	-	-	-	-	-	-	-	-	S	
983	T	-	-	-	-	-	-	-	-	-	-	-	-	C	C	C	C	C	C	C	C	C	C	C	C	S
1019	C	-	-	-	-	-	-	-	-	-	-	-	-	-	-	-	-	-	-	-	-	-	-	-	S	
1031	C	-	-	-	-	-	-	-	-	-	-	-	-	-	-	-	-	-	-	-	-	-	-	-	S	
1034	T	-	-	-	-	-	-	-	-	-	-	-	-	-	-	-	-	-	-	-	-	-	-	-	S	
1043	C	-	-	-	-	-	-	-	-	-	-	-	-	-	-	-	-	-	-	-	-	-	-	-	S	
1068	C	T	T	-	-	-	-	-	-	-	-	-	-	C	C	C	C	C	-	-	C	-	C	C	S	
1089	C	-	-	-	-	-	-	-	-	-	-	-	-	A	A	A	A	A	A	-	-	-	-	-	NS	
1101	G	-	-	-	-	-	-	-	-	-	-	-	-	A	A	A	A	A	A	A	A	A	A	A	NS	
1127	T	-	-	-	-	-	-	-	-	-	-	-	-	C	C	C	C	C	C	C	C	C	C	C	S	
1131	C	-	-	-	-	-	-	-	-	-	-	-	-	-	-	-	-	-	-	-	-	-	-	-	S	
1160	T	-	-	-	-	-	-	-	-	-	-	-	-	C	C	C	C	C	C	C	C	C	C	C	S	

- 118 from *D. simulans* have in the ADH gene?
B) How many fixed differences are there between *D. melanogaster*
120 and *D. yakuba*?

2.1 Allele frequencies

122 Allele frequencies are a central unit of population genetics analysis,
but from diploid individuals we only get to observe genotype counts.
124 Our first task then is to calculate allele frequencies from genotype
counts. Consider a diploid autosomal locus segregating for two alleles
126 (A_1 and A_2). We'll use these arbitrary labels for our alleles, merely
to keep this general. Let N_{11} and N_{12} be the number of A_1A_1 ho-
128 mozygotes and A_1A_2 heterozygotes, respectively. Moreover, let N
be the total number of diploid individuals in the population. We can
130 then define the relative frequencies of A_1A_1 and A_1A_2 genotypes as
 $f_{11} = N_{11}/N$ and $f_{12} = N_{12}/N$, respectively. The frequency of allele
132 A_1 in the population is then given by

$$p = \frac{2N_{11} + N_{12}}{2N} = f_{11} + \frac{1}{2}f_{12}. \quad (2.1)$$

Note that this follows directly from how we count alleles given in-
134 dividuals' genotypes, and holds independently of Hardy–Weinberg
proportions and equilibrium (discussed below). The frequency of the
136 alternate allele (A_2) is then just $q = 1 - p$.

2.1.1 Measures of genetic variability

138 **Nucleotide diversity (π)** One common measure of genetic diversity is
the average number of single nucleotide differences between haplotypes
140 chosen at random from a sample. This is called *nucleotide diversity*
and is often denoted by π . For example, we can calculate π for our
142 ADH locus from Table 2.1 above: we have 6 sequences from *D. sim-
ulans* (a-f), there's a total of 15 ways of pairing these sequences, and

Table 2.1: Variable sites in exons 2 and 3 of the ADH gene in *Drosophila* McDONALD and KREITMAN (1991). The first column (pos.) gives the position in the gene; exon 2 begins at position 778 and we've truncated the dataset at site 1175. The second column gives the consensus nucleotide (con.), i.e. the most common base at that position; individuals with nucleotides that match the consensus are marked with a dash. The first columns of sequence (a-l) are from *D. melanogaster*; the next columns (a-f) give sequences from *D. simulans*, and the final set of columns (a-l) from *D. yakuba*. The last column shows whether the difference is a non-synonymous (N) or synonymous (S) change.

144

$$\pi = \frac{1}{15} ((2+1+1+1+0)+(3+3+3+2)+(0+0+1)+(0+1)+(1)) = 1.2\bar{6} \quad (2.2)$$

where the first bracketed term gives the pairwise differences between
 146 a and b-f, the second bracketed term the differences between b and c-f
 and so on.

148 Our π measure will depend on the length of sequence it is calcu-
 lated for. Therefore, π is usually normalized by the length of sequence,
 150 to be a per site (or per base) measure. For example, our ADH se-
 quence covers 397bp of DNA and so $\pi = 1.2\bar{6}/397 = 0.0032$ per site
 152 in *D. simulans* for this region. Note that we could also calculate π
 per synonymous site (or non-synonymous). For synonymous site π , we
 154 would count up number of synonymous differences between our pairs
 of sequences, and then divide by the total number of sites where a
 156 synonymous change could have occurred.¹

Number of segregating sites. Another measure of genetic variability
 158 is the total number of sites that are polymorphic (segregating) in our
 sample. One issue is that the number of segregating sites will grow
 160 as we sequence more individuals (unlike π). Later in the course, we'll
 talk about how to standardize the number of segregating sites for the
 162 number of individuals sequenced (see eqn (3.38)).

The frequency spectrum. We also often want to compile information
 164 about the frequency of alleles across sites. We call alleles that are
 found once in a sample *singletons*, alleles that are found twice in a
 166 sample *doubletons*, and so on. We count up the number of loci where
 an allele is found i times out of n , e.g. how many singletons are there
 168 in the sample, and this is called the *frequency spectrum*. We'll want to
 do this in some consistent manner, such as calculating the frequency
 170 spectrum of the minor allele or the derived allele.

Question 2. How many minor-allele singletons are there in *D.*
 172 *simulans* in the ADH region?

Levels of genetic variability across species. Two observations have
 174 puzzled population geneticists since the inception of molecular popula-
 tion genetics. The first is the relatively high level of genetic variation
 176 observed in most obligately sexual species. This first observation,
 in part, drove the development of the Neutral theory of molecular
 178 evolution, the idea that much of this molecular polymorphism may
 simply reflect a balance between genetic drift and mutation. The sec-
 180 ond observation is the relatively narrow range of polymorphism across

¹ Technically we would need to divide by the total number of possible point mutations that would result in a synonymous change; this is because some mutational changes at a particular nucleotide will result in a non-synonymous or synonymous change depending on the base-pair change.

species with vastly different census sizes. This observation represented a puzzle as the Neutral theory predicts that levels of genetic diversity should scale with population size. Much effort in theoretical and empirical population genetics has been devoted to trying to reconcile models with these various observations. We'll return to discuss these ideas throughout our course.

The first observations of molecular genetic diversity within natural populations were made from surveys of allozyme data, but we can revisit these general patterns with modern data.

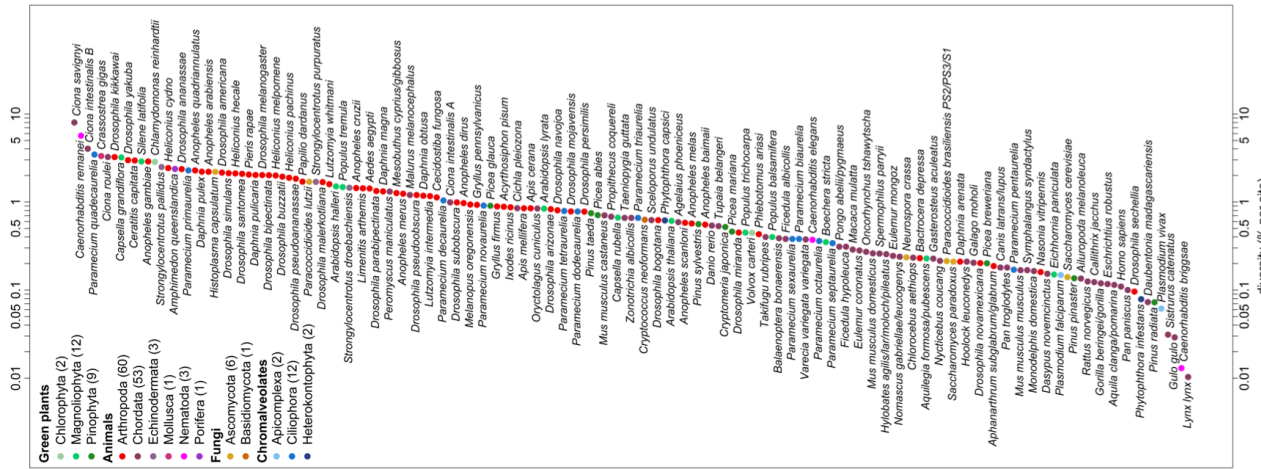


Figure 2.1: Sea Squirt (*Ciona intestinalis*).

Einleitung in die vergleichende gehirnphysiologie und Vergleichende psychologie. Loeb, J. 1899. Image from the Biodiversity Heritage Library. Contributed by MBLWHOI Library. No known copyright restrictions.

For example, LEFFLER *et al.* (2012) compiled data on levels of within-population, autosomal nucleotide diversity (π) for 167 species across 14 phyla from non-coding and synonymous sites (Figure 2.2). The species with the lowest levels of π in their survey was Lynx, with $\pi = 0.01\%$, i.e. only 1/10000 bases differed between two sequences. In contrast, some of the highest levels of diversity were found in *Ciona savignyi*, Sea Squirts, where a remarkable 1/12 bases differ between pairs of sequences. This 800-fold range of diversity seems impressive, but census population sizes have a much larger range.

2.1.2 Hardy–Weinberg proportions

Imagine a population mating at random with respect to genotypes, i.e. no inbreeding, no assortative mating, no population structure, and no sex differences in allele frequencies. The frequency of allele A_1 in the population at the time of reproduction is p . An A_1A_1 genotype is made by reaching out into our population and independently drawing two A_1 allele gametes to form a zygote. Therefore, the probability that an individual is an A_1A_1 homozygote is p^2 . This probability is also the expected frequencies of the A_1A_1 homozygote in the popula-

190 For example, LEFFLER *et al.* (2012) compiled data on levels of
191 within-population, autosomal nucleotide diversity (π) for 167 species
192 across 14 phyla from non-coding and synonymous sites (Figure 2.2).
The species with the lowest levels of π in their survey was Lynx, with
193 $\pi = 0.01\%$, i.e. only 1/10000 bases differed between two sequences. In
contrast, some of the highest levels of diversity were found in *Ciona*
196 *savignyi*, Sea Squirts, where a remarkable 1/12 bases differ between
pairs of sequences. This 800-fold range of diversity seems impressive,
but census population sizes have a much larger range.

Figure 2.2: Levels of autosomal nucleotide diversity for 167 species across 14 phyla. Figure 1 from LEFFLER *et al.* (2012), licensed under CC BY 4.0. Points are ranked by their π , and coloured by their phylum. Note the log-scale.

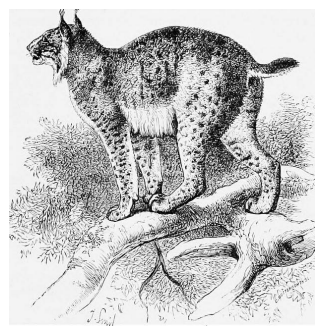


Figure 2.2: Levels of autosomal nucleotide diversity for 167 species across 14 phyla. Figure 1 from LEFFLER *et al.* (2012), licensed under CC BY 4.0. Points are ranked by their π , and coloured by their phylum. Note the log-scale.

An introduction to the study of mammals living and extinct. Flower, W.H. and Lydekker, R. 1891. Image from the Biodiversity Heritage Library. Contributed by Cornell University Library. No known copyright restrictions.

208 tion. The expected frequency of the three possible genotypes are

$$\begin{array}{ccc} f_{11} & f_{12} & f_{22} \\ \hline p^2 & 2pq & q^2 \end{array}$$

210 Note that we only need to assume random mating with respect to
our focal allele in order for these expected frequencies to hold in the
212 zygotes forming the next generation. Evolutionary forces, such as
selection, change allele frequencies within generations, but do not
214 change this expectation for new zygotes, as long as p is the frequency
of the A_1 allele in the population at the time when gametes fuse.

216 **Question 3.** On the coastal islands of British Columbia there is
a subspecies of black bear (*Ursus americanus kermodei*, Kermode's
218 bear). Many members of this black bear subspecies are white; they're
sometimes called spirit bears. These bears aren't hybrids with polar
220 bears, nor are they albinos. They are homozygotes for a recessive
change at the MC1R gene. Individuals who are *GG* at this SNP are
222 white while *AA* and *AG* individuals are black.

Below are the genotype counts for the MC1R polymorphism in
224 a sample of bears from British Columbia's island populations from
RITLAND *et al.* (2001).

	<i>AA</i>	<i>AG</i>	<i>GG</i>
226	42	24	21

What are the expected frequencies of the three genotypes under
228 HWE?

See Figure 2.5 for a nice empirical demonstration of Hardy–Weinberg
230 proportions. The mean frequency of each genotype closely matches its
HW expectations, and much of the scatter of the dots around the ex-
232 pected line is due to our small sample size (~ 60 individuals). While
HW often seems like a silly model, it often holds remarkably well
234 within populations. This is because individuals don't mate at random,
but they do mate at random with respect to their genotype at most of
236 the loci in the genome.

Question 4. You are investigating a locus with three alleles, A,
238 B, and C, with allele frequencies p_A , p_B , and p_C . What fraction of the
population is expected to be homozygotes under Hardy–Weinberg?

240 Microsatellites are regions of the genome where individuals vary
for the number of copies of some short DNA repeat that they carry.
242 These regions are often highly variable across individuals, making
them a suitable way to identify individuals from a DNA sample. This
244 so-called DNA fingerprinting has a range of applications from estab-
lishing paternity and identifying human remains to matching individ-
246 uals to DNA samples from a crime scene. The FBI make use of the

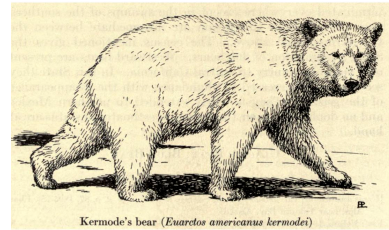


Figure 2.4: Kermode's bear.
Extinct and vanishing mammals of the western
hemisphere. 1942. Glover A. Image from the
Biodiversity Heritage Library. Contributed by
Prelinger Library. Not in copyright.

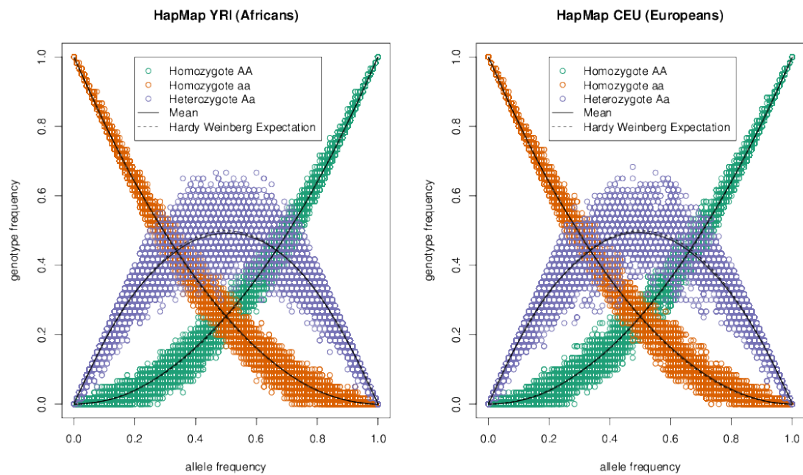


Figure 2.5: Demonstrating Hardy–Weinberg proportions using 10,000 SNPs from the HapMap European (CEU) and African (YRI) populations. Within each of these populations the allele frequency against the frequency of the 3 genotypes; each SNP is represented by 3 different coloured points. The solid lines show the mean genotype frequency. The dashed lines show the predicted genotype frequency from Hardy–Weinberg equilibrium. [Code here](#). [Blog post on figure here](#).

248 CODIS database². The CODIS database contains the genotypes of
over 13 million people, most of whom have been convicted of a crime.
250 Most of the profiles record genotypes at 13 microsatellite loci that are
tetranucleotide repeats (since 2017, 20 sites have been genotyped).

252 The allele counts for two loci (D16S539 and TH01) are shown in
table 2.2 and 2.3 for a sample of 155 people of European ancestry. You
can assume these two loci are on different chromosomes.

allele name	80	90	100	110	120	121	130	140	150
allele count	3	34	13	102	97	1	44	13	3

allele name	60	70	80	90	93	100	110
allele counts	84	42	37	67	77	1	2

254 **Question 5.** You extract a DNA sample from a crime scene. The
genotype is 100/80 at the D16S539 locus and 70/93 at TH01.

256 **A)** You have a suspect in custody. Assuming this suspect is in-
nocent and of European ancestry, what is the probability that their
258 genotype would match this profile by chance (a false-match probabil-
ity)?

260 **B)** The FBI uses ≥ 13 markers. Why is this higher number neces-
sary to make the match statement convincing evidence in court?

262 **C)** An early case that triggered debate among forensic geneticists
was a crime among the Abenaki, a Native American community in
264 Vermont (see LEWONTIN, 1994, for discussion). There was a DNA
sample from the crime scene, and the perpetrator was thought likely

² CODIS: Combined DNA Index System

Table 2.2: Data for 155 Europeans at the D16S539 microsatellite from CODIS from ALGEE-HEWITT *et al.* (2016). The top row gives the number of tetranucleotide repeats for each allele, the bottom row gives the sample counts.

Table 2.3: Same as 2.2 but for the TH01 microsatellite.

- 266 to be a member of the Abenaki community. Given that allele frequencies vary among populations, why would people be concerned about
 268 using data from a non-Abenaki population to compute a false match probability?

270 *2.2 Allele sharing among related individuals and Identity by Descent*

272 All of the individuals in a population are related to each other by a giant pedigree (family tree). For most pairs of individuals in a population these relationships are very distant (e.g. distant cousins),
 274 while some individuals will be more closely related (e.g. sibling/first
 276 cousins). All individuals are related to one another by varying levels
 278 of relatedness, or *kinship*. Related individuals can share alleles that
 have both descended from the shared common ancestor. To be shared,
 280 these alleles must be inherited through all meioses connecting the two
 282 individuals (e.g. surviving the $1/2$ probability of segregation each meio-
 sis). As closer relatives are separated by fewer meioses, closer relatives
 284 share more alleles. In Figure 2.6 we show the sharing of chromosomal
 regions between two cousins. As we'll see, many population and quan-
 286 titative genetic concepts rely on how closely related individuals are,
 and thus we need some way to quantify the degree of kinship among
 individuals.



Figure 2.6: First cousins sharing a stretch of chromosome identical by descent. The different grandparental diploid chromosomes are coloured so we can track them and recombinations between them across the generations. Notice that the identity by descent between the cousins persists for a long stretch of chromosome due to the limited number of generations for recombination.

We will define two alleles to be identical by descent (IBD) if they
 288 are identical due to transmission from a common ancestor in the past
 few generations³. For the moment, we ignore mutation, and we will
 290 be more precise about what we mean by ‘past few generations’ later
 on. For example, parent and child share exactly one allele identical
 292 by descent at a locus, assuming that the two parents of the child are
 randomly mated individuals from the population. In Figure 2.12, I
 294 show a pedigree demonstrating some configurations of IBD.

³ COTTERMAN, C. W., 1940 A calculus for statistico-genetics. Ph. D. thesis, The Ohio State University; and MALÉCOT, G., 1948 Les mathématiques de l'hérédité

One summary of how related two individuals are is the probability
 296 that our pair of individuals share 0, 1, or 2 alleles identical by descent
 (see Figure 2.7). We denote these probabilities by r_0 , r_1 , and r_2 re-
 298 spectively. See Table 2.4 for some examples. We can also interpret
 300 these probabilities as genome-wide averages. For example, on aver-
 age, at a quarter of all their autosomal loci full-sibs share zero alleles
 identical by descent.

302 One summary of relatedness that will be important is the prob-
 ability that two alleles picked at random, one from each of the two
 304 different individuals i and j , are identical by descent. We call this
 quantity the *coefficient of kinship* of individuals i and j , and denote it
 306 by F_{ij} . It is calculated as

$$F_{ij} = 0 \times r_0 + \frac{1}{4}r_1 + \frac{1}{2}r_2. \quad (2.3)$$

The coefficient of kinship will appear multiple times, in both our dis-
 308 cussion of inbreeding and in the context of phenotypic resemblance
 between relatives.

Relationship (i,j)*	r_0	r_1	r_2	F_{ij}
parent-child	0	1	0	$1/4$
full siblings	$1/4$	$1/2$	$1/4$	$1/4$
Monozygotic twins	0	0	1	$1/2$
1 st cousins	$3/4$	$1/4$	0	$1/16$

310 **Question 6.** What are r_0 , r_1 , and r_2 for $1/2$ sibs? ($1/2$ sibs share
 one parent but not the other).

Our r coefficients are going to have various uses. For example,
 they allow us to calculate the probability of the genotypes of a pair of
 relatives. Consider a biallelic locus where allele A_1 is at frequency p ,
 and two individuals who have IBD allele sharing probabilities r_0 , r_1 ,
 r_2 . What is the overall probability that these two individuals are both
 homozygous for allele 1? Well that's

$$\begin{aligned} P(A_1A_1) &= P(A_1A_1|0 \text{ alleles IBD})P(0 \text{ alleles IBD}) \\ &\quad + P(A_1A_1|1 \text{ allele IBD})P(1 \text{ allele IBD}) \\ &\quad + P(A_1A_1|2 \text{ alleles IBD})P(2 \text{ alleles IBD}) \end{aligned} \quad (2.4)$$

Or, in our r_0 , r_1 , r_2 notation:

$$\begin{aligned} P(A_1A_1) &= P(A_1A_1|0 \text{ alleles IBD})r_0 \\ &\quad + P(A_1A_1|1 \text{ allele IBD})r_1 \\ &\quad + P(A_1A_1|2 \text{ alleles IBD})r_2 \end{aligned} \quad (2.5)$$



Figure 2.7: A pair of diploid individuals (X and Y) sharing 0, 1, or 2 alleles IBD where lines show the sharing of alleles by descent (e.g. from a shared ancestor).

Table 2.4: Probability that two individuals of a given relationship share 0, 1, or 2 alleles identical by descent on the autosomes. *Assuming this is the only close relationship the pair shares.

312 If our pair of relatives share 0 alleles IBD, then the probability that
 they are both homozygous is $P(A_1A_1|0 \text{ alleles IBD}) = p^2 \times p^2$, as all
 314 four alleles represent independent draws from the population. If they
 share 1 allele IBD, then the shared allele is of type A_1 with probability
 316 p , and then the other non-IBD allele, in both relatives, also needs to
 be A_1 which happens with probability p^2 , so $P(A_1A_1|1 \text{ alleles IBD}) =$
 318 $p \times p^2$. Finally, our pair of relatives can share two alleles IBD, in which
 case $P(A_1A_1|2 \text{ alleles IBD}) = p^2$, because if one of our individuals is
 320 homozygous for the A_1 allele, both individuals will be. Putting this all
 together our equation (2.5) becomes

$$P(A_1A_1) = p^4r_0 + p^3r_1 + p^2r_2 \quad (2.6)$$

322 Note that for specific cases we could also calculate this by summing
 over all the possible genotypes their shared ancestor(s) had; however,
 324 that would be much more involved and not as general as the form we
 have derived here.

326 We can write out terms like eq (2.6) for all of the possible configura-
 tions of genotype sharing/non-sharing between a pair of individuals.
 328 Based on this we can write down the expected number of polymorphic
 sites where our individuals are observed to share 0, 1, or 2 alleles.

330 **Question 7.** The genotype of our suspect in Question 5 turns
 out to be 100/80 for D16S539 and 70/80 at TH01. The suspect is not
 332 a match to the DNA from the crime scene; however, they could be a
 sibling.

334 Calculate the joint probability of observing the genotype from the
 crime and our suspect:

- 336 A) Assuming that they share no close relationship.
- B) Assuming that they are full sibs.
- 338 C) Briefly explain your findings.

340 There's a variety of ways to estimate the relationships among in-
 dividuals using genetic data. An example of using allele sharing to
 identify relatives is offered by the work of Nancy Chen (in collabo-
 342 ration with Stepfanie Aguillon, see CHEN *et al.*, 2016; AGUILLO
et al., 2017). CHEN *et al.* has collected genotyping data from thou-
 344 sandes of Florida Scrub Jays at over ten thousand loci. These Jays
 live at the Archbold field site, and have been carefully monitored for
 346 many decades allowing the pedigree of many of the birds to be known.
 Using these data she estimates allele frequencies at each locus. Then
 348 by equating the observed number of times that a pair of individuals
 share 0, 1, or 2 alleles to the theoretical expectation, she estimates
 350 the probability of r_0 , r_1 , and r_2 for each pair of birds. A plot of these
 are shown in Figure 2.9, showing how well the estimates match those
 352 known from the pedigree.



Figure 2.8: Florida Scrub-Jays (*Aphelocoma coerulescens*).
 The birds of America : from drawings made in
 the United States and their territories. 1880.
 Audubon J.J. Image from the Biodiversity
 Heritage Library. Contributed by Smithsonian
 Libraries. Licensed under CC BY-2.0.



Figure 2.9: Estimated coefficient of kinship from Florida Scrub Jays. Each point is a pair of individuals, plotted by their estimated IBD (r_1 and r_2) from their genetic data. The points are coloured by their known pedigree relationships. Note that most pairs have low kinship, and no recent genealogical relationship, and so appear as black points in the lower left corner. Thanks to Nancy Chen for supplying the data. Code here.



Figure 2.10: A simulation of sharing between first cousins. The regions of your grandmother's 22 autosomes that you inherited are coloured red, those that your cousins inherited are coloured blue. In the third panel we show the overlapping genomic regions in purple, these regions will be IBD in you and your cousin. If you are full first cousins, you will also have shared genomic regions from your shared grandfather, not shown here. Details about how we made these simulations here.

Sharing of genomic blocks among relatives. We can more directly see the sharing of the genome among close relatives using high-density SNP genotyping arrays. Below we show a simulation of you and your first cousin's genomic material that you both inherited from your shared grandmother. Colored purple are regions where you and your cousin will have matching genomic material, due to having inherited it IBD from your shared grandmother.

You and your first cousin will share at least one allele of your genotype at all of the polymorphic loci in these purple regions. There's a

range of methods to detect such sharing. One way is to look for unusually long stretches of the genome where two individuals are never homozygous for different alleles. By identifying pairs of individuals who share an unusually large number of such putative IBD blocks, we can hope to identify unknown relatives in genotyping datasets. In fact, companies like 23&me and Ancestry.com use signals of IBD to help identify family ties.

As another example, consider the case of third cousins. You share one of eight sets of great-great grandparents with each of your (likely many) third cousins. On average, you and each of your third cousins each inherit one-sixteenth of your genome from each of those two great-great grandparents. This turns out to imply that on average, a little less than one percent of your and your third cousin's genomes ($2 \times (1/16)^2 = 0.78\%$) will be identical by virtue of descent from those shared ancestors. A simulated example where third cousins share blocks of their genome (on chromosome 16 and 2) due to their great, great grandmother is shown in Figure 2.11.

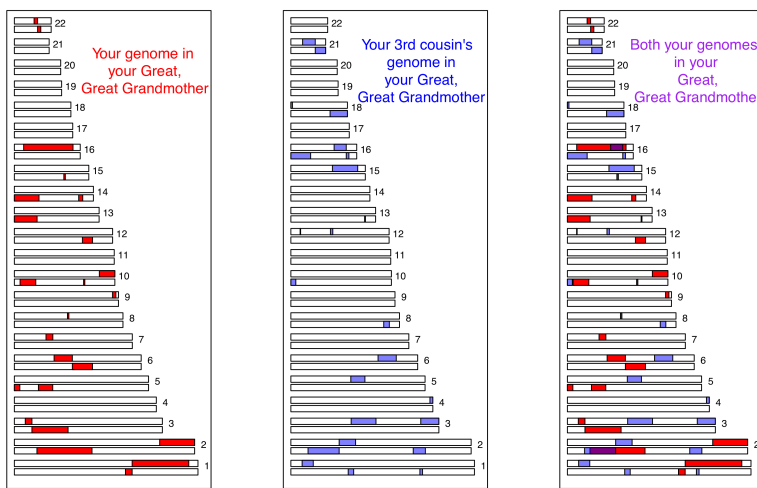


Figure 2.11: A simulation of sharing between third cousins, the details are the same as in Figure 2.10.

Note how if you compare Figure 2.11 and Figure 2.10, individuals inherit less IBD from a shared great, great grandmother than from a shared grandmother, as they inherit from more total ancestors further back. Also notice how the sharing occurs in shorter genomic blocks, as it has passed through more generations of recombination during meiosis. These blocks are still detectable, and so third cousins can be detected using high-density genotyping chips, allowing more distant relatives to be identified than single marker methods alone.⁴ More distant relations than third cousins, e.g. fourth cousins, start to have

⁴ Indeed the suspect in case of the Golden State Killer was identified through identifying third cousins that genetically matched a DNA sample from an old crime scene (see a [here](#) for more details).

- 388 a significant probability of sharing none of their genome IBD. But you
 have many fourth cousins, so you will share some of your genome IBD
 390 with some of them; however, it gets increasingly hard to identify the
 degree of relatedness from genetic data the deeper in the family tree
 392 this sharing goes.

2.2.1 Inbreeding

- 394 We can define an inbred individual as an individual whose parents are
 more closely related to each other than two random individuals drawn
 396 from some reference population.

When two related individuals produce an offspring, that individual can receive two alleles that are identical by descent, i.e. they can be homozygous by descent (sometimes termed autozygous), due to the fact that they have two copies of an allele through different paths through the pedigree. This increased likelihood of being homozygous relative to an outbred individual is the most obvious effect of inbreeding. It is also the one that will be of most interest to us, as it underlies a lot of our ideas about inbreeding depression and population structure. For example, in Figure 2.12 our offspring of first cousins is homozygous by descent having received the same IBD allele via two different routes around an inbreeding loop.

As the offspring receives a random allele from each parent (i and j), the probability that those two alleles are identical by descent is equal to the kinship coefficient F_{ij} of the two parents (Eqn. 2.3). This follows from the fact that the genotype of the offspring is made by sampling an allele at random from each of our parents.

f_{11}	f_{12}	f_{22}
$(1 - F)p^2 + Fp$	$(1 - F)2pq$	$(1 - F)q^2 + Fq$

The only way the offspring can be heterozygous (A_1A_2) is if their
 414 two alleles at a locus are not IBD (otherwise they would necessarily be
 homozygous). Therefore, the probability that they are heterozygous is

$$(1 - F)2pq, \quad (2.7)$$

416 where we have dropped the indices i and j for simplicity. The offspring can be homozygous for the A_1 allele in two different ways.
 418 They can have two non-IBD alleles that are not IBD but happen to be of the allelic type A_1 , or their two alleles can be IBD, such that they
 420 inherited allele A_1 by two different routes from the same ancestor.
 Thus, the probability that an offspring is homozygous for A_1 is

$$(1 - F)p^2 + Fp. \quad (2.8)$$



Figure 2.12: Alleles being transmitted through an inbred pedigree. The two sisters (mum and aunt) share two alleles identical by descent (IBD). The cousins share one allele IBD. The offspring of first cousins is homozygous by descent at this locus.

Table 2.5: Generalized Hardy–Weinberg

422 Therefore, the frequencies of the three possible genotypes can be
written as given in Table 2.5, which provides a generalization of the
424 Hardy–Weinberg proportions.

Note that the generalized Hardy–Weinberg proportions completely
426 specify the genotype probabilities, as there are two parameters (p
and F) and two degrees of freedom (as p and q have to sum to one).
428 Therefore, any combination of genotype frequencies at a biallelic site
can be specified by a combination of p and F .

430 **Question 8.** The frequency of the A_1 allele is p at a biallelic
locus. Assume that our population is randomly mating and that the
432 genotype frequencies in the population follow from HW. We select two
individuals at random to mate from this population. We then mate
434 the children from this cross. What is the probability that the child
from this full sib-mating is homozygous?

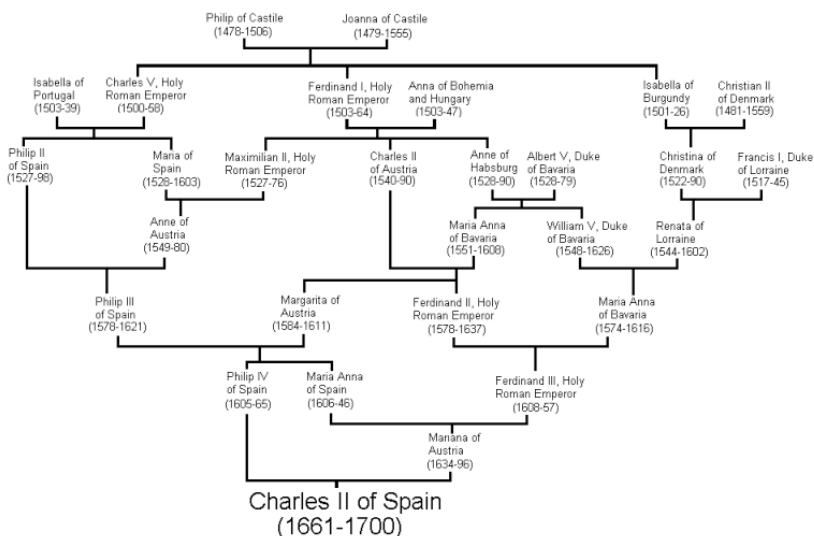
436 *Multiple inbreeding loops in a pedigree.* Up to this point we have as-
sumed that there is at most one inbreeding loop in the recent family
438 history of our individuals, i.e. the parents of our inbred individual
have at most one recent genealogical connection. However, an indi-
440 vidual who has multiple inbreeding loops in their pedigree can be
homozygous by descent thanks to receiving IBD alleles via multiple
442 different different loops. To calculate inbreeding in pedigrees of ar-
bitrary complexity, we can extend beyond our original relatedness
444 coefficients r_0 , r_1 , and r_2 to account for higher order sharing of alleles
IBD among relatives. For example, we can ask, what is the probability
446 that *both* of the alleles in the first individual are shared IBD with one
allele in the second individual? There are nine possible relatedness
448 coefficients in total to completely describe kinship between two diploid
individuals, and we won't go in to them here as it's a lot to keep track
450 of. However, we will show how we can calculate the inbreeding coeffi-
cient of an individual with multiple inbreeding loops more directly.

452 Let's say the parents of our inbred individual (B and C) have K
shared ancestors, i.e. individuals who appear in both B and C's recent
454 family trees. We denote these shared ancestors by A_1, \dots, A_K , and
we denote by n the total number of individuals in the chain from B
456 to C via ancestor A_i , including B, C, and A_i . For example, if B is C's
aunt, then B and C share two ancestors, which are B's parents and,
458 equivalently, C's grandparents. In this case, there are $n=4$ individuals
from B to C through each of these two shared ancestor. In the general
460 case, the kinship coefficient of B and C, i.e. the inbreeding coefficient
of their child, is

$$F = \sum_{i=1}^K \frac{1}{2^{n_i}} (1 + f_{A_i}) \quad (2.9)$$

where f_{A_i} is the inbreeding coefficient of the ancestor A_i . What's happening here is that we sum over all the mutually-exclusive paths in the pedigree through which B and C can share an allele IBD. With probability $1/2^{n_i}$, a pair of alleles picked at random from B and C is descended from the same ancestral allele in individual A_i , in which case the alleles are IBD.⁵ However, even if B inherits the maternal allele and C inherits the paternal allele of shared ancestor A_i , if A_i was themselves inbred, with probability f_{A_i} those two alleles are themselves IBD. Thus a shared *inbred* ancestor further increases the kinship of B and C.

⁵ For example, in the case of our aunt-nephew case, assuming that the aunt's two parents are their only recent shared ancestors, then $F = 1/2^4 + 1/2^4 = 1/8$, in agreement with the answer we would obtain from eqn (2.3).



Multiple inbreeding loops increase the probability that a child is homozygous by descent at a locus, which can be calculated simply by plugging in F , the child's inbreeding coefficient, into our generalized HW equation.

As one extreme example of the impact of multiple inbreeding loops in an individual's pedigree, let's consider king Charles II of Spain, the last of the Spanish Habsburgs. Charles was the son of Philip IV of Spain and Mariana of Austria, who were uncle and niece. If this were the only inbreeding loop, then Charles would have had an inbreeding coefficient of $1/8$. Unfortunately for Charles, the Spanish Habsburgs had long kept wealth and power within their family by arranging marriages between close kin. The pedigree of Charles II is shown in Figure 2.13, and multiple inbreeding loops are apparent. For example, Phillip III, Charles II's grandfather and great-grandfather, was himself

Figure 2.13: The pedigree of King Charles II of Spain. Pedigree from wikimedia drawn by Lec CRP1, public domain.



Figure 2.14: Charles II of Spain (by Juan Carreño de Miranda, 1685). Public Domain.

486 a child of an uncle-niece marriage.

488 ALVAREZ *et al.* (2009) calculated that Charles II had an inbreeding coefficient of 0.254, equivalent to a full-sib mating, thanks to all of the inbreeding loops in his pedigree. Therefore, he is expected to have 490 been homozygous by descent for a full quarter of his genome. As we'll talk about later in these notes, this means that Charles may have been 492 homozygous for a number of recessive disease alleles, and indeed he was a very sickly man who left no descendants due to his infertility.⁶ 494 Thus plausibly the end of one of the great European dynasties came about through inbreeding.

496 *2.2.2 Calculating inbreeding coefficients from genetic data*

If the observed heterozygosity in a population is H_O , and we assume 498 that the generalized Hardy–Weinberg proportions hold, we can set H_O equal to f_{12} , and solve Eq. (2.7) for F to obtain an estimate of the 500 inbreeding coefficient as

$$\hat{F} = 1 - \frac{f_{12}}{2pq} = \frac{2pq - f_{12}}{2pq}. \quad (2.10)$$

As before, p is the frequency of allele A_1 in the population. This 502 can be rewritten in terms of the observed heterozygosity (H_O) and the heterozygosity expected in the absence of inbreeding, $H_E = 2pq$, as

$$\hat{F} = \frac{H_E - H_O}{H_E} = 1 - \frac{H_O}{H_E}. \quad (2.11)$$

504 Hence, \hat{F} quantifies the deviation due to inbreeding of the observed heterozygosity from the one expected under random mating, relative 506 to the latter.

Question 9. Suppose the following genotype frequencies were observed 508 for an esterase locus in a population of *Drosophila* (A denotes the “fast” allele and B denotes the “slow” allele):

	AA	AB	BB
	0.6	0.2	0.2

510 What is the estimate of the inbreeding coefficient at the esterase locus?

If we have multiple loci, we can replace H_O and H_E by their means 514 over loci, \bar{H}_O and \bar{H}_E , respectively. Note that, in principle, we could also calculate F for each individual locus first, and then take the average 516 across loci. However, this procedure is more prone to introducing a bias if sample sizes vary across loci, which is not unlikely when we 518 are dealing with real data.

Genetic markers are commonly used to estimate inbreeding for wild 520 and/or captive populations of conservation concern. As an example of

⁶ Pedro Gargantilla, who performed Charles's autopsy, stated that his body “did not contain a single drop of blood; his heart was the size of a peppercorn; his lungs corroded; his intestines rotten and gangrenous; he had a single testicle, black as coal, and his head was full of water.” While some of this description may refer to actual medical conditions, some of these details seem a little unlikely. See here.

this, consider the case of the Mexican wolf (*Canis lupus baileyi*), also known as the lobo, a sub-species of gray wolf.

They were extirpated in the wild during the mid-1900s due to hunting, and the remaining five lobos in the wild were captured to start a breeding program. vonHOLDT *et al.* (2011) estimated the current-day, average expected heterozygosity to be 0.18, based on allele frequencies at over forty thousand SNPs. However, the average lobo individual was only observed to be heterozygous at 12% of these SNPs. Therefore, the average inbreeding coefficient for the lobo is $F = 1 - 0.12/0.18$, i.e. $\sim 33\%$ of a lobo's genome is homozygous due to recent inbreeding in their pedigree.

Genomic blocks of homozygosity due to inbreeding. As we saw above, close relatives are expected to share alleles IBD in large genomic blocks. Thus, when related individuals mate and transmit alleles to an inbred offspring, they transmit these alleles in big blocks through meiosis. An example, lets return to the case of our hypothetical first cousins from Figure 2.6. If this pair of individuals had a child, one possible pattern of genetic transmission is shown in Figure 2.16. The child has inherited the red stretch of chromosome via two different routes through their pedigree from the grandparents. This is an example of an autozygous segment, where the child is homozygous by descent at all of the loci in this red region. The inbreeding coefficient



of the child sets the proportion of their genome that will be in these autozygous segments. For example, a child of first full cousins is expected to have $1/16$ of their genome in these segments. The more distant the loop in the pedigree, the more meioses that chromosomes have been through and the shorter individual blocks will be. A child of first cousins will have longer blocks than a child of second cousins, for example.

Individuals with multiple inbreeding loops in their family tree can have a high inbreeding coefficient due to the combined effect of many



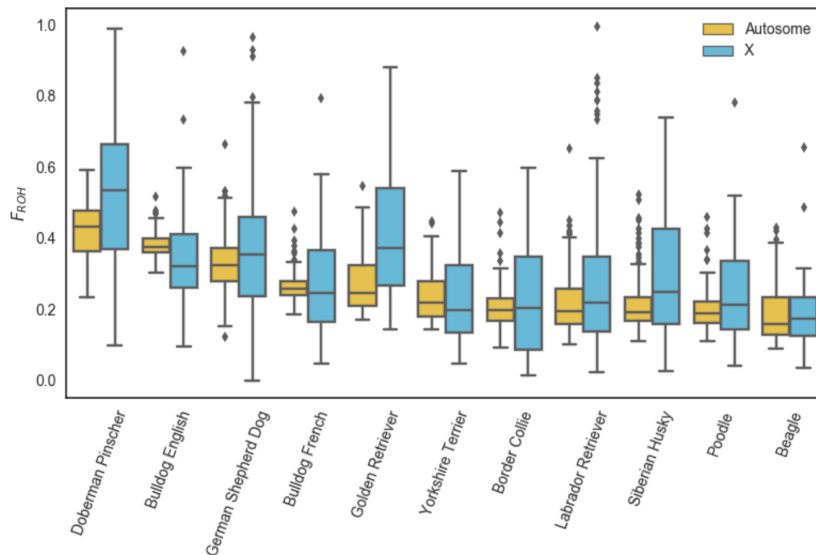
Figure 2.15: Grey wolf (*Canis lupus*). Dogs, jackals, wolves, and foxes: a monograph of the Canidae. 1890. y J.G. Keulemans. Image from the Biodiversity Heritage Library. Contributed by University of Toronto - Gerstein Science Information Centre. Not in copyright.

Figure 2.16: .

552 small blocks of autozygosity. For example, Charles II had an inbreeding
553 coefficient that is equivalent to that of the child of full-sibs, with
554 a quarter of his genome expected to homozygous by descent, but this
555 would be made up of many shorter blocks.

556 We can hope to detect these blocks by looking for unusually long
557 genomic runs of homozygosity (ROH) sites in an individual's genome.
558 One way to estimate an individual's inbreeding coefficient is then to
559 total up the proportion of an individual's genome that falls in such
560 ROH regions. This estimate is called F_{ROH} .

561 An example of using F_{ROH} to study inbreeding comes from the
562 work of SAMS and BOYKO (2018b), who identified runs of homozy-
563 gosity in 2,500 dogs, ranging from 500kb up to many megabases. Fig-



564 ure 2.18 shows the distribution of F_{ROH} of individuals in each dog
565 breed for the X and autosome. In Figure 2.19 this is broken down by
566 the length of ROH segments.

567 Dog breeds have been subject to intense breeding that has resulted
568 in high levels of inbreeding. Of the population samples examined,
569 Doberman Pinschers have the highest levels of their genome in runs
570 of homozygosity (F_{ROH}), somewhat higher than English bulldogs.
571 In 2.19 we can see that English bulldogs have more short ROH than
572 Doberman Pinschers, but that Doberman Pinschers have more of their
573 genome in very large ROH ($> 16Mb$). This suggests that English bulldogs
574 have had long history of inbreeding but that Doberman Pinschers
575 have a lot of recent inbreeding in their history.

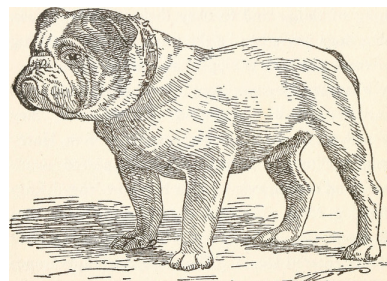


Figure 2.17: English bulldog. The dogs of Boytowm. 1918. Dyer, W. A.

Figure 2.18: The distribution of F_{ROH} of individuals from various dog breeds from SAMS and BOYKO (2018a), licensed under CC BY 4.0.



Figure 2.19: Cumulative density of ROH length, measured in megabases (Mb) from SAMS and BOYKO (2018a) for various dog breeds (licensed under CC BY 4.0). Note that longer lengths of ROH are on the left of the plot.

576 2.3 Summarizing population structure

INDIVIDUALS RARELY MATE COMPLETELY AT RANDOM; your
 578 parents weren't two Bilateria plucked at random from the tree of life.
 Even within species, there's often geographically-restricted mating
 580 among individuals. Individuals tend to mate with individuals from the
 same, or closely related sets of populations. This form of non-random
 582 mating is called population structure and can have profound effects
 on the distribution of genetic variation within and among natural
 584 populations.

2.3.1 Inbreeding as a summary of population structure.

586 It turns out that statements about inbreeding represent one natural
 way to summarize population structure. We defined inbreeding
 588 as having parents that are more closely related to each other than two
 individuals drawn at random from some reference population. The
 590 question that naturally arises is: Which reference population should
 we use? While I might not look inbred in comparison to allele frequen-
 592 cies in the United Kingdom (UK), where I am from, my parents cer-
 tainly are not two individuals drawn at random from the world-wide
 594 population. If we estimated my inbreeding coefficient F using allele
 frequencies within the UK, it would be close to zero, but would likely
 596 be larger if we used world-wide frequencies. This is because there is a
 somewhat lower level of expected heterozygosity within the UK than
 598 in the human population across the world as a whole.

WRIGHT⁷ developed a set of ‘F-statistics’ (also called ‘fixation indices’) that formalize the idea of inbreeding with respect to different levels of population structure. See Figure 2.20 for a schematic diagram. Wright defined F_{XY} as the correlation between random gametes, drawn from the same level X , relative to level Y . We will return to why F -statistics are statements about correlations between alleles in just a moment. One commonly used F -statistic is F_{IS} , which is the inbreeding coefficient between an individual (I) and the subpopulation (S). Consider a single locus, where in a subpopulation (S) a fraction $H_I = f_{12}$ of individuals are heterozygous. In this subpopulation, let the frequency of allele A_1 be p_S , such that the expected heterozygosity under random mating is $H_S = 2p_S(1 - p_S)$. We will write F_{IS} as

$$F_{IS} = 1 - \frac{H_I}{H_S} = 1 - \frac{f_{12}}{2p_S q_S}, \quad (2.12)$$

a direct analog of eqn. 2.10. Hence, F_{IS} is the relative difference between observed and expected heterozygosity due to a deviation from random mating within the subpopulation. We could also compare the observed heterozygosity in individuals (H_I) to that expected in the total population, H_T . If the frequency of allele A_1 in the total population is p_T , then we can write F_{IT} as

$$F_{IT} = 1 - \frac{H_I}{H_T} = 1 - \frac{f_{12}}{2p_T q_T}, \quad (2.13)$$

which compares heterozygosity in individuals to that expected in the total population. As a simple extension of this, we could imagine comparing the expected heterozygosity in the subpopulation (H_S) to that expected in the total population H_T , via F_{ST} :

$$F_{ST} = 1 - \frac{H_S}{H_T} = 1 - \frac{2p_S q_S}{2p_T q_T}. \quad (2.14)$$

We can relate the three F -statistics to each other as

$$(1 - F_{IT}) = \frac{H_I}{H_S} \frac{H_S}{H_T} = (1 - F_{IS})(1 - F_{ST}). \quad (2.15)$$

Hence, the reduction in heterozygosity within individuals compared to that expected in the total population can be decomposed to the reduction in heterozygosity of individuals compared to the subpopulation, and the reduction in heterozygosity from the total population to that in the subpopulation.

If we want a summary of population structure across multiple subpopulations, we can average H_I and/or H_S across populations, and use a p_T calculated by averaging p_S across subpopulations (or our samples from sub-populations). For example, the average F_{ST} across

⁷ WRIGHT, S., 1943 Isolation by Distance. *Genetics* 28(2): 114–138; and WRIGHT, S., 1949 The Genetical Structure of Populations. *Annals of Eugenics* 15(1): 323–354

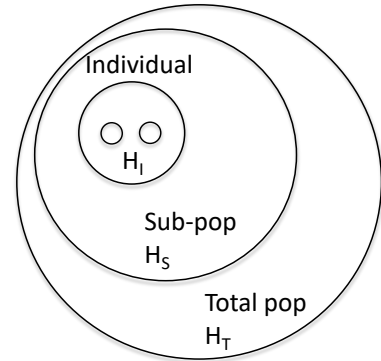


Figure 2.20: The hierarchical nature of F-statistics. The two dots within an individual represent the two alleles at a locus for an individual I . We can compare the heterozygosity in individuals (H_I), to that found by randomly drawing alleles from the sub-population (S), to that found in the total population (T).

632 K subpopulations (sampled with equal effort) is

$$F_{ST} = 1 - \frac{\bar{H}_S}{H_T}, \quad (2.16)$$

634 where $\bar{H}_S = 1/K \sum_{i=1}^K H_S^{(i)}$, and $H_S^{(i)} = 2p_i q_i$ is the expected heterozygosity in subpopulation i . It follows that the average heterozygosity of the sub-populations $\bar{H}_S \leq H_T$,⁸ and so $F_{ST} \geq 0$ and $F_{IS} \leq F_{IT}$.
636 Furthermore, if we have multiple sites, we can replace H_I , H_S , and H_T with their averages across loci (as above).⁹

638 As an example of comparing a genome-wide estimate of F_{ST} to that at individual loci we can look at some data from blue- and golden-winged warblers (*Vermivora cyanoptera* and *V. chrysoptera* 1-2 & 5-6 in Figure 2.21).

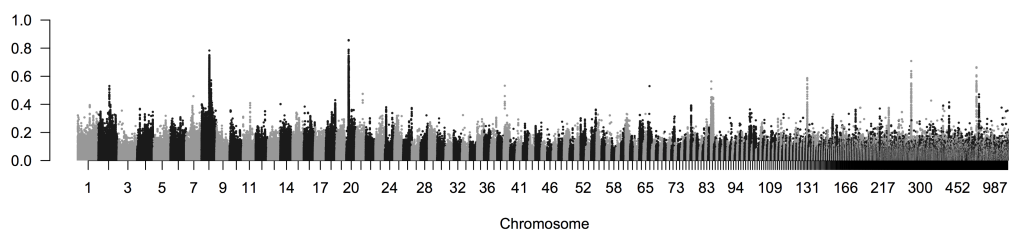
642 These two species are spread across eastern Northern America, with the golden-winged warbler having a smaller, more northerly range.
644 They're quite different in terms of plumage, but have long been known to have similar songs and ecologies. The two species hybridize readily
646 in the wild; in fact two other previously-recognized species, Brewster's and Lawrence's warbler (4 & 3 in 2.21), are actually found to just
648 be hybrids between these two species. The golden-winged warbler is listed as 'threatened' under the Canadian endangered species act. The
650 golden-winged warbler's habitat is under pressure from human activity and increased hybridization with the blue-winged warbler, which is
652 moving north into its range, also poses a significant issue. TOEWS
et al. (2016) investigated the population genomics of these warblers,
654 sequencing ten golden- and ten blue-winged warblers. They found
very low divergence among these species, with a genome-wide $F_{ST} =$
656 0.0045. In Figure 2.22, per SNP F_{ST} is averaged in 2000bp windows moving along the genome. The average is very low, but some regions

⁸ This observation that the average heterozygosity of the sub-populations must be less than or equal to that of the total population is called the Wahlund effect.

⁹ Averaging heterozygosity across loci first, then calculating F_{ST} , rather than calculating F_{ST} for each locus individually and then taking the average, has better statistical properties as statistical noise in the denominator is averaged out.



Figure 2.21: Blue-, golden-winged, and Lawrence's warblers (*Vermivora*). The warblers of North America. Chapman, F.M. 1907. Image from the Biodiversity Heritage Library. Contributed by American Museum of Natural History Library. Not in copyright.



658 of very high F_{ST} stand out. Nearly all of these regions correspond to large allele frequency differences at loci in, or close, to genes known
660 to be involved in plumage colouration differences in other birds. To illustrate these frequency differences TOEWS et al. genotyped a SNP
662 in each of these high- F_{ST} regions. Here's their genotyping counts from the SNP, segregating for an allele 1 and 2, in the *Wnt* region, a key

Figure 2.22: F_{ST} between blue- and golden-winged warbler population samples at SNPs across the genome. Each dot is a SNP, and SNPs are coloured alternating by scaffold. Thanks to David Toews for the figure.

664 regulatory gene involved in feather development:

Species	11	12	22
Blue-winged	2	21	31
Golden-winged	48	12	1

666 **Question 10.** With reference to the table of *Wnt*-allele counts:

- A) Calculate F_{IS} in blue-winged warblers.
- B) Calculate F_{ST} for the sub-population of blue-winged warblers compared to the combined sample.
- C) Calculate mean F_{ST} across both sub-populations.

672 *Interpretations of F-statistics* Let us now return to Wright's definition of the F -statistics as correlations between random gametes, drawn from the same level X , relative to level Y . Without loss of generality, 674 we may think about X as individuals and S as the subpopulation.

Rewriting F_{IS} in terms of the observed homozygote frequencies (f_{11} , 676 f_{22}) and expected homozygosities (p_S^2, q_S^2) we find

$$F_{IS} = \frac{2psq_S - f_{12}}{2psq_S} = \frac{f_{11} + f_{22} - p_S^2 - q_S^2}{2psq_S}, \quad (2.17)$$

678 using the fact that $p^2 + 2pq + q^2 = 1$, and $f_{12} = 1 - f_{11} - f_{22}$. The form of eqn. (2.17) reveals that F_{IS} is the covariance between pairs of alleles found in an individual, divided by the expected variance 680 under binomial sampling. Thus, F -statistics can be understood as the correlation between alleles drawn from a population (or an individual) 682 above that expected by chance (i.e. drawing alleles sampled at random from some broader population).

684 We can also interpret F -statistics as proportions of variance explained by different levels of population structure. To see this, let 686 us think about F_{ST} averaged over K subpopulations, whose frequencies are p_1, \dots, p_K . The frequency in the total population is 688 $p_T = \bar{p} = \frac{1}{K} \sum_{i=1}^K p_i$. Then, we can write

$$F_{ST} = \frac{2\bar{p}\bar{q} - \frac{1}{K} \sum_{i=1}^K 2p_i q_i}{2\bar{p}\bar{q}} = \frac{\left(\frac{1}{K} \sum_{i=1}^K p_i^2 + \frac{1}{K} \sum_{i=1}^K q_i^2\right) - \bar{p}^2 - \bar{q}^2}{2\bar{p}\bar{q}} = \frac{\text{Var}(p_1, \dots, p_K)}{\text{Var}(\bar{p})}, \quad (2.18)$$

690 which shows that F_{ST} is the proportion of the variance explained by the subpopulation labels.

2.3.2 Other approaches to population structure

692 There is a broad spectrum of methods to describe patterns of population structure in population genetic datasets. We'll briefly discuss two 694 broad-classes of methods that appear often in the literature: assignment methods and principal components analysis.

696 *2.3.3 Assignment Methods*

Here we'll describe a simple probabilistic assignment to find the probability that an individual of unknown population comes from one of K predefined populations. For example, there are three broad populations of common chimpanzee (*Pan troglodytes*) in Africa: western, central, and eastern. Imagine that we have a chimpanzee whose population of origin is unknown (e.g. it's from an illegal private collection). If we have genotyped a set of unlinked markers from a panel of individuals representative of these populations, we can calculate the probability that our chimp comes from each of these populations.

We'll then briefly explain how to extend this idea to cluster a set of individuals into K initially unknown populations. This method is a simplified version of what population genetics clustering algorithms such as STRUCTURE and ADMIXTURE do.¹⁰

710 A simple assignment method We have genotype data from unlinked S biallelic loci for K populations. The allele frequency of allele A_1 at locus l in population k is denoted by $p_{k,l}$, so that the allele frequencies in population 1 are $p_{1,1}, \dots, p_{1,L}$ and population 2 are $p_{2,1}, \dots, p_{2,L}$ and so on.

You genotype a new individual from an unknown population at these L loci. This individual's genotype at locus l is g_l , where g_l denotes the number of copies of allele A_1 this individual carries at this locus ($g_l = 0, 1, 2$).

The probability of this individual's genotype at locus l conditional on coming from population k , i.e. their alleles being a random HW draw from population k , is

$$P(g_l|\text{pop } k) = \begin{cases} (1 - p_{k,l})^2 & g_l = 0 \\ 2p_{k,l}(1 - p_{k,l}) & g_l = 1 \\ p_{k,l}^2 & g_l = 2 \end{cases} \quad (2.19)$$

722 Assuming that the loci are independent, the probability of the individual's genotype across all S loci, conditional on the individual 724 coming from population k , is

$$P(\text{ind.}|\text{pop } k) = \prod_{l=1}^S P(g_l|\text{pop } k) \quad (2.20)$$

We wish to know the probability that this new individual comes from population k , i.e. $P(\text{pop } k|\text{ind.})$. We can obtain this through Bayes' rule

$$P(\text{pop } k|\text{ind.}) = \frac{P(\text{ind.}|\text{pop } k)P(\text{pop } k)}{P(\text{ind.})} \quad (2.21)$$

¹⁰ PRITCHARD, J. K., M. STEPHENS, and P. DONNELLY, 2000 Inference of population structure using multilocus genotype data. *Genetics* 155(2): 945–959; and ALEXANDER, D. H., J. NOVEMBRE, and K. LANGE, 2009 Fast model-based estimation of ancestry in unrelated individuals. *Genome research* 19(9): 1655–1664

728 where

$$P(\text{ind.}) = \sum_{k=1}^K P(\text{ind.}|\text{pop } k)P(\text{pop } k) \quad (2.22)$$

is the normalizing constant. We interpret $P(\text{pop } k)$ as the prior probability of the individual coming from population k , and unless we have some other prior knowledge we will assume that the new individual has an equal probability of coming from each population $P(\text{pop } k) = 1/K$.

734 We interpret

$$P(\text{pop } k|\text{ind.}) \quad (2.23)$$

as the posterior probability that our new individual comes from each of our $1, \dots, K$ populations.

More sophisticated versions of this are now used to allow for hybrids, e.g., we can have a proportion q_k of our individual's genome come from population k and estimate the set of q_k 's.

740 Question 11.

Returning to our chimp example, imagine that we have genotyped a set of individuals from the Western and Eastern populations at two SNPs (we'll ignore the central population to keep things simpler). The frequency of the capital allele at two SNPs (A/a and B/b) is given by

Population	locus A	locus B
Western	0.1	0.85
Eastern	0.95	0.2

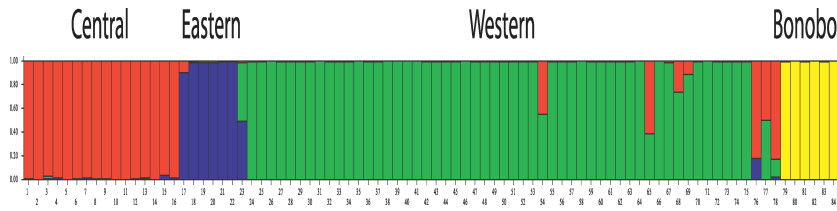
746 **A)** Our individual, whose origin is unknown, has the genotype AA at the first locus and bb at the second. What is the posterior probability 748 that our individual comes from the Western population versus Eastern chimp population?

750 **B)** Let's assume that our individual is a hybrid. At each locus, with probability q_W our individual draws an allele from the Western 752 population and with probability $q_C = 1 - q_W$ they draw an allele from the Eastern population. What is the probability of our individual's 754 genotype given q_C ?

756 **Optional** You could plot this probability as a function of q_W . How does your plot change if our individual is heterozygous at both loci?

Clustering based on assignment methods While it is great to be able 758 to assign our individuals to a particular population, these ideas can be pushed to learn about how best to describe our genotype data in 760 terms of discrete populations without assigning any of our individuals to populations *a priori*. We wish to cluster our individuals into K unknown populations. We begin by assigning our individuals at random 762 to these K populations.

- 764 1. Given these assignments we estimate the allele frequencies at all of
our loci in each population.
- 766 2. Given these allele frequencies we chose to reassign each individual
to a population k with a probability given by eqn. (2.20).
- 768 We iterate steps 1 and 2 for many iterations (technically, this ap-
proach is known as *Gibbs Sampling*). If the data is sufficiently infor-
770 mative, the assignments and allele frequencies will quickly converge on
a set of likely population assignments and allele frequencies for these
populations.



772 To do this in a full Bayesian scheme we need to place priors on
774 the allele frequencies (for example, one could use a beta distribution
prior). Technically we are using the joint posterior of our allele fre-
776 quencies and assignments. Programs like STRUCTURE, use this type
of algorithm to cluster the individuals in an “unsupervised” manner
778 (i.e. they work out how to assign individuals to an unknown set of
populations). See Figure 2.23 for an example of BECQUET *et al.*
780 using STRUCTURE to determine the population structure of chim-
panzees.

782 STRUCTURE-like methods have proven incredible popular and
useful in examining population structure within species. However, the
784 results of these methods are open to misinterpretation; see LAW-
SON *et al.* (2018) for a recent discussion. Two common mistakes
786 are 1) taking the results of STRUCTURE-like approaches for some
particular value of K and taking this to represent the best way to
788 describe population-genetic variation. 2) Thinking that these clusters
represent ‘pure’ ancestral populations.

790 There is no right choice of K , the number of clusters to partition
into. There are methods of judging the ‘best’ K by some statistical
792 measure given some particular dataset, but that is not the same as
saying this is the most meaningful level on which to summarize pop-
794 ulation structure in data. For example, running STRUCTURE on
world-wide human populations for low value of K will result in popula-
796 tion clusters that roughly align with continental populations (ROSEN-
BERG *et al.*, 2002). However, that does not tell us that assigning
798 ancestry at the level of continents is a particularly meaningful way of

Figure 2.23: BECQUET *et al.* (2007) genotyped 78 common chimpanzee and 6 bonobo at over 300 polymorphic markers (in this case microsatellites). They ran STRUCTURE to cluster the individuals using these data into $K = 4$ populations. In BECQUET *et al.* (2007) above figure they show each individual as a vertical bar divided into four colours depicting the estimate of the fraction of ancestry that each individual draws from each of the four estimated populations (licensed under CC BY 4.0). We can see that these four colours/populations correspond to: Red, central; blue, eastern; green, western; yellow, bonobo.

partitioning individuals. Running the same data for higher value of K,
 800 or within continental regions, will result in much finer-scale partitioning of continental groups (ROSENBERG *et al.*, 2002; LI *et al.*, 2008).
 802 No one of these layers of population structure identified is privileged as being more meaningful than another.

804 It is tempting to think of these clusters as representing ancestral populations, which themselves are not the result of admixture. However, that is not the case, for example, running STRUCTURE on
 806 world-wide human data identifies a cluster that contains many European individuals, however, on the basis of ancient DNA we know that
 808 modern Europeans are a mixture of distinct ancestral groups.

810 *2.3.4 Principal components analysis*

Principal component analysis (PCA) is a common statistical approach
 812 to visualize high dimensional data, and used by many fields. The idea of PCA is to give a location to each individual data-point on each of
 814 a small number principal component axes. These PC axes are chosen to reflect major axes of variation in the data, with the first PC being
 816 that which explains largest variance, the second the second most, and so on. The use of PCA in population genetics was pioneered by
 818 Cavalli-Sforza and colleagues and now with large genotyping datasets, PCA has made a comeback.¹¹

820 Consider a dataset consisting of N individuals at S biallelic SNPs. The i^{th} individual's genotype data at locus ℓ takes a value $g_{i,\ell} =$
 822 0, 1, or 2 (corresponding to the number of copies of allele A_1 an individual carries at this SNP). We can think of this as a $N \times S$ matrix
 824 (where usually $N \ll S$).

Denoting the sample mean allele frequency at SNP ℓ by p_ℓ , it's
 826 common to standardize the genotype in the following way

$$\frac{g_{i,\ell} - 2p_\ell}{\sqrt{2p_\ell(1-p_\ell)}} \quad (2.24)$$

i.e. at each SNP we center the genotypes by subtracting the mean
 828 genotype ($2p_\ell$) and divide through by the square root of the expected variance assuming that alleles are sampled binomially from the mean
 830 frequency ($\sqrt{2p_\ell(1-p_\ell)}$). Doing this to all of our genotypes, we form a data matrix (of dimension $N \times S$). We can then perform principal
 832 component analysis of this data matrix to uncover the major axes of genotype variance in our sample. Figure 2.24 shows a PCA from
 834 BECQUET *et al.* (2007) using the same chimpanzee data as in Figure 2.23.

836 It is worth taking a moment to delve further into what we are doing here. There's a number of equivalent ways of thinking about what
 838 PCA is doing. One of these ways is to think that when we do PCA we

¹¹ MENOZZI, P., A. PIAZZA, and L. CAVALLI-SFORZA, 1978 Synthetic maps of human gene frequencies in Europeans. *Science* 201(4358): 786–792; and PATTERSON, N., A. L. PRICE, and D. REICH, 2006 Population structure and eigenanalysis. *PLoS genetics* 2(12): e190

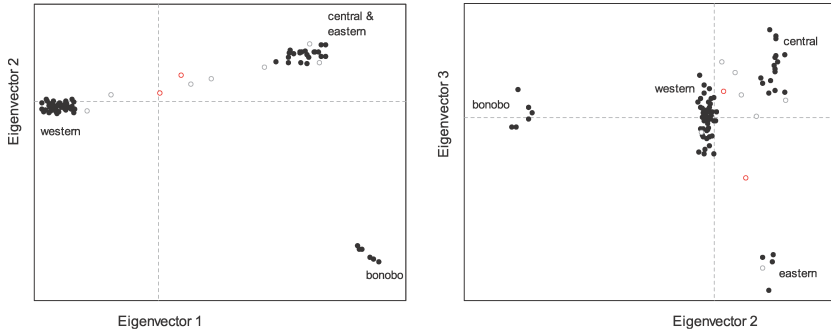


Figure 2.24: Principal Component Analysis by BECQUET *et al.* (2007) using the same chimpanzee data as in Figure 2.23. Here BECQUET *et al.* (2007) plot the location of each individual on the first two principal components (called eigenvectors) in the left panel, and on the second and third principal components (eigenvectors) in the right panel (licensed under CC BY 4.0). In the PCA, individuals identified as all of one ancestry by STRUCTURE cluster together by population (solid circles). While the nine individuals identified by STRUCTURE as hybrids (open circles) for the most part fall at intermediate locations in the PCA. There are two individuals (red open circles) reported as being of a particular population but that but appear to be hybrids.

are building the individual by individual covariance matrix and performing an eigenvalue decomposition of this matrix (with the eigenvectors being the PCs). This individual by individual covariance matrix has entries the $[i, j]$ given by

$$\frac{1}{S-1} \sum_{\ell=1}^S \frac{(g_{i,\ell} - 2p_\ell)(g_{j,\ell} - 2p_\ell)}{2p_\ell(1-p_\ell)} \quad (2.25)$$

Note that this is the covariance, and is very similar to those we encountered in discussing F -statistics as correlations (equation (2.17)), except now we are asking about the covariance between two individuals above that expected if they were both drawn from the total sample at random (rather than the covariance of alleles within a single individual). So by performing PCA on the data we are learning about the major (orthogonal) axes of the kinship matrix.

As an example of the application of PCA, let's consider the case of the putative ring species in the Greenish warbler (*Phylloscopus trochiloides*) species complex. This set of subspecies exists in a ring around the edge of the Himalayan plateau. ALCAIDE *et al.* (2014) collected 95 Greenish warbler samples from 22 sites around the ring, and the sampling locations are shown in Figure 2.25.

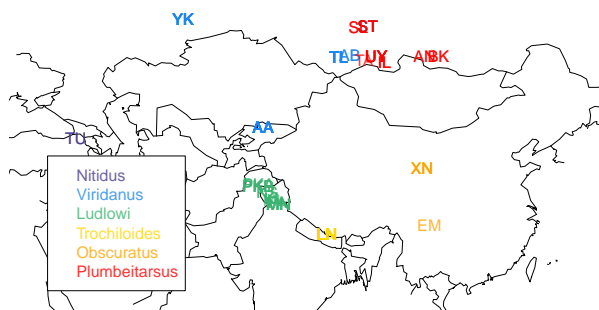


Figure 2.25: The sampling locations of 22 populations of Greenish warblers from ALCAIDE *et al.* (2014). The samples are coloured by the subspecies. Code here.

It is thought that these warblers spread from the south, northward in two different directions around the inhospitable Himalayan plateau, establishing populations along the western edge (green and blue populations) and the eastern edge (yellow and red populations). When they came into secondary contact in Siberia, they were reproductively isolated from one another, having evolved different songs and accumulated other reproductive barriers from each other as they spread independently north around the plateau, such that *P. t. viridianus* (blue) and *P. t. plumbeitarsus* (red) populations presently form a stable hybrid zone.

ALCAIDE *et al.* (2014) obtained sequence data for their samples at 2,334 snps. In Figure 2.27 you can see the matrix of kinship coefficients, using (2.25), between all pairs of samples. You can already see a lot about population structure in this matrix. Note how the red and yellow samples, thought to be derived from the Eastern route around the Himalayas, have higher kinship with each other, and blue and the (majority) of the green samples, from the Western route, form a similarly close group in terms of their higher kinship.

We can then perform PCA on this kinship matrix to identify the major axes of variation in the dataset. Figure 2.28 shows the samples plotted on the first two PCs. The two major routes of expansion clearly occupy different parts of PC space. The first principal component distinguishes populations running North to South along the western route of expansion, while the second principal component distinguishes among populations running North to South along the Eastern route of expansion. Thus genetic data supports the hypothesis that the Greenish warblers speciated as they moved around the Himalayan plateau. However, as noted by ALCAIDE *et al.* (2014), it also suggests additional complications to the traditional view of these

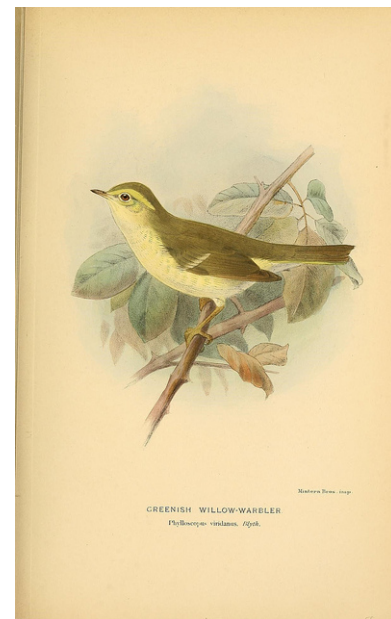


Figure 2.26: Greenish warbler, subsp. viridanus (*Phylloscopus trochiloides viridanus*). Coloured figures of the birds of the British Islands. 1885. Lilford T. L. P.. Image from the Biodiversity Heritage Library. Contributed by American Museum of Natural History Library. Not in copyright. (Greenish warblers are rare visitors to the UK.)

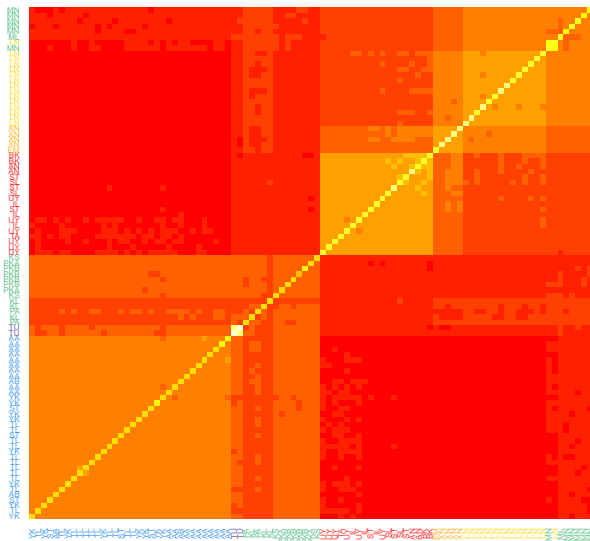


Figure 2.27: The matrix of kinship coefficients calculated for the 95 samples of Greenish warblers. Each cell in the matrix gives the pairwise kinship coefficient calculated for a particular pair. Hotter colours indicating higher kinship. The x and y labels of individuals are the population labels from Figure 2.25, and coloured by subspecies label as in that figure. The rows and columns have been organized to cluster individuals with high kinship. [Code here.](#)

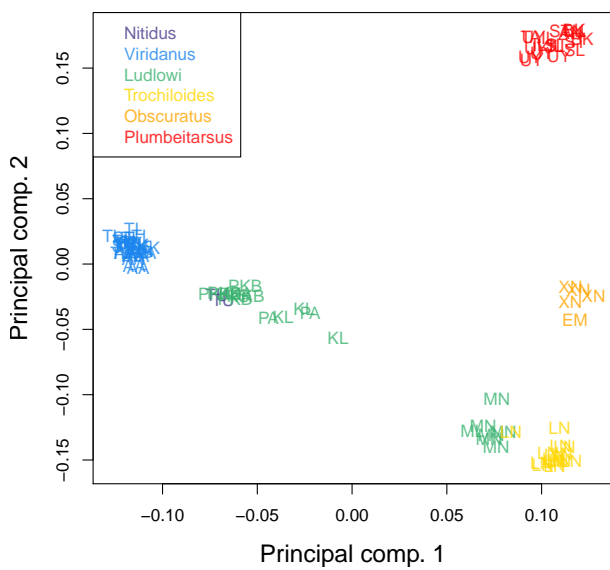


Figure 2.28: The 95 greenish warbler samples plotted on their locations on the first two principal components. The labels of individuals are the population labels from Figure 2.25, and coloured by subspecies label as in that figure. [Code here.](#)

warblers as an unbroken ring species, a case of speciation by continuous geographic isolation. The *Ludlowi* subspecies shows a significant genetic break, with the southern most MN samples clustering with the *Trochiloides* subspecies, in both the PCA and kinship matrix (Figures 2.28 and 2.27), despite being much more geographically close to the other *Ludlowi* samples. This suggests that genetic isolation is not just a result of geographic distance, and other biogeographic barriers must be considered in the case of this broken ring species.

Finally, while PCA is a wonderful tool for visualizing genetic data, care must be taken in its interpretation. The U-like shape in the case of the Greenish warbler PC might be consistent with some low level of gene flow between the red and the blue populations, pulling them genetically closer together and helping to form a genetic ring as well as a geographic ring. However, U-like shapes are expected to appear in PCAs even if our populations are just arrayed along a line, and more complex geometric arrangements of populations in PC space can result under simple geographic models (NOVEMBRE and STEPHENS, 2008). Inferring the geographical and population-genetic history of species requires the application of a range of tools; see ALCAIDE *et al.* (2014) and BRADBURD *et al.* (2016) for more discussion of the Greenish warblers.

906 2.3.5 Correlations between loci, linkage disequilibrium, and recombination

908 Up to now we have been interested in correlations between alleles
 at the same locus, e.g. correlations within individuals (inbreeding)
 910 or between individuals (relatedness). We have seen how relatedness
 between parents affects the extent to which their offspring is inbred.
 912 We now turn to correlations between alleles at different loci.

Recombination To understand correlations between loci we need
 914 to understand recombination a bit more carefully. Let us consider
 a heterozygous individual, containing AB and ab haplotypes. If no
 916 recombination occurs between our two loci in this individual, then
 these two haplotypes will be transmitted intact to the next genera-
 918 tion. While if a recombination (i.e. an odd number of crossing over
 events) occurs between the two parental haplotypes, then $1/2$ the time
 920 the child receives an Ab haplotype and $1/2$ the time the child receives
 an aB haplotype. Effectively, recombination breaks up the association
 922 between loci. We'll define the recombination fraction (r) to be the
 probability of an odd number of crossing over events between our loci
 924 in a single meiosis. In practice we'll often be interested in relatively
 short regions such that recombination is relatively rare, and so we
 926 might think that $r = r_{BP}L \ll \frac{1}{2}$, where r_{BP} is the average recombi-
 nation rate (in Morgans) per base pair (typically $\sim 10^{-8}$) and L is the
 928 number of base pairs separating our two loci.

Linkage disequilibrium The (horrible) phrase linkage disequilibrium
 930 (LD) refers to the statistical non-independence (i.e. a correlation)
 of alleles in a population at different loci. It's an awful name for a
 932 fantastically useful concept; LD is key to our understanding of diverse
 topics, from sexual selection and speciation to the limits of genome-
 934 wide association studies.

Our two biallelic loci, which segregate alleles A/a and B/b , have
 936 allele frequencies of p_A and p_B respectively. The frequency of the two
 locus haplotype AB is p_{AB} , and likewise for our other three combi-
 938 nations. If our loci were statistically independent then $p_{AB} = p_A p_B$,
 otherwise $p_{AB} \neq p_A p_B$. We can define a covariance between the A and
 940 B alleles at our two loci as

$$D_{AB} = p_{AB} - p_A p_B \quad (2.26)$$

and likewise for our other combinations at our two loci (D_{Ab} , D_{aB} , D_{ab}).
 942 Gametes with two similar case alleles (e.g. A and B, or a and b)
 are known as *coupling* gametes, and those with different case alleles
 944 are known as *repulsion* gametes (e.g. a and B, or A and b). Then,

we can think of D as measuring the *excess* of coupling to repulsion gametes. These D statistics are all closely related to each other as $D_{AB} = -D_{Ab}$ and so on. Thus we only need to specify one D_{AB} to know them all, so we'll drop the subscript and just refer to D . Also a handy result is that we can rewrite our haplotype frequency p_{AB} as

$$p_{AB} = p_A p_B + D. \quad (2.27)$$

If $D = 0$ we'll say the two loci are in linkage equilibrium, while if $D > 0$ or $D < 0$ we'll say that the loci are in linkage disequilibrium (we'll perhaps want to test whether D is statistically different from 0 before making this choice). You should be careful to keep the concepts of linkage and linkage disequilibrium separate in your mind. Genetic linkage refers to the linkage of multiple loci due to the fact that they are transmitted through meiosis together (most often because the loci are on the same chromosome). Linkage disequilibrium merely refers to the covariance between the alleles at different loci; this may in part be due to the genetic linkage of these loci but does not necessarily imply this (e.g. genetically unlinked loci can be in LD due to population structure).

i

Question 12. You genotype 2 bi-allelic loci (A & B) segregating in two mouse subspecies (1 & 2) which mate randomly among themselves, but have not historically interbreed since they speciated. On the basis of previous work you estimate that the two loci are separated by a recombination fraction of 0.1. The frequencies of haplotypes in each population are:

Pop	p_{AB}	p_{Ab}	p_{aB}	p_{ab}
1	.02	.18	.08	.72
2	.72	.18	.08	.02

A) How much LD is there within species? (i.e. estimate D)
 B) If we mixed individuals from the two species together in equal proportions, we could form a new population with p_{AB} equal to the average frequency of p_{AB} across species 1 and 2. What value would D take in this new population before any mating has had the chance to occur?

Our linkage disequilibrium statistic D depends strongly on the allele frequencies of the two loci involved. One common way to partially remove this dependence, and make it more comparable across loci, is to divide D through by its maximum possible value given the frequency of the loci. This normalized statistic is called D' and varies between +1 and -1. In Figure 2.29 there's an example of LD across the TAP2 region in human and chimp. Notice how physically close SNPs,



Figure 2.29: LD across the TAP2 gene region in a sample of Humans and Chimps, from PTAK *et al.* (2004), licensed under CC BY 4.0. The rows and columns are consecutive SNPs, with each cell giving the absolute D' value between a pair of SNPs. Note that these are different sets of SNPs in the two species, as shared polymorphisms are very rare.

i.e. those close to the diagonal, have higher absolute values of D' as
 984 closely linked alleles are separated by recombination less often allowing
 high levels of LD to accumulate. Over large physical distances, away
 986 from the diagonal, there is lower D' . This is especially notable in hu-
 mans as there is an intense, human-specific recombination hotspot in
 988 this region, which is breaking down LD between opposite sides of this
 region.

990 Another common statistic for summarizing LD is r^2 which we write
 as

$$r^2 = \frac{D^2}{p_A(1-p_A)p_B(1-p_B)} \quad (2.28)$$

992 As D is a covariance, and $p_A(1-p_A)$ is the variance of an allele drawn
 at random from locus A , r^2 is the squared correlation coefficient. Note
 994 that this r in r^2 is NOT the recombination fraction.

996 Figure 2.31 shows r^2 for pairs of SNPs at various physical distances
 in two population samples of *Mus musculus domesticus*. Again LD
 998 is highest between physically close markers as LD is being generated
 faster than it can decay via recombination; more distant markers have
 much lower LD as here recombination is winning out. Note the decay
 1000 of LD is much slower in the advanced-generation cross population than
 in the natural wild-caught population. This persistence of LD across
 1002 megabases is due to the limited number of generations for recombina-
 tion since the cross was created.

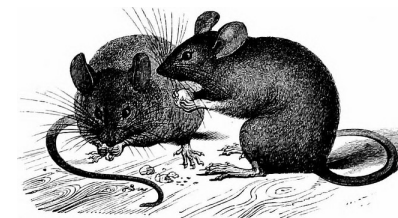
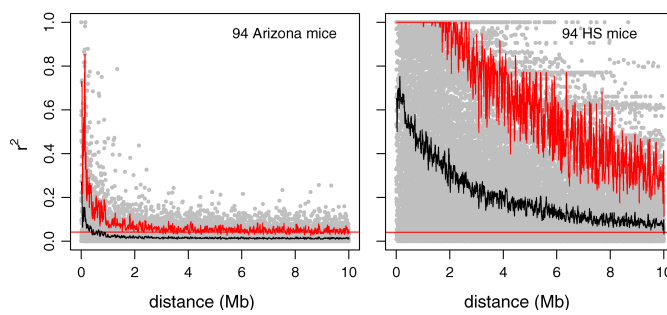


Figure 2.30: *Mus musculus*.
 A history of British quadrupeds, including the Cetacea. 1874. Bell T., Tomes, R. F.m Alston E. R. Image from the Biodiversity Heritage Library. Contributed by Cornell University Library. No known copyright restrictions.

Figure 2.31: The decay of LD for autosomal SNPs in *Mus musculus domesticus*, as measured by r^2 , in a wild-caught mouse population from Arizona and a set of advanced-generation crosses between inbred lines of lab mice. Each dot gives the r^2 for a pair of SNPs a given physical distance apart, for a total of ~ 3000 SNPs. The solid black line gives the mean, the jagged red line the 95th percentile, and the flat red line a cutoff for significant LD. From LAURIE *et al.* (2007), licensed under CC BY 4.0.

1004 *The generation of LD.* Various population genetic forces can generate LD. Selection can generate LD by favouring particular combinations
 1006 of alleles. Genetic drift will also generate LD, not because particular combinations of alleles are favoured, but simply because at random
 1008 particular haplotypes can by chance drift up in frequency. Mixing between divergent populations can also generate LD, as we saw in the
 1010 mouse question above.

1012 *The decay of LD due to recombination* We will now examine what happens to LD over the generations if, in a very large population (i.e.
 1014 no genetic drift and frequencies of our loci thus follow their expectations), we only allow recombination to occur. To do so, consider the frequency of our AB haplotype in the next generation, p'_{AB} . We lose
 1016 a fraction r of our AB haplotypes to recombination ripping our alleles apart but gain a fraction $rp_A p_B$ per generation from other haplotypes
 1018 recombining together to form AB haplotypes. Thus in the next generation

$$p'_{AB} = (1 - r)p_{AB} + rp_A p_B \quad (2.29)$$

1020 The last term above, in eqn 2.29, is $r(p_{AB} + p_{Ab})(p_{AB} + p_{aB})$ simplified, which is the probability of recombination in the different diploid
 1022 genotypes that could generate a p_{AB} haplotype.

We can then write the change in the frequency of the p_{AB} haplotype as

$$\Delta p_{AB} = p'_{AB} - p_{AB} = -rp_{AB} + rp_A p_B = -rD \quad (2.30)$$

So recombination will cause a decrease in the frequency of p_{AB} if there is an excess of AB haplotypes within the population ($D > 0$), and an increase if there is a deficit of AB haplotypes within the population ($D < 0$). Our LD in the next generation is

$$\begin{aligned} D' &= p'_{AB} - p'_A p'_B \\ &= (p_{AB} + \Delta p_{AB}) - (p_A + \Delta p_A)(p_B + \Delta p_B) \\ &= p_{AB} + \Delta p_{AB} - p_A p_B \\ &= (1 - r)D \end{aligned} \quad (2.31)$$

where we can cancel out Δp_A and Δp_B above because recombination
 1026 only changes haplotype, not allele, frequencies. So if the level of LD in generation 0 is D_0 , the level t generations later (D_t) is

$$D_t = (1 - r)^t D_0 \quad (2.32)$$

1028 Recombination is acting to decrease LD, and it does so geometrically at a rate given by $(1 - r)$. If $r \ll 1$ then we can approximate this by
 1030 an exponential and say that

$$D_t \approx D_0 e^{-rt} \quad (2.33)$$



Figure 2.32: The decay of LD from an initial value of $D_0 = 0.25$ over time (Generations) for a pair of loci a recombination fraction r apart. Code here.



Figure 2.33: The decay of LD from an initial value of $D_0 = 0.25$ due to recombination over t generations, plotted across possible recombination fractions (r) between our pair of loci. Code here.

- Question 13.** You find a hybrid population between the two mouse subspecies described in the question above, which appears to be comprised of equal proportions of ancestry from the two subspecies.
- 1032 You estimate LD between the two markers to be 0.0723. Assuming
1034 that this hybrid population is large and was formed by a single mix-
1036 ture event, can you estimate how long ago this population formed?

A particularly striking example of the decay of LD generated by the mixing of populations is offered by the LD created by the interbreeding between humans and Neanderthals. Neanderthals and modern Humans diverged from each other likely over half a million years ago, allowing time for allele frequency differences to accumulate between the Neanderthal and modern human populations. The two populations spread back into secondary contact when humans moved out of Africa over the past hundred thousand years or so. One of the most exciting findings from the sequencing of the Neanderthal genome was that modern-day people with Eurasian ancestry carry a few percent of their genome derived from the Neanderthal genome, via interbreeding during this secondary contact. To date the timing of this interbreeding, SANKARARAMAN *et al.* (2012) looked at the LD in modern humans between pairs of alleles found to be derived from the Neanderthal genome (and nearly absent from African populations). In Figure 2.35 we show the average LD between these loci as a function of the genetic distance (r) between them, from the work of SANKARARAMAN *et al.*

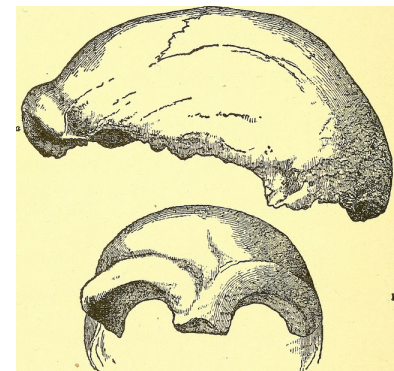
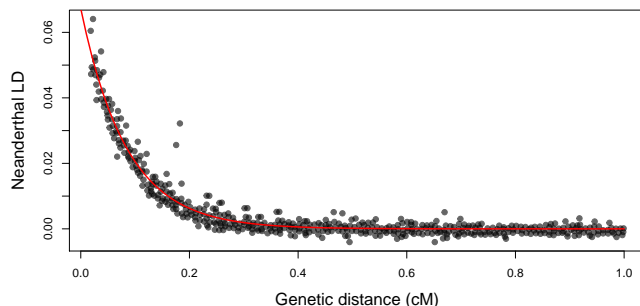


Figure 2.34: The earliest discovered fossil of a Neanderthal, fragments of skull found in a cave in the Neander Valley in Germany.
Man's place in nature. 1890. Huxley, T. H.
Image from the Internet Archive. Contributed by The Library of Congress. No known copyright restrictions.

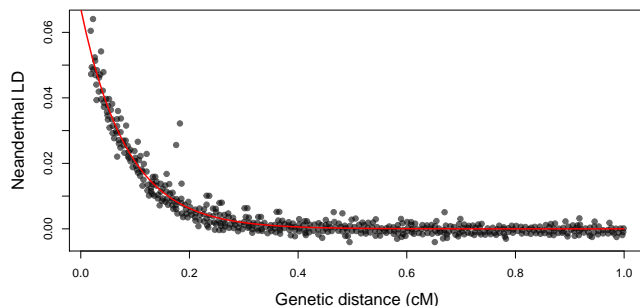


Figure 2.35: The LD between putative-Neanderthal alleles in a modern European population (the CEU sample from the 1000 Genomes Project). Each point represents the average D statistic between a pair of alleles at a given genetic distance apart (as given on the x-axis and measured in centiMorgans (cM)). The putative Neanderthal alleles are alleles where the Neanderthal genome has a derived allele that is at very low frequency in a modern-human West African population sample (thought to have little admixture from Neanderthals). The red line is the fit of an exponential decay of LD, using non-linear least squared (nls in R).

- 1054 Assuming a recombination rate r , we can fit the exponential decay
1056 of LD predicted by eqn. (2.33) to the data points in this figure; the fit
is shown as a red line. Doing this we estimate $t = 1200$ generations, or
1058 about 35 thousand years (using a human generation time of 29 years).
Thus the LD in modern Eurasians, between alleles derived from the
1060 interbreeding with Neanderthals, represents over thirty thousand years
of recombination slowly breaking down these old associations.¹²

¹² The calculation done by SANKARARAMAN *et al.* (2012) is actually a bit more involved as they account for inhomogeneity in recombination rates and arrive at a date of 47,334 – 63,146 years.

Genetic Drift and Neutral Diversity

1064 RANDOMNESS IS INHERENT TO EVOLUTION, from the lucky
 birds blown of course to colonize some new oceanic island, to which
 1066 mutations arise first in the HIV strain infecting an individual taking
 anti-retroviral drugs. One major source of stochasticity in evolution-
 1068 ary biology is genetic drift. Genetic drift occurs because more or less
 copies of an allele by chance can be transmitted to the next genera-
 1070 tion. This can occur because, by chance, the individuals carrying a
 particular allele can leave more or less offspring in the next generation.
 1072 In a sexual population, genetic drift also occurs because Mendelian
 transmission means that only one of the two alleles in an individual,
 1074 chosen at random at a locus, is transmitted to the offspring.

Genetic drift can play a role in the dynamics of all alleles in all
 1076 populations, but it will play the biggest role for neutral alleles. A
 neutral polymorphism occurs when the segregating alleles at a poly-
 1078 morphic site have no discernible differences in their effect on fitness.
 We'll make clear what we mean by "discernible" later, but for the
 1080 moment think of this as "no effect" on fitness.

The neutral theory of molecular evolution. The role of genetic drift
 1082 in molecular evolution has been hotly debated since the 60s when
 the Neutral theory of molecular evolution was proposed (see OHTA
 1084 and GILLESPIE, 1996, for a history)¹. The central premise of Neu-
 tral theory theory is that patterns of molecular polymorphism within
 1086 species and substitution between species can be well understood by
 supposing that the vast majority of these molecular polymorphisms
 1088 and substitutions were neutral alleles, whose dynamics were just sub-
 ject to the vagaries of genetic drift and mutation. Early proponents of
 1090 this view suggested that the vast majority of new mutations are either
 neutral or highly deleterious (e.g. mutations that disrupt important
 1092 protein functions). This latter class of mutations are too deleterious
 to contribute much to common polymorphisms or substitutions be-

¹ KIMURA, M., 1968 Evolutionary rate at the molecular level. *Nature* *217*(5129): 624–626; KING, J. L. and T. H. JUKES, 1969 Non-darwinian evolution. *Science* *164*(3881): 788–798; and KIMURA, M., 1983 *The neutral theory of molecular evolution*. Cambridge University Press

¹⁰⁹⁴ tween species, because they are quickly weeded out of the population by selection.

¹⁰⁹⁶ Neutral theory can sound strange given that much of the time our first brush with evolution often focuses on adaptation and phenotypic evolution. However, proponents of this world-view didn't deny the existence of advantageous mutations, they simply thought that beneficial mutations are rare enough that their contribution to the bulk of polymorphism or divergence can be largely ignored. They also often thought that much of phenotypic evolution may well be adaptive, but again the loci responsible for these phenotypes are a small fraction of all the molecular change that occur. The neutral theory of molecular evolution was originally proposed to explain protein polymorphism.
¹¹⁰⁶ However, we can apply it more broadly to think about neutral evolution genome-wide. With that in mind, what types of molecular changes could be neutral? Perhaps:

- ¹¹¹⁰ 1. Changes in non-coding DNA that don't disrupt regulatory sequences. For example, in the human genome only about 2% of the genome codes for proteins. The rest is mostly made up of old transposable element and retrovirus insertions, repeats, pseudo-genes, and general genomic clutter. Current estimates suggest that, even counting conserved, functional, non-coding regions, less than 10% of our genome is subject to evolutionary constraint (RANDS *et al.*, 2014).
 - ¹¹¹⁸ 2. Synonymous changes in coding regions, i.e. those that don't change the amino-acid encoded by a codon.
 - ¹¹²⁰ 3. Non-synonymous changes that don't have a strong effect on the functional properties of the amino acid encoded, e.g. changes that don't change the size, charge, or hydrophobic properties of the amino acid too much.
 - ¹¹²⁴ 4. An amino-acid change with phenotypic consequences, but little relevance to fitness, e.g. a mutation that causes your ears to be a slightly different shape, or that prevents an organism from living past 50 in a species where most individuals reproduce and die by their 20s.
- ¹¹²⁸ There are counter examples to all of these ideas, e.g. synonymous changes can affect the translation speed and accuracy of proteins and so are subject to selection. However, the list above hopefully convinces you that the general thinking that some portion of molecular change may not be subject to selection isn't as daft as it may have initially sounded.
- ¹¹³⁴ Various features of molecular polymorphism and divergence have been viewed as consistent with the neutral theory of molecular evo-

lution. The two we'll focus on in this chapter are the high level of molecular polymorphism in many species (see for example Figure 2.2) and the molecular clock. We'll see that various aspects of the original neutral theory have merit in describing some features and types of molecular change, but we'll also see that it is demonstrably wrong in some cases. We'll also see the primary utility of the neutral theory isn't whether it is right or wrong, but that it serves as a simple null model that can be tested and in some cases rejected, and subsequently built on. The broader debate currently in the field of molecular evolution is the balance of neutral, adaptive, and deleterious changes that drive different types of evolutionary change.

3.1 Loss of heterozygosity due to drift.

Genetic drift will, in the absence of new mutations, slowly purge our population of neutral genetic diversity, as alleles slowly drift to high or low frequencies and are lost or fixed over time.

Imagine a randomly mating population of a constant size N diploid individuals, and that we are examining a locus segregating for two alleles that are neutral with respect to each other. This population is randomly mating with respect to the alleles at this locus. See Figures 3.1 and 3.2 to see how genetic drift proceeds, by tracking alleles within a small population.

In generation t our current level of heterozygosity is H_t , i.e. the probability that two randomly sampled alleles in generation t are non-identical is H_t . Assuming that the mutation rate is zero (or vanishingly small), what is our level of heterozygosity in generation $t + 1$?

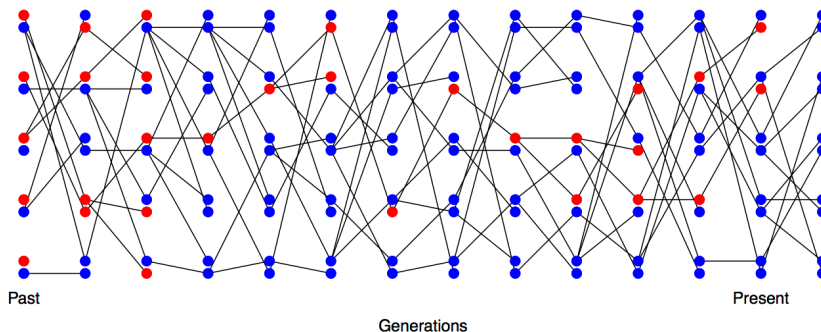


Figure 3.1: Loss of heterozygosity over time, in the absence of new mutations. A diploid population of 5 individuals over the generations, with lines showing transmission. In the first generation every individual is a heterozygote. Code here.

In the next generation ($t + 1$) we are looking at the alleles in the offspring of generation t . If we randomly sample two alleles in generation $t + 1$ which had different parental alleles in generation t , that is just like drawing two random alleles from generation t . So the probability that these two alleles in generation $t + 1$, that have different parental



Figure 3.2: Loss of heterozygosity over time, in the absence of new mutations. A diploid population of 5 individuals. In the first generation I colour every allele a different colour so we can track their descendants. Code here.

₁₁₆₆ alleles in generation t , are non-identical is H_t .

Conversely, if the two alleles in our pair had the same parental
₁₁₆₈ allele in the proceeding generation (i.e. the alleles are identical by descent one generation back) then these two alleles must be identical
₁₁₇₀ (as we are not allowing for any mutation).

In a diploid population of size N individuals there are $2N$ alleles.
₁₁₇₂ The probability that our two alleles have the same parental allele in the proceeding generation is $1/(2N)$ and the probability that they have
₁₁₇₄ different parental alleles is $1 - 1/(2N)$. So by the above argument, the expected heterozygosity in generation $t + 1$ is

$$H_{t+1} = \frac{1}{2N} \times 0 + \left(1 - \frac{1}{2N}\right) H_t \quad (3.1)$$

₁₁₇₆ Thus, if the heterozygosity in generation 0 is H_0 , our expected heterozygosity in generation t is

$$H_t = \left(1 - \frac{1}{2N}\right)^t H_0 \quad (3.2)$$

₁₁₇₈ i.e. the expected heterozygosity within our population is decaying geometrically with each passing generation. If we assume that $1/(2N) \ll 1$
₁₁₈₀ then we can approximate this geometric decay by an exponential decay (see Question 2 below), such that

$$H_t = H_0 e^{-t/(2N)} \quad (3.3)$$

₁₁₈₂ i.e. heterozygosity decays exponentially at a rate $1/(2N)$.

In Figure 3.3 we show trajectories through time for 40 independently simulated loci drifting in a population of 50 individuals. Each population was started from a frequency of 30%. Some drift up and some drift down, eventually being lost or fixed from the population, but, on average across simulations, the allele frequency doesn't change.
₁₁₈₆ We also track heterozygosity, you can see that heterozygosity sometimes goes up, and sometimes goes down, but on average we are losing heterozygosity, and this rate of loss is well predicted by eqn. (3.2).
₁₁₉₀

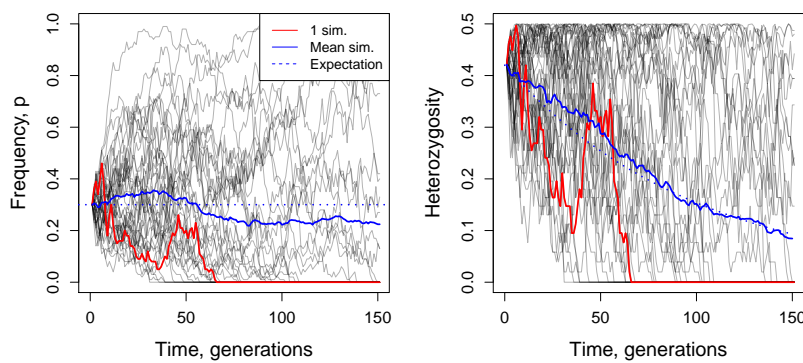


Figure 3.3: Change in allele frequency and loss of heterozygosity over time for 40 replicates. Simulations of genetic drift in a diploid population of 50 individuals, in the absence of new mutations. We start 40 independent, biallelic loci each with an initial allele at 30% frequency. The left panel shows the allele frequency over time and the right panel shows the heterozygosity over time, with the mean decay matching eqn. (3.2). Code here.

Question 1. You are in charge of maintaining a population of delta smelt in the Sacramento river delta. Using a large set of microsatellites you estimate that the mean level of heterozygosity in this population is 0.005. You set yourself a goal of maintaining a level of heterozygosity of at least 0.0049 for the next two hundred years. Assuming that the smelt have a generation time of 3 years, and that only genetic drift affects these loci, what is the smallest fully outbreeding population that you would need to maintain to meet this goal?

Note how this picture of decreasing heterozygosity stands in contrast to the consistency of Hardy-Weinberg equilibrium from the previous chapter. However, our Hardy-Weinberg *proportions* still hold in forming each new generation. As the offspring genotypes in the next generation ($t + 1$) represent a random draw from the previous generation (t), if the parental frequency is p_t , we *expect* a proportion $2p_t(1 - p_t)$ of our offspring to be heterozygotes (and HW proportions for our homozygotes). However, because population size is finite, the observed genotype frequencies in the offspring will (likely) not match exactly with our expectations. As our genotype frequencies likely change slightly due to sampling, biologically this reflects random variation in family size and Mendelian segregation, the allele frequency will change. Therefore, while each generation represents a sample from Hardy-Weinberg proportions based on the generation before, our genotype proportions are not at an equilibrium (an unchanging state) as the underlying allele frequency changes over the generations. We'll develop some mathematical models for these allele frequency changes later on. For now, we'll simply note that under our simple model of drift (formally the Wright-Fisher model), our allele count in the $t + 1^{th}$ generation represents a binomial sample (of size $2N$) from the popu-

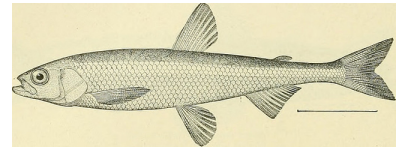


Figure 3.4: Pond smelt (*Hypomesus olidus*), a close relative of delta smelt. Bulletin of the United States Fish Commission, 1906. Image from the Biodiversity Heritage Library. Contributed by Smithsonian Libraries. Not in copyright.

lation frequency p_t in the previous generation. If you've read to here,
 1220 please email Prof Coop a picture of JBS Haldane in a striped suit with
 the title "I'm reading the chapter 3 notes". (It's well worth googling
 1222 JBS Haldane and to read more about his life; he's a true character and
 one of the last great polymaths.)

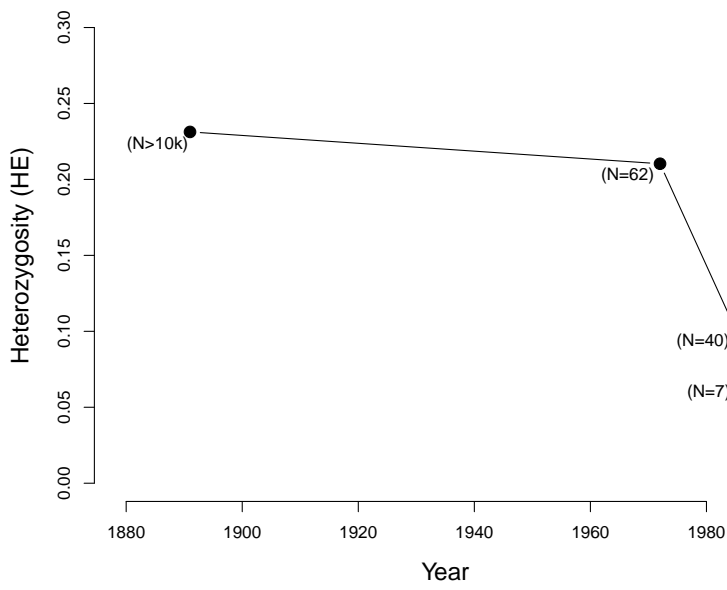


Figure 3.6: Loss of heterozygosity in the Black-footed Ferrets in their declining population. Numbers in brackets give estimated number of individuals alive at that time. Data from WISELY *et al.* (2002). Code here.



Figure 3.5: The black-footed ferret (*M. nigripes*).
 Wild animals of North America. The National geographical society, 1918. Image from the Biodiversity Heritage Library. Contributed by American Museum of Natural History Library. Not in copyright.

1224 To see how a decline in population size can affect levels of heterozygosity, let's consider the case of black-footed ferrets (*Mustela*
 1226 *nigripes*). The black-footed ferret population has declined dramatically through the twentieth century due to destruction of their habitat. In
 1228 1979, when the last known black-footed ferret died in captivity, they were thought to be extinct. In 1981, a very small wild population was
 1230 rediscovered (40 individuals), but in 1985 this population suffered a number of disease outbreaks. All of the 18 remaining wild individuals
 1232 were brought into captivity, 7 of which reproduced. Thanks to intense captive breeding efforts and conservation work, a wild population of
 1234 over 300 individuals has been established since. However, because all of these individuals are descended from those 7 individuals who
 1236 survived the bottleneck, diversity levels remain low. WISELY *et al.* measured heterozygosity at a number of microsatellites in individuals from museum collections, showing the sharp drop in diversity as
 1238 population sizes crashed (see Figure 3.6).

1240 **Question 2.** In mathematical population genetics, a commonly used approximation is $(1 - x) \approx e^{-x}$ for $x \ll 1$ (formally, this

1242 follows from the Taylor series expansion of $\exp(-x)$, ignoring second
 1244 order and higher terms of x). This approximation is especially useful
 1246 for approximating a geometric decay process by an exponential decay
 1248 process, e.g. $(1 - x)^t \approx e^{-xt}$. Using your calculator, or R, check how
 good of an approximation this is compared to the exact expression for
 two values of x , $x = 0.1$, and 0.01 , across two different values of t ,
 $t = 5$ and $t = 50$. Briefly comment on your results.

3.1.1 Levels of diversity maintained by a balance between mutation 1250 and drift

Next we're going to consider the amount of neutral polymorphism that
 1252 can be maintained in a population as a balance between genetic drift
 removing variation and mutation introducing new neutral variation,
 1254 see Figure 3.7 for an example. Note in our example, how no single
 allele is maintained at a stable equilibrium, rather an equilibrium level
 1256 of polymorphism is maintained by a constantly shifting set of alleles.

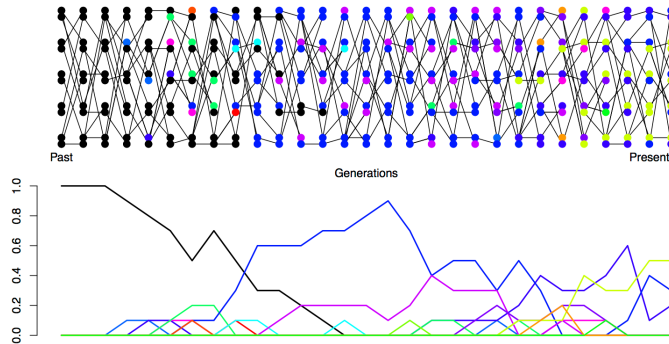


Figure 3.7: Mutation-drift balance. A diploid population of 5 individuals. In the first generation everyone has the same allele (black). Each generation the transmitted allele can mutate and we generate a new colour. In the bottom plot, I trace the frequency of alleles in our population over time. The mutation rate we use is very high, simply to maintain diversity in this small population. Code here.

The neutral mutation rate. We'll first want to consider the rate at
 1258 which neutral mutations arise in the population. Thinking back to our
 discussion of the neutral theory of molecular evolution, let's suppose
 1260 that there are only two classes of mutation that can arise in our ge-
 nomic region of interest: neutral mutations and highly deleterious mu-
 1262 tations. The total mutation rate at our locus is μ per generation, i.e.
 per transmission from parent to child. A fraction C of our mutations
 1264 are new alleles that are highly deleterious and so quickly removed
 from the population. We'll call this C parameter the constraint, and
 1266 it will differ according to the genomic region we consider. The remain-
 ing fraction $(1 - C)$ are our neutral mutations, such that our neutral
 1268 mutation rate is $(1 - C)\mu$. This is the per generation rate.

Question 3. It's worth taking a minute to get familiar with both
 1270 how rare, and how common, mutation is. The per base pair mutation

rate in humans is around 1.5×10^{-8} per generation. That means, on
 1272 average, we have to monitor a site for ~ 66.6 million transmissions
 from parent to child to see a mutation. Yet populations and genomes
 1274 are big places, so mutations are common at these levels.

A) Your autosomal genome is ~ 3 billion base pairs long (3×10^9).

1276 You have two copies, the one you received from your mum and one
 from your dad. What is the average (i.e. the expected) number of
 1278 mutations that occurred in the transmission from your mum and your
 dad to you?

1280 **B)** The current human population size is ~ 7 billion individuals.

How many times, at the level of the entire human population, is a
 1282 single base-pair mutated in the transmission from one generation to
 the next?

1284 *Levels of heterozygosity maintained as a balance between mutation
 and selection.* Looking backwards in time from one generation to
 1286 the previous generation, we are going to say that two alleles which
 have the same parental allele (i.e. find their common ancestor) in
 1288 the preceding generation have *coalesced*, and refer to this event as a
coalescent event.

1290 The probability that our pair of randomly sampled alleles have
 coalesced in the preceding generation is $1/(2N)$, and the probability
 1292 that our pair of alleles fail to coalesce is $1 - 1/(2N)$.

The probability that a mutation changes the identity of the trans-
 1294 mitted allele is μ per generation. So the probability of no mutation
 occurring is $(1 - \mu)$. We'll assume that when a mutation occurs it cre-
 1296 ates some new allelic type which is not present in the population. This
 assumption (commonly called the infinitely-many-alleles model) makes
 1298 the math slightly cleaner, and also is not too bad an assumption bi-
 logically. See Figure 3.7 for a depiction of mutation-drift balance in
 1300 this model over the generations.

This model lets us calculate when our two alleles last shared a
 1302 common ancestor and whether these alleles are identical as a result of
 failing to mutate since this shared ancestor. For example, we can work
 1304 out the probability that our two randomly sampled alleles coalesce 2
 generations in the past (i.e. they fail to coalesce in generation 1 and
 1306 then coalesce in generation 2), and that they are identical as

$$\left(1 - \frac{1}{2N}\right) \frac{1}{2N} (1 - \mu)^4 \quad (3.4)$$

Note the power of 4 is because our two alleles have to have failed to
 1308 mutate through 2 meioses each.

More generally, the probability that our alleles coalesce in gener-
 1310 ation $t + 1$ (counting backwards in time) and are identical due to no

mutation to either allele in the subsequent generations is

$$P(\text{coal. in } t+1 \& \text{ no mutations}) = \frac{1}{2N} \left(1 - \frac{1}{2N}\right)^t (1 - \mu)^{2(t+1)} \quad (3.5)$$

- ₁₃₁₂ To make this slightly easier on ourselves let's further assume that $t \approx t + 1$ and so rewrite this as:

$$P(\text{coal. in } t+1 \& \text{ no mutations}) \approx \frac{1}{2N} \left(1 - \frac{1}{2N}\right)^t (1 - \mu)^{2t} \quad (3.6)$$

- ₁₃₁₄ This gives us the approximate probability that two alleles will coalesce in the $(t + 1)^{\text{th}}$ generation. In general, we may not know ₁₃₁₆ when two alleles may coalesce: they could coalesce in generation $t = 1, t = 2, \dots$, and so on. Thus, to calculate the probability that ₁₃₁₈ two alleles coalesce in *any* generation before mutating, we can write:

$$\begin{aligned} P(\text{coal. in any generation \& no mutations}) &\approx P(\text{coal. in } t = 1 \& \text{ no mutations}) + \\ &\quad P(\text{coal. in } t = 2 \& \text{ no mutations}) + \dots \\ &= \sum_{t=1}^{\infty} P(\text{coal. in } t \text{ generations \& no mutation}) \end{aligned}$$

- ₁₃₂₀ which follows from basic probability and the fact that coalescing in a particular generation is mutually exclusive with coalescing in a different generation.

While we could calculate a value for this sum given N and μ , it's difficult to get a sense of what's going on with such a complicated expression. Here, we turn to a common approximation in population genetics (and all applied mathematics), where we assume that $1/(2N) \ll 1$ and $\mu \ll 1$. This allows us to approximate the geometric decay as an exponential decay. Then, the probability two alleles coalesce in generation $t + 1$ and don't mutate can be written as:

$$P(\text{coal. in } t+1 \& \text{ no mutations}) \approx \frac{1}{2N} \left(1 - \frac{1}{2N}\right)^t (1 - \mu)^{2t} \quad (3.7)$$

$$\approx \frac{1}{2N} e^{-t/(2N)} e^{-2\mu t} \quad (3.8)$$

$$= \frac{1}{2N} e^{-t(2\mu+1/(2N))} \quad (3.9)$$

- ₁₃₂₂ Then we can approximate the summation by an integral, giving us:

$$\frac{1}{2N} \int_0^{\infty} e^{-t(2\mu+1/(2N))} dt = \frac{1/(2N)}{1/(2N) + 2\mu} = \frac{1}{1 + 4N\mu} \quad (3.10)$$

- ₁₃₂₄ The equation above gives us the probability that our two alleles coalesce at some point in time, and do not mutate before reaching

their common ancestor. Equivalently, this can be thought of as the probability our two alleles coalesce *before* mutating, i.e. that they are homozygous.

Then, the complementary probability that our pair of alleles are non-identical (or heterozygous) is simply one minus this. The following equation gives the equilibrium heterozygosity in a population at equilibrium between mutation and drift:

$$H = \frac{4N\mu}{1 + 4N\mu} \quad (3.11)$$

The compound parameter $4N\mu$, the population-scaled mutation rate, will come up a number of times so we'll give it its own name:

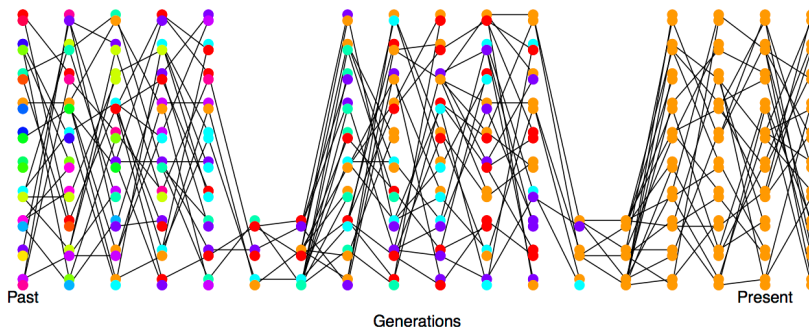
$$\theta = 4N\mu \quad (3.12)$$

So all else being equal, species with larger population sizes should have proportionally higher levels of neutral polymorphism.

Question 4. The sequence-level heterozygosity in *Capsella grandiflora* (grand shepherd's purse) is $\sim 2\%$ per base. Assuming a mutation rate of 10^{-9} bp^{-1} per generation, what is your estimate of the population size of *C. grandiflora*?

3.1.2 The effective population size

In practice, populations rarely conform to our assumptions of being constant in size with low variance in reproductive success. Real populations experience dramatic fluctuations in size, and there is often high variance in reproductive success. Thus rates of drift in natural populations are often a lot higher than the census population size would imply. See Figure 3.8 for a depiction of a repeatedly bottlenecked population losing diversity at a fast rate.



This result was derived by KIMURA and CROW (1964) and MALÉCOT (1948) (see MALÉCOT, 1969, for an English translation, the lack of earlier translation meant this result was missed). Technically we're assuming that every new mutation creates a new allele, the so-called "infinitely many alleles" model, otherwise our pair of sequences could be identical due to repeat or back mutation. See this GENETICS blog post and EWENS (2016) for a nice discussion of the history.

the effective population size (N_e) is the population size that would result in the same rate of drift in an idealized population of constant size (following our modeling assumptions) as that observed in our true population .

Figure 3.8: Loss of heterozygosity over time in a bottlenecking population. A diploid population of 10 individuals, that bottlenecks down to three individuals repeatedly. In the first generation, I colour every allele a different colour so we can track their descendants. There are no new mutations. Code here.

To cope with this discrepancy, population geneticists often invoke the concept of an *effective population size* (N_e). In many situations

1350 (but not all), departures from model assumptions can be captured by substituting N_e for N .

1352 If population sizes vary rapidly in size, we can (if certain conditions are met) replace our population size by the harmonic mean population size. Consider a diploid population of variable size, whose size is N_t t generations into the past. The probability our pairs of alleles have not coalesced by generation t is given by

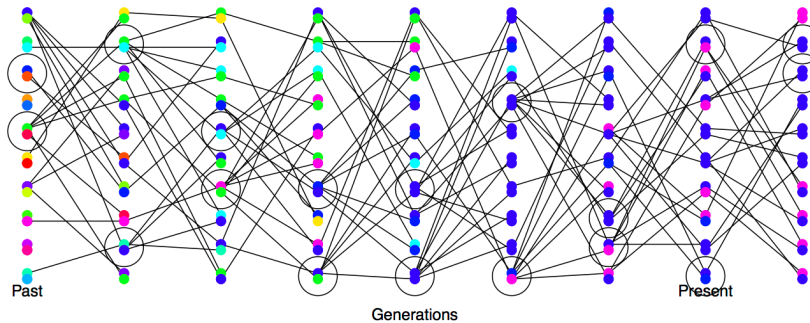
$$\prod_{i=1}^t \left(1 - \frac{1}{2N_i}\right) \quad (3.13)$$

1358 Note that this simply collapses to our original expression $(1 - \frac{1}{2N})^t$ if N_i is constant. Under this model, the rate of loss of heterozygosity in this population is equivalent to a population of effective size

$$N_e = \frac{1}{\frac{1}{t} \sum_{i=1}^t \frac{1}{N_i}}. \quad (3.14)$$

1360 This is the harmonic mean of the varying population size.²

1362 Thus our effective population size, the size of an idealized constant population which matches the rate of genetic drift, is the harmonic mean true population size over time. The harmonic mean is very 1364 strongly affected by small values, such that if our population size is one million 99% of the time but drops to 1000 every hundred or so generations, N_e will be much closer to 1000 than a million.



² To see this, note that if $1/(N_i)$ is small, then we can approximate (3.13) using the exponential approximation:

$$\prod_{i=1}^t \exp\left(-\frac{1}{2N_i}\right) = \exp\left(-\sum_{i=1}^t \frac{1}{2N_i}\right). \quad (3.15)$$

When we put the product inside the exponent, it becomes a sum. We can also write the probability of not coalescing by generation t in a population of constant size (N_e) as an exponential, so that it takes the same form as the expression above on the right. Comparing the exponent in the two cases, we see

$$\frac{t}{2N_e} = \sum_{i=1}^t 1/(2N_i) \quad (3.16)$$

So that if we want a constant effective population size (N_e) that has the same rate of loss of heterozygosity as our variable population, we need to rearrange and solve this equation to give (3.14).

Figure 3.9: High variance on reproductive success increases the rate of genetic drift. A diploid population of 10 individuals, where the circled individuals have much higher reproductive success. In the first generation I colour every allele a different colour so we can track their descendants, there are no new mutations. Code here.

1368 Variance in reproductive success will also affect our effective population size. Even if our population has a large constant size N individuals, if only small proportion of them get to reproduce, then the 1370 rate of drift will reflect this much smaller number of reproducing individuals. See Figure 3.9 for a depiction of the higher rate of drift in a 1372 population where there is high variance in reproductive success.

To see one example of this, consider the case where N_F of females 1374 get to reproduce and N_M males get reproduce. While every individual has a mother and a father, not every individual gets to be a parent. In

practice, in many animal species far more females get to reproduce than males, i.e. $N_M < N_F$, as a few males get many mating opportunities and many males get no/few mating opportunities (see JANICKE *et al.*, 2016, for a broad analysis, and note that there are certainly many exceptions to this general pattern). When our two alleles pick an ancestor, 25% of the time our alleles were both in a female ancestor, in which case they are IBD with probability $1/(2N_F)$, and 25% of the time they are both in a male ancestor, in which case they coalesce with probability $1/(2N_M)$. The remaining 50% of the time, our alleles trace back to two individuals of different sexes in the prior generation and so cannot coalesce. Therefore, our probability of coalescence in the preceding generation is

$$\frac{1}{4} \left(\frac{1}{2N_M} \right) + \frac{1}{4} \left(\frac{1}{2N_F} \right) \quad (3.17)$$

i.e. the rate of coalescence is the harmonic mean of the two sexes' population sizes, equating this to $\frac{1}{2N_e}$ we find

$$N_e = \frac{4N_F N_M}{N_F + N_M} \quad (3.18)$$

Thus if reproductive success is very skewed in one sex (e.g. $N_M \ll N/2$), our effective population size will be much reduced as a result. For more on how different evolutionary forces affect the rate of genetic drift, and their impact on the effective population size, see CHARLESWORTH (2009).

Question 5. You are studying a population of 500 male and 500 female Hamadryas baboons. Assume that all of the females but only 1/10 of the males get to mate: **A)** What is the effective population size for the autosome?

B) Do you expect the *ratio* of X-chromosome to autosomal diversity to be higher or lower in this species compared to a species where the sexes have more similar variance in reproductive success? Explain the intuition behind your answer.

3.2 The Coalescent and patterns of neutral diversity

“Life can only be understood backwards; but it must be lived forwards” – Kierkegaard

Pairwise Coalescent time distribution and the number of pairwise differences. Thinking back to our calculations we made about the loss of neutral heterozygosity and equilibrium levels of diversity (in Sections 3.1 and 3.1.1), you’ll note that we could first specify which generation a pair of sequences coalesce in, and then calculate some



Figure 3.10: Male Hamadryas baboons. Up to ten females live in a harem with a single male. Brehm's Tierleben (Brehm's animal life). Brehm, A.E. 1893. Image from the Biodiversity Heritage Library. Contributed by University of Illinois Urbana-Champaign. Not in copyright.

properties of heterozygosity based on that. That's because neutral mutations do not affect the probability that an individual transmits an allele, and so don't affect the way in which we can trace ancestral lineages back through the generations.

As such, it will often be helpful to consider the time to the common ancestor of a pair of sequences, and then think of the impact of that time to coalescence on patterns of diversity. See Figure 3.11 for an example of this.

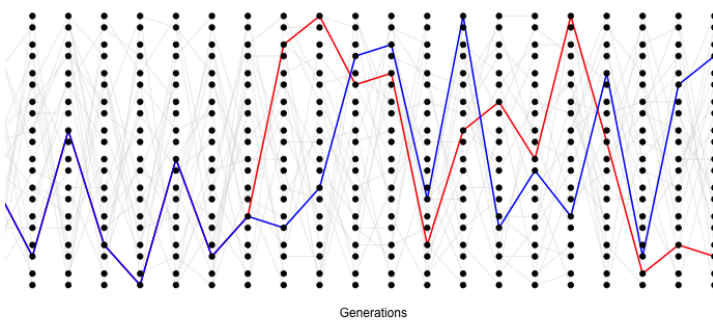


Figure 3.11: A simple demonstration of the coalescent process. The simulation consists of a diploid population of 10 individuals (20 alleles). In each generation, each individual is equally likely to be the parent of an offspring (and the allele transmitted is indicated by a light grey line). We track a pair of alleles, chosen in the present day, back 14 generations until they find a common ancestor. [Code here.](#)

The probability that a pair of alleles have failed to coalesce in t generations and then coalesce in the $t + 1$ generation back is

$$P(T_2 = t + 1) = \frac{1}{2N} \left(1 - \frac{1}{2N}\right)^t \quad (3.19)$$

Thus the coalescent time of our pair of alleles is a Geometrically distributed random variable, where the probability of success is $1/(2N)$; we denote this by $T_2 \sim \text{Geo}(1/(2N))$. The expected (i.e. the mean over many replicates) coalescent time of a pair of alleles is then

$$\mathbb{E}(T_2) = 2N \quad (3.20)$$

generations.

Conditional on a pair of alleles coalescing t generations ago, there are $2t$ generations in which a mutation could occur. If the per generation mutation rate is μ , then the expected number of mutations between a pair of alleles coalescing t generations ago is $2t\mu$ (the alleles have gone through a total of $2t$ meioses since they last shared a common ancestor). So we can write the expected number of mutations

Using our exponential approximation, we can see that 3.19 is

$$\approx \frac{1}{2N} e^{-t/(2N)} \quad (3.21)$$

and so think of a continuous random variable, i.e. we could say that the coalescent time of a pair of sequences (T_2) is approximately exponentially distributed with a rate $1/(2N)$, i.e. $T_2 \sim \text{Exp}(1/(2N))$. Formally we can do this by taking the limit of the discrete process more carefully.

(S_2) separating two alleles drawn at random from the population as

$$\begin{aligned}\mathbb{E}(S_2) &= \sum_{t=0}^{\infty} \mathbb{E}(S_2|T_2 = t)P(T_2 = t) \\ &= \sum_{t=0}^{\infty} 2\mu t P(T_2 = t) \\ &= 2\mu \mathbb{E}(T_2) \\ &= 4\mu N\end{aligned}\tag{3.22}$$

We'll assume that mutation is rare enough that it never happens at the same basepair twice, i.e. no multiple hits, such that we get to see all of the mutation events that separate our pair of sequences.³ Thus the number of mutations between a pair of sites is the observed number of differences between a pair of sequences. In the previous chapter we denote the observed number of pairwise differences at putatively neutral sites separating a pair of sequences as π (we usually average this over a number of pairs of sequences for a region). Therefore, under our simple, neutral, constant population-size model we expect

$$\mathbb{E}(\pi) = 4N\mu = \theta\tag{3.23}$$

So we can get an empirical estimate of θ from π , let's call this $\hat{\theta}_\pi$, by setting $\hat{\theta}_\pi = \pi$, i.e. our observed level of pairwise genetic diversity. If we have an independent estimate of μ , then from setting $\pi = \hat{\theta}_\pi = 4N\mu$ we can furthermore obtain an estimate of the population size N that is consistent with our levels of neutral polymorphism. If we estimate the population size this way, we should call it the effective coalescent population size (N_e). It's best to think about N_e estimated from neutral diversity as a long-term effective population size for the species, but there are many caveats that come along with that assumption. For example, past bottlenecks and population expansions are all subsumed into a single number and so this estimated N_e may not be very representative of the population size at any time. That said, it's not a bad place to start when thinking about the rate of genetic drift for neutral diversity in our population over long time-periods.⁴

Lets take a moment to distinguish our expected heterozygosity (eqn. 3.11) from our expected number of pairwise differences (π). Our expected heterozygosity is the probability that two alleles at a locus, sampled from a population at random, are different from each other. If one or more mutations have occurred since a pair of alleles last shared a common ancestor, then our sequences will be different from each other. On the other hand, our π measure keeps track of the average total number of differences between our loci. As such, π is often a more useful measure, as it records the number of differences between

³ This is called the infinitely-many-sites assumption, which should be fine if $N\mu_{BP} \ll 1$, where μ_{BP} is the mutation rate per base pair).

⁴ Up to this point we've been describing only neutral processes, however, selection can also alter levels of polymorphism. For example, if some synonymous sites directly experience selection, then even if we use π calculated for synonymous changes we may underestimate the coalescent effective population size. As we'll see later in the notes, selection at linked sites can also impact neutral diversity. As such, if we can, we may want to use genomic sites subject to the weakest selective constraints, and also far from gene-dense or otherwise very constrained regions of the genome, to estimate N_e from π . But even then caution is warranted.

the sequences, not just whether they are different from each other
 1460 (however, for certain types of loci, e.g. microsatellites, heterozygosity
 is often used as we cannot usually count up the minimum number of
 1462 mutations in a sensible way). In the case where our locus is a single
 basepair, the two measures will usually be close to one another, as
 1464 $H \approx \theta$ for small values of θ . For example, comparing two sequences
 at random in humans, $\pi \approx 1/1000$ per basepair, and the probability
 1466 that a specific base pair differs between two sequences is $\approx 1/1000$.
 However, these two quantities start to differ from each other when
 1468 we consider regions with higher mutation rates. For example, if we
 consider a 10kb region, our mutation rate will 10,000 times larger than
 1470 a single base pair. For this length of sequence the probability that two
 randomly chosen haplotypes differ is quite different from the number
 1472 of mutational differences between them. (Try a mutation rate of 10^{-8}
 per base and a population size of 10,000 in our calculations of $\mathbb{E}[\pi]$
 1474 and H to see this.)

Question 6. ROBINSON *et al.* (2016) found that the endangered
 1476 Californian Channel Island fox on San Nicolas had very low levels
 of diversity ($\pi = 0.000014\text{bp}^{-1}$) compared to its close relative the
 1478 California mainland gray fox (0.0012bp^{-1}).

- A) Assuming a mutation rate of 2×10^{-8} per bp, what effective
 1480 population sizes do you estimate for these two populations?
 B) Why is the effective population size of the Channel Island fox
 1482 so low? [Hint: quickly google Channel island foxes to read up on their
 history, also to see how ridiculously cute they are.]

Question 7. In your own words describe why the coalescent time
 1484 of a pair of lineages scales linearly with the (effective) population size.
 1486



Figure 3.12: Gray Fox, *Urocyon cinereoargenteus*.

Diseases and enemies of poultry. Pearson and Warren. (1897) Image from the Biodiversity Heritage Library. Contributed by University of California Libraries. Not in copyright.

More details on the pairwise coalescent and the randomness of mutation. We've derived the expected number of differences between a
 1488 pair of sequences and talked about how variable the coalescent time
 is for a pair of sequences. The mutation process is also very variable;
 1490 even if two sequences coalesce in the very distant past by chance, they
 may still be identical in the present if there was no mutation during
 1492 that time.

Conditional on the coalescent time t , the probability that our pair
 1494 of alleles are separated by S_2 mutations since they last shared a com-
 mon ancestor is
 1496

$$P(S_2|T_2 = t) = \binom{2t}{j} \mu^j (1 - \mu)^{2t-j} \quad (3.24)$$

i.e. mutations happen in j generations and do not happen in $2t - j$
 1498 generations (with $\binom{2t}{j}$ ways this combination of events can possibly

happen). Assuming that $\mu \ll 1$ and that $2t - j \approx 2t$, then we can
 1500 approximate the probability that we have S_2 mutations as a Poisson
 distribution:

$$P(S_2|T_2 = t) = \frac{(2\mu t)^j e^{-2\mu t}}{j!} \quad (3.25)$$

1502 i.e. a Poisson with mean $2\mu t$. We'll not make much use of this result,
 but it is very useful in thinking about how to simulate the process of
 1504 mutation.

3.3 The coalescent process of a sample of alleles.

1506 Usually we are not just interested in pairs of alleles, or the average
 pairwise diversity. Generally we are interested in the properties of di-
 1508 versity in samples of a number of alleles drawn from the population.
 Instead of just following a pair of lineages back until they coalesce, we
 1510 can follow the history of a sample of alleles back through the popula-
 tion.

1512 Consider first sampling three alleles at random from the population.
 The probability that all three alleles choose exactly the same ancestral
 1514 allele one generation back is $1/(2N)^2$. If N is reasonably large, then this
 is a very small probability. As such, it is very unlikely that our three
 1516 alleles coalesce all at once, and in a moment we'll see that it is safe to
 ignore such unlikely events.

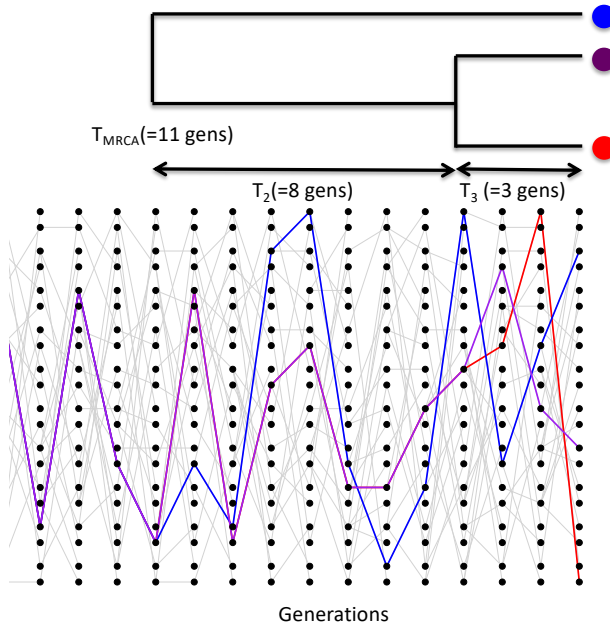


Figure 3.13: A simple simulation of the coalescent process for three lineages. We track the ancestry of three modern-day alleles, the first pair (blue and purple) coalesce four generations back, after which there are only two independent lineages we are tracking. This pair then coalesces twelve generations in the past. Note that different random realizations of this process will differ from each other a lot. The T_{MRCA} is $T_3 + T_2$. The total time in the tree is $T_{tot} = 3T_3 + 2T_2 = 25$ generations. Code here.

1518 The probability that a specific pair of alleles find a common ances-
 tor in the preceding generation is still $1/(2N)$. There are three possible

¹⁵²⁰ pairs of alleles, so the probability that no pair finds a common ancestor in the preceding generation is

$$\left(1 - \frac{1}{2N}\right)^3 \approx \left(1 - \frac{3}{2N}\right) \quad (3.26)$$

¹⁵²² In making this approximation we are multiplying out the right hand-side and ignoring terms of $1/N^2$ and higher. See Figure 3.13 for a ¹⁵²⁴ random realization of this process.

More generally, when we sample i alleles there are $\binom{i}{2}$ pairs,⁵ i.e. ¹⁵²⁶ $i(i - 1)/2$ pairs. Thus, the probability that no pair of alleles in a sample of size i coalesces in the preceding generation is

$$\left(1 - \frac{1}{(2N)}\right)^{\binom{i}{2}} \approx \left(1 - \frac{\binom{i}{2}}{2N}\right) \quad (3.27)$$

¹⁵²⁸ while the probability any pair coalesces is $\approx 2N/\binom{i}{2}$.

We can ignore the possibility that more than pairs of alleles (e.g. ¹⁵³⁰ tripletons) simultaneously coalesce at once as terms of $1/N^2$ and higher can be ignored as they are vanishingly rare. Obviously in reasonable ¹⁵³² sample sizes there are many more triples ($\binom{i}{3}$) and higher order combinations than there are pairs ($\binom{i}{2}$), but if $i \ll N$ then we are safe to ¹⁵³⁴ ignore these terms.

When there are i alleles, the probability that we wait until the $t + 1$ ¹⁵³⁶ generation before any pair of alleles coalesces is

$$P(T_i = t + 1) = \frac{\binom{i}{2}}{2N} \left(1 - \frac{\binom{i}{2}}{2N}\right)^t \quad (3.28)$$

Thus the waiting time to the first coalescent event while there are i ¹⁵³⁸ lineages is a geometrically distributed random variable with probability of success $\binom{i}{2}/2N$, which we denote by

$$T_i \sim \text{Geo}\left(\frac{\binom{i}{2}}{2N}\right). \quad (3.29)$$

¹⁵⁴⁰ The mean waiting time till any of pair within our sample coalesces is

$$\mathbb{E}(T_i) = \frac{2N}{\binom{i}{2}} \quad (3.30)$$

After a pair of alleles first finds a common ancestral allele some number of generations back in the past, we only have to keep track of that common ancestral allele for the pair when looking further into the ¹⁵⁴² past. Thus when a pair of alleles in our sample of i alleles coalesces, we then switch to having to follow $i - 1$ alleles back in time. Then ¹⁵⁴⁴ when a pair of these $i - 1$ alleles coalesce, we then only have to follow $i - 2$ alleles back. This process continues until we coalesce back ¹⁵⁴⁶ to a sample of two, and from there to a single most recent common ancestor (MRCA).

⁵ said as “i choose 2”

To see the continuous time version of this, note that (3.28) is

$$\approx \frac{\binom{i}{2}}{2N} \exp\left(-\frac{\binom{i}{2}}{2N} t\right) \quad (3.31)$$

The waiting time T_i to the first coalescent event in a sample of i alleles is thus exponentially distributed with rate $\binom{i}{2}/2N$, i.e. $T_i \sim \text{Exp}\left(\frac{\binom{i}{2}}{2N}\right)$.

1550 *Simulating a coalescent genealogy* To simulate a coalescent genealogy at a locus for a sample of n alleles we therefore simply follow the
1552 following algorithm:

1. Set $i = n$.
- 1554 2. Simulate a random variable to be the time T_i to the next coalescent event from $T_i \sim \text{Exp}((\frac{i}{2})/2N)$
- 1556 3. Choose a pair of alleles to coalesce at random from all possible pairs.
- 1558 4. Set $i = i - 1$
- 1560 5. Continue looping steps 2-4 until $i = 1$, i.e. the most recent common ancestor of the sample is found.

1562 By following this algorithm we are generating realizations of the genealogy of our sample.

3.3.1 Expected properties of coalescent genealogies and mutations.

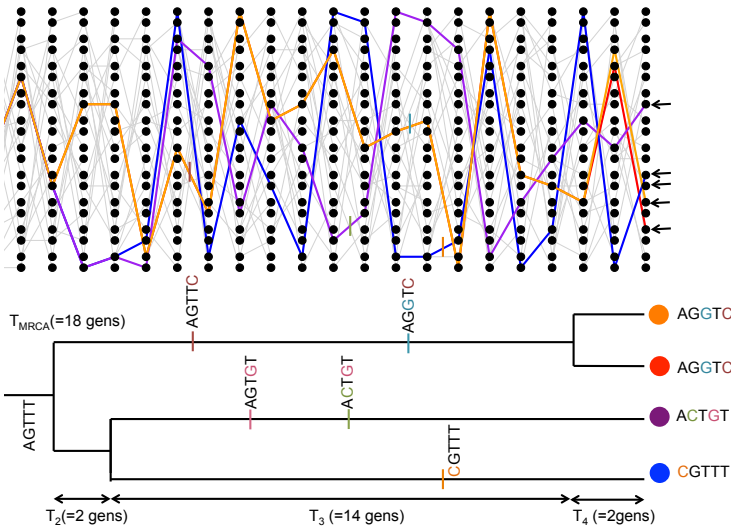


Figure 3.14: A simple coalescent tree from a single coalescent simulation, tracing the genealogy of 4 alleles with mutational changes marked with dashes showing transitions away from the MRCA sequence (AGTTT). The T_{MRCA} is $T_4 + T_3 + T_2$. The total time in the tree is $T_{tot} = 4T_4 + 3T_3 + 2T_2 = 54$ generations. [Code here.](#)

1564 *The expected time to the most recent common ancestor.* We will first consider the time to the most recent common ancestor of the entire
1566 sample (T_{MRCA}). This is

$$T_{MRCA} = \sum_{i=n}^2 T_i \quad (3.32)$$

generations back, where we are summing from $i = n$ alleles counting backwards to $i = 2$ alleles (see Figure 3.14 for example). As our coalescent times for different i are independent, the expected time to the most recent common ancestor is

$$\mathbb{E}(T_{MRCA}) = \sum_{i=n}^2 \mathbb{E}(T_i) = \sum_{i=n}^2 2N / \binom{i}{2} \quad (3.33)$$

Using the fact that $\frac{1}{i(i-1)} = \frac{1}{i-1} - \frac{1}{i}$ and a bit of rearrangement, we can rewrite this as

$$\mathbb{E}(T_{MRCA}) = 4N \left(1 - \frac{1}{n} \right) \quad (3.34)$$

So the average T_{MRCA} scales linearly with population size N . Interestingly, as we move to larger and larger samples (i.e. $n \gg 1$), the average time to the most recent common ancestor converges on $4N$. What's happening here is that in large samples our lineages typically coalesce rapidly at the start and very soon coalesce down to a much smaller number of lineages.

Question 8. Assume an autosomal effective population of 10,000 individuals (roughly the long-term human estimate) and a generation time of 30 years. What is the expected time to the most recent common ancestor of a sample of 20 people? What is this time for a sample of 500 people?

The expected total time in a genealogy and the number of segregating sites. Mutations fall on specific lineages of the coalescent genealogy and are transmitted to all descendants of their lineage. Furthermore, under the infinitely-many-sites assumption, each mutation creates a new segregating site. The mutation process is a *Poisson process*, and the longer a particular lineage, i.e. the more generations of meioses it represents, the more mutations that can accumulate on it. The total number of segregating sites in a sample is thus a function of the *total* amount of time in the genealogy of the sample, or the sum of all the branch lengths on the genealogical tree, T_{tot} . Our total amount of time in the genealogy is

$$T_{tot} = \sum_{i=n}^2 iT_i \quad (3.35)$$

as when there are i lineages, each contributes a time T_i to the total time (see Figure 3.14 for an example). Taking the expectation of the total time in the genealogy,

$$\mathbb{E}(T_{tot}) = \sum_{i=n}^2 i \frac{2N}{\binom{i}{2}} = \sum_{i=n}^2 \frac{4N}{i-1} = \sum_{i=n-1}^1 \frac{4N}{i} \quad (3.36)$$

1598 we see that our expected total amount of time in the genealogy scales
 linearly with our population size N . Our expected total amount of
 1600 time is also increasing with sample size n , but is doing so very slowly.
 This again follows from the fact that in large samples, the initial
 1602 coalescence usually happens very rapidly, so that extra samples add
 little to the total amount of time in the genealogical tree.

1604 We saw above that the number of mutational differences between
 a pair of alleles that coalescence T_2 generations ago was Poisson with
 1606 a mean of $2\mu T_2$, where $2T_2$ is the total branch length in this simple
 2-sample genealogical tree. A mutation that occurs on any branch of
 1608 our genealogy will cause a segregating polymorphism in the sample
 (meeting our infinitely-many-sites assumption). Thus, if the total time
 1610 in the genealogy is T_{tot} , there are T_{tot} generations for mutations. So
 the total number of mutations segregating in our sample (S) is Poisson
 1612 with mean μT_{tot} . Thus the expected number of segregating sites in a
 sample of size n is

$$\mathbb{E}(S) = \mu \mathbb{E}(T_{tot}) = \sum_{i=n-1}^1 \frac{4N\mu}{i} = \theta \sum_{i=n-1}^1 \frac{1}{i} \quad (3.37)$$

1614 Note that this is growing with the sample size n , albeit very slowly
 (roughly at the rate of the log of the sample size). We can use this
 1616 formula to derive another estimate of the population scaled mutation
 rate θ , by setting our observed number of segregating sites in a sample
 1618 (S) equal to this expectation. We'll call this estimator $\hat{\theta}_W$:

$$\hat{\theta}_W = \frac{S}{\sum_{i=n-1}^1 1/i} \quad (3.38)$$

This estimator of θ was devised by WATTERSON (1975), hence the
 1620 W .

The neutral site-frequency spectrum. We can use our coalescent process to find the expected number of derived alleles present i times out of a sample size n , e.g. how many singletons ($i = 1$) do we expect 1622 to find in our sample? For example, in Figure 3.14 in our sample of four sequences, there are 3 singletons and 2 doubletons. The number 1624 of sites with these different allele frequencies depends on the lengths of specific genealogical branches. A mutation that falls on a branch 1626 with i descendants will create a derived allele with frequency i . For example, in our example tree in Figure 3.14, the total number of generations where a mutation could arise and be a doubleton is $T_3 + 2T_2$, 1628 the total length of the branch ancestral to just the orange and red 1630 allele ($T_3 + T_2$) plus the branch ancestral to just the blue and purple 1632 allele (T_2).

To get a better sense of how T_{tot} grows with the sample size, we can approximate the sum 3.36 by an integral, which will work for large n . The result is $\int_1^{n-1} \frac{4N}{i} di = 4N \log(n - 1)$.

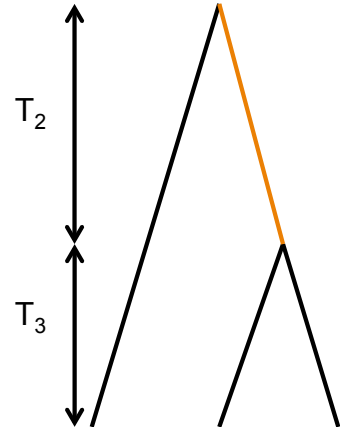


Figure 3.15: A tree for three samples; note that this is the only possible tree shape (treating the tips as unlabeled, i.e. I don't care which pair of sequences carry a doubleton, just that any two sequences carry a derived allele).

To see how we could go about working this out, lets start by considering the simple coalescent tree, shown in Figure 3.15, for sample of 3 alleles drawn from a population. Mutations that fall on the branches coloured in black will be derived singletons, while mutations that fall along the orange branch will be doubletons in the sample. The total number of generations where a singleton mutation could arise is $3T_3 + T_2$. Note that we only count the time where there are two lineages (T_2) once. So our expected number of singletons, using eqn (3.30), is

$$\mathbb{E}(S_i) = \mu (3\mathbb{E}(T_3) + \mathbb{E}(T_2)) = \mu \left(3 \frac{2N}{3} + 2N \right) = \theta \quad (3.39)$$

By similar logic, the time where doubletons could arise is T_2 and our expected number of doubletons is $\mathbb{E}(S_i) = \theta/2$. Thus, there are on average half as many doubletons as singletons.

Extending this logic to larger samples might be doable, but is tedious (I mean really tedious: for 10 alleles there are thousands of possible tree shapes and the task quickly gets impossible even computationally). A nice, relatively simple proof of the neutral site frequency spectrum is given by (HUDSON, 2015), but we won't give this here.

The general form is:

$$\mathbb{E}(S_i) = \frac{\theta}{i} \quad (3.40)$$

i.e. there are twice as many singletons as doubletons, three times as many singletons as tripletons, and so on. The other thing that will be helpful for us to know is that neutral alleles at intermediate frequency tend to be old, and those that are rare in the sample are young. We expect to see a lot more rare alleles in our sample than common alleles.

Question 9. There are two possible tree shapes that could relate four samples. Draw both of them and separately colour (or otherwise mark) the branches by where singletons, doubletons, and tripleton derived alleles could arise.

We can also ask the probability of observing a derived allele segregating at frequency i/n given that the site is polymorphic in our sample of size n (i.e. given that $0 < i < n$). We can obtain this probability by dividing the expected number of sites segregating for an allele at frequency i by the expected number segregating at all of the possible allele frequencies for polymorphisms in our sample

$$P(i|0 < i < n) = \frac{\mathbb{E}(S_i)}{\sum_{j=1}^{n-1} \mathbb{E}(S_j)} = \frac{1/i}{\sum_{j=1}^{n-1} 1/j}. \quad (3.41)$$

We can interpret this probability as the fraction of polymorphic sites we expect to find at a frequency i/n .

1670 *Tests based on the site frequency spectrum* Population geneticists
1672 have proposed a variety of ways to test whether an observed site fre-
1674 quency spectrum conforms to its neutral, constant-size expectations.
1676 These tests are useful for detecting population size changes using data
across many loci, or for detecting the signal of selection at individual
loci. One of the first tests was proposed by (TAJIMA, 1989), and is
called Tajima's D . Tajima's D is

$$D = \frac{\hat{\theta}_\pi - \hat{\theta}_W}{C} \quad (3.42)$$

1678 where the numerator is the difference between the estimate of θ based
on pairwise differences and that based on segregating sites. As these
1680 two estimators both have expectation θ under the neutral, constant-
size model, the expectation of D is zero. The denominator C is a
1682 positive constant; it's the square-root of an estimator of the variance of
this difference under the constant population size, neutral model. This
constant was chosen for D to have mean zero and variance 1 under the
1684 null model, so we can test for departures from this simple null model.

1686 An excess of rare alleles compared to the constant-size, neutral
model will result in a negative Tajima's D , because each additional
rare allele increases the number of segregating sites by 1, but only has
1688 a small effect on the number of pairwise differences between samples.
In contrast, a positive Tajima's D reflects an excess of intermediate
frequency alleles relative to the constant-size, neutral expectation.
1690 Alleles at intermediate-frequency increase pairwise diversity more per
segregating site than typical, thus increasing θ_π more than θ_W .

3.3.2 Demography and the coalescent

1694 We've already seen how changes in population size can change the rate
at which heterozygosity is lost from the population (see the discussion
1696 around eqn. (3.13)). If the population size in generation i is N_i , the
probability that a pair of lineages coalesce is $1/(2N_i)$; this conforms to
1698 our intuition that if the population size is small, the rate at which
pairs of lineages find their common ancestor is faster. We can poten-
tially accommodate rapid random fluctuations in population size by
simply using the effective population size N_e in place of N . However,
1702 longer term more systematic changes in population size will distort
the coalescent genealogies, and hence patterns of diversity, in more
1704 systematic ways.

1706 We can see how demography potentially distorts the observed fre-
quency spectrum away from the neutral expectation in a very large
sample of humans shown in Figure 3.16. For comparison, the neu-
1708 tral frequency spectrum, eqn (3.40), is shown as a red line. There are
vastly more rare alleles than expected under our neutral, constant-

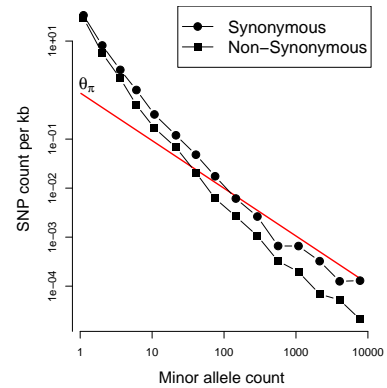
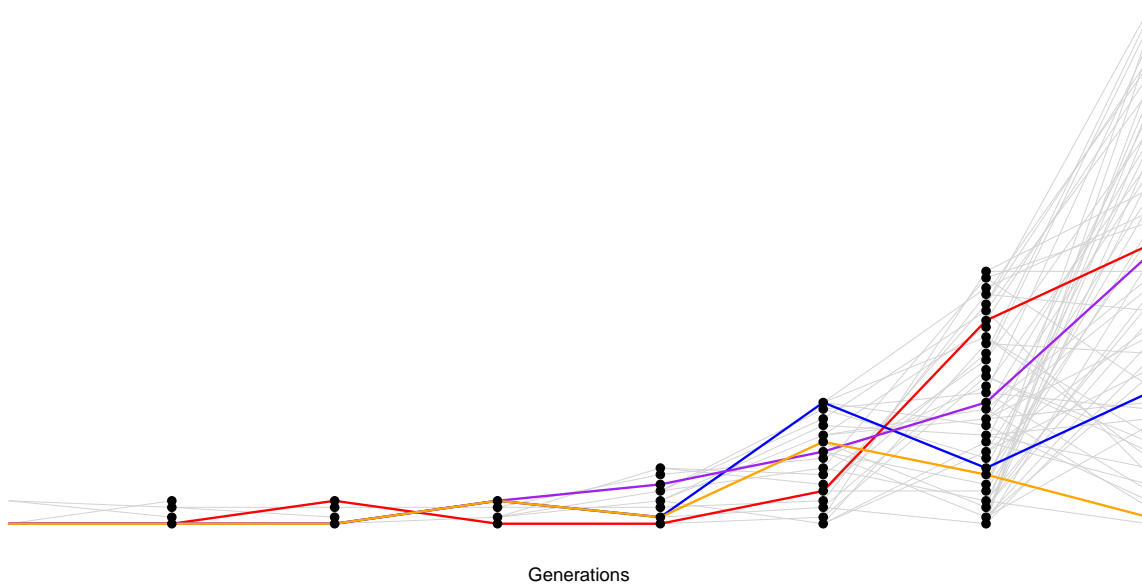


Figure 3.16: Data from 202 genes from 14002 people of European ancestry (28004 alleles). Note the double log-scale. The red line gives the neutral, constant population size estimate of the site frequency spectrum, our equation (3.40), using a θ estimated from π . Note how the non-synonymous changes are even more skewed towards rare alleles, likely due to selection against non-synonymous alleles preventing them from reaching high frequency. Data from NELSON *et al.* (2012). Code here.

¹⁷¹⁰ size-size model, but the neutral prediction and reality agree somewhat more for alleles that are more common.



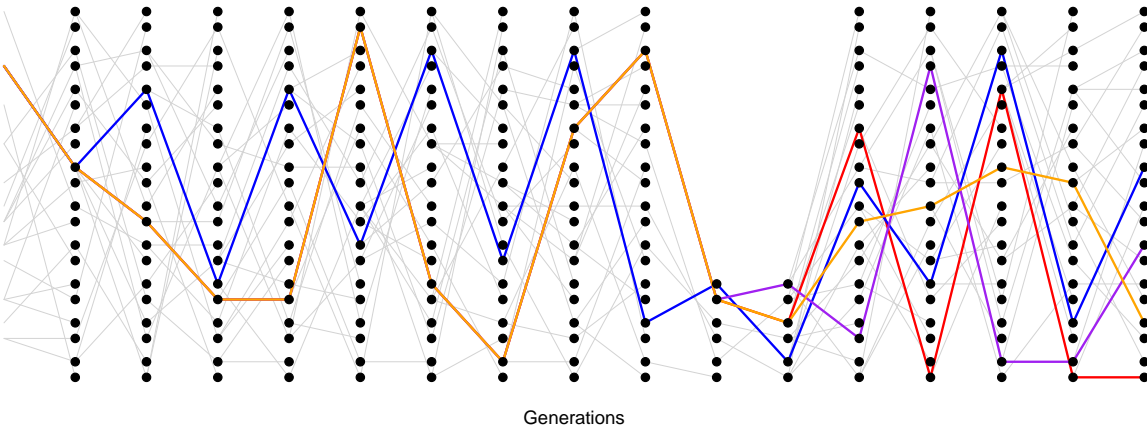
¹⁷¹² Why is this? Well, these patterns are likely the result of the very recent explosive growth in human populations. If the population has ¹⁷¹⁴ grown rapidly, then the pairwise-coalescent rate in the past may be much higher than the coalescent rate closer to the present. (see Figure ¹⁷¹⁶ 3.17).

¹⁷¹⁸ One consequence of a recent population expansion is that there is much less genetic diversity in the population than you'd predict using the census population size. Humans are one example of this ¹⁷²⁰ effect; there are 7 billion of us alive today, but this is due to very rapid population growth over the past thousand to tens of thousands of ¹⁷²² years. Our level of genetic diversity is very much lower than you'd predict given our census size, reflecting our much smaller ancestral ¹⁷²⁴ population. A second consequence of recent population expansion is that the deeper coalescent branches are much more squished together ¹⁷²⁶ in time compared to those in a constant-sized population. Mutations on deeper branches are the source of alleles at more intermediate ¹⁷²⁸ frequencies, and so there are even fewer intermediate-frequency alleles in growing populations. That's why there are so many rare alleles, ¹⁷³⁰ especially singletons, in this large sample of Europeans.

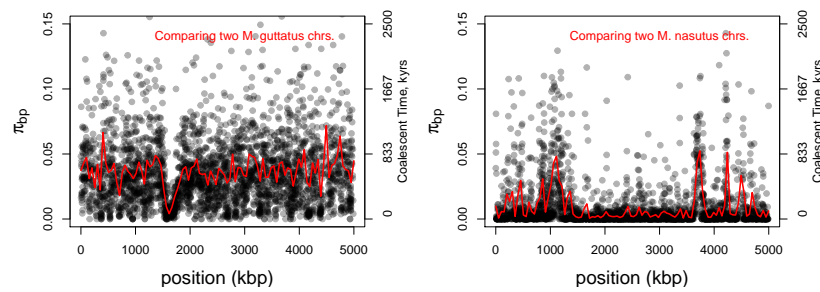
¹⁷³² Another common demographic scenario is a population bottleneck. In a bottleneck, the population size crashes dramatically, and subsequently recovers. For example, our population may have had size ¹⁷³⁴ N_{Big} and crashed down to N_{Small} . One example of a bottleneck is

Figure 3.17: A realization of the coalescent process in a growing population. The population underwent a period of doubling every generation. The initial population size of just two individuals, maintained for a number of generations, is obviously highly unrealistic but serves our purpose. [Code here.](#)

shown in Figure 3.18. Looking at a sample of lineages drawn from the



1736 population today, if the bottleneck was somewhat recent ($\ll N_{\text{Big}}$
 1738 generations in the past) many of our lineages will not have coalesced
 before reaching the bottleneck, moving backward in time. But during
 1740 the bottleneck our lineages coalesce at a much higher rate, such that
 1742 many of our lineages will coalesce if the bottleneck lasts long enough
 ($\sim N_{\text{Small}}$ generations). If the bottleneck is very strong, then all of
 1744 our lineages will coalesce during the bottleneck, and the resulting site
 frequency spectrum may look very much like our population growth
 model (i.e. an excess of rare alleles). However, if some pairs of lineages
 escape coalescing during the bottleneck, they will coalesce much more
 deeply in time (e.g. the blue and orange ancestral lineages in 3.18).



1746 An example of this is shown Figure 3.19, data from BRANDVAIN
 1748 et al.. *Mimulus nasutus* is a selfing species that arose recently from an
 out-crossing progenitor *M. guttatus*, and experienced a strong bottle-
 1750 neck. *M. guttatus* has very high levels of genetic diversity ($\pi = 4\%$
 at synonymous sites), but *M. nasutus* has lost much of this diversity
 1752 ($\pi = 1\%$). Looking along the genome, between a pair of *M. guttatus*
 chromosomes, levels of diversity are fairly uniformly high.

Figure 3.18: A realization of the coalescent process in a bottlenecked population. Our population underwent a bottleneck eight generations in the past. [Code here](#).

Figure 3.19: Diversity along a region of the *Mimulus* genome. Black dots give π in 1kb windows between chromosomes sampled from two individuals, the red line is a moving average (data from BRANDVAIN et al.). Pairwise coalescent times (t) estimated assuming $t = \pi/2\mu$ using $\mu_{BP} = 10^{-9}$. [Code here](#).



Figure 3.20: Yellow Monkeyflower *M. guttatus*.
Choix des plus belles fleurs et des plus beaux fruits. Pierre-Joseph Redouté. (1833). Contributed to Flickr by Swallowtail Garden Seeds. Public Domain.

1754 But in comparing two *M. nasutus* chromosomes, diversity is low
because the pair of lineages generally coalesce recently. Yet in a few
1756 places we see levels of diversity comparable to *M. guttatus*; these re-
gions correspond to genomic sites where our pair of lineages fail to
1758 coalesce during the bottleneck and subsequently coalesce much more
deeply in the ancestral *M. guttatus* population.

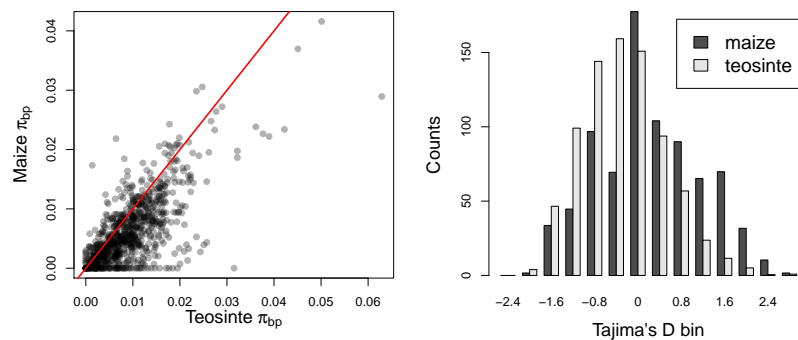


Figure 3.21: Data for polymorphism from Maize and Teosinte: 774 loci from WRIGHT *et al.* (2005). **Left)** Genetic diversity levels in maize and teosinte samples at each of these loci. Note how diversity levels are lower in maize than teosinte, i.e. most points are below the red $x = y$ line. **Right)** The distribution of Tajima's D in maize and teosinte, see how the maize distribution is shifted towards positive values. Code here.

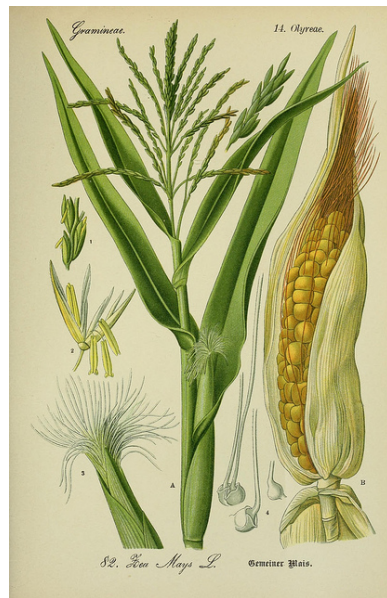


Figure 3.22: Maize (*Zea mays*). Prof. Dr. Thomé's Flora von Deutschland. 1886. Thomé, O. W. Image from the Biodiversity Heritage Library. Contributed by New York Botanical Garden. Not in copyright.

1760 Mutations that arise on deeper lineages will be at intermediate fre-
quency in our sample, and so mild bottlenecks can lead to an excess of
1762 intermediate frequency alleles compared to the standard constant-size
model. This can skew Tajima's D (see eqn 3.42) towards positive val-
1764 ues and away from its expectation of zero. One example of this skew
is shown in Figure 3.21. Maize (*Zea mays* subsp. *mays*) was domesti-
1766 cated from its wild progenitor teosinte (*Zea mays* subsp. *parviflora*)
roughly ten thousand years ago. We can see how the bottleneck as-
1768 sociated with domestication has resulted in a loss of genetic diversity
in maize compared to teosinte, and the polymorphism that remains is
1770 somewhat skewed towards intermediate frequencies resulting in more
positive values of Tajima's D.

1772 **Question 10.** VOIGHT *et al.* (2005) sequenced 40 autosomal
regions from 15 diploid samples of Hausa people from Yaounde,
1774 Cameroon. The average length of locus they sequenced for each re-
gion was 2365bp. They found that the average number of segregating
1776 sites per locus was $S = 11.1$ and the average $\pi = 0.0011$ per base over
the loci. Is Tajima's D positive or negative? Is a demographic model
1778 with a bottleneck or growth more consistent with this result?

3.4 Molecular Evolution and the fixation of neutral alleles

1780 "history is just one damn thing after another" -Arnold Toynbee

It is very unlikely that a rare neutral allele accidentally drifts up
 1782 to fixation; more likely, such an allele will be eventually lost from the
 population. However, populations experience a large and constant
 1784 influx of rare alleles due to mutation, so even if it is very unlikely that
 an individual allele fixes within the population, some neutral alleles
 1786 will fix by chance.

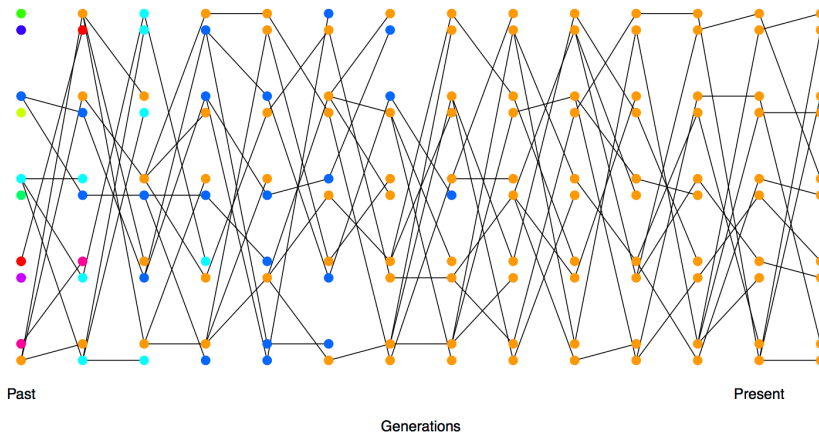


Figure 3.23: Each allele initially present in a small diploid population is given a different colour so we can track their descendants over time. By the 9th generation, all of the alleles present in the population can trace their ancestry back to the orange allele. [Code here.](#)

Probability of the eventual fixation of a neutral allele An allele which
 1788 reaches fixation within a population is an ancestor to the entire pop-
 ulation. In a particular generation there can only be a single allele
 1790 that all other alleles at the locus in a later generation can claim as an
 ancestor (See Figure 3.23). At a neutral locus, the actual allele does
 1792 not affect the number of descendants that the allele has (this follows
 from the definition of neutrality: neutral alleles don't leave more or
 1794 less descendants on average than other neutral alleles). An equivalent
 way to state this is that the allele labels don't affect anything; thus
 1796 the alleles are *exchangeable*. As a consequence of being exchangeable,
 any allele is equally likely to be the ancestor of the entire population.
 1798 In a diploid population of size N , there are $2N$ alleles, all of which
 1800 are equally likely to be the ancestor of the entire population at some
 1802 later time point. So if our allele is present in a single copy, the chance
 1804 that it is the ancestor to the entire population in some future genera-
 1806 tion is $1/(2N)$, i.e. the chance our neutral allele is eventually fixed is
 $1/(2N)$. In Figure 3.23, our orange allele in the first generation is one
 1808 of 10 differently coloured alleles, and so has a $1/10$ chance of being
 the ancestor of the entire population at some later time point (and
 in this simulation it does become the common ancestor, by the 9th
 generation).

More generally, if our neutral allele is present in i copies in the
 1808 population, of $2N$ alleles, the probability that this allele becomes fixed

¹⁸¹⁰ is $i/(2N)$, i.e. the probability that a neutral allele is eventually fixed
¹⁸¹² is simply given by its frequency (p) in the population. (We can also
¹⁸¹⁴ derive this result by letting $Ns \rightarrow 0$ in eqn. (8.11), a result we'll
¹⁸¹⁶ encounter later.)

¹⁸¹⁸ How long does it take on average for such an allele to fix within
¹⁸²⁰ our population? Well, in developing equation (3.34) we've seen that
¹⁸²² it takes $4N$ generations for a large sample of alleles to all trace their
¹⁸²⁴ ancestry back to a single most recent common ancestral allele. Any
¹⁸²⁶ single-base pair change which arose as a single mutation at a locus,
¹⁸²⁸ and fixed in the population, must have been present in the sequence
¹⁸³⁰ transmitted by the most recent common ancestor of the population
¹⁸³² at that locus. Thus it must take roughly $4N$ generations for a neu-
¹⁸³⁴ tral allele present in a single copy within the population to fix. This
¹⁸³⁶ argument can be made more precise, but in general we would still
¹⁸³⁸ find that it takes $\approx 4N$ generations for a neutral allele to go from its
¹⁸⁴⁰ introduction to fixation with the population.

¹⁸²⁶ *Rate of substitution of neutral alleles* A substitution between popula-
¹⁸²⁸ tions that do not exchange gene flow is simply a fixation event within
¹⁸³⁰ one population. The rate of substitution is therefore the rate at which
¹⁸³² new alleles fix in the population, so that the long-term substitution
¹⁸³⁴ rate is the rate at which mutations arise that will eventually become
¹⁸³⁶ fixed within our population.

¹⁸³⁸ Lets assume, based on our discussion of the neutral theory of molec-
¹⁸⁴⁰ ular evolution, that there are only two classes of mutational changes
¹⁸⁴² that can occur with a region, highly deleterious mutations and neutral
¹⁸⁴⁴ mutations. A fraction C of all mutational changes are highly deleteri-
¹⁸⁴⁶ ous, and cannot possibly contribute to substitution nor polymorphism.
¹⁸⁴⁸ The other $1 - C$ fraction of mutations are neutral. If our total mu-
¹⁸⁵⁰ tation rate is μ per transmitted allele per generation, then a total of
¹⁸⁵² $2N\mu(1 - C)$ neutral mutations enter our population each generation.

¹⁸⁵⁴ Each of these neutral mutations has a $1/(2N)$ probability chance of
¹⁸⁵⁶ eventually becoming fixed in the population. Therefore, the rate at
¹⁸⁵⁸ which neutral mutations arise that eventually become fixed within our
¹⁸⁶⁰ population is

$$2N\mu(1 - C) \frac{1}{2N} = \mu(1 - C) \quad (3.43)$$

¹⁸⁶² Thus the rate of substitution, under a model where newly arising
¹⁸⁶⁴ alleles are either highly deleterious or neutral, is simply given by the
¹⁸⁶⁶ mutation rate of neutral alleles, i.e. $\mu(1 - C)$.

¹⁸⁶⁸ Consider a pair of species that have diverged for T generations,
¹⁸⁷⁰ i.e. orthologous sequences shared between the species last shared a
¹⁸⁷² common ancestor T generations ago. If these species have maintained

1850 a constant μ over that time, they will have accumulated an average of

$$2\mu(1 - C)T \quad (3.44)$$

1852 neutral substitutions. This assumes that T is a lot longer than the
1854 time it takes to fix a neutral allele, such that the total number of
1856 alleles introduced into the population that will eventually fix is the
1858 total number of substitutions.

1859 This is a really pretty result as the population size has completely
1861 canceled out of the neutral substitution rate. However, there is an-
1863 other way to see this in a more straight forward way. If I look at a
1865 sequence in me compared to, say, a particular chimp, I'm looking at
1867 the mutations that have occurred in both of our germlines since they
1869 parted ways T generations ago. Since neutral alleles do not alter the
1871 probability of their transmission to the next generation, we are simply
1873 looking at the mutations that have occurred in $2T$ generations worth
1875 of transmissions. Thus the average number of neutral mutational dif-
1876 ferences separating our pair of species is simply $2\mu(1 - C)T$.

1866 A number of observations follow under this model, from equation
1868 (3.44). The first is that a primary determinant of patterns of molec-
1870ular evolution in a genomic region is the level of constraint (C). This
1872 pattern generally seems to hold empirically: non-coding regions often
1874 evolve more rapidly than coding regions, synonymous substitutions
1876 accumulate faster than nonsynonymous, and nonsynonymous sub-
1878stitutions accumulate faster in less vital proteins than ones that are
1880 absolutely necessary for early development. Note that this is not a
1882 unique prediction of the neutral model, e.g. less constrained regions
1884 may also be better able to evolve adaptively. However, it is a fan-
1886tastically useful general insight, e.g. it allows us to spot putatively
1888 functional non-coding regions by looking for genomic regions that have
1890 very low levels of divergence among distantly related species.

"functionally less impor-
 tant molecules or parts of a
 molecule evolve faster than
 more important ones."

- KIMURA and OHTA (1974)

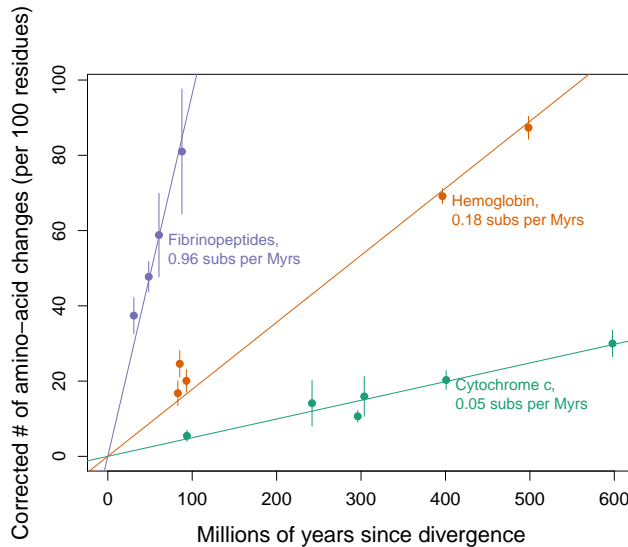


Figure 3.24: The numbers of substitutions in three proteins, corrected for multiple hits, between various pairs of groups plotted against the time these groups shared a common ancestor in the fossil record. Data from DICKERSON (1971). The lines give the linear regression through the origin for each protein. The slope of the regression is given next to the protein name. See (ROBINSON *et al.*, 2016) who revisited this classic study and confirmed the conclusions.

1878 The second important insight, and critical for the development of
 1880 the neutral theory, is that equation (3.44) is seemingly consistent with
 ZUCKERKANDL and PAULING (1965)'s hypothesis of a surprisingly
 constant, protein molecular clock. The protein molecular clock is the
 1882 observation that for some proteins there's a linear relationship be-
 1884 tween the number of non-synonymous (NS) substitutions and the time
 1886 species last shared a common ancestor in the fossil record. DICKER-
 1888 SON (1971) provided an early example of this observation (Figure
 1890 3.24), by comparing various organisms whose molecular sequences were
 1892 available to him. For example, he found that humans and rattlesnakes,
 1894 who last share a common ancestor in the fossil record around 300 mil-
 1896 lion years, are separated by roughly 15 NS substitutions per 100 sites
 1898 in the Cytochrome c protein. While, humans and dogfish, which di-
 1900 verged around 400 million years, are separated by 19 NS substitutions
 1902 per 100 sites in this gene.

In equation (3.44), if we double the amount of time separating a pair of species T , we double the number of substitutions predicted. Note that for this to be true T must be measured in generations. To explain a protein molecular clock between species that clearly differed dramatically in generation time it was hypothesized that the mutation rate actually scaled with generation time, i.e. short-lived organisms introduced fewer mutations per generation, e.g. as they had fewer rounds of mitosis. This generation-time assumption meant that the mutation rate per year could be constant, such that μT would be a constant for pairs of species that had diverged for similar geological



Figure 3.25: Eastern diamondback rattlesnake (*Crotalus adamanteus*). North American herpetology. Holbrook, J. E. Image from the Biodiversity Heritage Library. Contributed by Smithsonian Libraries. Licensed under CC BY-2.0.

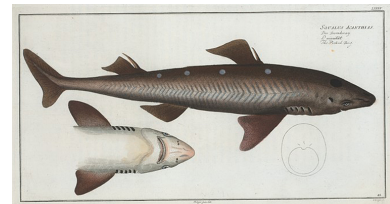


Figure 3.26: Spiny dogfish (*Squalus acanthias*).

Rare Book Division, The New York Public Library. "Squalus Acanthias, The Picked-Dog" The New York Public Library Digital Collections. 1785. Public domain.

times, which are measured in years, even if the organisms differed in generation time. This assumption would allow neutral theory to be consistent with a protein molecular clock measured in years. We now know that this critical generation time assumption is false: organisms with shorter generation times have somewhat higher mutation rates per year so a strict neutral model is inconsistent with the protein molecular clock. We'll return to these ideas when we discuss the fate of very weakly selected mutations in Chapter 8 and OHTA (1973)'s Nearly Neutral theory. grahamI currently dont do generation time effect in that chapter, need to update

The contribution of ancestral polymorphism to divergence. If we are considering T to represent the divergence between long-separated species, then we can think of T as the time that the species split. However, for more recently diverged populations and species, we need to include the fact that the sorting of ancestral polymorphism contributes to divergence among species. In Figure 3.27, we see our two populations split T_s generations ago. However, the coalescence of our A and B lineage is necessarily deeper in time than T_s . The top mutation was polymorphic in the ancestral population but now contributes to the divergence between A and B. Assuming that our ancestral population had effective size N_A individuals, and that our populations split cleanly with no subsequent gene flow, then

$$T = T_s + 2N_A. \quad (3.45)$$

If our species split time is very large compared to $2N$ then we can think of T as the split time.

Question 11. For this, and the next question, assume that humans and chimps diverged around 5.5×10^6 years ago, have a generation time 20 years, that the speciation occurred instantaneously in allopatry with no subsequent gene flow, and the ancestral effective population size of the human and chimp common ancestor population was 10,000 individuals.

Nachman and Crowell sequenced 12 pseudogenes in humans and chimps and found substitutions at 1.3% of sites.

- A) What is the mutation rate per site per generation at these genes?
- B) All of the pseudogenes they sequenced are on the autosomes. What would your prediction be for pseudogenes on the X and Y chromosomes, given that there are fewer rounds of replication in the female germline than in the male germline.

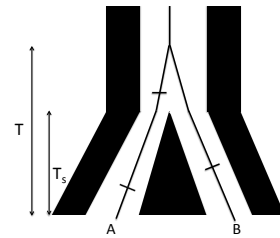


Figure 3.27: The genealogy of two alleles one sampled from population A and B. Mutations on the lineages are shown as dashes. The pair of alleles coalesce in the ancestral population of A and B. The two populations split T_s generations ago, with no subsequent gene flow, but the two lineages must coalesce deeper in time.

3.5 Tests of molecular evolution.

1942 3.5.1 Comparing the rates of non-synonymous to synonymous substitutions d_N/d_S

1944 One common tool in molecular evolution is to compare the estimated number (or rates) of substitutions in different classes of genomic sites, for example the ratio of the number of non-synonymous to synonymous substitutions in a given gene. The simplest way to calculate d_N is to count up the non-synonymous changes and divide by the total number of positions in the gene where a non-synonymous point mutation could occur. We can do likewise for synonymous changes d_S , and then take the ratio d_N/d_S .⁶

1952 For the vast majority of protein-coding genes in the genome we see that $d_N/d_S < 1$. This observation is consistent with the view that 1954 non-synonymous sites are much more constrained than synonymous sites, i.e. that most non-synonymous mutations are deleterious and 1956 quickly removed from the population. If we are willing to make the assumption that all synonymous changes are neutral, $d_S = 2T\mu$, then 1958 we can estimate the degree of constraint on non-synonymous sites. (Note that synonymous changes can sometimes be subject to both 1960 positive and negative selection, but this neutral assumption is a useful starting place.)

1962 Assume that a fraction C of non-synonymous changes are too deleterious to contribute to polymorphism. Then, after T generations of 1964 divergence have elapsed between two populations, we'd expect d_N neutral non-synonymous substitutions, where

$$d_N = 2T(1 - C)\mu \quad (3.46)$$

1966 Dividing by d_S , we find

$$d_N/d_S = (1 - C) \quad (3.47)$$

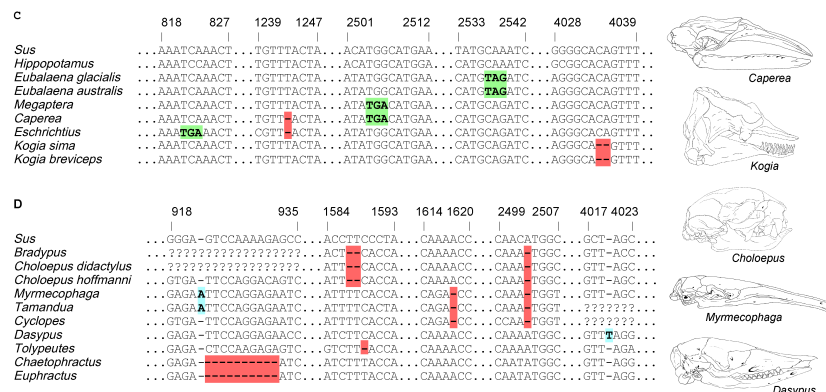
Therefore, if we assume that non-synonymous mutations can only be 1968 strongly deleterious or neutral, we estimate the fraction of mutational changes that are constrained by negative selection as $C = 1 - d_N/d_S$. 1970 C has the interpretations of being the fraction of non-synonymous mutations that are quickly weeded out of the population by selection, 1972 and so do not contribute to divergence among species.

We can test whether our gene is evolving in a constrained way at 1974 the protein level by estimating d_N/d_S and testing whether this is significantly less than 1. A d_N/d_S test can provide evolutionary evidence 1976 that a stretch of DNA proposed to be protein-coding is subject to selective constraint, and so likely does encode for a functional protein. 1978 We can also perform a d_N/d_S test on specific branches of a phylogeny

⁶ This ignores the fact that some changes are more likely to occur by mutation than others and also does not account for multiple hits (multiple mutations at the same bp position). Therefore, in practice the ratio d_N/d_S is more typically calculated by model-based likelihood and bayesian methods that can account for these features.

for a gene, to test on which branches the gene is subject to constraint,
 1980 or to test for changes in the level of constraint across the phylogeny.

Loss of constraint at pseudogenes. While most protein genes evolve
 1982 under constraint, we can find examples of genes that are evolving
 1984 in a less constrained manner. The simplest example of this is where
 1986 the gene has lost function. Genes can lose function because of inac-
 1988 tivating mutations that stop them being transcribed or translated
 1990 into functional proteins. Such genes are called ‘pseudogenes’. When
 1992 a gene completely loses function there is no longer selection against
 1994 non-synonymous changes and so such mutations are just as free to ac-
 1996 cumulate as synonymous changes, and so $d_N/d_S = 1$. Pseudogenes
 1998 are a wonderful example of the extension of Darwin’s ideas about
 vestigial traits (‘Rudimentary organs’) to the DNA level; we can still
 recognize a once useful word (gene) whose spelling is slowly degrading.
 Our genomes are filled with old pseudogenes whose original meanings
 (functional protein coding sequences) are slowly being eroded through
 the accumulation of neutral substitutions. One nice example of a
 gene that has repeatedly lost function, i.e. become repeatedly psue-
 1996 odogenized, is the Enamlin gene from the study of MEREDITH *et al.*
 1998 (2009).



The protein Enamlin is a key structural protein involved in the
 2000 outer cap of enamel on teeth. Various mammals have secondarily
 evolved diets that do not require hard teeth, and so greatly reduced
 2002 the selection pressure for hard enamel, or even teeth at all. For ex-
 ample, two-toed sloths (*Choloepus*), Pygmy sperm whales (*Kogia*),
 2004 and aardvark (*Orycteropus*) all lack enamel on teeth. Other mammals
 have lost their teeth entirely, e.g. giant anteaters (*Myrmecophaga*) and
 2006 Baleen whales. Due to this relaxation of constraint on the phenotype,
 the Enamlin gene has accumulated pseudogenizing substitutions such
 2008 as premature stop codons and frameshift mutations (see Figure 3.28)

“Rudimentary organs may be com-
 pared with the letters in a word,
 still retained in the spelling, but be-
 come useless in the pronunciation,
 but which serve as a clue .. for its
 derivation.” – DARWIN (1859) pg. 455

Figure 3.28: Examples of frameshift mutations (insertions blue, deletions red) and premature stop codons in Enamlin in Cetacea and Xenarthra. Figure from MEREDITH *et al.* (2009), licensed under CC BY 4.0.



Figure 3.29: Two-toed sloth (*Choloepus hoffmanni*). An introduction to the study of mammals, living and extinct. 1891. Flower W. H. and Lydekker R. Image from the Biodiversity Heritage Library. Contributed by University of Toronto. Not in copyright.

for examples). MEREDITH *et al.* sequenced Enamlin across a range of species and found that none of the species with enamel have frameshift mutations in Enamlin, while 17/20 of species that lack enamel or teeth have frameshifts in Enamlin, and all of them carry premature stop codons (Figure 3.30).

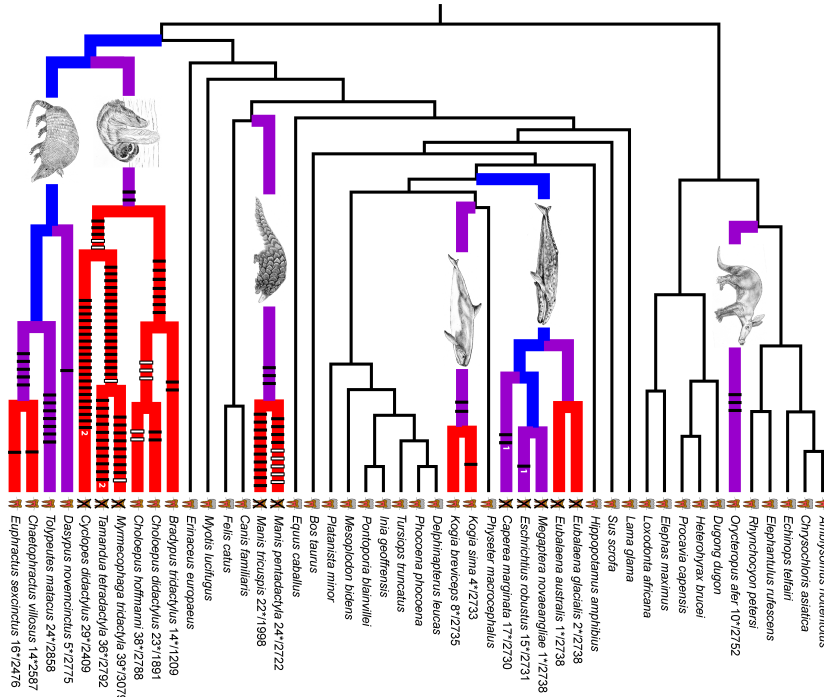


Figure 3.30: The tooth symbol next to each taxon shows whether they have teeth with enamel, lack enamel, or lack teeth. Branches of the phylogeny are coloured by whether their Enamlin is functional (black), pre-mutation (blue), mixed (purple), or pseudogenized (red). The black and white bars on branches show frameshift mutations. The numbers after taxon names indicate minimum number of stop codons in the sequence divided by the length of the sequence. Figure from MEREDITH *et al.* (2009), licensed under CC BY 4.0.

The branches of the Enamlin phylogeny with a functional Enamlin gene (black) had an estimated $d_N/d_S = 0.51$, consistent with the protein evolving in a constrained manner. In contrast, the branches with a pseudogenized Enamlin (red) had $d_N/d_S = 1.02$, consistent with the gene evolving an unconstrained way. The branches where the gene was likely transitioning from a functional to non-function state, i.e. pre-mutation (blue) and mixed (purple), had intermediate values of $d_N/d_S = 0.83 - 0.98$, consistent with a transition from a constrained to unconstrained mode of protein evolution somewhere along these branches of the phylogeny.

Adaptive evolution and d_N/d_S . Clearly genes are not only subject to neutral and deleterious mutations; beneficial mutations must also arise and fix from time to time. Let's assume that a fraction B of non-synonymous mutations that arise are beneficial such that $2N\mu B$ beneficial mutations arise per generation. Newly arisen beneficial alleles are not destined to fix in the population, as they may be lost to

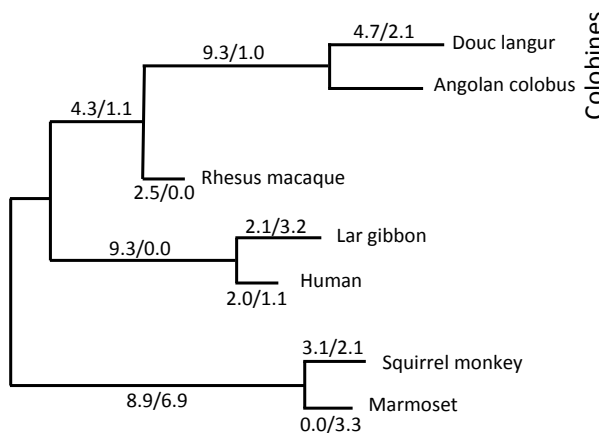
2030 genetic drift when they are rare in the population (we'll discuss how
 to calculate the fixation probability for beneficial alleles in Chapter
 2032 8). A newly arisen beneficial allele reaches fixation in the population
 with probability f_B from its initial frequency of $1/2N$. This fixation
 2034 probability may be much higher than that of neutral mutations, but
 still much less than 1. If $2T$ generations of divergence have elapsed
 2036 between the two populations then a total of

$$dN = 2T(1 - C - B)\mu + 2T \times (2N\mu B) \times f_B \quad (3.48)$$

non-synonymous substitutions will have accumulated. Then

$$d_N/d_S = (1 - C - B) + 2NBf_B \quad (3.49)$$

2038 assuming again that all synonymous mutations are neutral. Note that
 this means that our estimates of C using $1 - d_N/d_S$ will be a lower
 2040 bound on the true constraint if even a small fraction of mutations
 are beneficial. Those cases where the gene is evolving more rapidly
 2042 at the protein level than at synonymous sites, i.e. $d_N/d_S > 1$, are
 potentially strong candidates for positive selection rapidly driving
 2044 change at the protein level. We can identify genes that have d_N/d_S
 significantly greater than one, either on the complete gene phylogeny,
 2046 or on particular branches. Note that is a very conservative test that
 few genes in the genome meet, as many genes that are fixing adaptive
 2048 non-synonymous substitutions will have $d_N/d_S < 1$; even if adaptive
 mutations are common, genes may still evolve in a constrained way
 2050 (i.e. $d_N/d_S < 1$) if the rapid fixation of beneficial mutations due to pos-
 itive selection is outweighed by the loss of non-synonymous mutations
 2052 to negative selection.



A classic example for looking at adaptive evolution using d_N/d_S is
 2054 the evolution of the lysozyme protein in primates (MESSIER and

Figure 3.31: A phylogram for the primate lysozyme gene, data from YANG (1998). For each branch, the numbers give the estimated average number of non-synonymous to synonymous changes in the lysozyme protein.



Figure 3.32: Abyssinian black-and-white colobus (*Colobus guereza*). A member of the leaf-eating Colobines. Brehm's Tierleben, Brehm, A.E. 1893. Image from the Biodiversity Heritage Library. Contributed by University of Illinois Urbana-Champaign. Not in copyright.



STEWART, 1997; YANG, 1998). The lysozyme protein is a key component for the breakdown of bacterial walls. It shows very fast protein evolution (see the phylogeny in Figure 3.31), notably on the lineages leading to apes (e.g. gibbons and humans) and Colobines (e.g. colobus and langur monkeys). Colobines have leaf-based diets. They digest these leaves by bacterial fermentation in their foregut, and then use lysozymes to break down the bacteria to extract energy from the leaves. In Colobines, the lysozyme protein has evolved to work well in the high-PH environment of the stomach. Remarkably, the Colobine lysozyme has convergently evolved this activity via very similar amino-acid changes at 5 key residuals in cows and Hoatzins (a leaf eating bird, KORNEGAY *et al.*, 1994)

The McDonald-Kreitman test As noted above, a big issue with using d_N/d_S to detect adaptation is that it is very conservative. For a more powerful test of rapid divergence, what we need to do is adjust for the level of constraint a gene experiences at non-synonymous sites. One way to do this is to use polymorphism data as an internal control. If we see little non-synonymous polymorphism at a gene, but a lot of synonymous polymorphism, we now know that there is likely strong constraint on the gene (i.e. high C), thus we expect d_N/d_S to be low. McDONALD and KREITMAN (1991) devised a simple test of the neutral theory of molecular evolution at a gene based on this intuition (building on the conceptually similar HKA test HUDSON *et al.*, 1987). McDONALD and KREITMAN took the case where we have polymorphism data at a gene for one species and divergence to a closely related species. They partitioned polymorphism and fixed differences in their sample into non-synonymous and synonymous changes:

	Poly.	Fixed
Non-Syn.	P_N	D_N
Syn.	P_S	D_S
Ratio	P_N/P_S	D_N/D_S

Under neutral theory, we expect a smaller number of non-synonymous to synonymous fixed differences ($D_N/D_S < 1$) and exactly the same expectation holds for polymorphism (P_N/P_S). Let's consider a gene with L_S and L_N sites where synonymous and non-synonymous mutations could arise respectively. We can think of the underlying gene genealogy at our gene, see Figure 3.34, with the total time on the coalescent genealogy within the species as T_{tot} and the total time for fixed differences between our species as T'_{div} . Then under neutrality we expect $\mu L_N(1 - C)T_{tot}$ non-synonymous polymorphisms (i.e. our number of segregating sites), and $\mu L_N(1 - C)T'_{div}$ non-synonymous

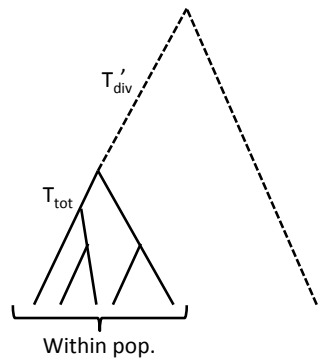


Figure 3.34: An example of a gene genealogy for a set of alleles sampled within a population and a single allele sampled from a distantly-related species.

²⁰⁹⁴ fixed differences. We can then fill out the rest of our table as follows:

	Poly.	Fixed
Non-Syn.	$\mu L_N(1 - C)T_{tot}$	$\mu L_N(1 - C)T'_{div}$
Syn.	$\mu L_S T_{tot}$	$\mu L_S T'_{div}$
Ratio	$L_N(1 - C)/(L_S)$	$L_N(1 - C)/(L_S)$

²⁰⁹⁶ Therefore, we expect the ratio of non-synonymous to synonymous changes to be the same for polymorphism and divergence under a ²⁰⁹⁸ strict neutral model. We can test this expectation of equal ratios via the standard tests of a 2×2 table. If the ratio of N/S is significantly ²¹⁰⁰ higher for divergence than polymorphism we have evidence that non-synonymous substitutions are accumulating more rapidly than we ²¹⁰² would predict given levels of constraint alone.

²¹⁰⁴ As example of a McDonald-Kreitman table consider the work of FRENTIU *et al.* (2007) on the molecular evolution of L Photopigment opsin in Admiral (*Limenitis*) butterflies, responsible for colour ²¹⁰⁶ vision in the long-wavelength part of the visual spectrum. FRENTIU *et al.* found that the sensitivity of this opsin had shifted towards blue ²¹⁰⁸ in its sensitivity in *L. archippus archippus* (viceroy) compared to *L. arthemis astyanax*. To test whether this molecular evolution reflected ²¹¹⁰ positive selection they sequenced 24 *L. arthemis astyanax* individuals and one *L. archippus archippus* sequence. They identified 11 poly- ²¹¹² morphic sites in *L. arthemis astyanax* and 16 fixed differences, which break down as follows:

	Poly.	Fixed
Non-Syn.	2	12
Syn.	9	4
Ratio	2/9	3/1

²¹¹⁴ Note the strong excess of non-synonymous to synonymous divergence compared to polymorphism (p-value of 0.006, Fisher's exact ²¹¹⁶ test), which is consistent with the gene evolving in an adaptive manner among the two species. We would expect roughly only 3 non- ²¹¹⁸ synonymous substitutions out of 16 substitutions if the gene was ²¹²⁰ evolving neutrally ($16 \times 2/11$).

3.6 Neutral diversity and population structure

²¹²² We've considered alleles drawn from a randomly-mating population, and divergence among alleles drawn from two distantly-related populations. ²¹²⁴ We'll now turn to consider divergence among more closely related populations. In thinking about the coalescent within populations we made the assumption that any pair of lineages is equally likely to coalesce with each other. However, when there is population ²¹²⁶ structure this assumption is violated.

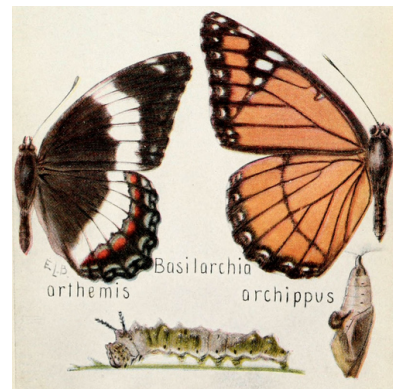


Figure 3.35: White admiral (*Limenitis arthemis*) and Viceroy (*Limenitis archippus*). *Basilarchia* is the old genus that these two species were originally placed in. Viceroy and Monarch butterflies are Müllerian mimics.
Field book of insects (1918). Lutz, F.E. . illustrations by Edna L. Beutenmüller. Image from the Biodiversity Heritage Library. Contributed by MBLWHOI Library. Not in copyright.

We have previously written the measure of population structure

²¹³⁰ F_{ST} as

$$F_{ST} = \frac{H_T - H_S}{H_T} \quad (3.50)$$

where H_S is the probability that two alleles sampled at random from ²¹³² a subpopulation differ, and H_T is the probability that two alleles sampled at random from the total population differ.

²¹³⁴ *A simple population split model* Imagine a population of constant size of N_e diploid individuals that T generations in the past split into two ²¹³⁶ daughter populations (sub-populations) each of size N_e individuals, which do not subsequently exchange migrants. In the current day we ²¹³⁸ sample an equal number of alleles from both subpopulations.

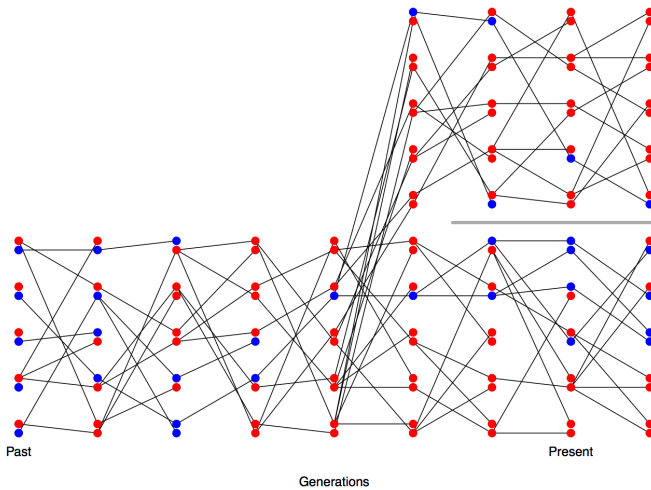


Figure 3.36: Change in allele frequencies following a population split. Code here.

²¹⁴⁰ Consider a pair of alleles sampled within one of our sub-populations and think about their per site heterozygosity. These alleles have experienced a population of size N_e and so the probability that they differ ²¹⁴² is $H_S \approx 4N_e\mu$ (assuming that $N_e\mu \ll 1$, using our equation 3.11 for heterozygosity within a population).

²¹⁴⁴ The heterozygosity in our total population is a little more tricky to calculate. Assuming that we equally sample both sub-populations, ²¹⁴⁶ when we draw two alleles from our total sample, 50% of the time they are drawn from the same subpopulation and 50% of the time ²¹⁴⁸ they are drawn from different subpopulations. Therefore, our total heterozygosity is given by

$$H_T = \frac{1}{2}H_S + \frac{1}{2}H_B \quad (3.51)$$

²¹⁵⁰ where H_B is the probability that a pair of alleles drawn from our two different sub-populations differ from each other. A pair of alleles from

2152 different sub-populations cannot find a common ancestor with each
2154 other for at least T generations into the past as they are in distinct
2156 populations (not connected by migration). Once our alleles find them-
2158 selves back in the combined ancestral population it takes them on
2160 average $2N$ generations to coalesce. So the total opportunity for mu-
2162 tation between our pair of alleles sampled from different populations is
2164 $2(T + 2N)$ generations of meioses, such that the probability that our
2166 pairs of alleles is different is

$$H_B \approx 2\mu(T + 2N) \quad (3.52)$$

2160 We can plug this into our expression for H_T , and then that in turn
into F_{ST} . Doing so we find that

$$F_{ST} \approx \frac{\mu T}{\mu T + 4N_e \mu} = \frac{T}{T + 4N_e} \quad (3.53)$$

2162 Note that μ cancels out of this equation. In this simple toy model,
 F_{ST} is increasing because the amount of between-population diversity
2164 increases with the divergence time of the two populations (initially
linearly with T). F_{ST} grows at a rate give by $T/(4N_e)$ so that differenti-
2166 ation will be higher between populations separated by long divergence
times or with small effective population sizes.

2168 **Question 12.** The genome-wide F_{ST} between Bornean and Suma-
tran orangutan species samples (*Pongo pygmaeus* and *Pongo abelii*)
2170 is ≈ 0.37 (LOCKE *et al.*, 2011), representing a deep population split
between the species (potentially with little subsequent gene flow).
2172 Within the populations the genome-wide average Watterson's θ is
 $\theta_W = 1.4\text{kb}^{-1}$, estimated from the number of segregating sites. As-
2174 sume a generation time of 20 years, and a mutation rate of 2×10^{-8}
per base per generation. How far in the past did the two populations
2176 diverge?

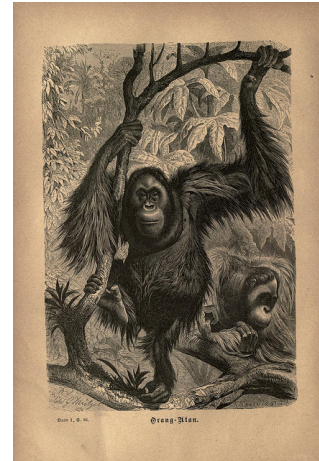


Figure 3.37: Orangutan (*Pongo*).
Brehms thierleben, allgemeine kunde des
thierreichs. Brehm, A. E. Image from the
Biodiversity Heritage Library. Contributed by
MBLWHOI Library. Not in copyright.

2178 *A simple model of migration between an island and the mainland.* We
can also use the coalescent to think about patterns of differentiation
under a simple model of migration-drift equilibrium. Let's consider a
2180 small island population that is relatively isolated from a large main-
land population, where both of these populations are constant in size.
2182 We'll assume that the expected heterozygosity for a pair of alleles
sampled on the mainland is H_M .

2184 Our island has a population size N_I that is very small compared
to our mainland population. Each generation some low fraction m of
2186 our individuals on the island have migrant parents from the mainland
the generation before. Our island may also send migrants back to the
2188 mainland, but these are a drop in the ocean compared to the large
population size on the mainland and their effect can be ignored.

If we sample an allele on the island and trace its ancestral lineage backward in time, each generation our ancestral allele has a low probability m of being descended from the mainland in the preceding generation (if we go back far enough the allele eventually has to be descended from an allele on the mainland). The probability that a pair of alleles sampled on the island are descended from a shared recent common ancestral allele on the island is the probability that our pair of alleles coalesces before either lineage migrates. For example, the probability that our pair of alleles coalesces $t + 1$ generations back on the island is

$$\frac{1}{2N_I} (1-m)^{2(t+1)} \left(1 - \frac{1}{2N_I}\right)^t \approx \frac{1}{2N_I} \exp\left(-t\left(\frac{1}{2N_I} + 2m\right)\right), \quad (3.54)$$

with the approximation following from assuming that $m \ll 1$ & $\frac{1}{(2N_I)} \ll 1$ (note that this is very similar to our derivation of heterozygosity above). The probability that our alleles coalesce before either one of them migrates off the island, irrespective of the time, is

$$\int_0^\infty \frac{1}{2N_I} \exp\left(-t\left(\frac{1}{2N_I} + 2m\right)\right) dt = \frac{1/(2N_I)}{1/(2N_I) + 2m}. \quad (3.55)$$

Let's assume that the mutation rate is very low such that it is very unlikely that the pair of alleles mutate before they coalesce on the island. Therefore, the only way that the alleles can be different from each other is if one or other of them migrates to the mainland, which happens with probability

$$1 - \frac{1/(2N_I)}{1/(2N_I) + 2m} \quad (3.56)$$

Conditional on one or other of our alleles migrating to the mainland, both of our alleles represent independent draws from the mainland and so differ from each other with probability H_M . Therefore, the level of heterozygosity on the island is given by

$$H_I = \left(1 - \frac{1/(2N_I)}{1/(2N_I) + 2m}\right) H_M \quad (3.57)$$

So the reduction of heterozygosity on the island compared to the mainland is

$$F_{IM} = 1 - \frac{H_I}{H_M} = \frac{1/(2N_I)}{1/(2N_I) + 2m} = \frac{1}{1 + 4N_I m}. \quad (3.58)$$

The level of inbreeding on the island compared to the mainland will be high if the migration rate is low and the effective population size of the island is low, as allele frequencies on the island are drifting and diversity on the island is not being replenished by migration. The key parameter here is the number individuals on the island replaced by immigrants from the mainland each generation ($N_I m$).

We have framed this problem as being about the reduction in genetic diversity on the island compared to the mainland. However, if we consider collecting individuals on the island and mainland in proportion to their population sizes, the total level of heterozygosity would be $H_T = H_M$, as samples from our mainland would greatly outnumber those from our island. Therefore, considering the island as our sub-population, we have derived another simple model of F_{ST} .

Question 13. You are investigating a small river population of sticklebacks, which receives infrequent migrants from a very large marine population. At a set of putatively neutral biallelic markers the freshwater population has frequencies:

0.2, 0.7, 0.8

at the same markers the marine population has frequencies:

0.4, 0.5 and 0.7.

From studying patterns of heterozygosity at a large collection of markers, you have estimated the long term effective size of your freshwater population is 2000 individuals.

What is your estimate of the migration rate from the marine populations into the river?

Incomplete lineage sorting Because it can take a long time for an polymorphism to drift up or down in frequency, multiple population splits may occur during the time an allele is still segregating. This can lead to incongruence between the overall population tree and the information about relationships present at individual loci. In Figure 3.39 and 3.40 we show a simulation of three populations where the bottom population splits off from the other two first, followed by the subsequent splitting of the top and the middle populations. We start both simulations with a newly introduced red allele being polymorphic in the combined ancestral population. The most likely fate of this allele is that it is quickly lost from the population, but sometimes the allele can drift up in frequency and be polymorphic when the populations split, as the allele in our two figures has done. If the allele is lost/fixed in the descendant populations before the next population split, our allele configuration will agree with the population tree, as it does in Figure 3.39, and so too the gene tree will agree with population tree (as shown in the left side of Figure 3.41). However, if the allele persists as a polymorphism in the ancestral population until the top and the middle populations split, then the allele could fix in one of these populations and not the other. Such an event leads to a substitution pattern that disagrees with the population tree, as in Figure 3.40. If we were to construct a phylogeny using the variation at this site we would see a disagreement between the gene tree and

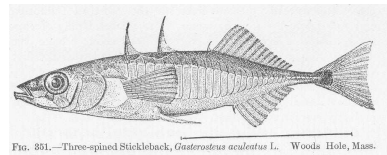


Fig. 331.—Three-spined Stickleback, *Gasterosteus aculeatus* L. Woods Hole, Mass.

Figure 3.38: Three-spined stickleback (*Gasterosteus aculeatus*).

Jordan, David Starr (1907) Fishes, New York City, NY: Henry Holt and Company. Image from Wikimedia Commons Public domain.

population tree. In Figure 3.40 an allele drawn from the top and the
 2264 bottom populations are necessarily more closely related to each other
 than either is to an allele drawn from population 2; tracing our allelic
 2266 lineages from the top and bottom populations back through time, they
 must coalesce with each other before we reach the point where the
 2268 red mutation arose; in contrast, a lineage from the middle population
 cannot have coalesced with either other lineage until past the time the
 2270 red mutation arose. An example of this ‘incomplete lineage sorting’ in
 terms of the underlying tree is shown on the right side of Figure 3.41.

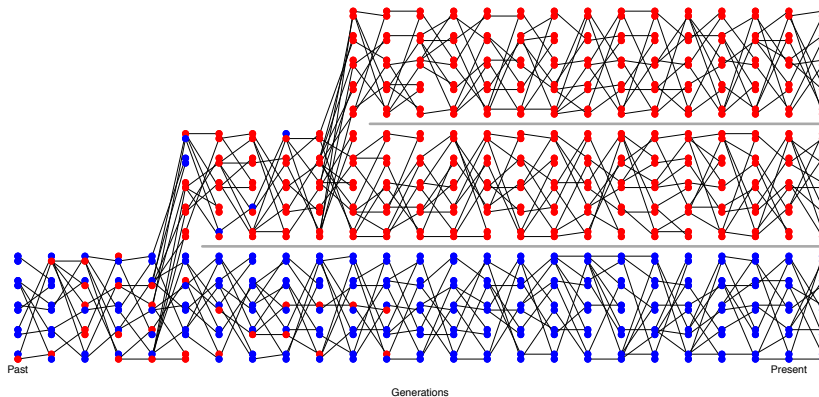


Figure 3.39: An example of alleles assorting among three populations such that there is no incomplete lineage sorting. [Code here.](#)

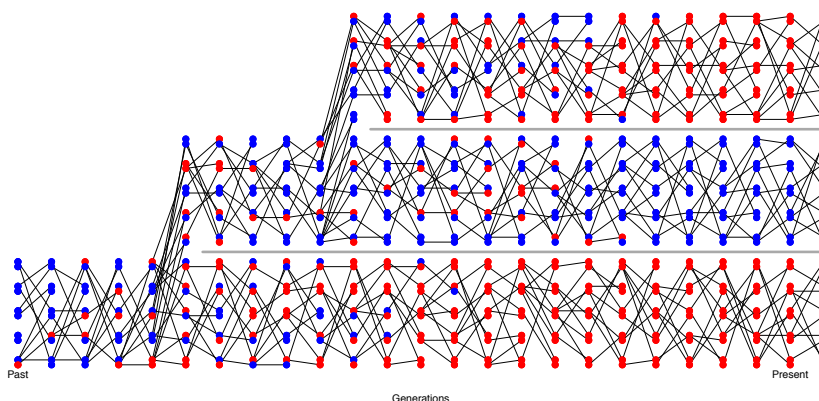


Figure 3.40: An example of alleles assorting among three populations leading to incomplete lineage sorting. [Code here.](#)



Figure 3.41: The population tree of three populations ((A, B), C) is shown blocked out with black shapes. Two different coalescent trees relating a single allele drawn from A, B, and C are shown with thinner lines.

2272 A natural pedigree analogy to incomplete lineage sorting is the fact
 2273 that while two biological siblings are more closely related to each other
 2274 genealogically than either is to their cousin, at any given locus one of
 2275 the siblings can share an allele IBD with their cousin that they do not
 2276 share with their own sibling, due to the randomness of Mendelian seg-
 2277 regation down their pedigree. In these cases, the average relatedness of
 2278 the individuals/populations disagrees with the patterns of relatedness
 2279 at a particular locus.

2280 As an empirical example of incomplete lineage sorting, let's con-
 2281 sider the work of JENNINGS and EDWARDS (2005) who sequenced
 2282 a single allele from three different species of Australian grass finches
(Poephila): two sister species of long-tailed finches (*Poephila acuticauda* and *P. hecki*) and the black-throated finch (*Poephila cincta*,
 2284 see Figure 3.42). They collected sequence data for 30 genes, and con-
 2285 structed phylogenetic gene trees at each of these loci, resulting in 28
 2286 well-resolved gene trees. 16 of the gene trees showed *P. acuticauda*
 2288 and *P. hecki* as sisters with *P. cincta* (the tree ((A,H),C)), while for
 twelve genes the gene tree was discordant with the population tree:
 2290 for seven of their genes *P. hecki* fell as an outgroup to the other two
 and at five *P. acuticauda* fell as an outgroup (the trees ((A,C),H) and
 2292 ((H,C),A) respectively).

2293 Let's use the coalescent to understand this discordance between
 2294 gene trees and species trees. Let's assume that two sister populations
 (A & B) split t_1 generations in the past, with a deeper split from a
 2296 third outgroup population (C) t_2 generations in the past. We'll as-
 2297 sume that there's no gene flow among our populations after each split.
 2298 We can trace back the ancestral lineages of our three alleles. The first
 opportunity for the A & B lineages to coalesce is t_1 generations ago.
 2299 If they coalesce with each other in their shared ancestral population
 before t_2 in the past (left side of Figure 3.41) their gene tree will def-
 2300 inately agree with the population tree. So the only way for the gene
 2301 tree to disagree with the population tree is for the A & B lineages to
 2302 fail to coalesce in their shared ancestral population between t_1 and t_2 ;
 2303 this happens with probability $(1 - 1/(2N))^{t_2 - t_1}$. We'll get a discordant
 2304 gene tree if A & B make it back to the shared ancestral population
 2305 with C without coalescing, and then one or the other of them coalesces
 2306 with the C lineage before they coalesce with each other. This happens
 2307 with probability 2/3, as at the first pairwise-coalescent event there are
 2308 are three possible pairs of lineages that could coalesce, two of which
 2309 (A & C and B & C) result in a discordant tree. So the probability
 2310 that we get a coalescent tree that is discordant with the population
 2311 tree is

$$\frac{2}{3} (1 - 1/(2N))^{t_2 - t_1}. \quad (3.59)$$

2312 Thus we should expect gene-tree population-tree discordance when



Figure 3.42: Banded Grass Finch (*P. cincta*). Illustration by Elizabeth Gould.
Birds of Australia Gould J. 1840. CC BY 4.0 uploaded to Flickr by rawpixel.com.

populations split in rapid succession and/or population sizes are large.

2316

Question 14. Let's return to JENNINGS and EDWARDS's Aus-

2318 tralian grass finches example. They estimated that the ancestral pop-
ulation size of our two long-tailed finches was four hundred thousand.

2320 What is your best estimate of the inter-speciation time, i.e. $t_2 - t_1$?

Testing for gene flow. We often want to test whether gene flow has

2322 occurred between populations. For example, we might want to es-
tablish a case that interbreeding between humans and Neanderthals
2324 occurred or demonstrate that gene flow occurred after two populations
began to speciate. A broad range of methods have been designed to
2326 test for gene flow and to estimate gene flow rates based on neutral ex-
pectations. Here we'll briefly just discuss one method based on some
2328 simple coalescent ideas. Above we assumed that gene-tree popula-
tion-tree discordance was due to incomplete lineage sorting due to popu-
2330 lations rapidly splitting. However, gene flow among populations can
also lead to gene-tree discordance. While both ILS and gene flow can
2332 lead to discordance, under simplifying assumptions, ILS implies more
symmetry in how these discordances manifest themselves.

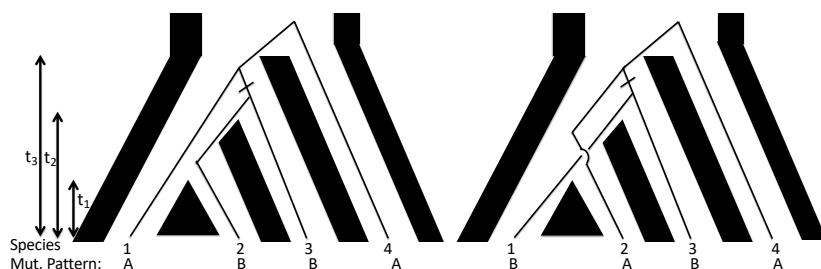


Figure 3.43: In both the left and right trees ILS has occurred between our single lineages sampled from populations A, B, and C. Imagine that population D is a somewhat distant outgroup such that the lineages from A through C (nearly) always coalesce with each other before any coalesce with D. The small dash on the branch indicates the mutation A → B occurring, giving rise to the ABBA or BABA mutational pattern shown at the bottom.

2334 Take a look at Figure 3.43. In both cases the lineages from A and
2336 B fail to coalesce in their initial shared ancestral population, and one
or the other of them coalesces with the lineage from C before they
2338 coalesce with each other. Each option is equally likely; therefore the
mutational patterns ABBA and BABA are equally likely to occur
under ILS.⁷

2340 However, if gene flow occurs from population C into population B,
in addition to ILS the lineage from B can more recently coalesce with
2342 the lineage from C, and so we should see more ABBAs than BABAs.
To test for this effect of gene flow, we can sample a sequence from
2344 each of our 4 populations and count up the number of sites that show
the two mutational patterns consistent with the gene-tree discordance

⁷ Here we have to assume no structure in the ancestral population.

²³⁴⁶ n_{ABBA} and n_{BABA} and calculate

$$\frac{n_{ABBA} - n_{BABA}}{n_{ABBA} + n_{BABA}} \quad (3.60)$$

This statistic will have expectation zero if the gene-tree discordance is
²³⁴⁸ due to ILS and will be skewed negative if gene flow occurred from C
into B (and skewed positive if gene flow occurred from C into A).

Phenotypic Variation and the Resemblance Between Relatives

THE DISTINCTION BETWEEN GENOTYPE AND PHENOTYPE is one of the most useful ideas in Biology.¹ The genotype of an individual (the genome), for most purposes, is decided when the sperm fertilizes egg. The phenotype of an individual represents any measurable aspect of an organism.

Your height, to the amount of RNA transcribed from a given gene, to what you ate last Tuesday: all of these are phenotypes. Nearly any phenotype we can choose to measure about an organism represents the outcome of the information encoded by their genome played out through an incredibly complicated developmental, physiological and/or behavioural processes that in turn interact with a myriad of environmental and stochastic factors. Honestly it boggles the mind how organisms work as well as they do, let alone that I managed to eat lunch last Tuesday.

There are many different ways to think about studying the path from genotype through to phenotype. The one we will take here is to think about how phenotypic variation among individuals in a population arises as a result of genetic variation in the population. One simple way to measure this genotype-phenotype relationship is to calculate the phenotypic mean for each genotype at a locus. For example, WANG *et al.* (2018) explored the genetic basis of budset time in European aspen (*Populus tremula*); the effect of one specific SNP on that phenotype is shown in Figure 4.2. Budset timing is a key trait underlying local adaptation to varying growing season length. The associated SNP falls in a gene (*PtFT2*) that is known to play a strong role in flowering time regulation in other plants.

One way for us to assess the relationship between genotype and phenotype is to find the best fitting linear line through the data, i.e. fit a linear regression of phenotypes for our individuals on their geno-

¹ JOHANNSEN, W., 1911 The Genotype Conception of Heredity. The American Naturalist 45(531): 129–159



Figure 4.1: European aspen *P. tremula*. H. Schacht. 1860. BHL Image from the Biodiversity Heritage Library. Contributed by The Library of Congress. Not in copyright.

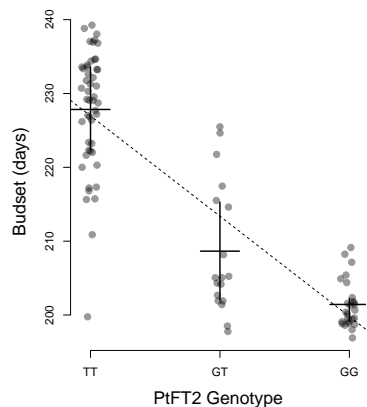


Figure 4.2: The effect of a flowering time gene (*PtFT2*) SNP on budset time in European aspen. Each dot gives the genotype-phenotype combination for an individual. The horizontal lines give the budset mean for each genotype and the vertical lines show the inter-quartile range. The dotted line gives the linear regression of phenotype on genotype. Thanks to Pär Ingvarsson for sharing these data from WANG *et al.* (2018).

2382 types at a particular SNP (l):

$$X \sim \mu + a_l G_l \quad (4.1)$$

2384 In the equation above, X is a vector of the phenotypes of a set of
2386 individuals and G_l is our vector of genotypes at locus l , with $G_{i,l}$
2388 taking the value 0, 1, or 2 depending on whether our individual i is
2390 homozygote, heterozygote, or the alternate homozygote at our locus of
2392 interest. Here μ is our phenotypic mean. The slope of this regression
2394 line (a_l) has the interpretation of being the average effect of substitut-
2396 ing a copy of allele 2 for a copy of allele 1. In our Aspen example the
2398 slope is -13.6 , i.e. swapping a single T for a G allele moves the budset
2400 forward by 13.6 days, such that the GG homozygote is predicted to set
 buds 27.2 days earlier than the TT homozygote.

2394 As a measure of the significance of this genotype-phenotype rela-
2396 tionship, we can calculate the p-value of our regression. To try and
2398 identify loci that are associated with our trait genome-wide, we can
2400 conduct this regression at each SNP we genotype in the genome.
 One common way to display the results of such an analysis (called
2398 a genome-wide association study or GWAS for short) is to plot the
2400 logarithm of the p-value for each SNP along genome (a so-called Man-
 hattan plot). Here's one from WANG *et al.* (2018) for their Aspen
 budset phenotype

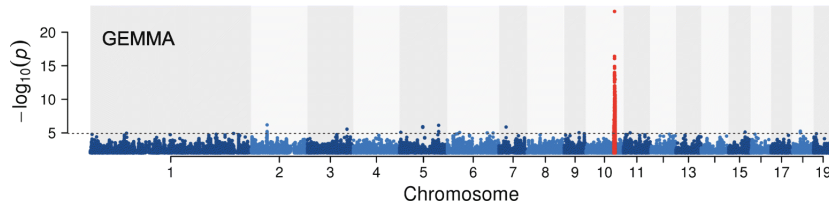


Figure 4.3: Manhattan plot of the p-value of the linear association between genotype and budset in Aspen. Each dot represents the test at a single SNP, plotted at its physical coordinate in the genome. Different chromosomes are plotted in alternating colours. The SNPs surrounding the PtFT2 gene are shown in red. From WANG *et al.* (2018), licensed under CC BY 4.0.

2402 The SNP with the most significant p-value is the PtFT2 SNP. Note
2404 that other SNPs in the surrounding region also light up as showing a
2406 significant association with budset timing. This is because loci that
2408 are in LD with a functional locus may in turn show an association,
2410 not because they directly affect the phenotype, but simply because
 the genotypes at the two loci are themselves non-randomly associated.
 Below is a zoomed in version (Figure 2 in WANG *et al.* (2018)) with
2412 SNPs coloured by the strength of their LD with the putatively func-
2414 tional SNP. Note how SNPs in strong LD with the functional allele
 (redder points) have more significant p-values.

2412 Variation in some traits seems to have a relatively simple genetic
2414 basis. In our Aspen example there is one clear large-effect locus, which
 explains 62% of the variation in budset. Note that even in this case,
 where we have an allele with a very strong effect on a phenotype, this

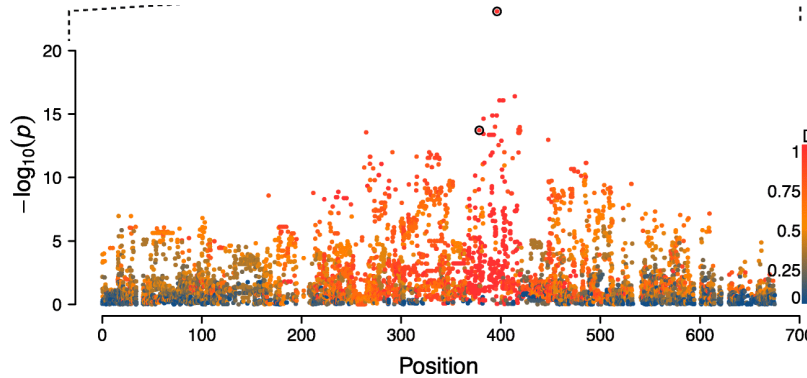


Figure 4.4: The Manhattan plot zoomed in on the top-hit (red SNPs from Figure 4.3). SNPs are now coloured by their D_f value with the most significant SNP. D_f is the LD covariance between a pair of loci (D) normalized by the largest value D can take given the allele frequencies. Figure from WANG *et al.* (2018), licensed under CC BY 4.0.

2416 is not an allele *for* budset, nor is PtFT2 a gene *for* budset. It is an
 2417 allele that is associated with budset in the sampled environments and
 2418 populations. In a different set of environments, this allele's effects
 2419 may be far smaller, and a different set of alleles may contribute to
 2420 phenotype variation. PtFT2, the gene our focal SNP falls close to, is
 2421 just one of many genes and molecular pathways involved in budset.
 2422 A mutant screen for budset may uncover many genes with larger ef-
 2423 fects; this gene is just a locus that happens to be polymorphic in this
 2424 particular set of genotyped individuals.

While phenotypic variation for some phenotypes has a relatively
 2425 simple genetic basis, many phenotypes are likely much more genetically
 2426 complex, involving the functional effect of many alleles at hun-
 2427 dreds or thousands of polymorphic loci. For example hundreds of
 2428 small effect loci affecting human height have been mapped in Euro-
 2429 pean populations to date. Such genetically complex traits are called
 2430 polygenic traits.

2432 In this chapter, we will use our understanding of the sharing of
 2433 alleles between relatives to understand the phenotypic resemblance
 2434 between relatives in quantitative phenotypes. This will allow us to
 2435 understand the contribution of genetic variation to phenotypic varia-
 2436 tion. In the next chapter, we will then use these results to understand
 2437 the evolutionary change in quantitative phenotypes in response to
 2438 selection.

4.0.1 A simple additive model of a trait

2440 Let's imagine that the genetic component of the variation in our trait
 2441 is controlled by L autosomal loci that act in an additive manner. The
 2442 frequency of allele 1 at locus l is p_l , with each copy of allele 1 at this
 2443 locus increasing your trait value by a_l above the population mean.
 2444 The phenotype of an individual, let's call her i , is X_i . Her genotype
 2445 at SNP l is $G_{i,l}$. Here $G_{i,l} = 0, 1$, or 2 , representing the number of

"All that we mean when we speak of a gene [allele] for pink eyes is, a gene which differentiates a pink eyed fly from a normal one —not a gene [allele] which produces pink eyes per se, for the character pink eyes is dependent on the action of many other genes." - STURTEVANT (1915)

²⁴⁴⁶ copies of allele 1 she has at this SNP. Her expected phenotype, given her genotype at all L SNPs, is then

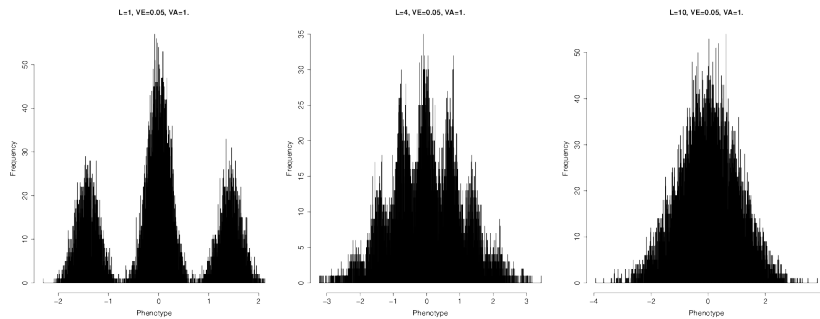
$$\mathbb{E}(X_i|G_{i,1}, \dots, G_{i,L}) = \mu + X_{A,i} = \mu + \sum_{l=1}^L G_{i,l}a_l \quad (4.2)$$

²⁴⁴⁸ where μ is the mean phenotype in our population, and $X_{A,i}$ is the deviation away from the mean phenotype due to her genotype. Now ²⁴⁵⁰ in reality the phenotype is a function of the expression of those alleles in a particular environment. Therefore, we can think of this expected ²⁴⁵² phenotype as being an average across a set of environments that occur in the population.

²⁴⁵⁴ When we measure our individual's observed phenotype we see

$$X_i = \mu + X_{A,i} + X_{E,i} \quad (4.3)$$

²⁴⁵⁶ where X_E is the deviation from the mean phenotype due to the environment. This X_E includes the systematic effects of the environment our individual finds herself in and all of the noise during development, ²⁴⁵⁸ growth, and the various random insults that life throws at our individual. If a reasonable number of loci contribute to variation in our ²⁴⁶⁰ trait then we can approximate the distribution of $X_{A,i}$ by a normal distribution due to the central limit theorem (see Figure 4.5). Thus if we can approximate the distribution of the effect of environmental ²⁴⁶² variation on our trait ($X_{E,i}$) also by a normal distribution, which is reasonable as there are many small environmental effects, then the ²⁴⁶⁴ distribution of phenotypes within the population (X_i) will be normally distributed (see Figure 4.5).



²⁴⁶⁸ Note that as this is an additive model; we can decompose eqn. 4.3 into the effects of the two alleles at each locus and rewrite it as

$$X_i = \mu + X_{iM} + X_{iP} + X_{iE} \quad (4.4)$$

²⁴⁷⁰ where X_{iM} and X_{iP} are the contribution to the phenotype of the alleles that our individual received from her mother (maternal alleles) and

Figure 4.5: The convergence of the phenotypic distribution to a normal distribution. Each of the three histograms shows the distribution of the phenotype in a large sample, for increasingly large numbers of loci ($L = 1, 4, \text{ and } 10$, with the proportion of variance explained held at $V_A = 1$). I have simulated each individual's phenotype following equations 4.2 and 4.3. Specifically, we've simulated each individual's biallelic genotype at L loci, assuming Hardy-Weinberg proportions and that the allele is at 50% frequency. We assume that all of the alleles have equal effects and combine them additively together. We then add an environmental contribution, which is normally distributed with variance 0.05. Note that in the left two pictures you can see peaks corresponding to different genotypes due to our low environmental noise (in practice we can rarely see such peaks for real quantitative phenotypes). Code here.

father (paternal alleles) respectively. This will come in handy in just
 2472 a moment when we start thinking about the phenotypic covariance of relatives.

2474 Now obviously this model seems silly at first sight as alleles don't
 only act in an additive manner, as they interact with alleles at the
 2476 same loci (dominance) and at different loci (epistasis). Later we'll
 relax this assumption, however, we'll find that if we are interested
 2478 in evolutionary change over short time-scales it is actually only the
 "additive component" of genetic variation that will (usually) concern
 2480 us. We will define this more formally later on, but for the moment
 we can offer the intuition that parents only get to pass on a single
 2482 allele at each locus on to the next generation. As such, it is the effect
 of these transmitted alleles, averaged over possible matings, that is
 2484 an individual's average contribution to the next generation (i.e. the
 additive effect of the alleles that their genotype consists of).

2486 *4.0.2 Additive genetic variance and heritability*

As we are talking about an additive genetic model, we'll talk about
 2488 the additive genetic variance (V_A), the phenotypic variance due to the
 additive effects of segregating genetic variation. This is a subset of the
 2490 total genetic variance if we allow for non-additive effects.

The variance of our phenotype across individuals (V) we can write
 2492 as

$$V = \text{Var}(X_A) + \text{Var}(X_E) = V_A + V_E \quad (4.5)$$

In writing the phenotypic variance as a sum of the additive and environmental contributions, we are assuming that there is no covariance
 2494 between $X_{G,i}$ and $X_{E,i}$ i.e. there is no covariance between genotype
 2496 and environment.

Our additive genetic variance can be written as

$$V_A = \sum_{l=1}^L \text{Var}(G_{i,l}a_l) \quad (4.6)$$

2498 where $\text{Var}(G_{i,l}a_l)$ is the contribution of locus l to the additive variance
 among individuals. Assuming random mating, and that our loci
 2500 are in linkage equilibrium, we can write our additive genetic variance
 as

$$V_A = \sum_{l=1}^L a_l^2 2p_l(1 - p_l) \quad (4.7)$$

2502 where the $2p_l(1 - p_l)$ term follows from the binomial sampling of two
 alleles per individual at each locus.

2504 **Question 1.** You have two biallelic SNPs contributing to variance
 in human height. At the first SNP you have an allele with an additive

2506 effect of 5cm which is found at a frequency of 1/10,000. At the second
 2508 SNP you have an allele with an additive effect of -0.5cm segregat-
 ing at 50% frequency. Which SNP contributes more to the additive
 genetic variance? Explain the intuition of your answer.

2510 *An example of calculating polygenic scores.* Now we don't usually
 get to see the individual loci contributing to highly polygenic traits.
 2512 Instead, we only get to see the distribution of the trait in the popu-
 lation. However, with the advent of GWAS in human genetics we can
 2514 see some of the underlying genetics using the many trait-associated
 loci identified to date. Using the estimated effect sizes at each locus,
 2516 each one of which is tiny, we can calculate the weighted sum over an
 individual's genotype as in equation 4.2. This weighted sum is called
 2518 the individual's polygenic score. To illustrate how polygenic scores
 work, we can take a set of 1700 SNPs, each chosen as the SNP with
 2520 the strongest signal of association with height in 1700 roughly inde-
 pendent bins spaced across the genome. The effects of these SNPs are
 2522 tiny; the medium, absolute additive effect size is 0.07cm. Figure 4.6
 shows the distribution of a thousand individuals' polygenic scores cal-
 2524 culated using these 1700 SNPs (simulated genotypes using the UKBB
 frequencies). The standard deviation of these polygenic scores $\sim 2\text{cm}$.
 2526 The individuals with higher polygenic scores for height are predicted
 to be taller than the individuals with lower polygenic scores.

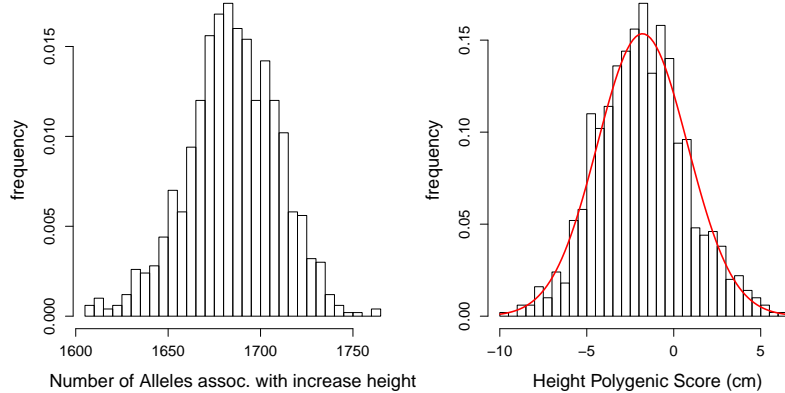


Figure 4.6: **Left)** The distribution of the number of height-increasing alleles that individuals carry at 1700 SNPs associated with height in the UK Biobank, for a sample of 1000 individuals. **right)** The distribution of the polygenic scores for these 1000 individuals. Plotted on top is a normal distribution with the same mean and variance. The empirical variance of these polygenic scores is 0.13, the additive genetic variance calculated by equation (4.7) is 0.135, so the two are in good agreement. Code here.

2528 *The narrow sense heritability* We would like a way to think about
 what proportion of the variation in our phenotype across individuals
 2530 is due to genetic differences as opposed to environmental differences.
 Such a quantity will be key in helping us think about the evolution of

2532 phenotypes. For example, if variation in our phenotype had no genetic basis, then no matter how much selection changes the mean phenotype
 2534 within a generation the trait will not change over generations.

We'll call the proportion of the variance that is genetic the *heritability*, and denote it by h^2 . We can then write heritability as

$$h^2 = \frac{Var(X_A)}{V} = \frac{V_A}{V} \quad (4.8)$$

Remember that we are thinking about a trait where all of the alleles
 2538 act in a perfectly additive manner. In this case our heritability h^2
 is referred to as the *narrow sense heritability*, the proportion of the
 2540 variance explained by the additive effect of our loci. When we allow
 dominance and epistasis into our model, we'll also have to define the
 2542 *broad sense heritability* (the total proportion of the phenotypic variance
 attributable to genetic variation).

The narrow sense heritability of a trait is a useful quantity; indeed
 2544 we'll see shortly that it is exactly what we need to understand the
 2546 evolutionary response to selection on a quantitative phenotype. We
 can calculate the narrow sense heritability by using the resemblance
 2548 between relatives. For example, if the phenotypic differences between
 individuals in our population were solely determined by environmental
 2550 differences experienced by these different individuals, we should not
 expect relatives to resemble each other any more than random individ-
 2552 uals drawn from the population. Now the obvious caveat here is that
 relatives also share an environment, so may resemble each other due to
 2554 shared environmental effects.

Note that the heritability is a property of a sample from the pop-
 2556 ulation in a particular set of environments at a particular time.

Changes in the environment may change the phenotypic variance.
 2558 Changes in the environment may also change how our genetic alleles
 are expressed through development and so change V_A . Thus estimates
 2560 of heritability are not transferable across environments or populations.

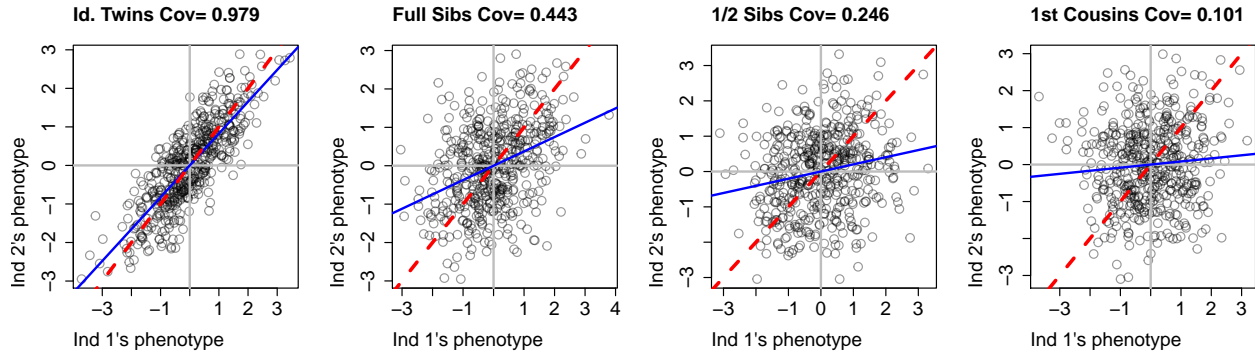
4.0.3 The covariance between relatives

2562 So we'll go ahead and calculate the covariance in phenotype between
 two individuals (1 and 2) who have phenotypes X_1 and X_2 respec-
 2564 tively. To think about imagine plotting the phenotypes of, say, sisters
 against each other. The x and y coordinates of each point will be
 2566 the, say, heights of the pair of siblings. Do tall women tend to have
 tall sisters, do short women tend to have short sisters? How much do
 2568 their phenotypes covary. If some of the variation in our phenotype is
 genetic we expect identical twins to resemble each other more than
 2570 full siblings, who in turn will resemble each other more than half-sibs
 and so on out (see Figure 4.7). Under our simple additive model of

2572 phenotypes we can write the covariance as

$$\text{Cov}(X_1, X_2) = \text{Cov}((X_{1M} + X_{1P} + X_{1E}), ((X_{2M} + X_{2P} + X_{2E})) \quad (4.9)$$

We can expand this out in terms of the covariance between the various
2574 components in these sums.



To make our task easier, we will make two commonly made assumptions:
2576

1. We can ignore the covariance of the environments between individuals (i.e. $\text{Cov}(X_{1E}, X_{2E}) = 0$)
2. We can ignore the covariance between the environment of one individual and the genetic variation in another individual (i.e. $\text{Cov}(X_{1E}, (X_{2M} + X_{2P})) = 0$). (We can actually incorporate these effects in later if we choose too.)

The failure of these assumptions to hold can undermine our estimates of heritability, but we'll return to that later. Moving forward
2584 with these assumptions, we can simplify our original expression above
2586 and write our phenotypic covariance between our pair of individuals as

$$\text{Cov}(X_1, X_2) = \text{Cov}((X_{1M}, X_{2M}) + \text{Cov}(X_{1M}, X_{2P}) + \text{Cov}(X_{1P}, X_{2M}) + \text{Cov}(X_{1P}, X_{2P}) \quad (4.10)$$

This equation is saying that, under our simple additive model, we can
2588 see the covariance in phenotypes between individuals as the covariance
2590 between the maternal and paternal allelic effects in our individuals.
We can use our results about the sharing of alleles between relatives to
2592 obtain these covariance terms. But before we write down the general case, let's quickly work through some examples.

2594 The covariance between identical twins Let's first consider the case of a pair of identical twins from two unrelated parents. Our pair of

Figure 4.7: Covariance of phenotypes between pairs of individuals of a given relatedness. Each point gives the phenotypes of a different pair of individuals. The additive genetic variance is held constant at $V_A = 1$, such that the expected covariances ($2F_{1,2}V_A$) should be 1, 0.5, 0.25, and 0.125 respectively din good agreement with the empirical covariances reported in the title of each graph. The data were simulated as described in the caption of Figure 4.5. The blue line shows $x = y$ and the red line shows the best fitting linear regression line. Code here.

2596 twins share their maternal and paternal allele identical by descent
 $(X_{1M} = X_{2M}$ and $X_{1P} = X_{2P})$. As their maternal and paternal alleles
 2598 are not correlated draws from the population, i.e. have no probability
 of being *IBD* as we've said the parents are unrelated, the covariance
 2600 between their effects on the phenotype is zero (i.e. $Cov(X_{1P}, X_{2M}) =$
 $Cov(X_{1M}, X_{2P}) = 0$). In that case, eqn. 4.10 is

$$Cov(X_1, X_2) = Cov((X_{1M}, X_{2M}) + Cov(X_{1P}, X_{2P}) = 2Var(X_{1M}) = V_A \quad (4.11)$$

2602 Now in general identical twins are not going to be super helpful for
 us in estimating h^2 , because under models with non-additive effects,
 2604 identical twins will have higher covariance than we'd expect just based
 on the alleles they share. This is because identical twins don't just
 2606 share alleles, they share their entire genotypes, and thus resemble each
 other in phenotype also because of shared dominance effects.

2608 *The covariance in phenotype between mother and child* If a mother
 and father are unrelated individuals (i.e. are two random draws from
 2610 the population) then this mother and her child share one allele IBD
 at each locus (i.e. $r_1 = 1$ and $r_0 = r_2 = 0$). Half the time our
 2612 mother (ind 1) transmits her paternal allele to the child (ind 2), in
 which case $X_{P1} = X_{M2}$, and so $Cov(X_{P1}, X_{M2}) = Var(X_{P1})$,
 2614 and all the other covariances in eqn. 4.10 are zero. The other half
 of the time she transmits her maternal allele to the child, in which
 2616 case $Cov(X_{M1}, X_{M2}) = Var(X_{M1})$ and all the other terms are zero.
 By this argument, $Cov(X_1, X_2) = \frac{1}{2}Var(X_{M1}) + \frac{1}{2}Var(X_{P1}) = \frac{1}{2}V_A$.

2618 *The covariance between general pairs of relatives under an additive
 model* The two examples above make clear that to understand
 2620 the covariance between phenotypes of relatives, we simply need
 to think about the alleles they share IBD. Consider a pair of rel-
 2622 atives (1 and 2) with a probability r_0 , r_1 , and r_2 of sharing zero,
 one, or two alleles IBD respectively. When they share zero alleles
 2624 $Cov((X_{1M} + X_{1P}), (X_{2M} + X_{2P})) = 0$, when they share one allele
 $Cov((X_{1M} + X_{1P}), (X_{2M} + X_{2P})) = Var(X_{1M}) = \frac{1}{2}V_A$, and when they
 2626 share two alleles $Cov((X_{1M} + X_{1P}), (X_{2M} + X_{2P})) = V_A$. Therefore,
 the general covariance between two relatives is

$$Cov(X_1, X_2) = r_0 \times 0 + r_1 \frac{1}{2}V_A + r_2 V_A = 2F_{1,2}V_A \quad (4.12)$$

2628 So under a simple additive model of the genetic basis of a pheno-
 type, to measure the narrow sense heritability we need to measure the
 2630 covariance between pairs of relatives (assuming that we can remove
 the effect of shared environmental noise). From the covariance be-
 2632 tween relatives we can calculate V_A , and we can then divide this by
 the total phenotypic variance to get h^2 .

2634 **Question 2.** A) In polygynous red-winged blackbird populations
 (i.e. males mate with several females), paternal half-sibs can be iden-
 2636 tified. Suppose that the covariance of tarsus lengths among half-sibs
 is 0.25 cm^2 and that the total phenotypic variance is 4 cm^2 . Use these
 2638 data to estimate h^2 for tarsus length in this population.

2640 B) Why might paternal half-sibs be preferable for measuring heri-
 tability than maternal half-sibs?

2642 *Parent-midpoint offspring regression* Another way that we can esti-
 mate the narrow sense heritability is through the regression of child's
 2644 phenotype on the parental mid-point phenotype. The parental mid-
 point phenotype is simply the average of the mum and dad's pheno-
 type. We denote the child's phenotype by X_{kid} and mid-point phe-
 2646 notype by X_{mid} , so that if we take the regression $X_{kid} \sim X_{mid}$ this
 regression has slope $\beta = \text{Cov}(X_{kid}, X_{mid})/\text{Var}(X_{mid})$. The covari-
 2648 ance of $\text{Cov}(X_{kid}, X_{mid}) = \frac{1}{2}V_A$, and $\text{Var}(X_{mid}) = \frac{1}{2}V$, as by taking
 the average of the parents we have halved the variance, such that the
 2650 slope of the regression is

$$\beta_{mid,kid} = \frac{\text{Cov}(X_{kid}, X_{mid})}{\text{Var}(X_{mid})} = \frac{V_A}{V} = h^2 \quad (4.13)$$

2652 i.e. the regression of the child's phenotype on the parental midpoint
 phenotype is an estimate of the narrow sense heritability. This way of
 estimating heritability has the problem of not controlling for environ-
 2654 mental correlations between relatives. But it's a useful way to think
 about heritability and will be directly relevant to our discussion of the
 2656 response to selection in the next chapter.

2658 Our regression allows us to attempt to predict the phenotype of
 the child given the phenotypes of the parents; how well we can do this
 depends on the slope. If the slope is close to zero then the parental
 2660 phenotypes hold no information about the phenotype of the child,
 while if the slope is close to one then the parental mid-point is a good
 2662 guess at the child's phenotype.

2664 More formally, the expected phenotype of the child given the
 parental phenotypes is

$$\mathbb{E}(X_{kid}|X_{mum}, X_{dad}) = \mu + \beta_{mid,kid}(X_{mid} - \mu) = \mu + h^2(X_{mid} - \mu) \quad (4.14)$$

2666 which follows from the definition of linear regression. So to find the
 child's predicted phenotype, we simply take the mean phenotype and
 add on the difference between our parental mid-point and the popula-
 2668 tion mean, multiplied by our narrow sense heritability.

2670 **Question 3.** Briefly explain what Galton meant by 'regression
 towards mediocrity', and why he observed this pattern in light of
 Mendelian inheritance.



Figure 4.8: Red-winged blackbird and Tricoloured Red-winged blackbirds (*Agelaius phoeniceus* and *Agelaius tricolor*).

Bird-lore (1899). National Association of Audubon Societies for the Protection of Wild Birds and Animals. Image from the Biodiversity Heritage Library. Contributed by American Museum of Natural History Library. Not in copyright.

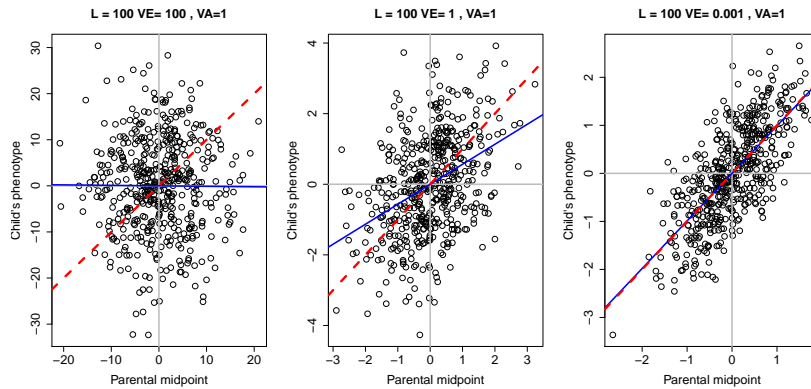


Figure 4.9: Regression of child's phenotype of the parental mid-point phenotype. The three panels show decreasing levels of environmental variance (V_E) holding the additive genetic variance constant ($V_A = 1$). In these figures, we simulate 100 loci, as described in the caption of Figure 4.5. We simulate the genotypes and phenotypes of the two parents, and then simulate the child's genotype following mendelian transmission. The blue line shows $x = y$ and the red line shows the best fitting linear regression line. Code here.

2672 *Estimating additive genetic variance across a variety of different relationships.* In many natural populations we may have access to
 2674 individuals with a range of different relationships to each other (e.g. through monitoring of the paternity of individuals), but relatively few
 2676 pairs of individuals for a specific relationship (e.g. sibs). We can try and use this information on various relatives as fully as possible in a
 2678 mixed model framework. Building from equation 4.3, we can write an individual's phenotype X_i as

$$X_i = \mu + X_{A,i} + X_{E,i} \quad (4.15)$$

2680 where $X_{E,i} \sim N(0, V_E)$ and $X_{A,i}$ is normally distributed across individuals with covariance matrix $V_A A$, where the entries for a pair
 2682 of individuals i and j are $A_{ij} = 2F_{i,j}$ and $A_{ii} = 1$. Given the matrix
 2684 A we can estimate V_A . We can also add fixed effects into this model to account for generation effects, additional mixed effects could also
 2686 be included to account for shared environments between particular individuals (e.g. a shared nest). This approach is sometimes called the
 2688 "animal model".

2688 4.1 Multiple traits

Traits often covary with each other, both due to environmentally induced effects (e.g. due to the effects of diet on multiple traits) and due to the expression of underlying genetic covariance between traits.
 2690 Genetic covariance, in turn, can reflect pleiotropy, a mechanistic effect of an allele on multiple traits (e.g. variants that affect skin pigmentation often affect hair color), the genetic linkage of loci independently
 2692 affecting multiple traits, or the effects of assortative mating.
 2694

2696 Consider two traits $X_{1,i}$ and $X_{2,i}$ in an individual i . These traits
 could be, say, the individual's leg length and nose length. As before,
 2698 we can write these as

$$\begin{aligned} X_{1,i} &= \mu_1 + X_{1,A,i} + X_{1,E,i} \\ X_{2,i} &= \mu_2 + X_{2,A,i} + X_{2,E,i} \end{aligned} \quad (4.16)$$

As before we can talk about the total phenotypic variance (V_1, V_2),
 2700 environmental variance ($V_{1,E}$ and $V_{2,E}$), and the additive genetic
 variance for trait one and two ($V_{1,A}, V_{2,A}$). But now we also have
 2702 to consider the total covariance between trait one and trait two,
 $V_{1,2} = \text{Cov}(X_1, X_2)$, as well as the environmentally induced covariance
 2704 ($V_{E,1,2} = \text{Cov}(X_{1,E}, X_{2,E})$) and the additive genetic covariance
 $(V_{A,1,2} = \text{Cov}(X_{1,A}, X_{2,A}))$. To better understand the covariance arising
 2706 due to pleiotropy, let's think about a set of L SNPs contributing
 to our two traits. If the additive effect of an allele at the i^{th} SNP is
 2708 $\alpha_{i,1}$ and $\alpha_{i,2}$ on traits 1 and 2, then the additive covariance between
 our traits is

$$V_{A,1,2} = \sum_{i=1}^L 2\alpha_{i,1}\alpha_{i,2}p_i(1-p_i) \quad (4.17)$$

2710 assuming our loci are in linkage disequilibrium. Thus a genetic correlation arises due to pleiotropy, because loci that tend to affect trait 1
 2712 also systematically affect trait 2. For example, alleles associated with later Age at Menarche (AAM) in European females also tend to be
 2714 positively associated with height (see Figure 4.10), thereby creating a genetic correlation between AAM and height.

2716 We can store our variance and covariance values in matrices, a way of gathering these terms that will be useful when we discuss selection:

$$\mathbf{V} = \begin{pmatrix} V_1 & V_{1,2} \\ V_{1,2} & V_2 \end{pmatrix} \quad (4.18)$$

2718 and

$$\mathbf{G} = \begin{pmatrix} V_{1,A} & V_{A,1,2} \\ V_{A,1,2} & V_{2,A} \end{pmatrix} \quad (4.19)$$

Here we've shown the matrices for two traits, but we can generalize
 2720 this to an arbitrary number of traits.

We can estimate these quantities, in a similar way as before, by
 2722 studying the covariance in different traits between relatives:

$$\text{Cov}(X_{1,i}, X_{2,j}) = 2F_{i,j}V_{A,1,2} \quad (4.20)$$

We can also talk about the genetic correlation between two phenotypes
 2724

$$r_g = \frac{V_{A,1,2}}{\sqrt{V_{A,1}V_{A,2}}} \quad (4.21)$$

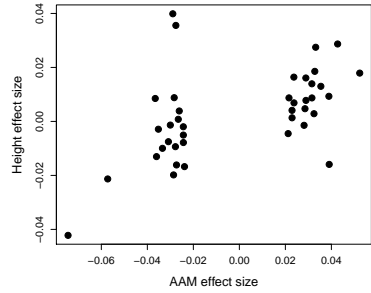


Figure 4.10: The additive effect sizes of loci associated with female Age at Menarche (AAM) and their effect size on Height in a European population. Data from PICKRELL *et al.* (2016). Code here.

where $V_{A,1}$ and $V_{A,2}$ are the additive genetic variance for trait 1 and 2 respectively. Here, r_g tells us to what extent the additive genetic variance in two traits is correlated.

One type of genetic covariance we often think about is the covariance of male and female phenotypes. For example, below is the relationship between the forehead patch size for Pied fly-catcher fathers and their sons and daughters. The phenotype has been standardized to have mean 0 and variance 1 in each group. The phenotypic covariance of the sample of fathers and sons is 0.35, while the phenotypic covariance of fathers and daughter is 0.23.

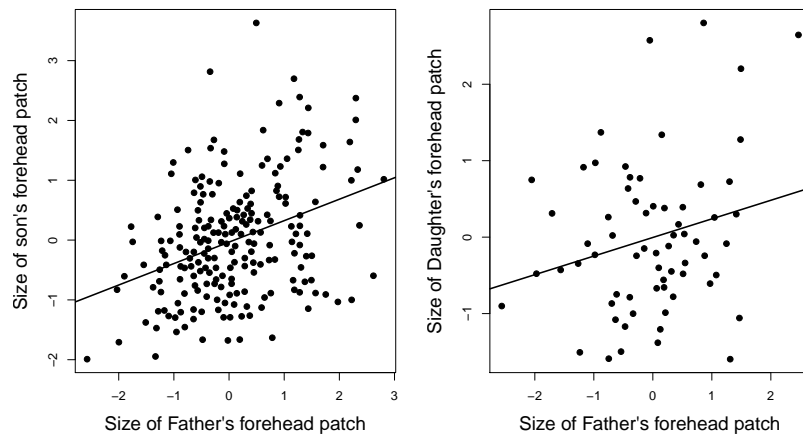


Figure 4.11: Relationship of standardized forehead patch size between fathers and sons and daughters in Pied fly-catchers. Data from POTTI and CANAL. Code here.



Figure 4.12: *Ficedula hypoleuca*, Pied fly-catcher.
Coloured illustrations of British birds, and their eggs (1842-1850). London :G.W. Nickisson. Image from the Biodiversity Heritage Library. Contributed by Smithsonian Libraries. Not in copyright.

Question 4. Assume we can ignore the effect of the shared environment in our Pied fly-catcher example.

A) What is the additive genetic covariance between male and female patch size?

B) What is the additive genetic correlation of male and female patch size? You can assume that the additive genetic variance is the same in males and females.

4.1.1 Non-additive variation.

Up to now we've assumed that our alleles contribute to our phenotype in an additive fashion. However, that does not have to be the case as there may be non-additivity among the alleles present at a locus (*dominance*) or among alleles at different loci (*epistasis*). We can accommodate these complications into our models. We do this by partitioning our total genetic variance into independent variance components.

2750 *Dominance.* To understand the effect of dominance, let's consider
2752 how the allele that a parent transmits influences their offspring's phe-
2754 notype. A parent transmits one of their two alleles at a locus to their
2756 offspring. Assuming that individuals mate at random, this allele is
2758 paired with another allele drawn at random from the population. For
2760 example, assume your mother transmitted an allele 1 to you: with
2762 probability p it would be paired with another allele 1, and you would
2764 be a homozygote; and with probability q it's paired with a 2 allele and
2766 you're a heterozygote.

2768 Now consider an autosomal biallelic locus ℓ , with frequency p for
2770 allele 1, and genotypes 0, 1, and 2 corresponding to how many copies
2772 of allele 1 individuals carry. We'll denote the mean phenotype of an
2774 individual with genotype 0, 1, and 2 as $\bar{X}_{\ell,0}$, $\bar{X}_{\ell,1}$, $\bar{X}_{\ell,2}$ respectively.
2776 This mean is taking an average phenotype over all the environments
2778 and genetic backgrounds the alleles are present on. We'll mean center
2780 (MC) these phenotypic values, setting $\bar{X}'_{\ell,0} = \bar{X}_{\ell,0} - \mu$, and likewise
2782 for the other genotypes.

2784 We can think about the average (marginal) MC phenotype of an
2786 individual who received an allele 1 from their parent as the average
2788 of the MC phenotype for heterozygotes and 11 homozygotes, weighted
2790 by the probability that the individual has these genotypes, i.e. the
2792 probability they receive an additional allele 1 or an allele 2 from their
2794 other parent:

$$a_{\ell,1} = p\bar{X}'_{\ell,2} + q\bar{X}'_{\ell,1}, \quad (4.22)$$

2796 Similarly, if your parent transmitted an 2 allele to you, your average
2798 MC phenotype would be

$$a_{\ell,2} = p\bar{X}'_{\ell,1} + q\bar{X}'_{\ell,0} \quad (4.23)$$

2798 Let's now consider the average phenotype of an offspring of each of
2800 our three genotypes

genotype:	0,	1,	2.
additive genetic value:	$a_{\ell,2} + a_{\ell,2}$,	$a_{\ell,1} + a_{\ell,2}$,	$a_{\ell,1} + a_{\ell,1}$

2802 i.e. the mean phenotype of each genotypes' offspring averaged over
2804 all possible matings to other individuals in the population (assuming
2806 individuals mate at random). These are the additive MC genetic
2808 values (breeding values) of our genotypes. Here we are simply adding
2810 up the additive contributions of the alleles present in each genotype
2812 and ignoring any non-additive effects of genotype.

2814 To illustrate this, in Figure 4.13 we plot two different cases of dom-
2816 inance relationships; in the top row an additive polymorphism and in
2818 the second row a fully dominant allele. The additive genetic values of
2820 the genotypes are shown as red dots. Note that the additive values of
2822 the genotypes line up with the observed MC phenotypic means in the



Figure 4.13: The average mean-centered (MC) phenotypes of each genotype. **Top Row:** Additive relationship between genotype and phenotype. **Bottom Row:** Allele 1 is dominant over allele 2, such that the heterozygote has the same phenotype as the 22 genotype (2). The area of each circle is proportion to the fraction of the population in each genotypic class (p^2 , $2pq$, and q^2). One the left column $p = 0.1$ and the right column is $p = 0.9$. The additive genetic values of the genotypes are shown as red dots. The regression between phenotype and additive genotype is shown as a red line. The black vertical arrows show the difference between the average MC phenotype and additive genetic value for each genotype. Code here.

top row, when our alleles interact in a completely additive manner.

2790 Our additive genetic values always fall along a linear line (the red line in our figure). The additive values are falling along the best fitting line
 2792 of linear regression for our population, when phenotype is regressed
 against the additive genotype (0, 1, 2 copies of allele 1) across all in-
 2794 dividuals in our population. Note in the dominant case the additive
 2796 genetic values differ from the observed phenotypic means, and are
 closer to the observed values for the genotypes that are most common
 in the population.

2798 The difference in the additive effect of the two alleles $a_{\ell,2} - a_{\ell,1}$
 2800 can be interpreted as an average effect of swapping an allele 1 for an
 2802 allele 2; we'll call this difference $\alpha_{\ell} = a_{\ell,2} - a_{\ell,1}$. Our α_{ℓ} is also the
 slope of the regression of phenotype against genotype (the red line
 2804 in Figure 4.13). Note that the slope of our regression of phenotype
 on genotype (α_{ℓ}) does not depend on the population allele frequency
 2806 for our completely additive locus (top row of 4.13). In contrast, when
 there is dominance, the slope between genotype and phenotype (α_{ℓ})
 2808 is a function of allele frequency (bottom row of 4.13). When a domi-
 nant allele (1) is rare there is a strong slope of phenotype on genotype,
 2810 bottom left Figure 4.13. This strong slope is because replacing a single
 copy of the 2 allele with a 1 allele in an individual has a big effect on
 2812 average phenotype, as it will most likely move an individual from be-
 ing a 22 homozygote to being a 12 heterozygote. In contrast, when the
 dominant allele (1) is common in the population, replacing a 2 allele
 by a 1 allele in an individual on average has little phenotypic effect,

2814 leading to a weak slope bottom right Figure 4.13. This small effect is
2815 because as we are mainly turning heterozygotes into homozygotes (11),
2816 who have the same mean phenotype as each other.

2817 As as an example of how dominance and population allele frequen-
2818 cies can change the additive effect of an allele, let's consider the ge-
2819 netics of the age of sexual maturity in Atlantic Salmon. A single allele
2820 of large effect segregates in Atlantic Salmon that influences the sexual
2821 maturation rate in salmon (AYLLON *et al.*, 2015; BARSON *et al.*,
2822 2015), and hence the timing of their return from the sea to spawn
2823 (sea age). The allele falls close to the autosomal gene VGLL3 (COUS-
2824 MINER *et al.*, 2013, variation at this gene in humans also influences
2825 the timing of puberty). The left side of Figure 4.15 shows the age at
2826 sexual maturity in males. The allele (E) associated with slower sex-
2827 ual maturity is recessive in males. While the LL homozygotes mature
2828 on average a whole year later, the additive effect of the allele is weak
2829 while the L allele is rare in the population. The right panel shows
2830 the effect of the L allele in females. Note how the allele is much more
2831 dominant in females, and has a much more pronounced additive ef-
2832 fect. The dominance of an allele is not a fixed property of the allele
2833 but rather a statement of the relationship of genotype to phenotype,
2834 such that the dominance relationship between alleles may vary across
phenotypes and contexts (e.g. sexes).

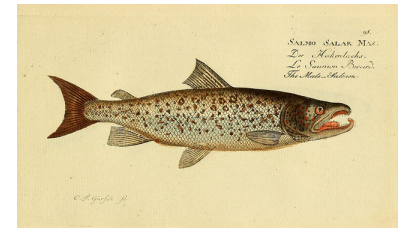


Figure 4.14: Atlantic Salmon (*Salmo salar*).

Histoire naturelle des poissons. 1796. Bloch, M. E. Image from the Biodiversity Heritage Library. Contributed by Ernst Mayr Library, Museum of Comparative Zoology. Not in copyright.

Figure 4.15: The average age at sexual maturity for each genotype, broken down by sex. The area of each circle is proportional to the fraction of the population in each genotypic class. The regression between phenotype and additive genotype is shown as a red line. Data from BARSON *et al.* (2015). Code here.

The variance in the population phenotype due to these additive breeding values at locus ℓ , assuming HW proportions, is

$$\begin{aligned}
V_{A,\ell} &= p^2(2a_{\ell,2})^2 + 2pq(a_{\ell,1} + a_{\ell,0})^2 + q^2(2a_{\ell,0})^2 \\
&= 2(pa_{\ell,1}^2 + qa_{\ell,2}^2) \\
&= 2pq\alpha_{\ell}^2
\end{aligned} \tag{4.24}$$

2836 The total additive variance for the whole genotype can be found by

summing the individual additive genetic variances over loci

$$V_A = \sum_{\ell=1}^L V_{A,\ell} = \sum_{\ell=1}^L 2p_\ell q_\ell \alpha_\ell^2. \quad (4.25)$$

Having assigned the additive genetic variance to be the variance explained by the additive contribution of the alleles at a locus, we define the dominance variance as the population variance among genotypes at a locus due to their deviation from additivity. We can calculate how much each genotypic mean deviates away from its additive prediction at locus ℓ (the length of the arrows in Figure 4.13). For example, the heterozygote deviates

$$d_{\ell,1} = \bar{X}'_{\ell,1} - (a_{\ell,1} + a_{\ell,2}) \quad (4.26)$$

away from its additive genetic value, with similar expressions for each of the homozygotes ($d_{\ell,0}$ and $d_{\ell,2}$). We can then write the dominance variance at our locus as the genotype-frequency weighted sum of our squared dominance deviations

$$V_{D,\ell} = p^2 d_{\ell,0}^2 + 2pq d_{\ell,1}^2 + q^2 d_{\ell,2}^2. \quad (4.27)$$

Writing our total dominance variance as the sum across loci

$$V_D = \sum_{\ell=1}^L V_{D,\ell}. \quad (4.28)$$

Having now partitioned all of the genetic variance into additive and dominant terms, we can write our total genetic variance as

$$V_G = V_A + V_D. \quad (4.29)$$

We can do this because by construction the covariance between our additive and dominant deviations for the genotypes is zero. We can define the narrow sense heritability as before $h^2 = V_A/V_P = V_A/(V_G + V_E)$, which is the proportion of phenotypic variance due to additive genetic variance. We can also define the total proportion of the phenotypic variance due to genetic differences among individuals, as the broad-sense heritability $H^2 = V_G/(V_G + V_E)$.

Relationship (i,j)*	$Cov(X_i, X_j)$
parent-child	$1/2V_A$
full siblings	$1/2V_A + 1/4V_D$
identical (monozygotic) twins	$V_A + V_D$
1 st cousins	$1/8V_A$

Table 4.1: Phenotypic covariance between some pairs of relatives, include the dominance variation. * Assuming this is the only relationship the pair of individuals share (above that expected from randomly sampling individuals from the population).

When dominance is present in the loci influencing our trait ($V_D > 0$), we need to modify our phenotype covariance among relatives to

account for this non-additivity. Specifically, our equation for the
 2862 covariance among a general pair of relatives (eqn. 4.12 for additive variation) becomes

$$\text{Cov}(X_1, X_2) = 2F_{1,2}V_A + r_2V_D \quad (4.30)$$

2864 where r_2 is the probability that the pair of individuals share 2 alleles identical by descent, making the same assumptions (other than
 2866 additivity) that we made in deriving eqn. 4.12. In table 4.1 we show the phenotypic covariance for some common pairs of relatives. The
 2868 regression of offspring phenotype on parental midpoint still has a slope V_A/V_P .

2870 Full sibs and parent-offspring have the same covariance if there
 2872 is no dominance variance (as they have the same kinship coefficient $F_{1,2}$). However, when dominance is present ($V_D > 0$), full-sibs resemble each other more than parent-offspring pairs. That's because
 2874 parents and offspring share precisely one allele, while full-sibs can share both alleles (i.e. the full genotype at a locus) identical by descent. We can attempt to estimate V_D by comparing different sets of relationships. For example, non-identical twins (full sibs born at same
 2876 time) should have 1/2 the phenotypic covariance of identical twins if $V_D = 0$. Therefore, we can attempt to estimate V_D by looking at
 2880 whether identical twins have more than twice the phenotypic covariance than non-identical twins.

2882 The most important aspect of this discussion for thinking about evolutionary genetics is that the parent-offspring covariance is still
 2884 only a function of V_A . This is because our parent (e.g. the mother) transmits only a single allele, at each locus, to its offspring. The other
 2886 allele the offspring receives is random (assuming random mating), as it comes from the other unrelated parent (the father). Therefore, the
 2888 average effect on the child's phenotype of an allele the child receives from their mother is averaged over all possible random alleles the child
 2890 could receive from their father (weighted by their frequency in the population). Thus we only care about the additive effect of the allele,
 2892 as parents transmit only alleles (not genotypes) to their offspring.
 This means that the short-term response to selection, as described by
 2894 the breeder's equation, depends only on V_A and the additive effect of alleles. Therefore, if we can estimate the narrow-sense heritability
 2896 we can predict the short-term response. However, if alleles display dominance, our value of V_A will change as alleles at our loci change in
 2898 frequency, e.g. as dominant alleles become common in the population their contribution to V_A decreases. Therefore, if there is dominance
 2900 our value of V_A will not be constant across generations.

Up to this point we have only considered dominance and not epistasis. However, we can include epistasis in a similar manner (for ex-

ample among pairs of loci). This gets a little tricky to think about,
2904 so we will only briefly explain it. We can first estimate the additive
effect of the alleles by considering the effect of the alleles averaging
2906 over their possible genetic backgrounds (including the other interact-
ing alleles they are possibly paired with), just as before. We can then
2908 calculate the additive genetic variance from this. We can estimate the
dominance variance, by calculating the residual variance among geno-
2910 types at a locus unexplained by the additive effect of the loci. We can
then estimate the epistatic variance by estimating the residual vari-
2912 ance left unexplained among the two locus genotypes after accounting
for the additive and dominant deviations calculated from each locus
2914 separately. In practice these high variance components are hard to
estimate, and usually small as much of our variance is assigned to the
2916 additive effect. Again we would find that we mostly care about V_A for
predicting short-term evolution, but that the contribution of loci to
2918 the additive genetic variance will depend on the epistatic relationships
among loci.

2920 **Question 5.** How could you use 1/2 sibs vs. full-sibs to estimate
 V_D ? Why might this be difficult in practice? Why are identical vs.
2922 non-identical twins better suited for this?

2924 **Question 6.** Can you construct a case where $V_A = 0$ and $V_D > 0$?
You need just describe it qualitatively; you don't need to work out the
math. (tricker question).

The Response to Phenotypic Selection

- ²⁹²⁸ Evolution by natural selection requires:
1. Variation in a phenotype

²⁹³⁰ 2. That survival is non-random with respect to this phenotypic variation.

²⁹³² 3. That this variation is heritable.

Points 1 and 2 encapsulate our idea of Natural Selection, but evolution by natural selection will only occur if the 3rd condition is also met.

²⁹³⁴ ¹ It is the heritable nature of variation that couples change within a generation due to natural selection to change across generations (evolutionary change).

²⁹³⁸ Let's start by thinking about the change within a generation due to directional selection, where selection acts to change the mean phenotype within a generation. For example, a decrease in mean height within a generation, due to taller organisms having a lower chance of surviving to reproduction than shorter organisms. Specifically, we'll denote our mean phenotype at reproduction by μ_S , i.e. after selection has acted, and our mean phenotype before selection acts by μ_{BS} . This second quantity may be hard to measure, as obviously selection acts throughout the life-cycle, so it might be easier to think of this as the mean phenotype if selection hadn't acted. So the change in mean phenotype within a generation is $\mu_S - \mu_{BS} = S$.

We are interested in predicting the distribution of phenotypes in the next generation. In particular, we are interested in the mean phenotype in the next generation to understand how directional selection has contributed to evolutionary change. We'll denote the mean phenotype in offspring, i.e. the mean phenotype in the next generation before selection acts, as μ_{NG} . The change across generations we'll call the response to selection R and put this equal to $\mu_{NG} - \mu_{BS}$.

²⁹⁵⁶ The mean phenotype in the next generation is

$$\mu_{NG} = \mathbb{E}(\mathbb{E}(X_{kid}|X_{mom}, X_{dad})) \quad (5.1)$$

See LEWONTIN (1970). Note that these requirements are not specific to DNA, i.e. the concept of evolution by natural selection is substrate independent.

¹ Some people consider natural selection to only operate on heritable phenotype variation and so require all three conditions to say that natural selection occurs. This is mostly a semantic point, however, it is useful to be able to distinguish the action of selection from a possible response.

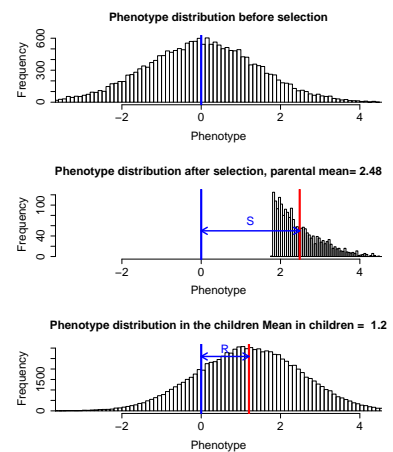


Figure 5.1: **Top.** Distribution of a phenotype in the parental population prior to selection, $V_A = V_E = 1$. **Middle.** Only individuals in the top 10% of the phenotypic distribution are selected to reproduce; the resulting shift in the phenotypic mean is S . **Bottom.** Phenotypic distribution of children of the selected parents; the shift in the mean phenotype is R . Code here.

where the outer expectation is over possible pairs of randomly mating individuals who survive to reproduce. We can use eqn. 4.14 to obtain an expression for this expectation:

$$\mu_{NG} = \mu_{BS} + \beta_{mid,kid}(\mathbb{E}(X_{mid}) - \mu_{BS}) \quad (5.2)$$

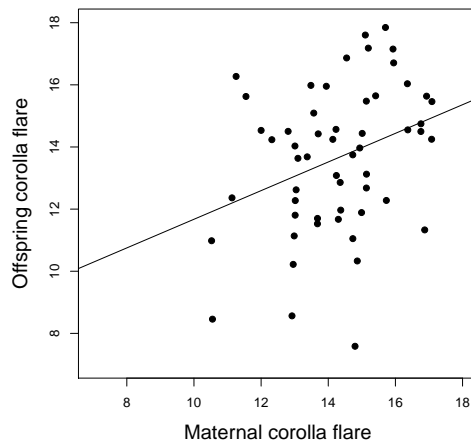
So to obtain μ_{NG} we need to compute $\mathbb{E}(X_{mid})$, the expected mid-point phenotype of pairs of individuals who survive to reproduce. Well this is just the expected phenotype in the individuals who survived to reproduce (μ_S), so

$$\mu_{NG} = \mu_{BS} + h^2(\mu_S - \mu_{BS}) \quad (5.3)$$

So we can write our response to selection as

$$R = \mu_{NG} - \mu_{BS} = h^2(\mu_S - \mu_{BS}) = h^2S \quad (5.4)$$

So our response to selection is proportional to our selection differential, and the constant of proportionality is the narrow sense heritability. This equation is sometimes termed the Breeder's equation. It is a statement that the evolutionary change across generations (R) is proportional to the change caused by directional selection within a generation (S), and that the strength of this relationship is determined by the narrow sense heritability (h^2).



Question 1. GALEN (1996) explored selection on flower shape in *P. viscosum*. She found that plants with larger corolla flare had more bumblebee visits, which resulted in higher seed set and a 17% increase in corolla flare in the plants contributing to the next generation. Based on the data in the caption of Figure 5.3 what is the expected response in the next generation?

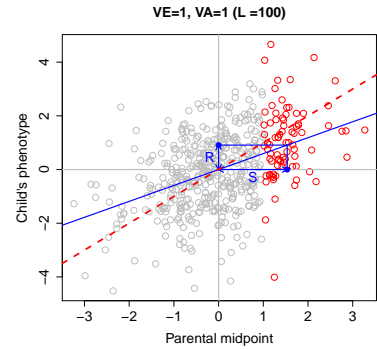


Figure 5.2: A visual representation of the Breeder's equation. Regression of child's phenotype on parental midpoint phenotype ($V_A = V_E = 1$). Under truncation selection, only individuals with phenotypes > 1 (red) are bred. [Code here](#).

Figure 5.3: The relationship between maternal and offspring corolla flare (flower width) in *P. viscosum*. From GALEN's data the covariance of mother and child is 1.3, while the variance of the mother is 2.8. Data from GALEN (1996). [Code here](#).



Figure 5.4: Sticky jacob's ladder (*Polemonium viscosum*). Flowers of Mountain and Plain (1920). Clements, E. Image from the Biodiversity Heritage Library. Contributed by New York Botanical Garden, Mertz Library. Not in copyright. Cropped from original.

2978 To understand the genetic basis of the response to selection take a look at Figure 5.5. The setup is the same as in our previous simulation figures. The individuals who are selected to form our next

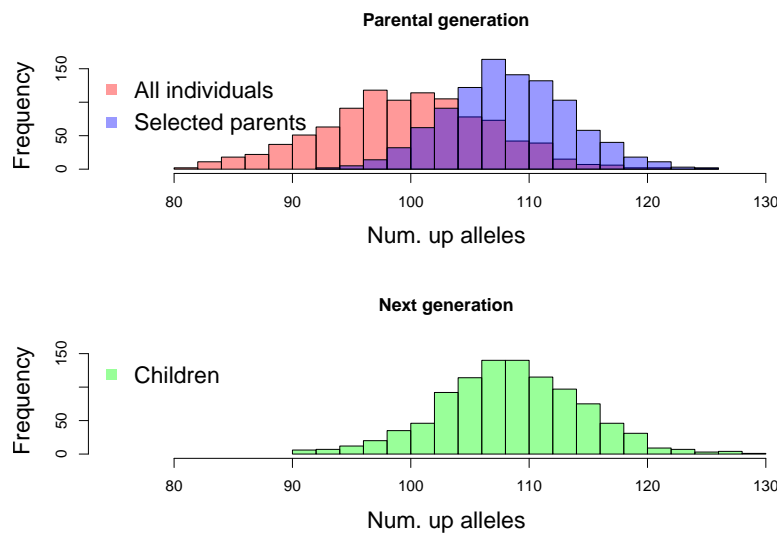


Figure 5.5: **Top.** Distribution of the number of up alleles in the parental population prior to selection (red), for the selected individuals the top 10% of the population (blue) **Bottom.** The same distribution for the offspring of the selected parents in the next generation (green). Code here.

2980 generation carry more alleles that increase the phenotype, in the current range of environments currently experienced by the population. 2982 The average individual before selection carried 100 of these ‘up’ alleles, the average individual surviving selection 108 ‘up’ alleles. As 2984 individuals faithfully transmit their alleles to the next generation the average child of the selected parents carries 108 up alleles. Note that 2986 the variance has changed little, the children have plenty of variation in 2988 their genotype, such that selection can readily drive evolution in future generations. The average frequency of an ‘up’ allele has changed from 2990 50% to 54%. Our gains due to selection will be stably inherited to 2992 future generations.

2992 *The long-term response to selection* If our selection pressure is sustained over many generations, we can use our breeder’s equation to 2994 predict the response. If we are willing to assume that our heritability does not change and we maintain a constant selection gradient, then 2996 after n generations our phenotype mean will have shifted

$$nh^2S \quad (5.5)$$

i.e. our population will keep up a linear response to selection.

2998 **Question 2.** A population of red deer were trapped on Jersey (an island off of England) during the last inter-glacial period. From the



Figure 5.6: It’s not just deer that evolve to be small on islands, pygmy mammoths and elephants have evolved from large mainland species on numerous islands. For example, the California Channel Islands were home to a dwarf mammoth until about 13,000 years ago. Santa Rosa *Mammuthus exilis*. wikimedia, CC BY 3.0.

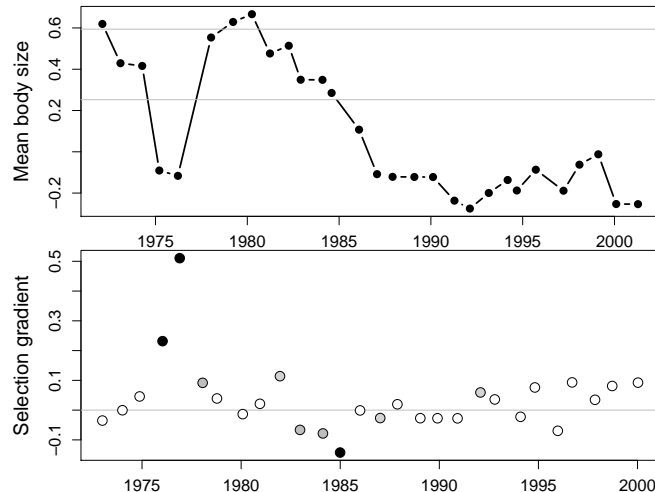
fossil record² we can see that the population rapidly adapted to their new conditions, perhaps due to selection for shorter reproductive times in the absence of predation. Within 6,000 years they evolved from an estimated mean weight of the population of 200kg to an estimated mean weight of 36kg (a 6 fold reduction)! You estimate that the generation time of red deer is 5 years and, from a current day population, that the narrow sense heritability of the phenotype is 0.5.

A) Estimate the mean change per generation in the mean body weight.

B) Estimate the change in mean body weight caused by selection within a generation. State your assumptions.

C) Assuming we only have fossils from the founding population and the population after 6000 years, should we assume that the calculations accurately reflect what actually occurred within our population?

3014



² LISTER, A., 1989 Rapid dwarfing of red deer on Jersey in the last interglacial. *Nature* 342(6249): 539

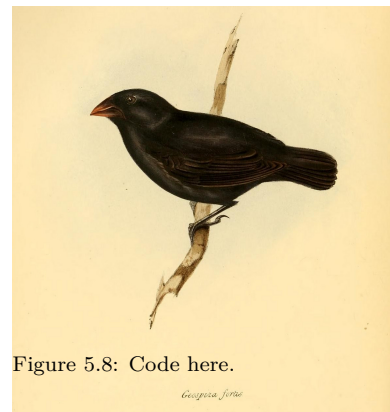


Figure 5.8: Code here.

Geospiza fortis

Figure 5.7: Medium ground-finch (*Geospiza fortis*).

The zoology of the voyage of H.M.S. Beagle. Birds Part 3. (1841) Gould G. Edited by Darwin, C. Illustration by Elizabeth Gould. Image from the Biodiversity Heritage Library. Contributed by Natural History Museum Library, London . Not in copyright.

Alternative formulations of the Breeder's equation. A change in mean phenotype within a generation occurs because of the differential fitness of our organisms. To think more carefully about this change within a generation, let's think about a simple fitness model where our phenotype affects the viability of our organisms (i.e. the probability they survive to reproduce). The probability that an individual has a phenotype X before selection is $p(X)$, so that the mean phenotype before selection is

$$\mu_{BS} = \mathbb{E}[X] = \int_{-\infty}^{\infty} xp(x)dx \quad (5.6)$$

The probability that an organism with a phenotype X survives to
 3024 reproduce is $w(X)$, and we'll think about this as the fitness of our
 organism. The probability distribution of phenotypes in those who do
 3026 survive to reproduce is

$$\mathbb{P}(X|\text{survive}) = \frac{p(x)w(x)}{\int_{-\infty}^{\infty} p(x)w(x)dx}. \quad (5.7)$$

where the denominator is a normalization constant which ensures that
 3028 our phenotypic distribution integrates to one. The denominator also
 has the interpretation of being the mean fitness of the population,
 3030 which we'll call \bar{w} , i.e.

$$\bar{w} = \int_{-\infty}^{\infty} p(x)w(x)dx. \quad (5.8)$$

Therefore, we can write the mean phenotype in those who survive
 3032 to reproduce as

$$\mu_S = \frac{1}{\bar{w}} \int_{-\infty}^{\infty} xp(x)w(x)dx \quad (5.9)$$

If we mean center our population, i.e. set the phenotype before
 3034 selection to zero, then

$$S = \frac{1}{\bar{w}} \int_{-\infty}^{\infty} xp(x)w(x)dx = \mathbb{E}(Xw(X)) \quad (5.10)$$

where the final part follows from the fact that the integral is taking
 3036 the mean of $Xw(X)$ over the population.

As our phenotype is mean centered ($\mathbb{E}(X) = 0$), we can see that
 3038 S has the form of a covariance between our phenotype X and our
 relative fitness $w(X)$

$$S = \mathbb{E}(Xw(X)) - \mathbb{E}(X)\mathbb{E}(w(X)) = Cov(X, w(X)/\bar{w}) \quad (5.11)$$

3040 Thus our change in mean phenotype is directly a measure of the co-
 variance of our phenotype and our fitness. Rewriting our breeder's
 3042 equation using this observation we see

$$R = \frac{V_A}{V} Cov(X, w(X)/\bar{w}) \quad (5.12)$$

we see that the response to selection is due to the fact that our
 3044 fitness (viability) of our organisms/parents covaries with our pheno-
 type, and that our child's phenotype is correlated with our parent's
 3046 phenotype.

Fisher's fundamental theorem of natural selection If we choose fitness
 to be our phenotype ($X = w(X)/\bar{w}$), then the response in fitness is

$$\begin{aligned} R &= \frac{V_A}{V} Cov(w(X)/\bar{w}, w(X)/\bar{w}) = \frac{V_A}{V} V \\ &= V_A \end{aligned} \quad (5.13)$$



Figure 5.9: Red deer (*Cervus elaphus*).

British mammals. Thorburn, A. (1920) Image from the Biodiversity Heritage Library. Contributed by Field Museum of Natural History Library. Licensed under CC BY-2.0.

i.e. the response to selection is equal to the additive genetic variance
 3048 for fitness. Or as Fisher put it

“The rate of increase in fitness of any organism at any time is equal to
 3050 its genetic variance in fitness at that time.” -FISHER (1930) (pg 37)

Fisher called this ‘the fundamental theorem of natural selection’. Our
 3052 proof here is just a sketch, and more formal approaches are needed
 to show it in generality. There has been much nashing of teeth over
 3054 exactly how broadly this result holds, and exactly what Fisher meant
 (see EWENS, 2010, for a recent overview).

3056 *Fitness Gradients and linear regressions* To understand this in more
 detail let imagine that we calculate the linear regression of an individ-
 3058 ual i ’s mean-centered phenotype (X_i) on fitness (W_i), i.e.

$$W_i \sim \beta X_i + \bar{w} \quad (5.14)$$

The best fitting slope of this regression (β), lets call it the ‘fitness
 3060 gradient’, is given by

$$\beta = \text{Cov}(X, w(X)/\bar{w})/V \quad (5.15)$$

i.e. the fitness gradient is the covariance of phenotype-fitness covari-
 3062 ance divided by the phenotypic variance. Using this result we can
 rewrite the breeder’s equation as

$$R = V_A \beta \quad (5.16)$$

3064 i.e. we’ll see a directional response to selection if there is a linear
 relationship of phenotype on fitness, and if there is additive genetic
 3066 variance for the phenotype. As one example of a fitness gradient, in
 Figure 5.10 the lifetime reproductive success (LRS) of male Red Deer
 3068 is plotted against the weight of their antlers. The red line gives the
 linear regression of fitness (LRS) on antler mass and the slope of this
 3070 line is the fitness gradient (β).

5.0.1 Fitness landscapes

3072 ??

One common metaphor when talk about evolution is that of a
 3074 population exploring an adaptive landscape with natural selection
 pushing a population towards higher fitness states corresponding to
 3076 peaks in this landscape (see e.g. Figure ??). LANDE (1976) found
 an evocative formulation of the Breeder’s equation which aids our
 3078 intuition of phenotypic fitness landscapes. LANDE showed that, if the
 phenotype is normally distributed, the response to selection (R) could

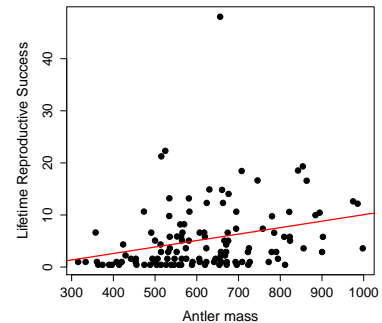


Figure 5.10: Lifetime reproductive success (LRS) of male Red Deer as a function of their antler mass. Data from KRUUK *et al.* (2002), see the paper for discussion of the complexities of equating this selection gradient with the evolutionary response. Code here..

This follows from the fact that we can then move the derivative inside the integral of \bar{w}

$$\begin{aligned} \frac{1}{\bar{w}} \frac{\partial \bar{w}}{\partial \bar{x}} &= \frac{1}{\bar{w}} \int_{-\infty}^{\infty} w(x) \frac{\partial p(x)}{\partial \bar{x}} dx \\ &= \int_{-\infty}^{\infty} \frac{w(x)}{\bar{w}} \frac{(x - \bar{x})}{V} dx \\ &= \frac{\text{cov}(w(x), x)}{\text{var}(x)} \end{aligned} \quad (5.17)$$

which is β . The middle line holds when $p(x)$ is the normal distribution.

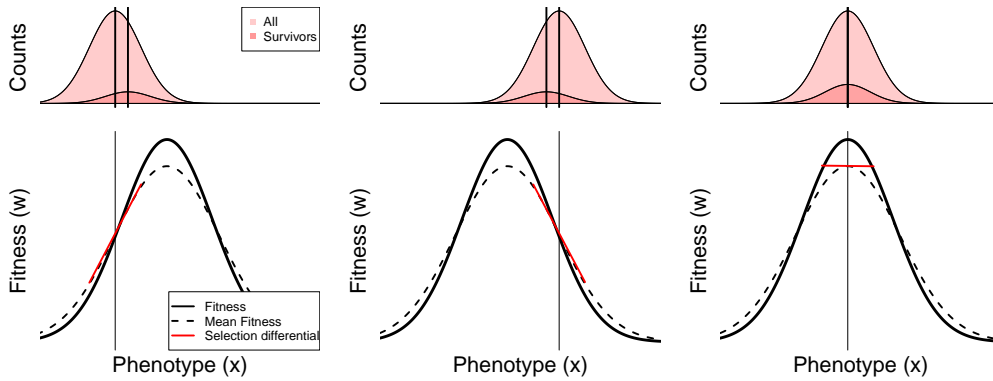


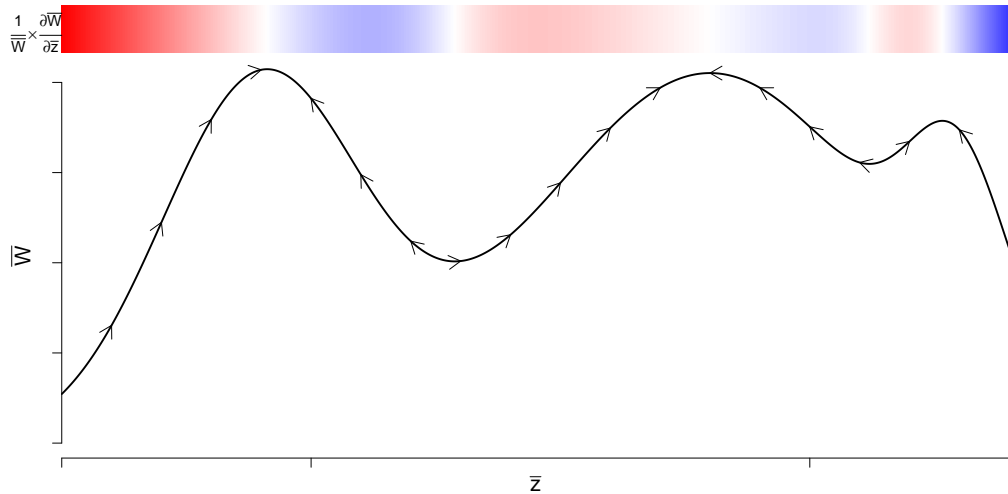
Figure 5.11: A population evolving on a (gaussian) fitness surface. The bottom panel shows the expected individual fitness ($w()$) and mean fitness as a function of phenotype. The red line shows the best fitting linear approximation to the relationship between phenotype and fitness, eqn (??), whose slope is β . The top panel shows the distribution of the phenotype before and after selection. Code here..

3080 be written in terms of the gradient (derivative) of the mean fitness (\bar{w})
of the population as a function of the mean phenotype:

$$R = \frac{V_A}{\bar{w}} \frac{\partial \bar{w}}{\partial \bar{x}} \quad (5.18)$$

3082 What does this mean? Well V_A/\bar{w} is always positive, so the direction
our population responds to selection is predicted by the sign of the
3084 derivative. If increasing the mean phenotype of the population slightly
would increase mean fitness ($\partial \bar{w} / \partial \bar{x} > 0$) our population will respond
3086 that generation by evolving toward higher values of the trait ($R > 0$),
left panel of Figure 5.11. Conversely if decreasing the population mean
3088 phenotype slightly would increase the mean fitness ($\partial \bar{w} / \partial \bar{x} < 0$) the
population will that generation evolve towards lower values of the
3090 phenotype, middle panel of Figure 5.11. Thus we can think of the
population as evolving on an adaptive landscape where the elevation
3092 is given by the population mean fitness. Natural selection operates on
the basis of individual-level fitness, but as a result of this our popula-
3094 tion is increasing in its average fitness, it is becoming more adapted.
What happens when it reaches the top? Well at the top of a peak
3096 $\partial \bar{w} / \partial \bar{x} = 0$, as it is a local maximum, and so $R = 0$. Assuming that the
relationship between fitness and phenotype stays constant, our pop-
3098 ulation will stay at the top of the fitness peak. This view of natural
selection does not imply that the population is evolving to the best
3100 possible state. Our population is just marching up the hill of mean
fitness end panel Figure 5.11. However, this peak isn't necessarily
3102 the highest fitness peak it's just which ever peak was closest and so
our population can become trapped on a local, but not global peak of
3104 fitness (see, for example Figure ??).

CAVEATS



One nice example documenting adaptive evolution to a new fitness optimum is offered by a remarkable time-series of stickleback evolution from a fossil lake-bed in Nevada (BELL *et al.*, 2006). In this lake the layers of sediment are laid down each year allowing a very detailed time series with over five thousand fossils measured. The time-series documents the evolution towards a new set of optimum phenotypes in the fifteen thousand years after the initial invasion of the lake by a heavily armoured stickleback species. In Figure ?? the population mean number of touching pterygiophores, the bones supporting the dorsal spines, through the fossil record. Note how quickly the species evolves toward its new value, presumably a fitness optimum in their new environment, and the long time subsequent time interval over which the population mean phenotype fluctuates about its new value.

HUNT *et al.* (2008) fitted a model of a population adapting to a fitness landscape, with a single peak, to these time-series data. Their fitted fitness surface is shown in the lower panel of Figure 5.13 . The arrows show the moves that the population mean phenotype is making on this inferred fitness surface. The population initially takes large steps up toward the peak of this surface and subsequently fluctuates around the peak. Under the interpretation that there is a single stationary peak these fluctuations represent genetic drift randomly knocking the population off its optimum, with selection acting to restore the population towards this local optimum.

3128 Stabilizing and Disruptive selection Up to now we have just looked at directional selection, where selection acts to change the mean phenotype. However, we can also use quantitative genetic models to describe



Figure 5.12: Fossil stickleback. Photo by Peter J. Park from LOSOS *et al.* (2013), licensed under CC BY 4.0.

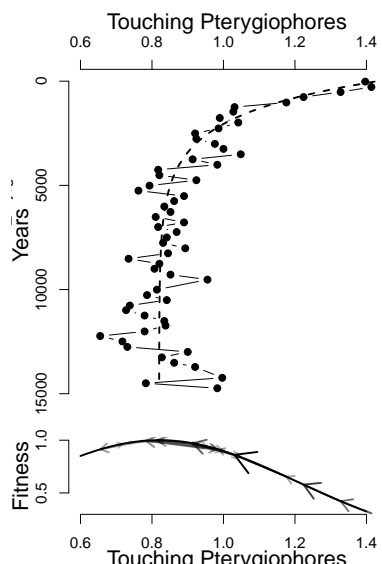


Figure 5.13: **Top)** A time series of stickleback phenotypic evolution from the fossil record. After a heavily armoured stickleback invades the lake it quickly evolves towards touching pterygiophores (the bones supporting the dorsal spines). Fossil measurements means are calculated in 250 year bins. **Bottom)** How our population moves on the Inferred fitness landscape. The arrows show each

other modes of selection, extending from effects on the population
 3132 mean the next natural step is to think about selection which acts on
 the population variance. Selection might act against more strongly
 3134 against individuals in the tails of the distribution, with those closer
 to the mean phenotype having higher fitness, which lowers the vari-
 3136 ance. Selection could also disfavour individuals close to the population
 mean, with individuals with extreme phenotypes having higher fitness,
 3138 which acts to increase the fitness.

Directional selection occurs because of the covariance between our
 3140 phenotype and fitness, eqn (5.11). Just as we expressing directional
 selection as a covariance allowed us to characterize directional selec-
 3142 tion as the linear relationship between fitness and and phenotype,
 β , we can summarize the variance reducing selection by including a
 3144 quadratic term in the regression of fitness on phenotype

$$w_i \sim \beta x_i + 1/2\gamma x_i^2 + \bar{w} \quad (5.19)$$

This γ , the coefficient of the quadratic term in our model, is the
 3146 quadratic selection gradient: the covariance of fitness and the squared
 deviation from the phenotypic mean (μ_{BS}), i.e.

$$\gamma = \frac{\text{Cov}(w(X), (X - \mu_{BS})^2)}{V^2} \quad (5.20)$$

3148 Our γ describes the curvature of the fitness surface around the mean.
 Values of $\gamma < 0$ are consistent with stabilizing selection, reducing
 3150 the variance. While values of $\gamma > 0$ are consistent with disruptive
 selection, increasing the variance.

3152 Under stabilizing selection the individuals with extreme phenotypes
 in either tail have lower fitness, the result of which is to reduce the
 3154 phenotypic variance within a generation. A classic case of stablizing
 selection is birth weight in humans (KARN and PENROSE, 1951).
 3156 Mary Karn collected data for nearly fourteen thousand pregnancies
 from 1935-46 for birth weight and mortality. These data are replotted
 3158 in Figure 5.14. The variance of all births is 1.575lb^2 , while in live
 births this was reduced to 1.26lb^2 , a 20% reduction in variance due to
 3160 stabilizing selection. It is worth noting, that this selection pressure has
 been greatly reduced over the decades in societies with access to good
 3162 prenatal care (ULIZZI and TERRENATO, 1992).

In Central Africa, Black-bellied seedcrackers (*P. ostrinus*) show
 3164 remarkable size polymorphism in their beaks (Figure 5.16). The small-
 beaked individuals feed on soft seeds from one species of marsh sedge
 3166 while the big-beaked individuals feed on hard seeds from another
 sedge, which requires ten times the force to crack. SMITH (1993)
 3168 recorded the fates of hundreds of juveniles, and found that individ-
 uals with intermediate beak sizes survived at much lower rates, Fig-
 3170 ure 5.16, because they were not well adapted to either seed resource.

Just like how β could be interpreted as the mean gradient of the fitness surface, our γ is the mean curvature of the fitness surface

$$\gamma = \mathbb{E} [\partial^2 w(x)/\partial x^2] = \int \partial^2 w(x)/\partial x^2 p(x) dx \quad (5.21)$$

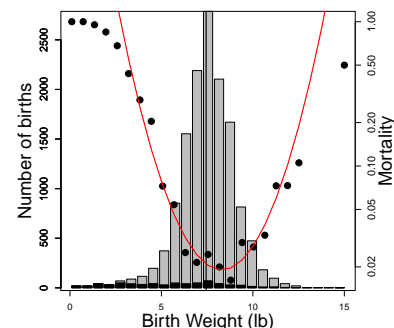


Figure 5.14: Bars show the total number of births with different birth weights (left axis). Dots show the mortality probability for different birth-weight bins (right axis). Data from KARN and PENROSE (1951) Table 2, collapsing male and female births, Code here.



Break length is subject to disruptive selection, as can also be seen by
 3172 the significant negative quadratic term in the regression of survival
 probability on break length. The variance of mandible in the total
 3174 sample of individuals was 0.5mm^2 in the survivors this variance in-
 creased by a factor of almost $\times 2.5$ to 1.3mm^2 .

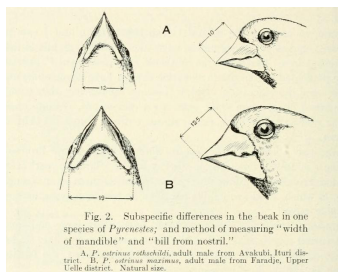


Fig. 2. Subspecific differences in the beak in one species of *Pyrenestes*, and method of measuring "width of mandible" and "bill from nostril".
 A, *P. ostrinus rothschildi*, adult male from Avauab, Huri district; B, *P. ostrinus ostrinus*, adult male from Parape, Upper Uelle district. Natural size.

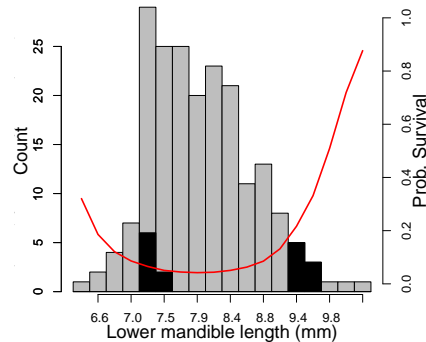


Figure 5.16: **Left** An illustration of the remarkable variation in beak size within Black-bellied seedcrackers (*P. ostrinus*). **Right** A histogram of a beak size measurement in Black-bellied seedcrackers, all juveniles are shown in white the black bars show the survivors. The red curve shows the best fitting linear and quadratic model to the probability of survival, fitted using a binomial generalized linear models with a logit link function.

Left illustration from: Size variation in *Pyrenestes* by Chapin J.P. in the Bulletin of the American Museum of Natural History (Vol. X Heritag ersity Library

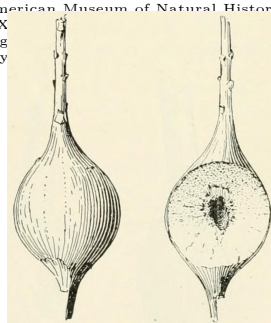


Figure 5.17: The gall formed by the goldenrod ball gallmaker (*Eurosta solidaginis*) in a goldenrod plant. The one on the right is cut to show a partial cross-section.

Annual report of the New York State Museum (1917) Image from the Biodiversity Heritage Library. Contributed by The LuEsther T Mertz Library, the New York Botanical Garden. Not in copyright.

3176 To illustrate how directional selection and quadratic terms play
 off during adaptation, lets consider the goldenrod gall fly (*Eurosta
 3178 solidaginis*), aka the goldenrod ball gallmaker. See Figure 5.18. As it's
 wonderful name implies this insect lays its eggs in Goldenrod plants,
 3180 and the larvae release chemicals forcing the plant to form a gall that
 forms a home for the larvae as they develop. While this seems like a
 3182 pretty sweet deal for the larvae, it is not without its perils.

When the small, ball galls fall risk of parasitism from parasitoid
 3184 wasps. This selection drives strong positive directional selection on
 gall size, with little stabilizing selection, notice that the good agree-
 3186 ment between the linear selection gradient and the fit including a
 linear and quadratic term. However, bigger galls fall under the pall of
 3188 predation from downy woodpeckers and black-capped chickadees, who
 seek out the tasty larvae. Thus intermediate size galls are favoured,
 3190 a fitness peak that the population quickly reaches this fitness peak.
 Once on this peak, there is no directional selection, i.e. no linear slope,
 3192 but there is strong stabilizing selection, i.e. a quadratic term.

5.0.2 The response of multiple traits to selection, the multivariate breeder's equation.

We can generalize these results for multiple traits, to ask how selection
 3196 on multiple phenotypes plays out over short time intervals.³ Considering two traits we can write our responses in both traits as

$$\begin{aligned} R_1 &= V_{A,1}\beta_1 + V_{A,1,2}\beta_2 \\ R_2 &= V_{A,2}\beta_2 + V_{A,1,2}\beta_1 \end{aligned} \tag{5.22}$$

³ LANDE, R., 1979 Quantitative genetic analysis of multivariate evolution, applied to brain: body size allometry. Evolution 33(1Part2): 402–416

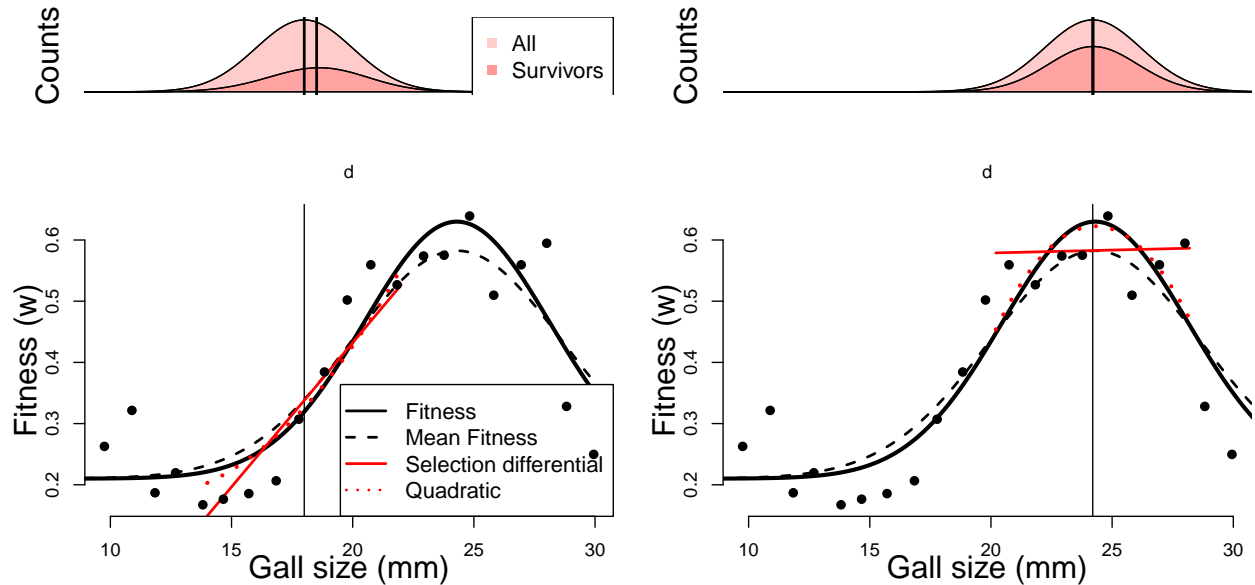


Figure 5.18: Fitness surface for gall diameter in goldenrod ball gall-makers. The dots are the measured survival probabilities of different sized galls. The solid line is a fitted individual fitness surface ($w()$). Dotted line is \bar{w} plotted as a function of the population mean assuming a normal distribution with a standard deviation of 2mm. Data from WEIS and GORMAN (1990), Code here.

3198 where the 1 and 2 index our two different traits. Here $V_{A,1,2}$ is our
 3199 additive covariance between our traits. Our selection gradient for trait
 3200 1, β_1 , represents the change in fitness changing trait 1 alone holding
 3201 everything else constant. This is a statement that our response in any
 3202 one phenotype is modified by selection on other traits that covary with
 3203 that trait. This offers a good way to think about how genetic trade
 3204 offs play out over short-term evolution.

We can also write this in matrix form. We can write our change in
 3206 the mean of our multiple phenotypes within a generation as the vector
 3207 \mathbf{S} and our response across multiple generations as the vector \mathbf{R} . These
 3208 two quantities are related by

$$\mathbf{R} = \mathbf{GV}^{-1}\mathbf{S} = \mathbf{G}\boldsymbol{\beta} \quad (5.23)$$

where \mathbf{V} and \mathbf{G} are our matrices of the variance-covariance of phenotypes and additive genetic values (eqn. (4.19) (4.18)) and $\boldsymbol{\beta}$ is a vector of selection gradients (i.e. the change within a generation as a fraction of the total phenotypic variance).

Question 3. You collect observations of red deer within a generation, recording an individual's number of offspring and phenotypes for a number of traits which are known to have additive genetic variation. Using your data, you construct the plots shown in Figure 5.19 (standardizing the phenotypes). Answer the following questions by choosing one of the bold options. Briefly justify each of your answers with reference to the breeder's equation and multi-trait breeder's equation.

3220 A) Looking just at figure 5.19 A, in what direction do you expect
male antler size to evolve?

3222 Insufficient information, increase, decrease.

3224 B) Looking just at figures 5.19 B and C, in what direction do you
expect male antler size to evolve?

3226 Insufficient information, increase, decrease.

3228 C) Looking at figures 5.19 A, B, and C, in what direction do you
expect male antler size to evolve?

3228 Insufficient information, increase, decrease.

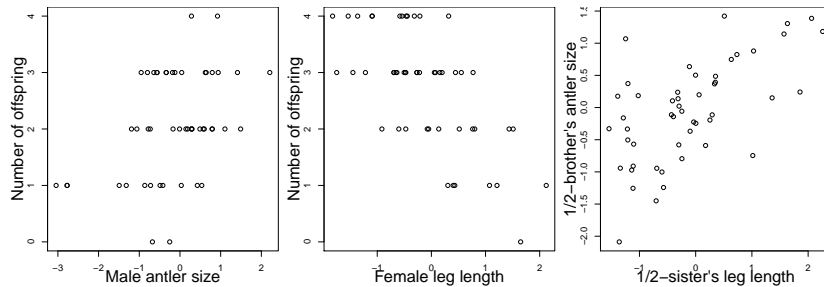
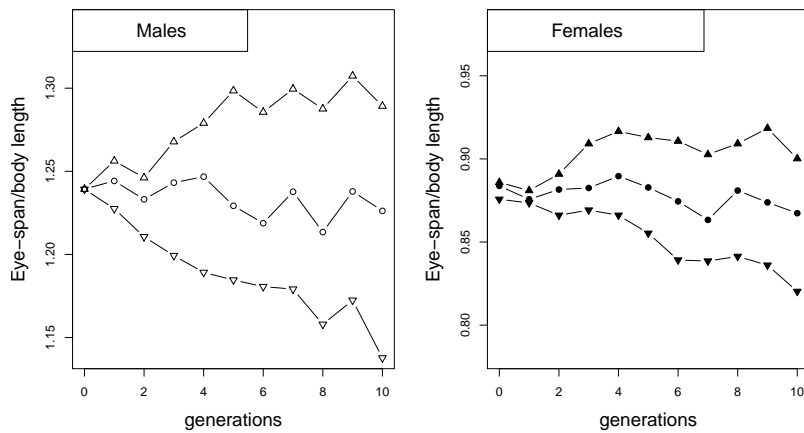


Figure 5.19: Observations of red deer within a generation; recording an individual's number of offspring and phenotypes (simulated data), which are known to have additive genetic variation. The figures left to right are A-C. (Data are simulated. Code here.)

As an example of correlated responses to selection, consider the

3230 WILKINSON (1993) selection experiment on Stalk-eyed flies (*Cyrtodiopsis dalmanni*). Stalk-eyed flies have evolved amazingly long
3232 eye-stalks. In the lab, WILKINSON established six populations of
wild-caught flies and selected up and down on males eye-stalk to body
size ratio for 10 generations (left plot in Figure 5.20). Despite the
fact that he did not select on females, he saw a correlated response in
3234 the females from each of the lines (right plot), because of the genetic
correlation between male and female body proportions.

Figure 5.20: WILKINSON selected two populations for flies for increased and eye-stalk to body length ratio. QUANTITATIVE males (mean shown as up triangles) and two for a decreased ratio (down triangles), by taking the top 10 males with the highest (lowest) ratio out of 50 measures. He also established two control populations (circles). He constructed each generation of females by sampling 10 at random from each population. Data from WILKINSON (1993). Code here.



3238 Question 4.

At the end of ten generations in WILKINSON's experiment (Figure 3240 5.20), the males from the up- and down-selected lines had mean eye- 3242 stalk to body ratios of 1.29 and 1.14 respectively, while the females 3244 from the up- and down-selected lines had means of 0.9 and 0.82.

A) WILKINSON estimated that by selecting the top/bottom 10 3246 males, he had on average shifted the mean body ratio by 0.024 within each generation. What is the male heritability of eye-stalk to body-length ratio?

B) Assume that the additive genetic variance of male and female 3248 phenotypes are equal and that there is no direct selection on female 3250 body-proportion in this experiment, i.e. that all of the response in females is due to correlated selection. Can you estimate the male-female genetic correlation of the eye-stalk ratio?

3252 *Estimating multivariate selection gradients* We can estimate multi- 3254 variate directional (β) and quadratic selection gradients (γ) just as we did for a single traits (x_1 and x_2), using linear models. For example, for two traits we can write

$$w_i \sim \beta_1 x_{1,i} + 1/2\gamma_1 x_{1,i}^2 + \beta_2 x_{2,i} + 1/2\gamma_2 x_{2,i}^2 + \gamma_{1,2} x_{1,i} x_{2,i} + \bar{w} \quad (5.24)$$

3256 where β_1 and γ_1 are the directional and quadratic selection gradients for trait one, and similarly for trait two. The covariance selection 3258 gradient between between traits is given by $\gamma_{1,2}$.

BRODIE III (1992)'s work provides a nice example of selection 3260 on multiple predation-avoidance traits in northwestern garter snakes

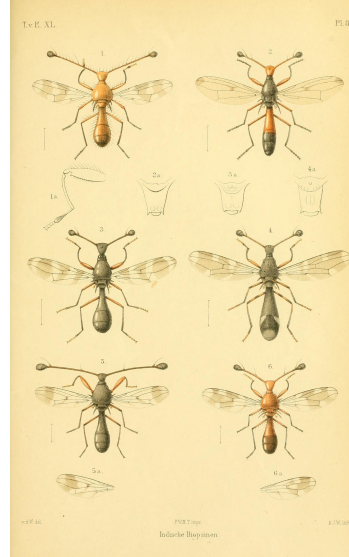


Figure 5.21: Stalk-eyed Flies (*Diopsidae*).

Diptera. van der Wulp. 1898. Image from the Biodiversity Heritage Library. Contributed by Smithsonian Libraries. Not in copyright.

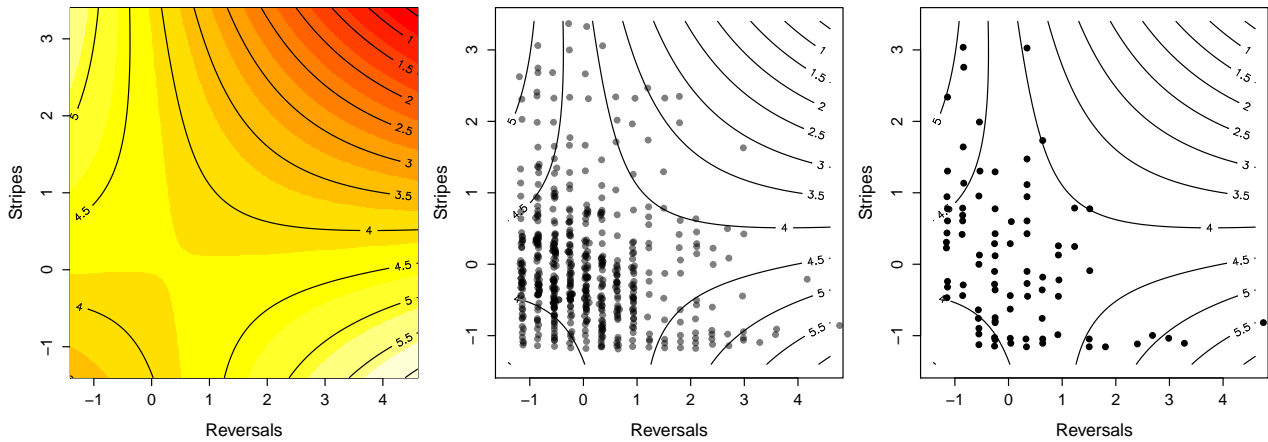


Figure 5.22: Left) The garter snake fitness surface estimated by BRODIE III (1992) lighter colours indicate higher fitness; middle) snake is an intermediate type; right) the snake (1992)

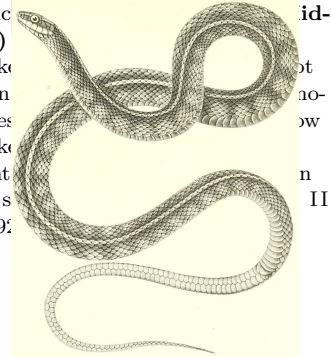


Figure 5.23: Northwestern garter snake (*Eutaenia cooperi*, now *Thamnophis ordinoides*)
The natural history of Washington territory, with much relating to Minnesota, Nebraska, Kansas, Oregon, and California (1859). Cooper J.G. and Suckley, G. Image from the Biodiversity Heritage Library. Contributed by Smithsonian Libraries. Not in copyright.

(*Thamnophis ordinoides*). BRODIE III released hundreds of snakes born in the lab into the wild, and then performed mark-recapture observations to monitor their fate.

Before releasing them he measured how stripey they were, and their behavioural tendency to reversals of direction during simulated flight from a predator. His quadratic fitness surface is shown in Figure 5.22, based on fitting the regression given by eqn (5.24) to juvenile survival. He found that neither single trait directional or quadratic gradients were significant, ie there was no apparent selection on one trait ignoring the other. However, there was a significant, negative covariance ($\gamma_{1,2} < 0$). The individuals with the highest chance of survival are either highly striped and perform few reversals (top left corner), or have little striping but reverse course frequently (bottom right corner).

5.1 Some applications of the multivariate trait breeder's equation

The multivariate breeders equation has a lot of different uses in understanding the response of multiple traits to selection. It also offers some insights into kin selection and sexual selection. We'll discuss these next.

Hamilton's Rule and the evolution of altruistic and selfish behaviours
Individuals frequently behave in ways that sacrifice their own fitness for the benefit of others. That selection favours such apparent acts of altruism is puzzling at first sight. HAMILTON (1964a,b) supplied the first general evolutionary explanation of such altruism. His intuition was that while an individual is losing out of some reproductive output,

MAYNARD SMITH (1964) coined the name kin selection to describe Hamilton's approach to this problem. It's also sometimes called the inclusive fitness approach, as we need to include not just one individual's fitness but the weighted sum of all the fitness of all their relatives.

the alleles underlying an altruistic behaviour can still spread in the population if this cost is outweighed by benefits gained through the transmission of these alleles through a related individual. Note that this means that the allele is not acting in an self-sacrificing manner, even though individuals may as a result.

Altruism reflects social interactions. So as a simple model let's imagine that individuals interact in pairs, with our focal individual i being paired with an individual j . This could be pairs of siblings interacting. Imagine that individuals have two possible phenotypes $X = 1$ or 0 , corresponding to providing or withholding some small act of 'altruism' (we could just as easily flip these labels and call them an unselfish act and a selfish act respectively). Our pairs of individuals interacting could, for example, be siblings sharing a nest. The altruistic trait could be as simple as growing at a slightly slower rate so as to reducing sibling-competition for food from parents, or more complicated acts of altruism such as children foregoing their own reproduction so as to help their parents raise their siblings.

Providing the altruistic act has a cost C to the fitness of our individual and failing to provide this act has no cost. Receiving this altruistic act confers a fitness benefit B over individuals who did not receive this act. HAMILTON's rule states that such a trait will spread through the population if

$$2FB > C \quad (5.25)$$

where F is the average kinship coefficient between the interacting individuals (i and j). In the usual formulation of Hamilton's Rule our $2F$ is replaced by the 'Coefficient of relationship', which is the proportion of alleles shared between the individuals. Here we use two times the kinship coefficient to keep things inline with our notation for these chapters. Note that if our individuals are themselves inbred we need to do a little more careful to reconcile these two measures. So the altruistic behaviour will spread even if it is costly to the individual if its cost is paid off by the benefit to sufficiently related individuals.

As one example of kin-selection consider KRAKAUER (2005)'s work on co-operative courtship in wild turkeys (*Meleagris gallopavo*). Male turkeys often form display partnerships, with a subordinate male helping a dominant male with displaying to females and defending the females from other groups of males.

These pairs are often full brothers ($F = 0.25$), with the subordinate male often being the younger of the two. The subordinate male often loses out on mating opportunities over their entire lifetime by acting as a wingman to their older brothers. KRAKAUER (2005) estimated that dominant males gained an extra 6.1 offspring when they display with a partner than males who display alone. While the subordinate males lose out on fathering 0.9 offspring compared

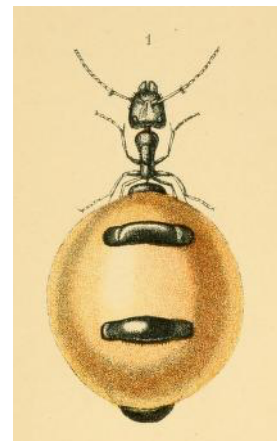


Figure 5.24: Australian Honey-pot Ant (*Camponotus inflatus*). Honey ants are gorged with honeydew collected by their nest mates, till they swell to the size of grapes, and used as a food storage device.

Ants, bees, and wasps; a record of observations on the habits of the social Hymenoptera (1897)
Lubbock, J. Image from the Biodiversity Heritage Library. Contributed by Smithsonian Libraries. Not in copyright.



Figure 5.25: Turkey (*Meleagris gallopavo*).

Bilder-atlas zur Wissenschaftlich-populären Naturgeschichte der Vögel in ihren sämmtlichen Hauptformen (1864). Wien,K.K. Hof Image from the Biodiversity Heritage Library. Contributed by Smithsonian Libraries. Not in copyright.

to solitary males. Thus the costs of helping by subordinate males is more than compensated by the fitness gains of their brothers ($(2 \times 0.25) \times 6.1 > 0.9$), and so the evolution of this altruistic helping in co-operative courtship is potentially well explained by kin-selection (see AKÇAY and VAN CLEVE, 2016, for more analysis).

Question 5. How would this answer be changed if the male Turkey partnerships were only $1/2$ sibs, or first cousins?

Where does this result come from? Well, we can use our quantitative genetics framework to gain some intuition by deriving a simple version of Hamilton's Rule by thinking about the phenotypes of an individual's kin as genetically correlated phenotypes. To sketch a proof of this result, let's assume that our focal i individual's fitness can be written as

$$W(i, j) = W_0 + W_i + W_j \quad (5.26)$$

where W_i is the contribution of the fitness of the individual i due to their own phenotype, and W_j is the contribution to our individual i 's fitness due to the interacting individual j 's behaviour (i.e. j 's phenotype). With the benefit B and cost C , our $W(i, j)$ are depicted in Figure 5.26.

Following our multivariate breeder's equation, we can write the expected change of our behavioural phenotype as

$$R = \beta_i V_A + \beta_j V_{A,i,j}, \quad (5.27)$$

Our altruistic phenotype is increasing in the population if $R > 0$, i.e. if

$$\beta_i V_A + \beta_j V_{A,i,j} > 0 \quad (5.28)$$

The slope β_i of the regression of our focal individual's behavioural phenotype on fitness is proportional to $-C$. The slope β_j of the regression of our interacting partner's phenotype on our focal individual's fitness is proportional to B (with the same constant of proportionality). Therefore, our altruistic phenotype is increasing in the population if

$$\begin{aligned} \beta_i V_A + \beta_j V_{A,i,j} &> 0 \\ B \frac{V_{A,i,j}}{V_A} &> C \end{aligned} \quad (5.29)$$

So what's the average genetic covariance between individual i and j 's altruistic phenotype? Well it's the same behavioural phenotype in both individuals, so the phenotypes are genetically correlated if our individuals are related to each other. The covariance of the same phenotype between two individuals is just $2F_{i,j}V_A$ (see (4.12)). So our

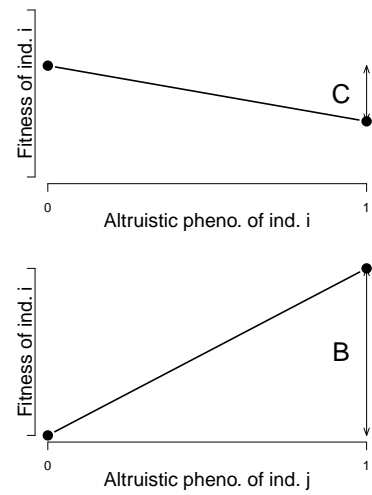


Figure 5.26: **Top**) The fitness of individual i as a function of their behavioural phenotype, where altruistic/non-altruistic behavioural phenotypes are encoded as 1 and 0 respectively. The direct fitness cost of behaving altruistically is C . **Bottom**) The fitness of our focal individual i as a function of the behavioural phenotype of their interacting partner (j). Our focal individual gets an increase B in fitness if their partner behaves altruistically. Code here.

Here we've following a simplified version of QUELLER (1992)'s treatment, to re-derive Hamilton's rule in a quantitative genetics framework (Hamilton's original papers did this in a population genetics framework).

altruistic phenotype is increasing in the population if

$$\begin{aligned} B \frac{2F_{i,j}V_A}{V_A} &> C \\ 2F_{i,j}B &> C \end{aligned} \quad (5.30)$$

Seen from this perspective, HAMILTON's rule is simply a statement that altruistic behaviours can spread via kin-selection, if the average cost to an individual of carrying altruistic alleles is paid back through the average benefit of interacting with altruistic relatives (kin)

Sexual selection and the evolution of mate preference by indirect benefits. Organisms often put an enormous effort into finding and attracting mates, sometimes at a considerable cost to their chances of survival. Why are individuals so choosy about who they mate with, particularly when their choice seems to be based on elaborate characters and arbitrary displays that surely lower the viability of their mates?

One major reason why individuals evolve to be choosy about who they mate with is that it can directly impact their fitness. By choosing a mate with particular characteristics, individuals can gain more parental care for their offspring, avoid parasites, or be choosing a mate with higher fertility. For example, female glow-worms flash at night to attract males flying by. Females with larger, brighter lanterns have higher fecundity, so males with a preference for brighter flashes will gain a direct benefit to their own fitness. (Note that males will benefit even if these differences in female fecundity are entirely driven by differences in environment, and so non-heritable.) Indeed male glow worms have evolved to be attracted to brighter flashing lures.

However, even in the absence of direct benefits of choice, selection can still indirectly favour the evolution of choosiness. These indirect benefits occur because individuals can have higher fitness offspring by choosing a mate whose phenotype indicates high viability (the so-called good genes hypothesis), or by choosing a mate whose phenotype is simply attractive, and likely to produce similarly attractive offspring (the 'runaway' or sexy sons hypothesis).

We'll denote a display trait, e.g. tail length, in males by σ and a preference trait in females by φ . Our display trait is under direct selection in males, such that its response to selection can be written as

$$R_\sigma = \beta_\sigma V_{A,\sigma} \quad (5.31)$$

Let's assume that the female preference trait, the degree to which females are attracted to long tails, is not under direct selection $\beta_\varphi = 0$. Then the response to selection of the preference trait can be written as

$$R_\varphi = \beta_\varphi V_{A,\varphi} + \beta_\sigma V_{A,\varphi\sigma} = \beta_\sigma V_{A,\varphi\sigma} \quad (5.32)$$

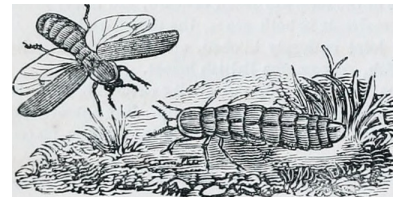


Figure 5.27: Male (left) and female (right) common glow worm (*Lampyris noctiluca*).

The animal kingdom : arranged after its organization; forming a natural history of animals, and an introduction to comparative anatomy. (1863) Cuvier, G. Image from the Biodiversity Heritage Library. Contributed by University of Toronto - Gerstein Science Information Centre. Not in copyright.

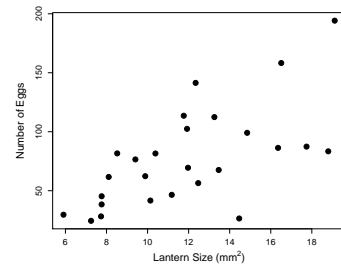


Figure 5.28: Female Glow worms who have the largest, and therefore brightest, lanterns have the highest fecundity. Data from HOPKINS *et al.* (2015). Code here.

3400 So the female preference will respond to selection if it is genetically correlated with the male trait, i.e. if $V_{A,\varphi\sigma}$ is not zero. There's a
 3402 number of different ways this genetic correlation could arise; the simplest is that the loci underlying the male trait may have a pleiotropic
 3404 effect on female preference. However, female preference may often have quite a distinct genetic basis from male display traits.

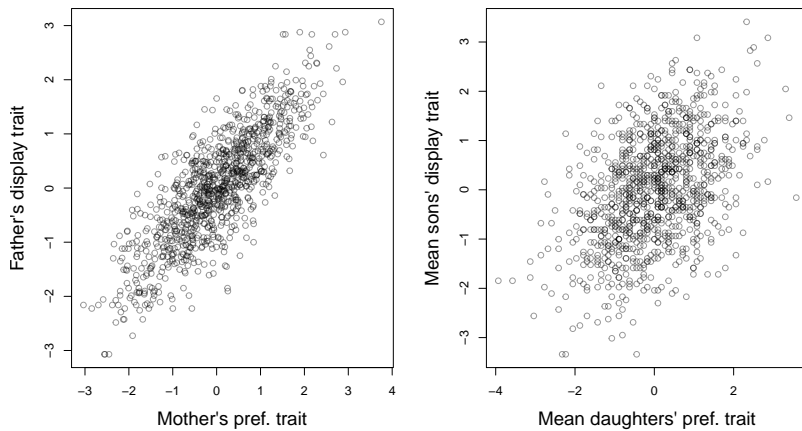


Figure 5.29: **Left)** Assortative mating between males and females. Males vary in a display trait (e.g. tail length), females vary in their preference for this trait. We see evidence of assortative mating as females with a preference for a particular value of the male trait tend to mate with those males. **Right)** As both male trait and female preference are genetic this establishes a genetic correlation in the next generation. This is simulated data. Code here.

3406 A more general way in which trait-preference genetic correlations may arise is through assortative mating. As females vary in their tail-
 3408 length preference, the ones with a preference for longer tails will mate with long-tailed males and the opposite for females with a preference
 3410 for shorter-tails. Therefore, a genetic correlation between mates display and preference traits will become established (see Figure 5.29).

3412 The males with the longer tails will also carry the alleles associated with the preference for longer tails, as their long-tailed dads tended
 3414 to mate with females with a genetic preference for long tails. Similarly, the the males with shorter tails will carry alleles associated with
 3416 the preference for shorter tails. Thus if there is direct selection for males with longer tails, then the female preference for longer tails will
 3418 increase too, as it is genetically correlated via assortative mating.

As an example of how direct selection on display traits can drive
 3420 the evolution of preference traits, let's consider some data from guppies. Guppies (*Poecilia reticulata*) are a classic system for studying
 3422 the interplay of natural and sexual selection. In some populations of guppies, females show a preference for males with more orange
 3424 colouration.

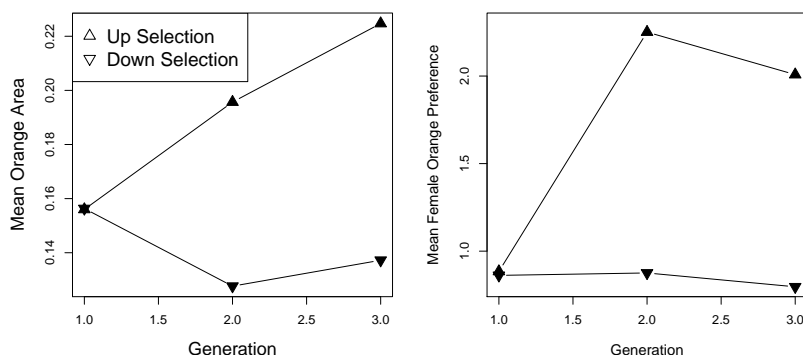


Figure 5.30: Mean phenotypes for the two up- and two down-selected populations of Guppies. Left panel: A response to selection was seen due to the direct selection on male colouration. Right panel: An indirect, correlated response was also seen in female preference. Data from HOUDE (1994). Code here.

HOUDE established four replicate population pairs of guppies and selected one of each pair for an increased or decreased orange coloration in males, selecting the top/bottom 20 out of 50 males. She randomly chose females from each population to form the next generation, and so did not exert direct selection on females. She measured the response to selection on male colouration and on female preference for orange (left and right panels of Figure 5.1 respectively). In the lines that were selected for more orange males females showed an increased preference for orange. While in those lines that she selected males for less orange in their display females showed a decreased preference for orange. This is consistent with indirect selection on female orange preference as a response to selection on male colouration, due to a genetic correlation between female preference and male trait. It is *a priori* unlikely that pleiotropy is the source of the genetic correlation between these traits, rather it is likely caused by females assortative mating with males that match their colour preference.

Returning to our bird tail example, what could drive the direct selection on male tail length? The selection for longer tails in males could come about because longer tails are genetically correlated with higher male viability, for example perhaps only males who gather an excess of food have the resources to invest in growing long tail, i.e. a long tail is an honest signal. This would be a good genes explanation of female mate choice evolution.

There's another subtler way that selection could favour our male trait. Imagine that the variation in female preference trait is because some females have no strong preference for the male-tail length, but some females have a strong preference for males with longer tails. Males with longer tails would then have higher fecundity than the short-tailed males as there's a subset of females who are strongly at-



Figure 5.31: Guppy (*Poecilia reticulata*).
From a set of 1962 stamps of Hungary.
Contributed to wikipedia by Darjac, not covered by copyright

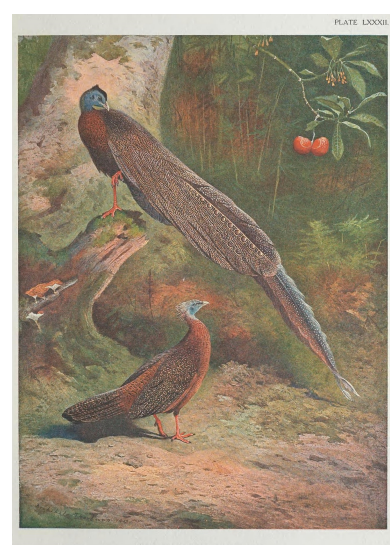


Figure 5.32: Argus Pheasant.
A monograph of the pheasants. (1918). Beebe, W Image from the Biodiversity Heritage Library. Contributed by Smithsonian Institution Libraries. Licensed under CC BY-2.0.

"The case of the male Argus Pheasant is eminently interesting, because it affords good evidence that the most refined beauty may serve as

3454 tracted to long tails, and these males also get to mate with the other
females. Thus selection favours long-tailed males, and so indirectly
3456 favours female preference for longer tails; females with a preference
for longer-tails have sons who in turn who are more attractive. This
3458 model is sometimes called the sexy-son model. It is also called the
Fisherian runaway model (FISHER, 1915), as female preference and
3460 male trait can coevolve in an escalating fashion driving more and more
extreme preferences for arbitrary traits. Thus many extravagant dis-
3462 play traits in males and females may exist purely because individuals
find them beautiful and are attracted to them.

3464

6

One-Locus Models of Selection

3466 “Socrates consisted of the genes his parents gave him, the experiences
3468 they and his environment later provided, and a growth and development
mediated by numerous meals. For all I know, he may have been
3470 very successful in the evolutionary sense of leaving numerous offspring.
His phenotype, nevertheless, was utterly destroyed by the hemlock
and has never since been duplicated. The same argument holds also
3472 for genotypes. With Socrates’ death, not only did his phenotype dis-
appear, but also his genotype.[...] The loss of Socrates’ genotype is
3474 not assuaged by any consideration of how prolifically he may have
reproduced. Socrates’ genes may be with us yet, but not his genotype,
3476 because meiosis and recombination destroy genotypes as surely as
death.” –WILLIAMS (1966)

3478 Individuals are temporary, their phenotypes are temporary, and
their genotypes are temporary. However, the alleles that individuals
3480 transmit across generations have permanence. Sustained phenotypic
evolutionary change due to natural selection occurs because of changes
3482 in the allelic composition of the population. To understand these
changes, we need to understand how the frequency of alleles (genes)
3484 changes over time due to natural selection.

As we have seen, natural selection occurs when there are differences
3486 between individuals in fitness. We may define fitness in various ways.
Most commonly, it is defined with respect to the contribution of a
3488 phenotype or genotype to the next generation. Differences in fitness
can arise at any point during the life cycle. For instance, different
3490 genotypes or phenotypes may have different survival probabilities from
one stage in their life to the stage of reproduction (viability), or they
3492 may differ in the number of offspring produced (fertility), or both.
Here, we define the absolute fitness of a genotype as the expected
3494 number of offspring of an individual of that genotype. Differences in
fitness among genotypes drive allele frequency change. In this chapter
3496 we’ll study the dynamics of alleles at a single locus. In this chapter
we’ll ignore the effects of genetic drift, and just study the determin-
3498 istic dynamics of selection. We’ll return to discuss the interaction of

selection and drift in the next chapter.

3500 *6.0.1 Haplod selection model*

We start out by modeling selection in a haploid model, as this is
 3502 mathematically relatively simple. Let the number of individuals carrying
 3504 alleles A_1 and A_2 in generation t be P_t and Q_t . Then, the relative
 3506 frequencies at time t of alleles A_1 and A_2 are $p_t = P_t/(P_t + Q_t)$ and
 $q_t = Q_t/(P_t + Q_t) = 1 - p_t$. Further, assume that individuals of
 type A_1 and A_2 on average produce W_1 and W_2 offspring individuals,
 respectively. We call W_i the absolute fitness.

3508 Therefore, in the next generation, the absolute number of carriers
 3510 of A_1 and A_2 are $P_{t+1} = W_1 P_t$ and $Q_{t+1} = W_2 Q_t$, respectively. The
 mean absolute fitness of the population at time t is

$$\bar{W}_t = W_1 \frac{P_t}{P_t + Q_t} + W_2 \frac{Q_t}{P_t + Q_t} = W_1 p_t + W_2 q_t, \quad (6.1)$$

i.e. the sum of the fitness of the two types weighted by their relative
 3512 frequencies. Note that the mean fitness depends on time, as it is a
 3514 function of the allele frequencies, which are themselves time depen-
 dent.

As an example of a rapid response to selection on an allele in a
 3516 haploid population, we can consider some data on the evolution of
 3518 drug resistant viruses. FEDER *et al.* (2017) studied viral dynamics
 in a macaque infected with a strain of simian immunodeficiency virus
 (SHIV) that carries the HIV-1 reverse transcriptase coding region.
 3520 The viral load of the macaque's blood plasma is shown as a black line
 in Figure 6.1. Twelve weeks after infection, the macaque was treated
 3522 with an anti-retroviral drug that targeted the the virus' reverse tran-
 scriptase protein. Note how the viral load initially starts to drop once
 3524 the drug is administered, suggesting that the absolute fitness of the
 original strain is less than one ($W_2 < 1$) in the presence of the drug (as
 3526 their numbers are decreasing). However, the viral population rebounds
 as a mutation that confers drug resistance to the anti-retroviral drug
 3528 arises in the SHIV and starts to spread. Viruses carrying this mu-
 tation (let's call them allele 1) likely have absolute fitness $W_1 > 1$.
 3530 The frequency of the drug-resistant allele is shown in red; it quickly
 spreads from being undetectable in week 13, to being fixed in the
 3532 SHIV population in week 20.

The rapid spread of this drug-resistant allele through the popula-
 3534 tion is driven by the much greater relative fitness of the drug-resistant
 allele over the original strain in the presence of the anti-retroviral
 drug.

The main focus of FEDER *et al.*'s work was modeling the complicated spatial dynamics of drug-resistant SHIV adaptation in different organ systems.

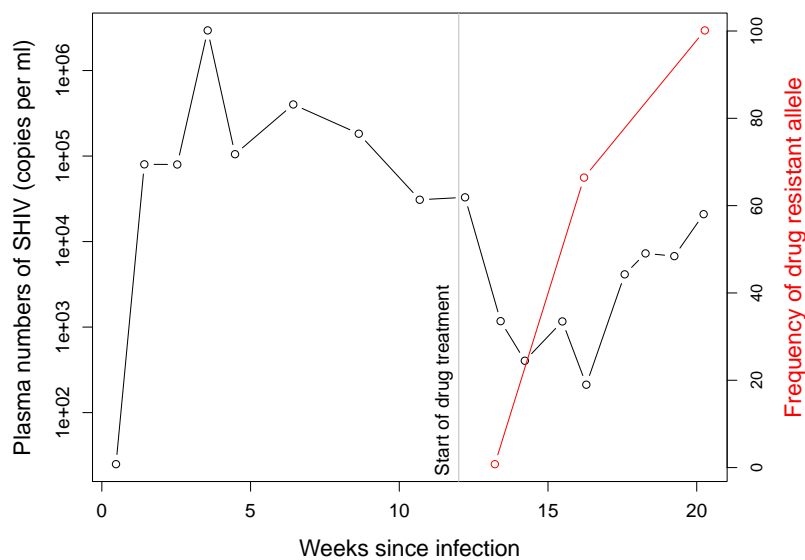


Figure 6.1: The rapid evolution of drug-resistant SHIV. The viral load of SHIV in the blood of a macaque (black line), the frequency of a drug resistance mutation (red line). Data from FEDER *et al.* (2017). Code here.

The frequency of allele A_1 in the next generation is given by

$$p_{t+1} = \frac{P_{t+1}}{P_{t+1} + Q_{t+1}} = \frac{W_1 P_t}{W_1 P_t + W_2 Q_t} = \frac{W_1 p_t}{W_1 p_t + W_2 q_t} = \frac{W_1}{\bar{W}_t} p_t. \quad (6.2)$$

Importantly, eqn. (6.2) tells us that the change in p only depends on a ratio of fitnesses. Therefore, we need to specify fitness only up to an arbitrary constant. As long as we multiply all fitnesses by the same value, that constant will cancel out and eqn. (6.2) will hold.

Based on this argument, it is very common to scale absolute fitnesses by the absolute fitness of one of the genotypes, e.g. the most or the least fit genotype, to obtain relative fitnesses. Here, we will use w_i for the relative fitness of genotype i . If we choose to scale by the absolute fitness of genotype A_1 , we obtain the relative fitnesses $w_1 = W_1/W_1 = 1$ and $w_2 = W_2/W_1$.

Without loss of generality, we can therefore rewrite eqn. (6.2) as

$$p_{t+1} = \frac{w_1}{\bar{w}} p_t, \quad (6.3)$$

dropping the subscript t for the dependence of the mean fitness on time in our notation, but remembering it. The change in frequency from one generation to the next is then given by

$$\Delta p_t = p_{t+1} - p_t = \frac{w_1 p_t}{\bar{w}} - p_t = \frac{w_1 p_t - \bar{w} p_t}{\bar{w}} = \frac{w_1 p_t - (w_1 p_t + w_2 q_t) p_t}{\bar{w}} = \frac{w_1 - w_2}{\bar{w}} p_t q_t, \quad (6.4)$$

recalling that $q_t = 1 - p_t$.

Assuming that the fitnesses of the two alleles are constant over time, the number of the two allelic types τ generations after time t are

$P_{t+\tau} = (W_1)^\tau P_t$ and $Q_{t+\tau} = (W_2)^\tau Q_t$, respectively. Therefore, the
 3556 relative frequency of allele A_1 after τ generations past t is

$$p_{t+\tau} = \frac{(W_1)^\tau P_t}{(W_1)^\tau P_t + (W_2)^\tau Q_t} = \frac{(w_1)^\tau P_t}{(w_1)^\tau P_t + (w_2)^\tau Q_t} = \frac{p_t}{p_t + (w_2/w_1)^\tau q_t}, \quad (6.5)$$

where the last step includes dividing the whole term by $(w_1)^\tau$ and
 3558 switching from absolute to relative allele frequencies.

Rearranging eqn. (6.5) and setting $t = 0$, we can work out the time
 3560 τ for the frequency of A_1 to change from p_0 to p_τ . First, we write

$$p_\tau = \frac{p_0}{p_0 + (w_2/w_1)^\tau q_0} \quad (6.6)$$

and rearrange this to obtain

$$\frac{p_\tau}{q_\tau} = \frac{p_0}{q_0} \left(\frac{w_1}{w_2} \right)^\tau. \quad (6.7)$$

3562 Solving this for τ yields

$$\tau = \log \left(\frac{p_\tau q_0}{q_\tau p_0} \right) / \log \left(\frac{w_1}{w_2} \right). \quad (6.8)$$

In practice, it is often helpful to parametrize the relative fitnesses
 3564 w_i in a specific way. For example, we may set $w_1 = 1$ and $w_2 = 1 - s$,
 where s is called the selection coefficient. Using this parametrization,
 3566 s is simply the difference in relative fitnesses between the two alleles.
 Equation (6.5) becomes

$$p_{t+\tau} = \frac{p_t}{p_t + q_t(1-s)^\tau}, \quad (6.9)$$

3568 as $w_2/w_1 = 1 - s$. Then, if $s \ll 1$, we can approximate $(1 - s)^\tau$ in the
 denominator by $\exp(-s\tau)$ to obtain

$$p_{t+\tau} \approx \frac{p_t}{p_t + q_t e^{-s\tau}}. \quad (6.10)$$

3570 This equation takes the form of a logistic function. That is because we
 are looking at the relative frequencies of two ‘populations’ (of alleles
 3572 A_1 and A_2) that are growing (or declining) exponentially, under the
 constraint that p and q always sum to 1.

3574 Moreover, eqn. (6.7) for the number of generations τ it takes for a
 certain change in frequency to occur becomes

$$\tau = -\log \left(\frac{p_\tau q_0}{q_\tau p_0} \right) / \log(1 - s). \quad (6.11)$$

3576 Assuming again that $s \ll 1$, this simplifies to

$$\tau \approx \frac{1}{s} \log \left(\frac{p_\tau q_0}{q_\tau p_0} \right). \quad (6.12)$$

One particular case of interest is the time it takes to go from an
 3578 absolute frequency of 1 to near fixation in a population of size N . In
 this case, we have $p_0 = 1/N$, and we may set $p_\tau = 1 - 1/N$, which is
 3580 very close to fixation. Then, plugging these values into eqn. (6.12), we
 obtain

$$\begin{aligned}\tau &= \frac{1}{s} \log \left(\frac{1 - 2/N + 1/N^2}{1/N^2} \right) \\ &\approx \frac{1}{s} (\log(N) + \log(N - 2)) \\ &\approx \frac{2}{s} \log(N)\end{aligned}\tag{6.13}$$

3582 where we make the approximations $N^2 - 2N + 1 \approx N^2 - 2N$ and later
 $N - 2 \approx N$.

3584 **Question 1.** In our example of the evolution of drug resistance,
 the drug-resistant SHIV virus spread from undetectable frequencies to
 3586 $\sim 65\%$ frequency by 16 weeks post infection. An estimated effective
 population size of SHIV is 1.5×10^5 , and its generation time is ~ 1
 3588 day. Assuming that the mutation arose as a single copy allele very
 shortly the start of drug treatment at 12 weeks, what is the selection
 3590 coefficient favouring the drug resistance allele?

Haploid model with fluctuating selection Selection pressures may
 3592 change while a polymorphism persists in the population due to environmental changes. We can use our haploid model to consider this
 3594 case where the fitnesses depend on time (DEMPSTER, 1955), and say that $w_{1,t}$ and $w_{2,t}$ are the fitnesses of the two types in generation t .
 3596 The frequency of allele A_1 in generation $t + 1$ is

$$p_{t+1} = \frac{w_{1,t}}{\bar{w}_t} p_t,\tag{6.14}$$

which simply follows from eqn. (6.3). The ratio of the frequency of
 3598 allele A_1 to that of allele A_2 in generation $t + 1$ is

$$\frac{p_{t+1}}{q_{t+1}} = \frac{w_{1,t}}{w_{2,t}} \frac{p_t}{q_t}.\tag{6.15}$$

Therefore, if we think of the two alleles starting in generation t at
 3600 frequencies p_t and q_t , then τ generations later,

$$\frac{p_{t+\tau}}{q_{t+\tau}} = \left(\prod_{i=t}^{\tau-1} \frac{w_{1,i}}{w_{2,i}} \right) \frac{p_t}{q_t}.\tag{6.16}$$

The question of which allele is increasing or decreasing in frequency
 3602 comes down to whether $\left(\prod_{i=t}^{\tau-1} w_{1,i}/w_{2,i} \right)$ is > 1 or < 1 . As it is a little

hard to think about this ratio, we can instead take the τ^{th} root of it

3604 and consider

$$\sqrt[\tau]{\left(\prod_{i=t}^{\tau-1} \frac{w_{1,i}}{w_{2,i}}\right)} = \frac{\sqrt[\tau]{\prod_{i=t}^{\tau-1} w_{1,i}}}{\sqrt[\tau]{\prod_{i=t}^{\tau-1} w_{2,i}}} \quad (6.17)$$

The term

$$\sqrt[\tau]{\prod_{i=t}^{\tau-1} w_{1,i}} \quad (6.18)$$

3606 is the geometric mean fitness of allele A_1 over the τ generations past generation t . Therefore, allele A_1 will only increase in frequency 3608 if it has a higher geometric mean fitness than allele A_2 (at least in our simple deterministic model). This implies that an allele with higher 3610 geometric mean fitness can even invade and spread to fixation if its (arithmetic) mean fitness is lower than the dominant type. To see this 3612 consider two alleles that experience the fitnesses given in Table 6.1. The allele A_1 does much better in dry years, but suffers in wet years; 3614 while the A_2 is generalist and is not affected by the variable environment. If there is an equal chance of a year being wet or dry, the A_1 3616 allele has higher (arithmetic) mean fitness, but it will be replaced by the A_2 allele as the A_2 allele has higher geometric mean fitness (See 3618 Figure 6.2).

	A_1	A_2
Dry	2	1.57
Wet	1.16	1.57
Arithmetic Mean	1.58	1.57
Geometric Mean	1.52	1.57

Table 6.1: Fitnesses of two alleles in wet and dry years. Means calculated assuming equal chances of wet and dry years. The geometric mean is calculated as $\sqrt{w_{\text{wet}} w_{\text{dry}}}$. Example numbers taken from SEGER and BROCKMANN (1987).

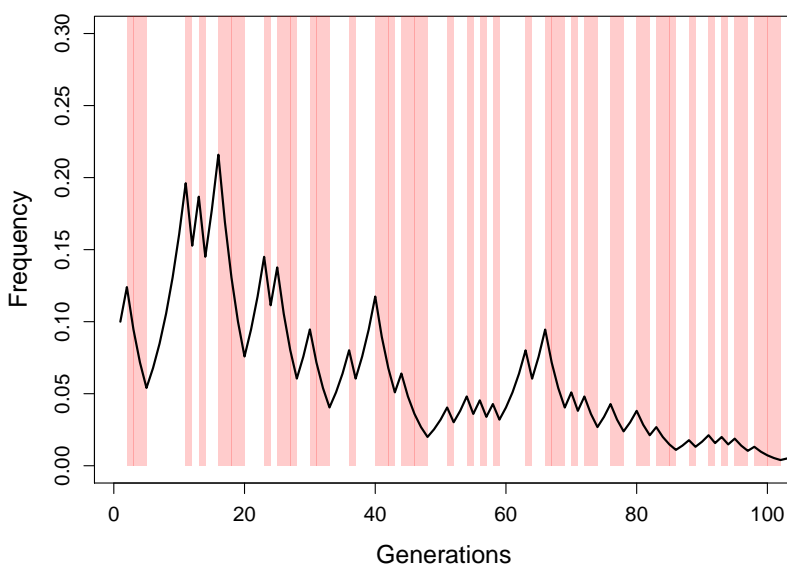


Figure 6.2: An example frequency trajectory of the A_2 allele under variable environments (using the fitnesses from Table 6.1). Dry years (generations) are shown in red, wet years in white. Note how the A_2 allele decreases in frequency in the dry years as A_1 has higher fitness, and yet the A_2 allele still wins out. Code here.

Evolution of bet hedging Don't put your eggs in one basket, it makes
 3620 a lot of sense to spread your bets. Financial advisors often advise you
 to diversify your portfolio, rather than placing all your investments
 3622 in one stock. Even if that stock looks very strong, you can come a
 cropper that $1/20$ times some particular part of the market crashes.
 3624 Likewise, evolution can result in risk averse strategies. Some species of
 bird lay multiple nests of eggs; some plants don't put all of their en-
 3626 ergy into seeds that will germinate next year. It can even make sense
 to hedge your bets even if that comes at an average cost (SEGER and
 3628 BROCKMANN, 1987).

To see this lets think more about geometric fitness. We can write
 3630 the fitness in a given generation i as $w_i = 1 + s_i$, such that we can
 write your geometric fitness as

$$\bar{g} = \sqrt[\tau]{\prod_{i=t}^{\tau-1} 1 + s_i} \quad (6.19)$$

when we think about products it's often natural to take the log to
 turn it into a sum

$$\begin{aligned} \log(\bar{g}) &= \frac{1}{\tau} \sum_{i=t}^{\tau-1} \log(1 + s_i) \\ &= \mathbb{E}[\log(1 + s_i)] \end{aligned} \quad (6.20)$$

equating the mean and the expectation. Assuming that s_i is small
 $\log(1 + s_i) \approx s_i - s_i^2/2$, ignoring terms s_i^3 and higher then this is

$$\begin{aligned} \log(\bar{g}) &\approx \mathbb{E}[s_i - s_i^2/2] \\ &= \mathbb{E}[s_i] - \text{var}(s_i)/2 \end{aligned} \quad (6.21)$$

3632 So genotypes with high arithmetic mean fitness can be selected against,
 i.e. have low geometric mean fitness against, if their fitness has too

3634 high a variance across generations (GILLESPIE, 1973, 1977). See our
 example above, Table 6.1 and Figure 6.2).

3636 A classic example of bet-hedging is in delayed seed germination
 in plants (COHEN, 1966). In variable environments, such as deserts,
 3638 it may make sense to spread your bets over years by having only a
 proportion of your seeds germinate in the first year. However, delay-
 3640 ing germination can come at a cost due to seed mortality. GREMER
 and VENABLE (2014), using data from a long-term study various
 3642 species of Sonoran Desert winter showed that annual plants were in-
 deed pursuing adaptive bet-hedging strategies. The plant species with

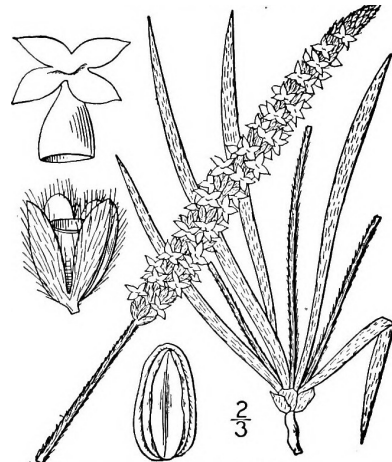


Figure 6.3: Woolly plantain (*Plantago patagonica*). One of the desert annuals shown to have a bet-hedging germination strategy by GREMER and VENABLE (2014).

An illustrated flora of the northern United States, Canada and the British possessions, from Newfoundland to the parallel of the southern boundary of Virginia, and from the Atlantic Ocean westward to the 102d meridian (1913) Britton, N.L. Image from the Biodiversity Heritage Library. Contributed by Cornell University Library. Not in copyright.

³⁶⁴⁴ the highest variation in among-year yield had the lowest germination fraction per year. Further, GREMER and VENABLE showed through
³⁶⁴⁶ modeling life that by having per-year germination proportions < 1 all of the species were achieving higher geometric fitness at the expense
³⁶⁴⁸ of arithmetic fitness in the variable desert environment. See Figure 6.4 for an example of bet hedging in Woolly plantain.

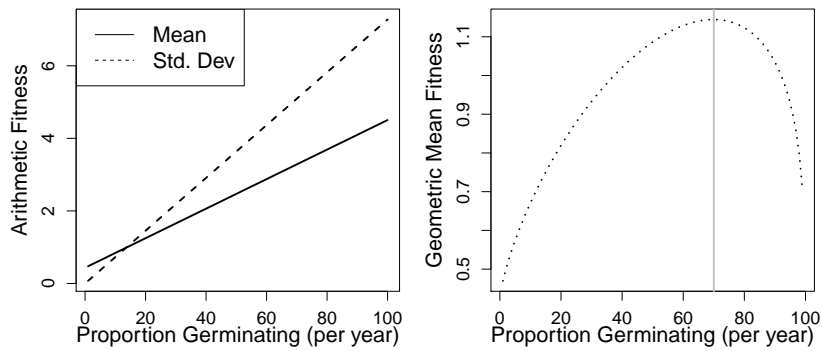


Figure 6.4: *Plantago patagonica*'s arithmetic fitness is an increasing function of the proportion of seeds germinating, due to seeds not surviving a germination delay. However, the standard deviation of fitness also increases with this proportion as they are more likely to have all of their seeds germinate in a bad year. Thus *Plantago patagonica* can achieve higher geometric fitness by only having a proportion of their seeds germinate. Thanks to Jenny Gremer for sharing these data from GREMER and VENABLE (2014)

³⁶⁵⁰ Delayed reproduction is also a common example of bet-hedging in micro-organisms. For example, the Chicken Pox virus, varicella
³⁶⁵² zoster virus, has a very long latent phase. After it causes chicken pox it enters a latent phase, residing, inactive, in neurons in the spinal
³⁶⁵⁴ cord, only to emerge 5-40 years later to cause the disease shingles. It is hypothesized that the virus actively suppresses itself as a strategy
³⁶⁵⁶ to allow it to emerge at a later time point as insurance against there being no further susceptible hosts at the time of its first infection
³⁶⁵⁸ (STUMPF *et al.*, 2002).

6.0.2 Diploid model

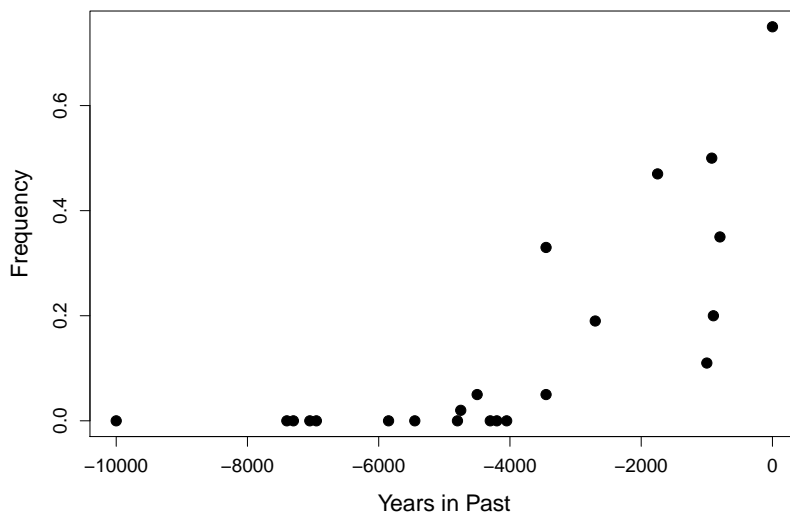


Figure 6.5: Frequency of the Lactase persistence allele in ancient and modern samples from Central Europe. Data compiled by MARCINIAK and PERRY (2017) from various sources. Thanks to Stephanie Marciniak for sharing these data. Code here.

3660 We will now move on to a diploid model of a single locus with two
 3662 segregating alleles. As an example of the change in the frequency of an
 3664 allele driven by selection, let's consider the evolution of Lactase persis-
 3666 tence. A number of different human populations that historically have
 3668 raised cattle have convergently evolved to maintain the expression
 3670 of the protein Lactase into adulthood (in most mammals the pro-
 3672 tein is switched off after childhood), with different lactase-persistence
 3674 mutations having arisen and spread in different pastoral human pop-
 3676ulations. This continued expression of Lactase allows adults to break
 3678 down Lactose, the main carbohydrate in milk, and so benefit nutri-
 3680 tionally from milk-drinking. This seems to have offered a strong fitness
 3682 benefit to individuals in pastoral populations.

3672 With the advent of techniques to sequence ancient human DNA,
 3674 researchers can now potentially track the frequency of selected muta-
 3676tions over thousands of years. The frequency of a Lactase persistence
 3678 allele in ancient Central European populations is shown in Figure
 3680 6.5. The allele is absent more than 5,000 years ago, but now found at
 3682 frequency of upward of 70% in many European populations.

3678 We will assume that the difference in fitness between the three
 3680 genotypes comes from differences in viability, i.e. differential survival
 3682 of individuals from the formation of zygotes to reproduction. We
 denote the absolute fitnesses of genotypes A_1A_1 , A_1A_2 , and A_2A_2
 by W_{11} , W_{12} , and W_{22} . Specifically, W_{ij} is the probability that a
 zygote of genotype A_iA_j survives to reproduction. Assuming that



Figure 6.6: Auroch (*Bos primigenius*). Aurochs are an extinct species of large wild cattle that cows were domesticated from.
Dictionnaire des sciences naturelles. 1816
 Cuvier, F.G. Image from the Internet Archive.
 Contributed by NCSU Libraries. No known
 copyright restrictions.

³⁶⁸⁴ individuals mate at random, the number of zygotes that are of the three genotypes and form generation t are

$$Np_t^2, \quad N2p_tq_t, \quad Nq_t^2. \quad (6.22)$$

³⁶⁸⁶ The mean fitness of the population of zygotes is then

$$\bar{W}_t = W_{11}p_t^2 + W_{12}2p_tq_t + W_{22}q_t^2. \quad (6.23)$$

Again, this is simply the weighted mean of the genotypic fitnesses.

³⁶⁸⁸ How many zygotes of each of the three genotypes survive to reproduce? An individual of genotype A_1A_1 has a probability of W_{11} ³⁶⁹⁰ of surviving to reproduce, and similarly for other genotypes. Therefore, the expected number of A_1A_1 , A_1A_2 , and A_2A_2 individuals who ³⁶⁹² survive to reproduce is

$$NW_{11}p_t^2, \quad NW_{12}2p_tq_t, \quad NW_{22}q_t^2. \quad (6.24)$$

It then follows that the total number of individuals who survive to ³⁶⁹⁴ reproduce is

$$N(W_{11}p_t^2 + W_{12}2p_tq_t + W_{22}q_t^2). \quad (6.25)$$

This is simply the mean fitness of the population multiplied by the ³⁶⁹⁶ population size (i.e. $N\bar{w}$).

The relative frequency of A_1A_1 individuals at reproduction is ³⁶⁹⁸ simply the number of A_1A_1 genotype individuals at reproduction ($NW_{11}p_t^2$) divided by the total number of individuals who survive to ³⁷⁰⁰ reproduce ($N\bar{W}$), and likewise for the other two genotypes. Therefore, ³⁷⁰² the relative frequency of individuals with the three different genotypes at reproduction is

$$\frac{NW_{11}p_t^2}{N\bar{W}}, \quad \frac{NW_{12}2p_tq_t}{N\bar{W}}, \quad \frac{NW_{22}q_t^2}{N\bar{W}} \quad (6.26)$$

(see Table 6.2).

	A_1A_1	A_1A_2	A_2A_2
Absolute no. at birth	Np_t^2	$N2p_tq_t$	Nq_t^2
Fitnesses	W_{11}	W_{12}	W_{22}
Absolute no. at reproduction	$NW_{11}p_t^2$	$NW_{12}2p_tq_t$	$NW_{22}q_t^2$
Relative freq. at reproduction	$\frac{W_{11}}{\bar{W}}p_t^2$	$\frac{W_{12}}{\bar{W}}2p_tq_t$	$\frac{W_{22}}{\bar{W}}q_t^2$

³⁷⁰⁴ As there is no difference in the fecundity of the three genotypes, the allele frequencies in the zygotes forming the next generation are simply ³⁷⁰⁶ the allele frequency among the reproducing individuals of the previous generation. Hence, the frequency of A_1 in generation $t + 1$ is

$$p_{t+1} = \frac{W_{11}p_t^2 + W_{12}2p_tq_t}{\bar{W}}. \quad (6.27)$$

Table 6.2: Relative genotype frequencies after one episode of viability selection.

³⁷⁰⁸ Note that, again, the absolute value of the fitnesses is irrelevant to the frequency of the allele. Therefore, we can just as easily replace the ³⁷¹⁰ absolute fitnesses with the relative fitnesses. That is, we may replace W_{ij} by $w_{ij} = W_{ij}/\bar{W}$, for instance.

³⁷¹² Each of our genotype frequencies is responding to selection in a manner that depends just on its fitness compared to the mean fitness ³⁷¹⁴ of the population. For example, the frequency of the 11 homozygotes increases from birth to adulthood in proportion to W_{11}/\bar{W} . In fact, ³⁷¹⁶ we can estimate this fitness ratio for each genotype by comparing the frequency at birth compared to adults. As an example of this ³⁷¹⁸ calculation, we'll look at some data from sticklebacks.

³⁷²⁰ Marine threespine stickleback (*Gasterosteus aculeatus*) independently colonized and adapted to many freshwater lakes as glaciers receded following the last ice age, making sticklebacks a wonderful system ³⁷²² for studying the genetics of adaptation. In marine habitats, most of the stickleback have armour plates to protect them from predation, ³⁷²⁴ but freshwater populations repeatedly evolve the loss of armour plates due to selection on an allele at the Ectodysplasin gene (EDA). This ³⁷²⁶ allele is found as a standing variant at very low frequency marine populations; BARRETT *et al.* took advantage of this fact and collected ³⁷²⁸ and bred a population of marine individuals carrying both the low- (L) and completely-plated (C) alleles. They introduced the offspring of this cross into four freshwater ponds and monitored genotype frequencies ³⁷³⁰ ¹ over their life courses:

	CC	LC	LL
Juveniles	0.55	0.23	0.22
Adults	0.21	0.53	0.26
Adults/Juv. (W_{\bullet}/\bar{W})	0.4	2.3	1.2
rel. fitness (W_{\bullet}/W_{12})	0.17	1.0	0.54

³⁷³² The heterozygotes have increased in frequency dramatically in the population as their fitness is more than double the mean fitness of the population. We can also calculate the relative fitness of each genotype by dividing through by the fitness of the fittest genotype, the heterozygote in this case (doing this cancels through \bar{W}). The relative fitness of the CC is $\sim 1/5$ of the heterozygote. Note that this calculation does not rely on the genotype frequencies being at their HWE in ³⁷³⁶ the juveniles.

Question 2. A What is the frequency of the low-plated EDA allele (L) at the start of the stickleback experiment?

B What is the frequency in the adults?

³⁷⁴⁴ **Question 3.** For many generations you have been studying an annual wildflower that has two color morphs, orange and white. You

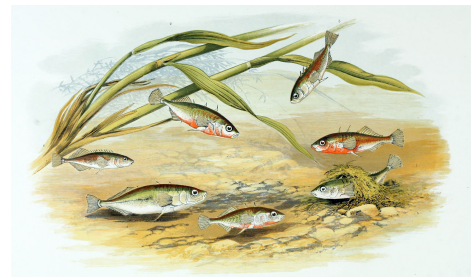


Figure 6.7: Freshwater threespine Stickleback (*G. aculeatus*).
British fresh-water fishes. Houghton W 1879.
Image from the Biodiversity Heritage Library.
Contributed by Ernst Mayr Library, Harvard..
Not in copyright.

¹ The actual dynamics observed by BARRETT *et al.* are more complicated as in the very young fish selection reverses direction.

³⁷⁴⁶ have discovered that a single bi-allelic locus controls flower color, with
 the white allele being recessive. The pollinator of these plants is an
³⁷⁴⁸ almost blind bat, so individuals are pollinated at random with respect
 to flower color. Your population census of 200 individuals showed that
³⁷⁵⁰ the population consisted of 168 orange-flowered individuals, and 32
 white-flowered individuals.

³⁷⁵² Heavy February rainfall creates optimal growing conditions for
 an exotic herbivorous beetle with a preference for orange-flowered
³⁷⁵⁴ individuals. This year it arrives at your study site with a ravenous
 appetite. Only 50% of orange-flowered individuals survive its wrath,
³⁷⁵⁶ while 90% of white-flowered individuals survive until the end of the
 growing season.

³⁷⁵⁸ **A** What is the initial frequency of the white allele, and what do you
 have to assume to obtain this?

³⁷⁶⁰ **B** What is the frequency of the white allele in the seeds forming the
 next generation?

³⁷⁶² The change in frequency from generation t to $t + 1$ is

$$\Delta p_t = p_{t+1} - p_t = \frac{w_{11}p_t^2 + w_{12}p_tq_t}{\bar{w}} - p_t. \quad (6.28)$$

To simplify this equation, we will first define two variables \bar{w}_1 and \bar{w}_2
³⁷⁶⁴ as

$$\bar{w}_1 = w_{11}p_t + w_{12}q_t, \quad (6.29)$$

$$\bar{w}_2 = w_{12}p_t + w_{22}q_t. \quad (6.30)$$

These are called the marginal fitnesses of allele A_1 and A_2 , respectively.
³⁷⁶⁶ They are so called as \bar{w}_1 is the average fitness of an allele A_1 ,
 i.e. the fitness of A_1 in a homozygote weighted by the probability it is
³⁷⁶⁸ in a homozygote (p_t) plus the fitness of A_1 in a heterozygote weighted
 by the probability it is in a heterozygote (q_t). We further note that
³⁷⁷⁰ the mean relative fitness can be expressed in terms of the marginal
 fitnesses as

$$\bar{w} = \bar{w}_1p_t + \bar{w}_2q_t, \quad (6.31)$$

³⁷⁷² where, for notational simplicity, we have omitted subscript t for the
 dependence of mean and marginal fitnesses on time.

³⁷⁷⁴ We can then rewrite eqn. (6.28) using \bar{w}_1 and \bar{w}_2 as

$$\Delta p_t = \frac{(\bar{w}_1 - \bar{w}_2)}{\bar{w}} p_t q_t. \quad (6.32)$$

The sign of Δp_t , i.e. whether allele A_1 increases or decreases in frequency, depends only on the sign of $(\bar{w}_1 - \bar{w}_2)$. The frequency of A_1 will keep increasing over the generations so long as its marginal fitness is higher than that of A_2 , i.e. $\bar{w}_1 > \bar{w}_2$, while if $\bar{w}_1 < \bar{w}_2$, the frequency of A_1 will decrease. Note the similarity between eqn. (6.32)

³⁷⁸⁰ and the respective expression for the haploid model in eqn. (6.4). (We will return to the special case where $\bar{w}_1 = \bar{w}_2$ shortly).

³⁷⁸² We can also rewrite (6.28) as

$$\Delta p_t = \frac{1}{2} \frac{p_t q_t}{\bar{w}} \frac{dw}{dp}, \quad (6.33)$$

³⁷⁸⁴ the demonstration of which we leave to the reader (see question below). This form shows that the frequency of A_1 will increase ($\Delta p_t > 0$) if the mean fitness is an increasing function of the frequency of A_1 (i.e. if $\frac{d\bar{w}}{dp} > 0$). On the other hand, the frequency of A_1 will decrease ($\Delta p_t < 0$) if the mean fitness is a decreasing function of the frequency of A_1 (i.e. if $\frac{d\bar{w}}{dp} < 0$). Thus, although selection acts on individuals, under this simple model, selection is acting to increase the mean fitness of the population. The rate of this increase is proportional to the variance in allele frequencies within the population ($p_t q_t$). This formulation suggested to WRIGHT (1932) the view of natural selection as moving populations up local fitness peaks, as we encountered in ³⁷⁹² Section ?? in discussing phenotypic fitness peaks. Again this view of selection as maximizing mean fitness only holds true if the genotypic ³⁷⁹⁴ fitnesses are frequency independent, later in this chapter we'll discuss some important cases where that doesn't hold.

³⁷⁹⁸ **Question 4.** Show that eqns. (6.33) and (6.32) are equivalent.

(Trickier question.)

³⁸⁰⁰ So far, our treatment of the diploid model of selection has been in terms of generic fitnesses w_{ij} . In the following, we will use particular ³⁸⁰² parameterizations to gain insight about two specific modes of selection: directional selection and heterozygote advantage.

³⁸⁰⁴ 6.0.3 Diploid directional selection

Directional selection means that one of the two alleles always has ³⁸⁰⁶ higher marginal fitness than the other one. Let us assume that A_1 is the fitter allele, so that $w_{11} \geq w_{12} \geq w_{22}$, and hence $\bar{w}_1 > \bar{w}_2$. As ³⁸⁰⁸ we are interested in changes in allele frequencies, we may use relative fitnesses. We parameterize the reduction in relative fitness in terms ³⁸¹⁰ of a selection coefficient, similar to the one we met in the haploid selection section, as follows:

genotype	$A_1 A_1$	$A_1 A_2$	$A_2 A_2$
absolute fitness	W_{11}	$\geq W_{12} \geq$	W_{22}
relative fitness (generic)	$w_{11} = W_{11}/W_{11}$	$w_{12} = W_{12}/W_{11}$	$w_{22} = W_{22}/W_{11}$
relative fitness (specific)	1	$1 - sh$	$1 - s$.

³⁸¹⁴ Here, the selection coefficient s is the difference in relative fitness between the two homozygotes, and h is the dominance coefficient. For

selection to be directional, we require that $0 \leq h \leq 1$ holds. The dominance coefficient allows us to move between two extremes. One is when $h = 0$, such that allele A_1 is fully dominant and A_2 fully recessive. In this case, the heterozygote A_1A_2 is as fit as the A_1A_1 homozygote genotype. The inverse holds when $h = 1$, such that allele A_1 is fully recessive and A_2 fully dominant.

We can then rewrite eqn. (6.32) as

$$\Delta p_t = \frac{p_t h s + q_t s(1-h)}{\bar{w}} p_t q_t, \quad (6.34)$$

where

$$\bar{w} = 1 - 2p_t q_t s h - q_t^2 s. \quad (6.35)$$

Question 5. Throughout the Californian foothills are old copper and gold-mines, which have dumped out soils that are polluted with heavy metals. While these toxic mine tailing are often depauperate of plants, *Mimulus guttatus* and a number of other plant species have managed to adapt to these harsh soils. WRIGHT *et al.* (2015) have mapped one of the major loci contributing to the adaptation to soils at two mines near Copperopolis, CA. WRIGHT *et al.* planted homozygote seedlings out in the mine tailings and found that only 10% of the homozygotes for the non-copper-tolerant allele survived to flower, while 40% of the copper-tolerant seedlings survived to flower.

A) What is the selection coefficient acting against the non-copper-tolerant allele on the mine tailing?

B) The copper-tolerant allele is fairly dominant in its action on fitness. If we assume that $h = 0.1$, what percentage of heterozygotes should survive to flower?

Question 6. Comparing the red ($h = 0$) and black ($h = 0.5$) trajectories in Figure 6.8, provide an explanation for why A_1 increases faster initially if $h = 0$, but then approaches fixation more slowly compared to the case of $h = 0.5$.

To see how dominance affects the trajectory of a real polymorphism, we'll consider an example from a colour polymorphism in red foxes (*Vulpes vulpes*). There are three colour morphs of red foxes: silver, cross, and red (see Figure 6.11), with this difference primarily controlled by a single polymorphism with genotypes RR, Rr, and rr respectively. The fur pelts of the silver morph fetched three times the price for hunters compared to cross (a smoky red) and red pelts, the latter two being seen as roughly equivalent in worth. Thus the desirability of the pelts acts as a recessive trait, with much stronger selection against the silver homozygotes. As a result of this price difference, silver foxes were hunted more intensely and declined as a

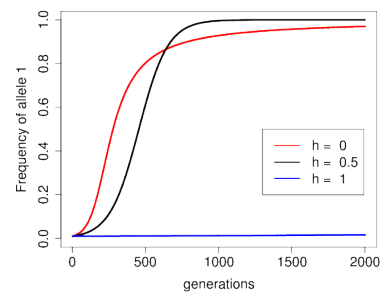


Figure 6.8: The trajectory of the frequency of allele A_1 , starting from $p_0 = 0.01$, for a selection coefficient $s = 0.01$ and three different dominance coefficients. The recessive beneficial allele ($h = 1$) will eventually fix in the population, but it takes a long time. Code here.



Figure 6.9: Keystone Copper Mine
1866, Copperopolis, Calaveras County.
Image from picryl. Source Library of Congress, Public Domain.

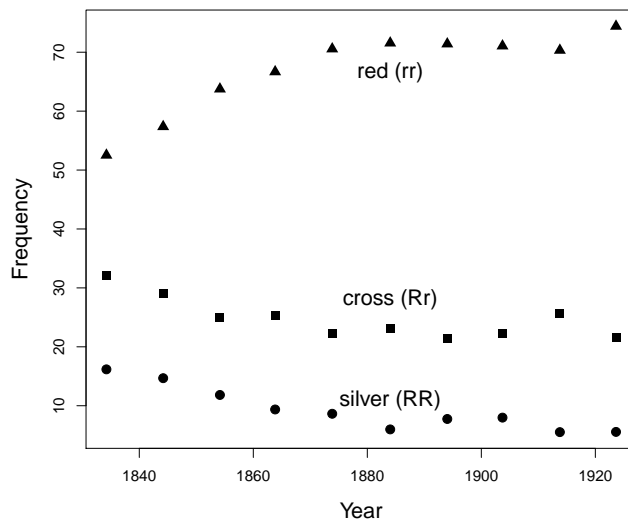


Figure 6.10: The frequency of red, cross, and silver fox morphs over the decades in Eastern Canada. These data are well described by recessive selection acting against the silver fox morph. Data from ELTON (1942), compiled by ALLENDORF and HARD (2009). [Code here.](#)

3854 proportion of the population in Eastern Canada, see Figure 6.10, as
documented by ELTON, from 16% to 5% from 1834 to 1937. HAL-
3856 DANE reanalyzed these data and showed that they were consistent
with recessive selection acting against the silver morph alone.

3858 Note how the heterozygotes (cross) decline somewhat as a result of
selection on the silver homozygotes, but overall the R allele is slow to
3860 respond to selection as it is ‘hidden’ from selection in the heterozygote
state.

3862 *Directional selection on an additive allele.* A special case is when
 $h = 0.5$. This case is the case of no dominance, as the interaction
3864 among alleles with respect to fitness is strictly additive. Then, eqn.
(6.34) simplifies to

$$\Delta p_t = \frac{1}{2} \frac{s}{\bar{w}} p_t q_t. \quad (6.36)$$

3866 If selection is very weak, i.e. $s \ll 1$, the denominator (\bar{w}) is close to
1 and we have

$$\Delta p_t = \frac{1}{2} s p_t q_t. \quad (6.37)$$

3868 It is instructive to compare eqn. (6.37) to the respective expression
under the haploid model. To this purpose, start from the generic term
3870 for Δp_t under the haploid model in eqn. (6.4) and set $w_1 = 1$ and
 $w_2 = 1 - s$. Again, assume that s is small, so that eqn. (6.4) becomes
3872 $\Delta p_t = s p_t q_t$. Hence, if s is small, the diploid model of directional
selection without dominance is identical to the haploid model, up to a
3874 factor of 1/2. That factor is due to the choice of the parametrisation;



Figure 6.11: Three colour morphs in red fox *V. vulpes*, cross, red, and silver foxes from left to right.
The larger North American mammals” Nelson,
E.W., Fuertes, L.A. 1916. Image from the
Biodiversity Heritage Library. Contributed
by Cornell University Library. No known
copyright restrictions.

we could have set $w_{11} = 1$, $w_{12} = 1 - s$, and $w_{22} = 1 - 2s$ in our diploid model instead, in which case the agreement with the haploid model would be perfect.

From this analogy, we can borrow some insight we gained from the haploid model. Specifically, the trajectory of the frequency of allele A_1 in the diploid model without dominance follows a logistic growth curve similar to (6.10). From this similarity, we can extrapolate from Equation (6.12) to find the time it takes for our diploid, beneficial, additive allele (A_1) to move from frequency p_0 to p_τ :

$$\tau \approx \frac{2}{s} \log \left(\frac{p_\tau q_0}{q_\tau p_0} \right) \quad (6.38)$$

generations; this just differs by a factor of 2 from our haploid model. Using this result we can find the time it takes for our favourable, additive allele (A_1) to transit from its entry into the population ($p_0 = 1/(2N)$) to close to fixation ($p_\tau = 1 - 1/(2N)$):

$$\tau \approx \frac{4}{s} \log(2N) \quad (6.39)$$

generations. Note the similarity to eqn. 6.13 for the haploid model, with a difference by a factor of 2 due to the choice of parametrization (and that the number of alleles is $2N$ in the diploid model, rather than N). Doubling our selection coefficient halves the time it takes for our allele to move through the population.

Question 7. Gulf killifish (*Fundulus grandis*) have rapidly adapted to the very high pollution levels in the Houston shipping canal since the 1950s. One of the ways that they've adapted is through the deletion of their aryl hydrocarbon receptor (AHR) gene. Oziolor et al. estimated that individuals who were homozygote for the intact AHR gene had a relative fitness of 20% of that of homozygotes for the deletion. Assuming an effective population size of 200 thousand individuals, how long would it take for the deletion to reach fixation, starting as a single copy in this population?

3902 6.1 Balancing selection and the selective maintenance of polymorphism.

3904 Directional selection on genotypes is expected to remove variation from populations, yet we see plentiful phenotypic and genetic variation in every natural population. Why is this? Three broad explanations for the maintenance of polymorphisms are

- 3908 1. Variation is maintained by a balance of genetic drift and mutation (we discussed this explanation in Chapter 3).

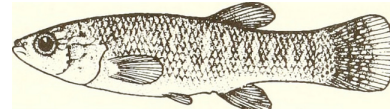


Figure 6.12: Gulf killifish (*Fundulus grandis*).

Distribution and abundance of fishes and invertebrates in Gulf of Mexico estuaries. Nelson D M and Pattillo M E Image from the Biodiversity Heritage Library. Contributed by MBLWHOI Library. No known copyright restrictions.

- 3910 2. Selection can sometimes act to maintain variation in populations
(balancing selection).
- 3912 3. Deleterious variation can be maintained in the population as a bal-
ance between selection removing variation and mutation constantly
3914 introducing new variation into the population.

We'll turn to these latter two explanations through this chapter and
3916 the next. Note that these explanations are not mutually exclusive,
and each of them will explain some proportion of the variation.

3918 *6.1.1 Heterozygote advantage*

One form of balancing selection occurs when the heterozygotes are
3920 fitter than either of the homozygotes. In this case, it is useful to pa-
rameterize the relative fitnesses as follows:

3922

genotype	$A_1 A_1$	$A_1 A_2$	$A_2 A_2$
absolute fitness	w_{11}	$w_{12} < w_{11} >$	w_{22}
relative fitness (generic)	$w_{11} = W_{11}/W_{12}$	$w_{12} = W_{12}/W_{11}$	$w_{22} = W_{22}/W_{12}$
relative fitness (specific)	$1 - s_1$	1	$1 - s_2$

3924 Here, s_1 and s_2 are the differences between the relative fitnesses
of the two homozygotes and the heterozygote. Note that to obtain
3926 relative fitnesses we have divided absolute fitness by the heterozygote
fitness. We could use the same parameterization as in the model of
3928 directional selection, but the reparameterization we have chosen here
makes the math easier.

3930 In this case, when allele A_1 is rare, it is often found in a heterozy-
gous state, while the A_2 allele is usually in the homozygous state, and
3932 so A_1 is more fit and increases in frequency. However, when the allele
 A_1 is common, it is often found in a less fit homozygous state, while
3934 the allele A_2 is often found in a heterozygous state; thus it is now al-
lele A_2 that increases in frequency at the expense of allele A_1 . Thus,
3936 at least in the deterministic model, neither allele can reach fixation
and both alleles will be maintained at an equilibrium frequency as a
3938 balanced polymorphism in the population.

We can solve for this equilibrium frequency by setting $\Delta p_t = 0$
3940 in eqn. (6.32), i.e. $p_t q_t (\bar{w}_1 - \bar{w}_2) = 0$. Doing so, we find that there
are three equilibria, all of which are stable. Two of them are not very
3942 interesting ($p = 0$ or $q = 0$), but the third one is the polymorphic equi-
librium, where $\bar{w}_1 - \bar{w}_2 = 0$ holds. Using our s_1 and s_2 parametrization
3944 above, we see that the marginal fitnesses of the two alleles are equal
when

$$p_e = \frac{s_2}{s_1 + s_2} \quad (6.40)$$

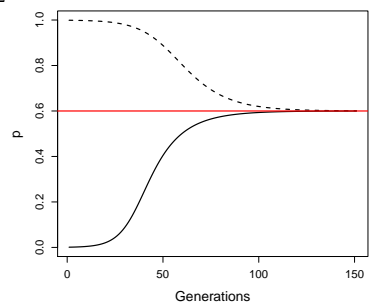
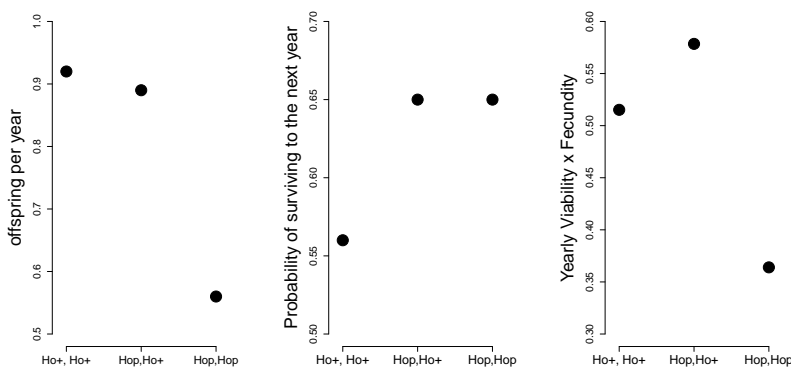


Figure 6.13: Two allele frequency trajectories of the A_1 allele subject to heterozygote advantage ($w_{11} = 0.9$, $w_{12} = 1$, and $w_{22} = 0.85$). In one simulation the allele is started from being rare in the population ($p = 1/1000$, solid line) and increases in frequency/ In the other simulation the allele is almost fixed ($p = 999/1000$, dashed line). In both cases the frequency moves toward the equilibrium frequency. The red line shows the equilibrium frequency (p_e). Code here.

for the equilibrium frequency of interest. This is also the frequency of A_1 at which the mean fitness of the population is maximized. The highest possible fitness of the population would be achieved if every individual was a heterozygote. However, Mendelian segregation of alleles in the gametes of heterozygotes means that a sexual population can never achieve a completely heterozygote population. This equilibrium frequency represents an evolutionary compromise between the advantages of the heterozygote and the comparative costs of the two homozygotes.



One example of a polymorphism maintained by heterozygote advantage is a horn-size polymorphism found in Soay sheep, a population of feral sheep on the island of Soay (about 40 miles off the coast of Scotland). The horns of the soay sheep resemble those of the wild Mouflon sheep, and the male Soay sheep use their horns to defend females during the rut. JOHNSTON *et al.* (2013) found a large-effect locus, at the RXFP2 gene, that controls much of the genetic variation for horn size. Two alleles Ho^p and Ho^+ segregate at this locus. The Ho^+ allele is associated with growing larger horns, while the Ho^p allele is associated with smaller horns, with a reasonable proportion of Ho^p homozygotes developing no horns at all. JOHNSTON *et al.* (2013) found that the Ho locus had substantial effects on male, but not female, fitness (see Figure 6.16).

The Ho^p allele has a mostly recessive effect on male fecundity, with the Ho^p homozygotes having lower yearly reproductive success presumably due to the fact that they perform poorly in male-male competition (left plot Figure 6.16). Conversely, the Ho^+ has a mostly recessive effect on viability, with Ho^+ homozygotes having lower yearly survival (middle plot Figure 6.16), likely because they spend little time feeding during the rut and so lose substantial body weight. Thus both of the homozygotes suffer from trade-offs between viability and

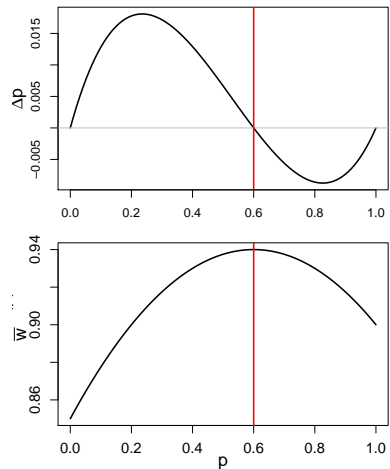


Figure 6.14: **Top)** The change in frequency of an allele with heterozygote advantage within a generation (Δp) as a function of the allele frequency. Fitnesses as in Figure 6.13. Note how the frequency change is positive below the equilibrium frequency (p_e) and negative above. **Bottom)** Mean fitness (\bar{w}) as a function of the allele frequency. The red line shows the equilibrium frequency (p_e). Code here.

Figure 6.15: For the three Soay sheep genotypes: the offspring per year (left), the probability of surviving a year (middle), and the product of the two (right). Thanks to Susan Johnston for supplying these simplified numbers from JOHNSTON *et al.* (2013). Code here.

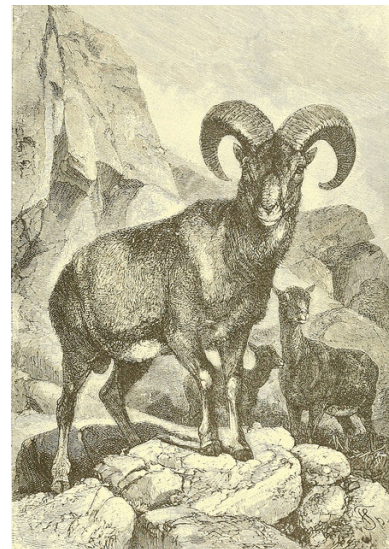


Figure 6.16: Mouflon (*Ovis orientalis orientalis*). Animate creation. (1898). Wood, J. G. Image from the Biodiversity Heritage Library. Contributed by Smithsonian Libraries. Not in copyright.

fecundity. As a result, the Ho^pHo^+ heterozygotes have the highest fitness (right plot Figure 6.16). The allele is thus balanced at intermediate frequency (50%) in the population due to this trade off between fitness at different life history stages.

Question 8. Assume that the frequency of the Ho^P allele is 10%, that there are 1000 males at birth, and that individual adults mate at random.

A) What is the expected number of males with each of the three genotypes in the population at birth?

B) Assume that a typical male individual of each genotypes has the following probability of surviving to adulthood:

$$\begin{array}{cccccc} \text{Ho}^+ & \text{Ho}^+ & \text{Ho}^+ & \text{Ho}^p & \text{Ho}^p & \text{Ho}^p \\ 0.5 & & 0.8 & & 0.8 & \end{array}$$

Making the assumptions from above, how many males of each genotype survive to reproduce? **C)** Of the males who survive to reproduce, let's say that males with the Ho^+Ho^+ and Ho^+Ho^p genotype have on average 2.5 offspring, while Ho^pHo^p males have on average 1 offspring. Taking into account both survival and reproduction, how many offspring do you expect each of the three genotypes to contribute to the total population in the next generation?

D) What is the frequency of the Ho^+ allele in the sperm that will form this next generation?

E) How would your answers to B-D change if the Ho^p allele was at 90% frequency?

The fitnesses here are chosen to roughly match those of the real Soay sheep example, as a full model would require us to more carefully model the life-histories of the sheep.

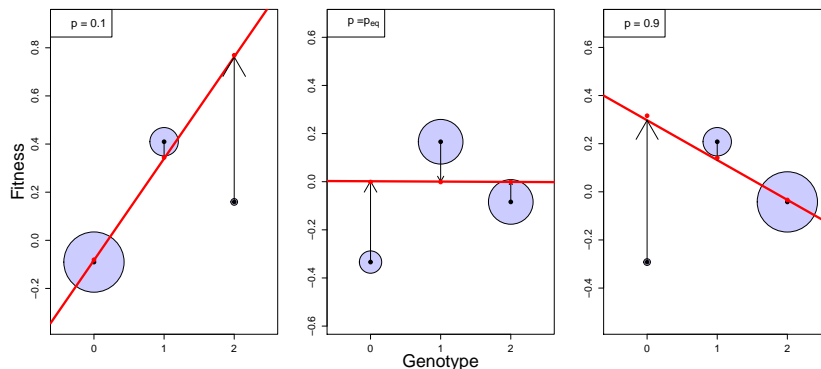


Figure 6.17: The deviation of the fitness of each genotype away from the mean population fitness (0) is shown as black dots. The area of each circle is proportion to the fraction of the population in each genotypic class (p^2 , $2pq$, and q^2). The additive genetic fitness of each genotype is shown as a red dot. The linear regression between fitness and additive genotype is shown as a red line. The black vertical arrows show the difference between the average mean-centered phenotype and additive genetic value for each genotype. The left panel shows $p = 0.1$ and the right panel shows $p = 0.9$; in the middle panel the frequency is set to the equilibrium frequency. Code here.

To push our understanding of heterozygote advantage a little further, note that the marginal fitnesses of our alleles are equivalent to the additive effects of our alleles on fitness. Recall from our discussion of non-additive variation (Section 4.1.1) that the difference in the additive effects of the two alleles gives the slope of the regression of additive genotypes on fitness, and that there is additive variance in fitness when this slope is non-zero. So what's happening here in our

4006 heterozygote advantage model is that the marginal fitness of the A_1
 allele, the additive effect of allele A_1 on fitness, is greater than the
 4008 marginal fitness of the A_2 allele ($\bar{w}_1 > \bar{w}_2$) when A_1 is at low fre-
 quency in the population. In this case, the regression of fitness on the
 4010 number of A_1 alleles in a genotype has a positive slope. This is true
 when the frequency of the A_1 allele is below the equilibrium frequency.
 4012 If the frequency of A_1 is above the equilibrium frequency, then the
 marginal fitness of allele A_2 is higher than the marginal fitness of allele
 4014 A_1 ($\bar{w}_1 < \bar{w}_2$) and the regression of fitness on the number of copies
 of allele A_1 that individuals carry is negative. In both cases there is
 4016 additive genetic variance for fitness ($V_A > 0$) and the population has
 a directional response. Only when the population is at its equilibrium
 4018 frequency, i.e. when $\bar{w}_1 = \bar{w}_2$, is there no additive genetic variance
 ($V_A = 0$), as the linear regression of fitness on genotype is zero.

4020 *Underdominance.* Another case that is of potential interest is the
 case of fitness underdominance, where the heterozygote is less fit than
 4022 either of the two homozygotes. Underdominance can be parametrized
 as follows:

genotype	A_1A_1	A_1A_2	A_2A_2
absolute fitness	w_{11}	$> w_{12} <$	w_{22}
relative fitness (generic)	$w_{11} = W_{11}/W_{12}$	$w_{12} = W_{12}/W_{12}$	$w_{22} = W_{22}/W_{12}$
relative fitness (specific)	$1 + s_1$	1	$1 + s_2$

4024 Underdominance also permits three equilibria: $p = 0$, $p = 1$, and
 a polymorphic equilibrium $p = p_U$. However, now only the first two
 4026 equilibria are stable, while the polymorphic equilibrium is unstable. If
 $p < p_U$, then Δp_t is negative and allele A_1 will be lost, while if $p > p_U$,
 4030 allele A_1 will become fixed.

4032 While strongly-selected, underdominant alleles might not spread
 within populations (if $p_U \gg 0$), they are of special interest in the
 study of speciation and hybrid zones. That is because alleles A_1 and
 4034 A_2 may have arisen in a stepwise fashion, i.e. not by a single mutation,
 but in separate subpopulations. In this case, heterozygote disadvan-
 4036 tage will play a potential role in species maintenance.

Question 9. You are studying the polymorphism that affects
 4038 flight speed in butterflies. The polymorphism does not appear to affect
 fecundity. Homozygotes for the B allele are slow in flight and so only
 4040 40% of them survive to have offspring. Heterozygotes for the poly-
 morphism (Bb) fly quickly and have a 70% probability of surviving
 4042 to reproduce. The homozygotes for the alternative allele (bb) fly very
 quickly indeed, but often die of exhaustion, with only 10% of them
 4044 making it to reproduction.



Figure 6.18: In *Pseudacraea eurytus* there are two homozygotes morphs that mimic a different blue and orange butterfly; the heterozygote fails to mimic either successfully and so suffers a high rate of predation (OWEN and CHANTER, 1972). Illustrations of new species of exotic butterflies (1868) Hewitson. Image from the Biodiversity Heritage Library. Contributed by Smithsonian Libraries. Not in copyright.

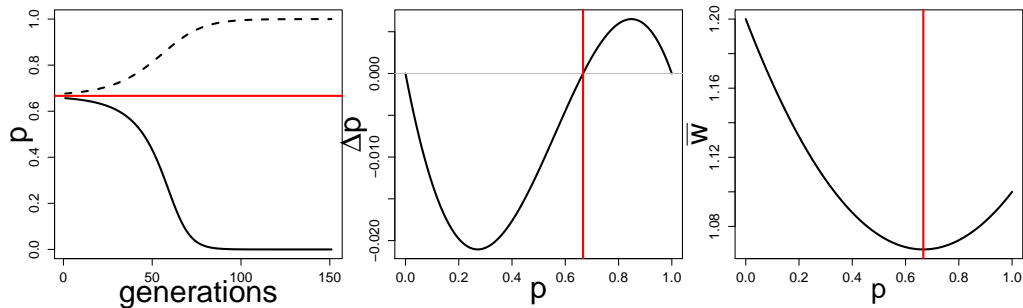


Figure 6.19: **Left)** Two allele frequency trajectories of an A_1 allele subject to heterozygote disadvantage ($w_{11} = 1.1$, $w_{12} = 1$, and $w_{22} = 1.2$). The allele is started from just above and below the equilibrium frequency, in both cases the frequency move away the equilibrium frequency. The red line shows the unstable equilibrium frequency (p_e). **Middle)** The change in frequency of an allele with heterozygote disadvantage within a generation (Δp) as a function of the allele frequency. Fitnesses as in Figure 6.13. Note how the frequency change is negative below the equilibrium frequency (p_e) and positive above. **Right)** Mean fitness (\bar{w}) as a function of the allele frequency. Code here.

A) What is the equilibrium frequency of the B allele?

B) Calculate the marginal absolute fitnesses of the B and the b allele at the equilibrium frequency.

Diploid fluctuating fitness Selection pressures fluctuate over time and can potentially maintain polymorphisms in the population. Two examples of polymorphisms fluctuating in frequency in response to temporally-varying selection are shown in Figure 6.20; thanks to the short lifespan of *Drosophila* we can see seasonally-varying selection. The first example is an inversion allele in *Drosophila pseudoobscura* populations. Throughout western North America, two orientations of the chromosome, two ‘inversion alleles’, exist: the Chiricahua and Standard alleles. DOBZHANSKY (1943) and WRIGHT and DOBZHANSKY (1946) investigated the frequency of these inversion alleles over four years at a number of locations and found that their frequency fluctuated systematically over the seasons in response to selection (left side of 6.20). If you’re still reading these notes send Prof. Coop a picture of Dobzhansky; Dobzhansky was one of the most important evolutionary geneticists of the past century and spent a bunch of time at UC Davis in his later years. Our second example is an insertion-deletion polymorphism in the Insulin-like Receptor gene in *Drosophila melanogaster*. PAABY *et al.* (2014) tracked the frequency of this allele over time and found it oscillated with the seasons (right side of 6.20). She and her coauthors also determined that these alleles had large effects on traits such as developmental time and fecundity, which could mediate the maintenance of this polymorphism through life-history trade-offs.

To explore temporal fluctuations in fitness, we’ll need to think about the diploid absolute fitnesses being time-dependent, where the three genotypes have fitnesses $w_{11,t}$, $w_{12,t}$, and $w_{22,t}$ in generation t . Modeling the diploid case with time-dependent fitness is much less tractable than the haploid case, as segregation makes it tricky to keep track of the genotype frequencies. However, we can make some

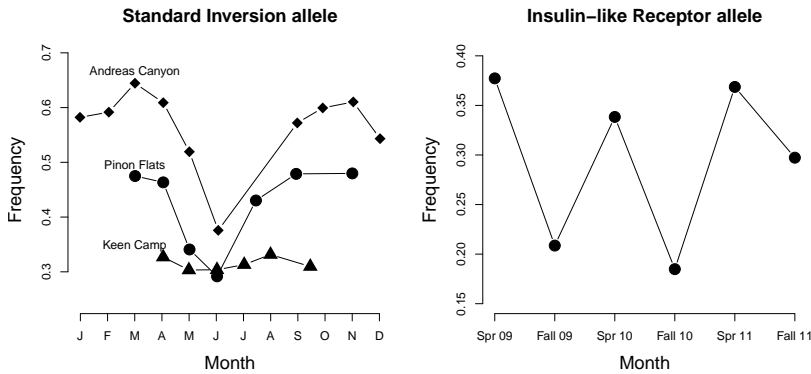


Figure 6.20: **Left)** Seasonal variation in the frequency of the ‘Standard’ inversion allele in *Drosophila pseudoobscura* for three populations from Mount San Jacinto, CA. These frequencies are an average over four years. Data from WRIGHT and DOBZHANSKY (1946). **Right)** The frequency of an allele at the Insulin-like Receptor gene over three years in *Drosophila melanogaster* samples from an Orchard in Pennsylvania. Data from PAABY *et al.* (2014). Code here.

progress and gain some intuition by thinking about how the frequency of allele A_1 changes when it is rare (following the work of HALDANE and JAYAKAR, 1963).

When A_1 is rare, i.e. $p_t \ll 1$, the frequency of A_1 in the next generation (6.27) can be approximated as

$$p_{t+1} \approx \frac{w_{12}}{\bar{w}} p_t. \quad (6.41)$$

To obtain this equation, we have ignored the p_t^2 term (because it is very small when p_t is small) and we have assumed that $q_t \approx 1$ in the numerator. Following a similar argument to approximate q_{t+1} , we can write

$$\frac{p_{t+1}}{q_{t+1}} = \frac{w_{12,t} p_t}{w_{22,t} q_t}. \quad (6.42)$$

Starting from out from p_0 and q_0 in generation 0, then $t+1$ generations later we have

$$\frac{p_{t+1}}{q_{t+1}} = \left(\prod_{i=0}^t \frac{w_{12,i}}{w_{22,i}} \right) \frac{p_0}{q_0}. \quad (6.43)$$

From this we can see, following our haploid argument from above, that the frequency of allele A_1 will increase when rare only if

$$\frac{\sqrt[t]{\prod_{i=0}^t w_{12,i}}}{\sqrt[t]{\prod_{i=0}^t w_{22,i}}} > 1, \quad (6.44)$$

i.e. if the heterozygote has higher geometric mean fitness than the $A_2 A_2$ homozygote.

The question now is whether allele A_1 will approach fixation in the population, or whether there are cases in which we can obtain a balanced polymorphism. To investigate that, we can simply repeat our analysis for $q \ll 1$, and see that in that case

$$\frac{p_{t+1}}{q_{t+1}} = \left(\prod_{i=0}^t \frac{w_{11,i}}{w_{12,i}} \right) \frac{p_0}{q_0}. \quad (6.45)$$

Now, for allele A_1 to carry on increasing in frequency and to approach fixation, the A_1A_1 genotype has to be out-competing the heterozygotes. For allele A_1 to approach fixation, we need the geometric mean of $w_{11,i}$ to be greater than the geometric mean fitness of heterozygotes ($w_{12,i}$). At the same time, if heterozygotes have higher geometric mean fitness than the A_1A_1 homozygotes, then the A_2 allele will increase in frequency when it is rare.

Intriguingly, we can thus have a balanced polymorphism even if the heterozygote is never the fittest genotype in any generation, as long as the heterozygote has a higher geometric mean fitness than either of the homozygotes. In this case, the heterozygote comes out ahead when we think about long-term fitness across heterogeneous environmental conditions, despite never being the fittest genotype in any particular environment.

As a toy example of this type of balanced polymorphism, consider a plant population found in one of two different environments each generation. These occur randomly; $1/2$ of time the population experiences the dry environment and with probability $1/2$ it experiences the wet environment. The absolute fitnesses of the genotypes in the different environments are as follows:

Environment	AA	Aa	aa
Wet	6.25	5.0	3.75
Dry	3.85	5.0	6.15
arithmetic mean	5.05	5.0	4.95

Let's write $w_{AA,dry}$ and $w_{AA,wet}$ for the fitnesses of the AA homozygote in the two environments. Then, if the two environments are equally common, $\prod_{i=0}^t w_{AA,i} \approx w_{AA,dry}^{t/2} w_{AA,wet}^{t/2}$ for large values of t . To obtain an estimate of this product normalized over the t generations, we can take the t^{th} root to obtain the geometric mean fitness. Taking the t^{th} root, we find the geometric mean fitness of the AA allele is $w_{AA,dry}^{1/2} w_{AA,wet}^{1/2}$. Doing this for each of our genotypes, we find the geometric mean fitnesses of our alleles to be:

	AA	Aa	aa
Geometric mean	4.91	5.0	4.80

i.e. the heterozygote has higher geometric mean fitnesses than either of the homozygotes, despite not being the fittest genotype in either environment (nor having the highest arithmetic mean fitness). So the A_1 allele can invade the population when it is rare as it spread thanks to the higher fitness of the heterozygotes. Similarly the A_2 allele can invade the population when it is rare. Thus both alleles will persist in the population due to the environmental fluctuations, and the higher geometric mean fitness of the heterozygotes.

This example is loosely based on the work of SCHEMSKE and BIERZYCHUDEK (2001) on *Linanthus parryae*, a desert annual, endemic to California. There are blue- and a white-flowered colour morphs polymorphic many populations, with this polymorphism being controlled by a single dominant allele. The blue-flowered plants produce more seeds in dry years, i.e. they have higher fitness in these years, while the white-flowered plants have higher seed production in wet years. Thus both morphs can potentially be maintained in the population. See TURELLI *et al.* (2001) for a more detailed analysis.

4134 *Negative frequency-dependent selection.* In the models and examples
 above, heterozygote advantage maintains multiple alleles in the pop-
 4136ulation because the common allele has a disadvantage compared to
 the other rarer allele. In the case of heterozygote advantage, the rel-
 4138ative fitnesses of our three genotypes are not a function of the other
 4140genotypes present in the population. However, there's a broader set of
 4142models where the relative fitness of a genotype depends on the geno-
 typic composition of the population; this broad family of models is
 4144called frequency-dependent selection. Negative frequency-dependent
 4146selection, where the fitness of an allele (or phenotype) decreases as it
 4148becomes more common in the population, can act to maintain genetic
 and phenotypic diversity within populations. While cases of long-term
 4146heterozygote advantage may be somewhat rare in nature, negative
 4148frequency-dependent selection is likely a common form of balancing
 4148selection.

4150 One common mechanism that may create negative frequency-
 4152dependent selection is the interaction between individuals within or
 among species. For example, negative frequency-dependent dynamics
 4154can arise in predator-prey or pathogen-host dynamics, where alleles
 conferring common phenotypes are at a disadvantage because preda-
 tors or pathogens learn or evolve to counter the phenotypic effects of
 4156common alleles.

4158 As one example of negative frequency-dependent selection, con-
 sider the two flower colour morphs in the deceptive Elderflower orchid
 4160(*Dactylorhiza sambucina*). Throughout Europe, there are popula-
 tions of these orchids polymorphic for yellow- and purple-flowered
 4162individuals, with the yellow flower corresponding to a recessive al-
 lele. Neither of these morphs provide any nectar or pollen reward to
 4164their bumblebee pollinators. Thus these plants are typically polli-
 nated by newly emerged bumblebees who are learning about which
 4166plants offer food rewards, with the bees alternating to try a different
 coloured flower if they find no food associated with a particular flower-
 4168colour morph (SMITHSON and MACNAIR, 1997). GIGORD *et al.*
 4170(2001) explored whether this behaviour by bees could result in nega-
 tive frequency-dependent selection; out in the field, the researchers set
 up experimental orchid plots in which they varied the frequency of the
 4172two colour morphs. Figure 6.22 shows their measurements of the rela-
 tive male and female reproductive success of the yellow morph across
 4174these experimental plots. When the yellow morph is rare, it has higher
 reproductive success than the purple morph, as it receives a dispropor-
 4176tionate number of visits from bumblebees that are dissatisfied with the
 purple flowers. This situation is reversed when the yellow morph be-
 comes common in the population; now the purple morph outperforms
 the yellow morph. Therefore, both colour morphs are maintained in



Figure 6.21: Elderflower orchid (*Dactylorhiza sambucina*). Abbildungen der in Deutschland und den angrenzenden gebieten vorkommenden grundformen der orchideenarten (1904). Müller, W. Image from the Biodiversity Heritage Library. Contributed by New York Botanical Garden. Not in copyright.

4178 this population, and presumably Europe-wide, due to this negative frequency-dependent selection.

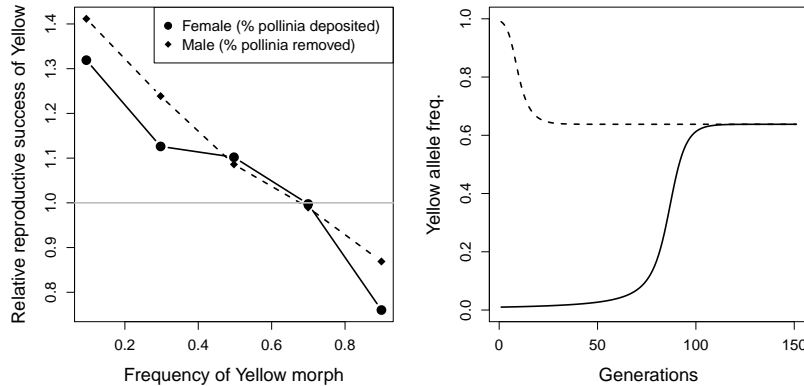


Figure 6.22: **Left)** Measures of the relative male- and female- reproductive success of the yellow Elderflower orchid morph as a function of the yellow morph in experimental plots. **Right)** Two allele frequency trajectories of the Yellow allele subject to negative frequency scheme given in the left plot (for an initial frequency of 0.01 and 0.99, solid and dotted line respectively). Note that the yellow Male reproductive success is measured in terms of the % of pollinia removed front a plant and female reproductive success is measured in terms of the % of stigmas receiving pollinia on a plant. These measures are made relative by dividing the reproductive success of the yellow morph by the mean of the yellow and purple morphs. Pollinia are the pollen masses of orchids, and other plants, where individual pollinium are transferred as a single unit by pollinators. Data from GIGORD *et al.* (2001). Code here.

4180 Negative frequency-dependent selection can also maintain different breeding strategies due to interactions amongst individuals within
 4182 a population. One dramatic example of this occurs in ruffs (*Philomachus pugnax*), a marsh-wading sandpiper that summers in Northern
 4184 Eurasia. The males of this species lek, with the males gathering on open ground to display and attract females. There are three different
 4186 male morphs differing in their breeding strategy. The large majority of males are ‘Independent’, with black or chestnut ruff plumage, and try
 4188 to defend and display on small territories. ‘Satellite’ males, with white ruff plumage, make up ~ 16% of males and do not defend territories,
 4190 but rather join in displays with Independent males and opportunistically mate with females visiting the lek. Finally, the rare ‘Faeder’
 4192 morph was only discovered in 2006 (JUKEMA and PIERSMA, 2006) and makes up less than 1% of males. These Faeder males are female
 4194 mimics who hang around the territories of Independents and try to ‘sneak’ in matings with females. Faeder males have plumage closely
 4196 resembling that of females and a smaller body size than other males, but with larger testicles (presumably to take advantage of rare mating
 4198 opportunities). All three of these morphs, with their complex behavioural and morphological differences, are controlled by three alleles
 4200 at a single autosomal locus, with the Satellite and Faeder alleles being genetically dominant over the high frequency Independent allele. The
 4202 genetic variation for these three morphs is potential maintained by negative frequency-dependent selection, as all three male strategies are
 4204 likely at an advantage when they are rare in the population. For example, while the Satellites mostly lose out on mating opportunities to
 4206 Independents, they may have longer life-spans and so may have equal



Figure 6.23: Lekking Ruffs (*Philomachus pugnax*). Three Independent males, one Satellite male, and one female (or Faeder male?).

Painting by Johann Friedrich Naumann (1780–1857). Public Domain, wikimedia.

life-time reproductive success (WIDEMO, 1998). However, Satellite
 4208 and Faeder males are totally reliant on the lekking Independent males,
 and so both of these alternative strategies cannot become overly com-
 4210 mon in the population. The locus controlling these differences has
 been mapped, and the underlying alleles have persisted for roughly
 4212 four million years (KÜPPER *et al.*, 2016; LAMICHHANEY *et al.*,
 2016). While this mating system is bizarre, the frequency dependent
 4214 dynamics mean that it has been around longer than we've been using
 stone tools.

4216 While these examples may seem somewhat involved, they must be
 simple compared to the complex dynamics that maintain the hundreds
 4218 of alleles present at the genes in the Major histocompatibility complex
 (MHC). MHC genes are key to the coordination of the vertebrate
 4220 immune system in response to pathogens, and are likely caught in an
 endless arms race with pathogens adapting to common MHC alleles,
 4222 allowing rare MHC alleles to be favoured. Balancing selection at the
 MHC locus has maintained some polymorphisms for tens of millions
 4224 of years, such that some of your MHC alleles may be genetically more
 closely related to MHC alleles in other primates than they are to
 4226 alleles in your close human friends.

6.2 Sex ratios, sex ratio distorters, and other selfish elements.

4228 We have seen that when selection acts in a simple manner it can act
 4230 to increase the mean fitness of the population. However, when the ab-
 solute fitnesses of individuals are frequency dependent, e.g. depend on
 4232 the strategies deployed by others in the population, natural selection
 is not guaranteed to increase mean fitness. One place where this is
 4234 particularly apparent is in the evolution of a 50/50 sex ratio. In fact

as we'll see that selection can drive the evolution of traits that are actively harmful to the fitness of an individual, when selection acts below the level of an individual.

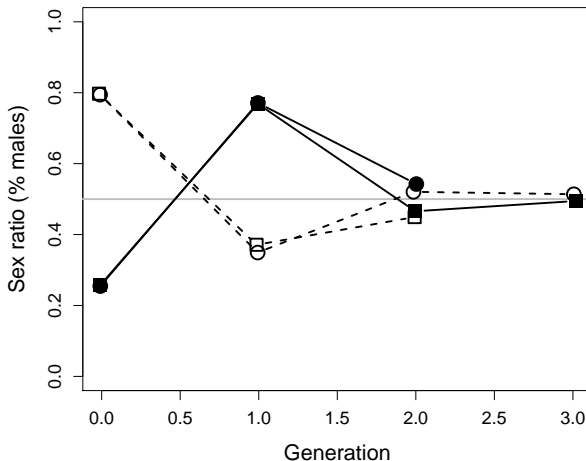


Figure 6.24: BASOLO (1994) explored sex ratio dynamics in platyfish (*Xiphophorus maculatus*), which has manipulable sex ratio due to its three factor sex determination. She started two replicates with a strong female bias (black) and two replicates with strong male bias (white). In all four cases the sex ratio quickly oscillated to a 50/50 sex ratio. Data from BASOLO (1994), Code here.

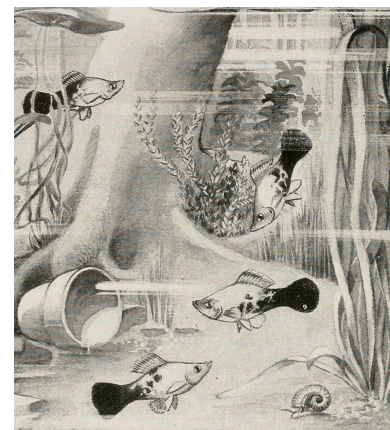


Figure 6.25: Poecilid Hybrid, *Xiphophorus helleri* × *Platypoecilus maculatus*.

Aquatic life, chapter by Curtis F.S. (1915)
Image from the Biodiversity Heritage Library.
Contributed by Harvard University, Museum of Comparative Zoology, Ernst Mayr Library. Not in copyright.

In many species, regardless of the mechanism of sex determination, the sex ratio is close to 50/50. Yet this is far from the optimum sex ratio from the perspective of the population viability. In many species females are the limiting sex, investing more in gametes and (sometimes) more in parental care, thus a population having many females and few males would offer the fastest rate of population growth (i.e. the highest mean fit). Imagine if the population sex ratio was strongly skewed towards females. A rare autosomal allele that caused a mother to produce sons would have high fitness, as the mother's sons would have high reproductive success in this population of most females. Thus our initially rare allele would initially increase in frequency. Conversely if the sex ratio was strongly skewed towards males, a rare autosomal allele that causes a mother to produce daughters would spread. So selection on autosomal alleles favours the production of the rare sex, a form of negative frequency dependence, this pushes the sex ratio away from being too skewed. Only the 50/50 sex ratio is evolutionarily stable as there is no rarer sex, and so no (autosomal) sex-ratio-altering mutation can invade a population with a 50/50. The 50/50 sex ratio is an example of an Evolutionary stable strategy (ESS), described in more detail in Section 6.2.2. Our population is held well away from its female-bias optimum for population growth as individual-level selection favours the production of the rarer sex, which results in a 50/50 sex ratio.

"An ESS is a strategy such that, if all the members of a population adopt it, then no mutant strategy could invade the population under the influence of natural selection" SMITH (1982), pg 10.

A version of this sex ratio argument was first put forward by DÜsing in 1884 and popularized by FISHER (1930), see EDWARDS (1998).

Adaptive adjustments to sex ratio in response to local mate competition.

There are, however, situations where we see strong deviations away from a 50/50 sex ratio. This can represent an adaptive strategy to situations where individuals compete against relatives for access to resources or mating opportunities. to see this consider fig wasps. There are many species of fig wasp, which form a tight pollination symbiosis with many species of Fig. Wasp females enter the inverted fig flower structure, top right Figure 6.26, pollinating the flowers.

They lay their eggs in some of the flowers, which form galls in response. The young, wingless, male wasps emerge from their galls first, Figure 6.27f, but they never leave the fig. Their only role in this is to fertilize the female wasps, Figure 6.27d, in the fig and then die. The female offspring, Figure 6.27a & e, emerge in the fig just as the male fig flowers are emerging, the female wasps burrow out and take the fig pollen with them as they fly off.

Female wasps have control over the sex of their offspring, what's a wasp mamma to do, i.e. what is their optimal strategy? They have this degree of control as sex determination in wasps is haplo-diploid, with fertilized eggs developing as diploid females and unfertilized males; thus by choosing to lay fertilized eggs they can control their number of daughters. If a female wasp lays her eggs into a fig with no other eggs, her sons will mate with her daughters and then die. Thus a lone female can maximize her contribution to the next generation by having many daughters, and just enough sons to fertilize them. And that's exactly what female wasps do, in many species of fig wasp 95% of individuals born are female.

6.2.1 Selfish genetic elements and selection below the level of the individual.

This section will be somewhat of a rogues gallery tour of some of the various genetic conflicts that occur and selfish genetic elements that can arise.

Selfish sex chromosomes and sex ratio distortion Now from the perspective of the autosomes a 50/50 sex ratio normally represents a stable strategy, but all is not harmonious in the genome. In systems with XY sex determination, male fertilization by Y-bearing sperm leads to sons, while male fertilization by X-bearing sperm leads to daughters. From the viewpoint of the X chromosome the Y-bearing sperm, and a male's sons, are an evolutionary deadend. We can imagine a mutation arising on the X chromosome, that causes a poison to be released during gametogenesis that kills Y-bearing sperm. This would cause much of the ejaculate of the males carrying this mutation to be

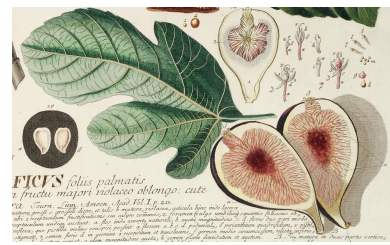


Figure 6.26: Common Fig (*Ficus carica*). Despite urban legends the crunch in figs isn't dead wasps, edible figs are dioecious and female wasps can't lay in the female flowers that form the fruit we eat.

Plantae selectae quarum imagines ad exemplaria naturalia Londini, in hortis curiosorum nutrita (1750) Trew, C.J. Image from the Biodiversity Heritage Library. Contributed by Missouri Botanical Garden. Not in copyright.

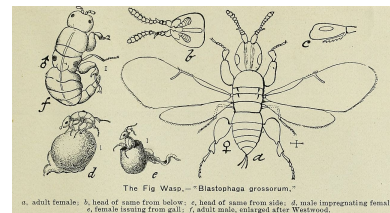


Figure 6.27: Life stages of Fig wasp (*Blastophaga psenes*, synonym *Blastophaga grossorum*); the primary pollinator of the common fig *Ficus carica*.

A descriptive catalogue of fruit and forest trees, vines and shrubs, choice palms and roses (1903) by Fancher Creek Nurseries Image from the Biodiversity Heritage Library. Contributed by National Agricultural Library, USDA. Not in copyright.

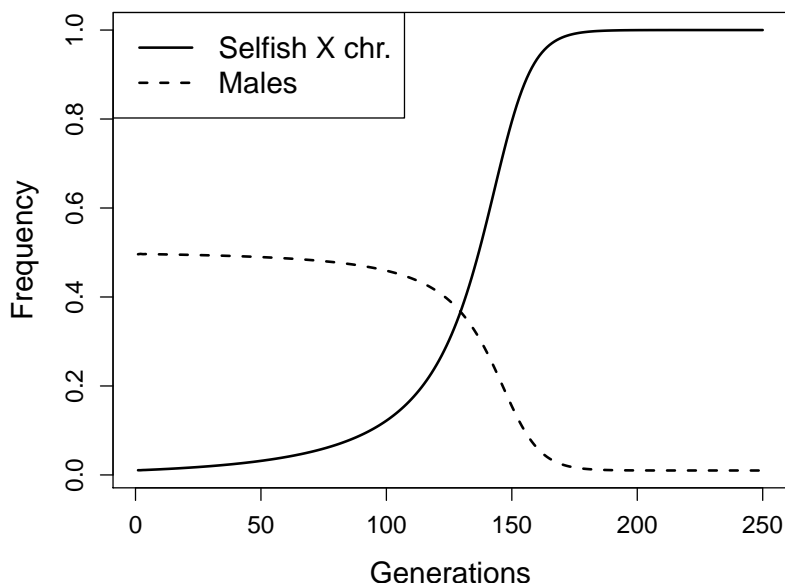


Figure 6.28: The increase in frequency of a sex-ratio distorting X allele in the population of X chromosomes (solid line) and the frequency of males in the population. Males carrying the selfish X allele have 99% daughters, and the selfish X allele reduces the viability of the carriers by 20% in a dominant manner. The model set up as in EDWARDS (1961), Code here.

4302 X-bearing sperm, and so these males would have mostly daughters.
 Such an allele would potentially spread in the population as it is over
 4304 transmitted through males, even if it somewhat reduces the fitness of
 the individuals who carry it. The spread of this allele would strongly
 4306 bias the population sex ratio towards females. Such ‘selfish’ X alleles
 turn out to be relatively common. They do not spread because they
 4308 are good for the individual, they can often substantially low the fitness
 of the bearer, but rather they spread because they are favoured due to
 4310 selection below the level of the individual.

One example of a selfish X chromosome allele is the *Winters sex-*
 4312 *ratio* system found in *Drosophila simulans*, so named as it was found
 in flies collected around Winters, California (just a few miles down the
 4314 road from Davis). In a cross the selfish X chromosome carrying males
 have > 80% daughters. The gene responsible, Dox (*Distorter on the*
 4316 *X*), appears to be a transposition from a parental gene, and produces
 a transcript which targets a region on the Y chromosome preventing
 4318 the Y-bearing sperm from developing TAO *et al.* (see Figure 6.29
 from 2007).

4320 The spread of such selfish sex chromosomes, distorting the sex
 ratio strongly away from 50/50, and can have profound effects for
 4322 population growth rates.² However, the other sex chromosome and au-
 tosomes are not helpless against the spread of selfish sex chromosome

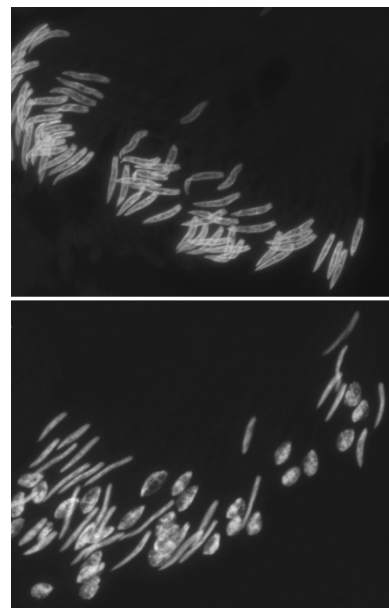


Figure 6.29: **Top)** Normally developing spermatids in *D. simulans*.
Bottom) Abnormally developing spermatids in a male expressing *dox*. The spermatids that look like rice crispies carry the Y chromosome, the normal, slender spermatids are X-bearing spermatids. Figure from TAO *et al.* (2007), cropped, licensed under CC BY 4.0.

² Indeed people have long discussed using selfish Y chromosomes, driving an over production of sons, for population control of malaria-spreading mosquitos. Natural selfish systems on the Y appear rare, likely because of its low gene content.

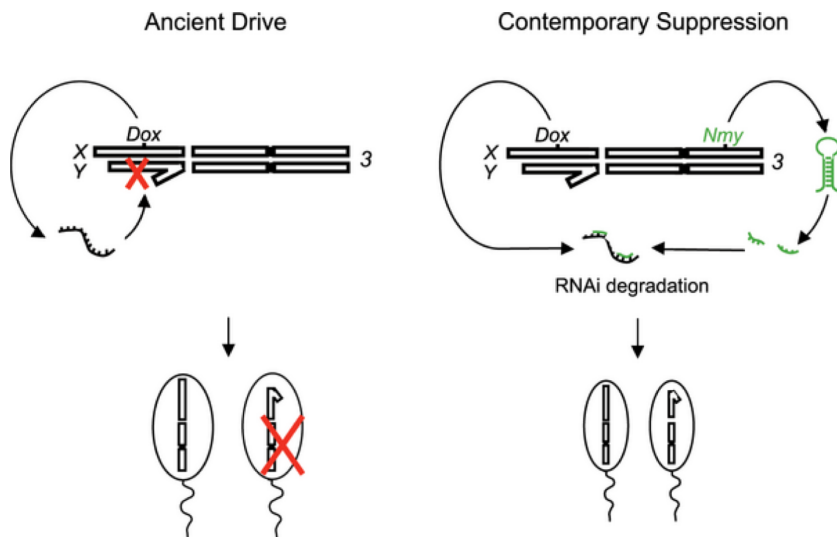


Figure 6.30: Mechanistic and Evolutionary Model for sex-ratio Distortion
Left) The X-linked Dox gene evolved to target the Y chromosome, blocking Y-bearing sperm from developing and so favouring its own transmission.
Right) Subsequently Dox was retrotransposed to an autosome forming the Nmy gene. Nmy was subsequently rearranged by a small duplication, and now blocks the action of dox by the formation of a hairpin small interfering RNA. Figure from FERREE and BARBASH (2007), licensed under CC BY 4.0. See LIN *et al.* (2018) for an update on the fascinating biology and further loci uncovered in this system.

elements. In the case of a selfish X chromosome that has achieved appreciable frequency in the population, there will be a strong excess of females in the population, such that suppressors of drive can arise on the autosomes and spread due to the fact that they allele causes the male bearer to produce sons and so spread due to Fisherian sex-ratio advantage. This has happened in the case of the Winters sex chromosome system. An autosomal allele has spread through the population that suppresses the selfish X chromosome, restoring the 50/50 sex ratio. Now the sex ratio distorter can only be found by crosses to naive populations, where the suppressor has not spread yet. The autosomal suppressor gene turns out to be a duplicate of the selfish dox gene, *NMY* (Not Much Yang), that moved to the autosome through retrotransposition and now blocks the action of dox through RNA-interference degradation of the dox transcript (see TAO *et al.*, 2007, , see Figure 6.30).

Conflict due to maternally transmitted elements. Chromosomes transmitted maternally, i.e. only through mothers, also have divergent interests from the individual. Many plants are hermaphrodite producing both pollen and seeds. But from the perspective of the Mitochondria in an individual, pollen is a waste of energy as the Mitochondria won't be transmitted through it. Thus a mutation that arises on the Mitochondria abolishing male sexual function, pollen, and shunting energy into other processes, can spread as this selfish outcome is favourable from the perspective of the mitochondrial allele.

The self spread of a CMS allele creates a population of females and hermaphrodite plants (a gynodioecious population). This strong excess



Figure 6.31: Bladder Campion (*Silene vulgaris*), on left, has both hermaphrodite and female plants due to a CMS and nuclear restorer polymorphisms (CHARLESWORTH and LAPORTE, 1998). (*S. nutans* on right)

4350 of female plants in turn can select for the spread of autosomal suppressors of CMS that are favoured by producing the rarer gamete (pollen),
 4352 and so restore the population to hermaphroditism. The spread of such Cytoplasmic Male Sterility (CMS) alleles, and subsequent autosomal suppression, is thought to be common in hermaphrodite species and often uncovered in crosses between diverged hermaphrodite populations.
 4354 The discovery or deliberate creation of CMS alleles in agricultural plants is prized because it gives breeders more control over hybridization as they can more carefully control the pollen donor to the plants.
 4358

4360 The maternal transmission of mtDNA also causes genetic conflicts in organisms with separate sexes. Males are an evolutionary dead end as far as mitochondria are concerned, and so mitochondrial mutations that lower a male's fitness are not removed from the population of mitochondria. Thus the Mitochondria genome may be a hotspot of alleles that are deleterious in males (an effect termed the "Mother's curse"). One example of a male-deleterious mitochondrial mutations



Figure 6.32: Arrival of the fille du roi, the 'king's daughters' to Quebec city in 1667. Painting by Eleanor Fortescue-Brickdale. The fille du roi were some 800 women whose emigration to New France (Quebec) was paid for by a program established by King Louis XIV of France to address the strong gender imbalance of the new colony. You can read more in this Atlantic article by Sarah Zhang.
Painting from the Library and Archives Canada collection, Wikimedia, Public Domain.

4366 underlying Leber's 'hereditary optic neuropathy' (LHON) in humans.
 4368 LHON causes degeneration of the optic nerve and loss of vision in teenage males (with much lower penetrance in women). One such
 4370 LHON mutation is present at low frequency in the Quebec population. The Québécois population grew rapidly from a relatively small number of founders, leading to the prevalence of some disease mutations due to the founder effect. Thanks to the detailed genealogical records
 4372 kept by French Canadian since the founding of Quebec, we know that nearly all the Québécois LHON alleles are descended from the
 4374 mitochondria of a single woman, one of the fille du roi, who arrived in

Quebec City in 1669 (LABERGE *et al.*, 2005). Using the genealogy, 4378 MILOT *et al.* (2017) tracked all of her mitochondrial descendants, individuals who's mother was in her matrilineal line, and so identified 4380 all the individuals in the Québécois who carried this allele. There was no significant difference in the fitness of females who carried or didn't 4382 carry the mutation. In contrast, the fitness of male carriers of the mutation was only 65.3% that of male non-carriers. This mitochondria 4384 mutation has increased in frequency slightly over the past 290 years, despite its strong effects in males, due to the fact that its effects have 4386 no consequence for female fitness.

Question 10. The frequency of the LHON allele was roughly

4388 1/2000 in 1669. If females suffered the same ill consequences as males what would be the frequency today? [assume there are ~29 years a 4390 generation]

Question 11. Kin selection has been proposed as a way that the

4392 male deleterious effects of mitochondrial mutation could be removed from the population. Can you explain this idea?

4394 It's not just chromosomes that get in on the act of the battle of the sexes. Numerous arthropods, including a high proportion of insects, are infected with the intracellular bacteria *Wolbachia*, which 4396 are passed to offspring through the maternal cytoplasm. As they are only transmitted by females, *Wolbachia* increase their transmission in 4398 a variety of selfish ways including feminization of males and killing male embryos. In one dramatic case, a male-killing *Wolbachia* strain 4400 forced a sex ratio of 100 females to every 1 male in *Hypolimnas bolina* 4402 (eggspot butterflies) throughout Southeast Asia. This extreme sex ratio persisted for many decades, according to the analysis of museum 4404 collections from the late 19C, before the sex ratio was rapidly restored to 50/50 by the spread of an autosomal suppressing allele. The autosomal 4406 suppressor allele spread very rapidly within populations taking just 5 years to spread through the population from 2001 to 2006.

4408 *Autosomal selfish systems* Self genetic systems can also arise and cause genetic conflicts on the autosomes. The interests of autosomal 4410 alleles are usually relatively well aligned with promoting the fitness. However, these interests can diverge during meiosis and gametogenesis. 4412 After all, There are two alleles at each autosomal locus but only one of them will get passed to a child, therefore there can be competition 4414 between alleles in an individual to be transmitted gamete to the next generation (Figure 6.34).

4416 Male and female gametogenesis offer different opportunities for selfish systems. Just as how selfish X chromosome systems can spread by



Figure 6.33: male Eggspot butterfly (*Hypolimnas bolina*).
P. Cramer's Uitlandsche kapellen (1780)
Image from the Biodiversity Heritage Library.
Contributed by Smithsonian Libraries. Not in copyright.

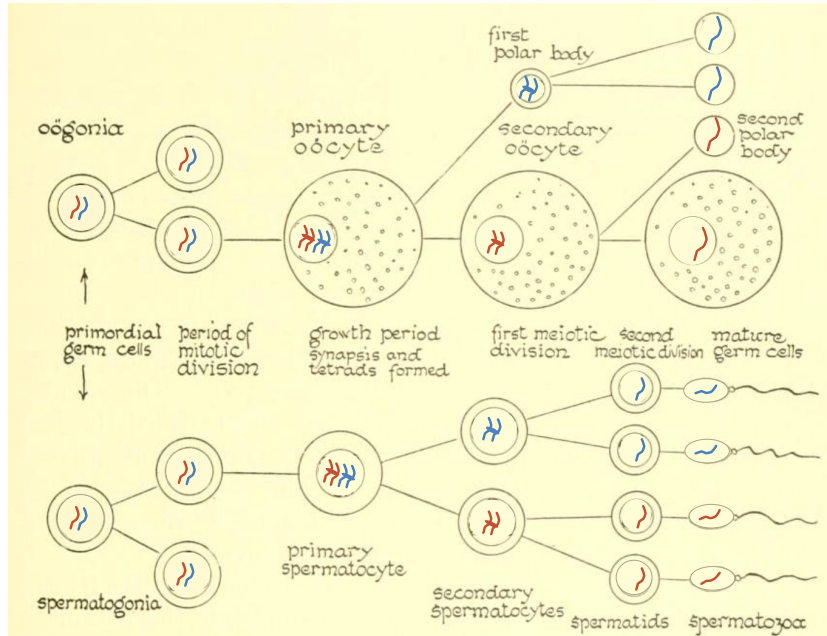


Figure 6.34: The two copies of a chromosome are shown in red and blue through the process of female and male meiosis and gametogenesis. Crossovers are omitted to keep things simpler, they should occur between at least one red and one blue chromosome. Modified from original to include chromosomes transmitted.

Biology: the story of living things (1937). Hunter, G.W., Walter H.E. Image from the Biodiversity Heritage Library. Contributed by MBLWHOI Library. No known copyright restrictions.

4418 targeting sperm that carry the Y chromosome, selfish autosomal alleles can spread by targeting sperm carrying the other chromosome in
 4420 heterozygotes. Both the Drosophila Segregation Distortion allele and the mouse T-allele are selfish autosomal systems that game transmission
 4422 in heterozygotes by killing off sperm that don't carry the allele in heterozygotes.

4424 In females meiosis there is a unique opportunity for cheating. In male meiosis all four products of meiosis become gametes. However,
 4426 only 1 of the four products of female meiosis becomes the egg, the other 3 products are fated to become the polar bodies. Thus alleles
 4428 can cheat in female meiosis by preferentially getting transmitted into the egg rather than the polar body. If an allele on red chromosome
 4430 can manipulate any asymmetry of meioses so that it can be present in the egg > 50% of the time it will be a transmission advantage in
 4432 female heterozygotes.

To see how such drivers can spread through the population lets
 4434 consider the case of a population where an allele drives in both male and female gametogenesis. (Most selfish alleles will be sex-specific, but
 4436 that makes the math a little more tricky.) Imagine a randomly-mating population of hermaphrodites. In this population, a derived allele (D)
 4438 segregates that distorts transmission in its favour over the ancestral allele (d) in the production of all the gametes of heterozygotes. The
 4440 drive leads to a fraction α of the gametes of heterozygotes (D/d) to carry the D allele ($\alpha \geq 0.5$). The D allele causes viability problems

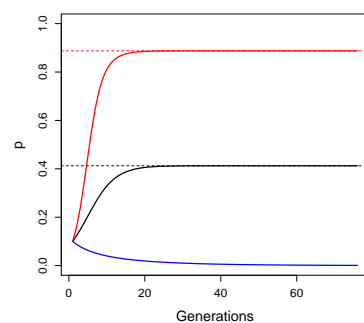


Figure 6.35: The fate of an unfit transmission distorter allele. If transmission is fair ($\alpha = 1/2$) the allele is lost, but the stronger its drive in heterozygotes the faster its spread and the higher its final frequency in the population (black and red curves, $\alpha = 0.7$ & 0.9 respectively). With fitnesses $w_{dd} = 1$, $w_{Dd} = 0.95$, and $w_{DD} = 0.1$. The dotted lines show the predicted equilibrium. Code here.

⁴⁴⁴² such that the relative fitnesses are $w_{dd} = 1$, $1 > w_{Dd} \geq w_{DD}$. If
⁴⁴⁴³ the D allele is currently at frequency p in the population at birth, its
⁴⁴⁴⁴ frequency at birth in the next generation will be

$$p' = \frac{w_{DD}p^2 + w_{Dd}\alpha 2pq}{\bar{w}} \quad (6.46)$$

⁴⁴⁴⁵ when $\alpha = 1/2$, i.e. fair Mendelian transmission this is exactly the same
⁴⁴⁴⁶ as our directional selection, which results in our D allele being selected
⁴⁴⁴⁷ out of the population (blue line, Figure 6.35). However, if $\alpha > 1/2$, i.e.
⁴⁴⁴⁸ our deleterious allele cheats, it can potentially increase in the popula-
⁴⁴⁴⁹ tion when it is rare (red and black lines, Figure 6.35)). However, the
⁴⁴⁵⁰ allele can become trapped in the population at a polymorphic equilib-
⁴⁴⁵¹ rium if its cost is sufficient in homozygotes. This is akin to the case
⁴⁴⁵² of heterozygote advantage, but now our allele offers no advantage to
⁴⁴⁵³ heterozygote but has a self advantage in heterozygotes.

⁴⁴⁵⁴ **Question 12.** (Tricker question) Thinking of our autosomal driver
⁴⁴⁵⁵ from equation 6.46. **B)** Imagine the cost of the driver were additive,
⁴⁴⁵⁶ i.e. $w_{dd} = 1$, $w_{Dd} = 1 - e$, $w_{DD} = 1 - 2e$. Under what conditions can
⁴⁴⁵⁷ the driver invade the population? Can a polymorphic equilibrium be
⁴⁴⁵⁸ maintained?

⁴⁴⁵⁹ **A)** Imagine the allele is completely recessive, i.e. $w_{dd} = w_{Dd} =$
⁴⁴⁶⁰ 1. What conditions do you need for a polymorphic equilibrium to
⁴⁴⁶¹ be maintained? What is the equilibrium frequency of this balanced
⁴⁴⁶² polymorphism?

⁴⁴⁶³ Many of the known autosomal drive systems are polymorphic in
⁴⁴⁶⁴ populations, unable to reach fixation in the population due to their
⁴⁴⁶⁵ costs in homozygotes. It seems like that this represents an ascer-
⁴⁴⁶⁶ tainment bias, and that many over selfish systems, which had lower
⁴⁴⁶⁷ selective costs, have swept to fixation.

⁴⁴⁶⁸ 6.2.2 Appendix: ESS for the sex ratio

⁴⁴⁶⁹ Let R be the sources and C_{σ} and C_{φ} be the cost of producing a son
⁴⁴⁷⁰ and daughter respectively. If our focal mother directs s of her effort
⁴⁴⁷¹ towards sons and $(1 - s)$ of her effort towards daughters, she'll pro-
⁴⁴⁷² duces $\frac{Rs}{C_{\sigma}}$ sons and $\frac{R(1-s)}{C_{\varphi}}$ daughters. We will assume that the mean
⁴⁴⁷³ reproductive value of daughters is 1. Given this the reproductive value
⁴⁴⁷⁴ of sons is the average number of matings that a male will have, i.e.
⁴⁴⁷⁵ the ratio # females/# males. So if the population has a sex ratio s_p , the
⁴⁴⁷⁶ fitness of our focal female is

$$W(s, s_p) = \left(\frac{R(1-s)}{C_{\varphi}} \times 1 \right) + \left(\frac{Rs}{C_{\sigma}} \times \frac{R(1-s_p)/C_{\varphi}}{Rs_p/C_{\sigma}} \right) \quad (6.47)$$

⁴⁴⁷⁷ expressing fitness in terms the number of grandkids our focal female is
⁴⁴⁷⁸ expected to have.

To find the ESS we want a sex ratio s^* for the population that no
 4480 mutant has higher fitness, i.e. $W(s^*, s^*) > W(s, s^*)$ for $s \neq s^*$, We can
 find this by

$$\frac{\partial W(s, s_p)}{\partial s} \Big|_{s^*=s=s_p} = 0 \quad (6.48)$$

4482 taking the derivative of Eqn 6.47 we obtain

$$\frac{\partial W(s, s_p)}{\partial s} = -\frac{R}{C_\varphi} + \frac{R}{C_\sigma} \left(\frac{R(1-s_p)/C_\varphi}{Rs_p/C_\sigma} \right) \quad (6.49)$$

setting $s^* = s = s_p$ and rearranging

$$\frac{R}{C_\varphi} = \frac{R}{C_\sigma} \left(\frac{R(1-s^*)/C_\varphi}{Rs^*/C_\sigma} \right) \quad (6.50)$$

4484 which is satisfied when $s^* = 1/2$, i.e. devoting equal resources to male
 and female offspring is the ESS, which corresponds to a 50/50 sex
 4486 ratio if male and female offspring are equally costly.

7

4488 *The interaction of Selection, Mutation, and Migration.*

4490 7.0.1 Mutation-selection balance

Mutation is constantly introducing new alleles into the population.
4492 Therefore, variation can be maintained within a population not only if selection is balancing (e.g. through heterozygote advantage or fluctuating selection over time, as we have seen in the previous section),
4494 but also due to a balance between mutation introducing deleterious
4496 alleles and selection acting to purge these alleles from the population (HALDANE, 1937). To study mutation-selection balance, we return to
4498 the model of directional selection, where allele A_1 is advantageous, i.e.

genotype	A_1A_1	A_1A_2	A_2A_2
absolute fitness	W_{11}	$\geq W_{12} \geq$	W_{22}
relative fitness	$w_{11} = 1$	$w_{12} = 1 - sh$	$w_{22} = 1 - s.$

4500 We'll begin by considering the case where allele A_2 is not completely recessive ($h > 0$), so that the heterozygotes suffer at least some dis-
4502 advantage. We denote by $\mu = \mu_{1 \rightarrow 2}$ the mutation rate per generation from A_1 to the deleterious allele A_2 , and assume that there is no re-
4504 verse mutation ($\mu_{2 \rightarrow 1} = 0$). Let us assume that selection against A_2 is relatively strong compared to the mutation rate, so that it is justified
4506 to assume that A_2 is always rare, i.e. $q_t = 1 - p_t \ll 1$. Compared to previous sections, for mathematical clarity, we also switch from fol-
4508 lowing the frequency p_t of A_1 to following the frequency q_t of A_2 . Of course, this is without loss of generality. The change in frequency of
4510 A_2 due to selection can be written as

$$\Delta_S q_t = \frac{\bar{w}_2 - \bar{w}_1}{\bar{w}} p_t q_t \approx -hsq_t. \quad (7.1)$$

This approximation can be found by assuming that $q^2 \approx 0$, $p \approx 1$,
4512 and that $\bar{w} \approx w_1$. All of these assumptions make sense if $q \ll 1$. From eqn. (7.1) we see that selection acts to reduce the frequency of

⁴⁵¹⁴ A_2 (as both h and s are positive), and it does so geometrically across the generations. That is, if the initial frequency of A_2 is q_0 , then its ⁴⁵¹⁶ frequency at time t is approximately

$$q_t = q_0(1 - hs)^t. \quad (7.2)$$

We will now consider the change in frequency induced by mutation.

⁴⁵¹⁸ Recalling that μ is the mutation rate from A_1 to A_2 per generation, the frequency of A_2 after mutation is

$$q' = \mu p_t + q_t = \mu(1 - q_t) + q_t. \quad (7.3)$$

⁴⁵²⁰ Assuming that $\mu \ll 1$ and that $q \ll 1$, the change in the frequency of allele A_2 due to mutation ($\Delta_M q_t$) can be approximated by

$$\Delta_M q_t = q' - q_t = \mu. \quad (7.4)$$

⁴⁵²² Hence, when A_2 is rare and the mutation rate is low, mutation acts to linearly increase the frequency of the deleterious allele A_2 .

⁴⁵²⁴ If selection is to balance deleterious mutation, their combined effect over one generation has to be zero. Therefore, to find the mutation–⁴⁵²⁶ selection equilibrium, we set

$$\Delta_M q_t + \Delta_S q_t = 0, \quad (7.5)$$

insert eqns. (7.1) and (7.4), and solve for q to obtain

$$q_e = q_t = \frac{\mu}{hs}. \quad (7.6)$$

⁴⁵²⁸ We see that the frequency of the deleterious allele A_2 is balanced at a frequency equal to the mutation rate (μ) divided by the reduction in ⁴⁵³⁰ relative fitness in the heterozygote (hs).

⁴⁵³² It is worth pointing out that the fitness of the $A_2 A_2$ homozygote has not entered this calculation, as A_2 is so rare that it is hardly ever found in the homozygous state. Therefore, if A_2 has any deleterious effect in a heterozygous state (i.e. if $h > 0$), it is this effect that ⁴⁵³⁴ determines the frequency at which A_2 is maintained in the population. Also, note that by writing the total change in allele frequency as $\Delta_M q_t + \Delta_S q_t$ we have implicitly assumed that we can ignore terms ⁴⁵³⁶ of order $\mu \times s$. That is, we have assumed that mutation and selection are both relatively weak. This assumption is valid under our prior ⁴⁵³⁸ assumption that both μ and s are small.

⁴⁵⁴⁰ If an allele is truly recessive (although few likely are), we have $h = 0$, and so eqn. (7.6) is not valid. However, we can make an argument similar to the one above to show that, for truly recessive alleles,

$$q_e = \sqrt{\frac{\mu}{s}}. \quad (7.7)$$

4544 **Question 1.** Oblong-winged katydids (*Amblycorypha oblongifolia*)
 4545 are usually green. However, some are bright pink, thanks to an
 4546 erythrism mutation (a nice example of early Mendelian reasoning in a
 4547 wonderfully titled paper¹). This pink condition is thought to be due
 4548 to a dominant mutation (Crew, 2013). Assume that roughly one in
 4549 ten thousand katydids is bright pink and that the mutation rate at the
 4550 gene underlying this condition is 10^{-5} . What is the relative fitness of
 heterozygotes for the pink mutation?

4552 *The genetic load of deleterious alleles* What effect do such deleterious
 mutations at mutation-selection balance have on the population? It
 4554 is common to quantify the effect of deleterious alleles in terms of a
 reduction of the mean relative fitness of the population. For a single
 4556 site at which a deleterious mutation is segregating at frequency $q_e = \mu/(hs)$, the population mean relative fitness is reduced to

$$\bar{w} = 1 - 2p_e q_e hs - q_e^2 s \approx 1 - 2\mu. \quad (7.8)$$

4558 Somewhat remarkably, the drop in mean fitness due to a site segregating at mutation-selection balance is independent of the selection
 4560 coefficient against the heterozygote; it depends only on the mutation
 rate. Intuitively this is because, given a fixed mutation rate, less dele-
 4562 terious alleles can rise to a higher equilibrium frequency, and thus
 contribute the same total load as more deleterious (rarer) alleles, but
 4564 this load is spread across more individuals in the population. Note
 that this result applies only if the mutation is not totally recessive, i.e.
 4566 if $h > 0$.

4568 A fitness reduction of 2μ is very small, given that the mutation
 rate of a gene is likely $< 10^{-5}$. However, if there are many loci seg-
 4570 regating at mutation-selection balance, small fitness reductions can
 accumulate to a substantial so-called genetic load, a major cause of
 variation in fitness-related traits among individuals. For example,
 4572 the human genome contains over twenty thousand genes, and many
 other functional regions, the vast majority of which will be subject
 4574 to purifying selection against mutations that disrupt their function.
 In humans, most loss of function (LOF) variants, which severely dis-
 4576 rupt a protein-coding gene, are found at low frequencies. However,
 each human genome typically carries over a hundred LOF variants
 4578 (MACARTHUR *et al.*, 2012; LEK *et al.*, 2016). Not every LOF allele
 will be deleterious; some could even be advantageous. However, the
 4580 combined load of these LOF alleles must on average lower our fitness,
 otherwise selection wouldn't be removing them from the population.
 4582 Each one of us carries a unique set of these LOF alleles, usually in a



Figure 7.1: Oblong-winged katydid. Field book of insects (1918). Lutz, F.E. Illustrations by Edna L. Beutemüller. Image from the Biodiversity Heritage Library. Contributed by MBLWHOI Library. Not in copyright. WHEELER, W. M., 1907 Pink Insect Mutants. The American Naturalist 41(492): 773–780

heterozygous state. We differ slightly in how many of these alleles we carry. For example, the left side of Figure 7.2 shows the distribution of the number of LOF alleles carried by 769 individuals of Dutch ancestry. The individuals who carry fewer of these LOF alleles will on average have higher fitness than those individuals with more.

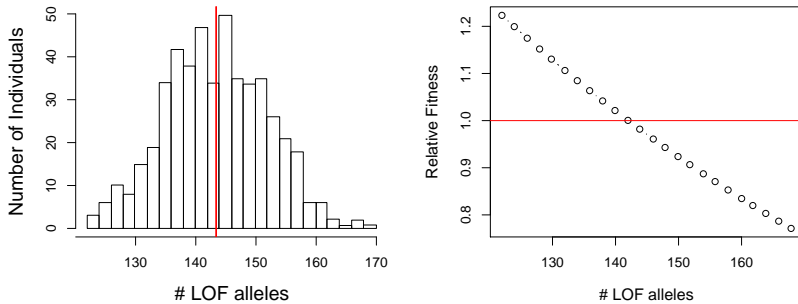


Figure 7.2: **Left)** The distribution of LOF alleles in 769 individuals from the Genome of the Netherlands project. Data from FRANCIOLI *et al.*. The average individual (red line) carries 144 LOF alleles. **Right).** The relative fitness of individuals carrying these varying numbers of LOF alleles, assuming multiplicative selection and a selection coefficient of $sh = 10^{-2}$ acting against these alleles (CASSA *et al.*, 2017). Code here.

How do these differences across individuals in total LOF mutations mount up? Well, if we are willing to assume that the fitness costs of deleterious alleles interact multiplicatively, we can make some progress. If an individual who carries one LOF mutation has a fitness $1 - hs$, then an individual who's heterozygote for two LOF mutations would have fitness $(1 - hs)^2$, and an individual who is heterozygote for L LOF alleles would have fitness $(1 - hs)^L$. The right-hand side of Figure 7.2 shows the predicted fitness of individuals carrying varying number of LOF alleles, relative to the mean fitness of the sample, using this multiplicative model. We don't yet know how much lower the fitness of these individuals really is, nor do we know how most of these LOF alleles manifest their fitness consequences through disease and other mechanisms. However, it's a reasonable guess that this variation in LOF alleles, presumably maintained by mutation-selection balance, is a major source of variation in fitness.

7.0.2 Inbreeding depression

All else being equal, eqn. (7.6) suggests that mutations that have a smaller effect in the heterozygote can segregate at higher frequency under mutation-selection balance. As a consequence, alleles that have strongly deleterious effects in the homozygous state can still segregate at low frequencies in the population, as long as they do not have too strong a deleterious effect in heterozygotes. Thus, outbred populations may have many alleles with recessive deleterious effects segregating within them.

4612 **Question 2.** Assume that a deleterious allele has a relative fitness .99 in heterozygotes and a relative fitness 0.2 when present in 4614 the homozygote state. Assume that the deleterious allele is at a frequency 10^{-3} at birth and the genotype frequencies follow from HWE. 4616 Only considering the fitness effects of this locus, and measuring fitness relative to the most fit genotype, answer the following questions:

4618 A) What is the average fitness of an individual in the population?
 B) What is the average fitness of the child of a full-sib mating?

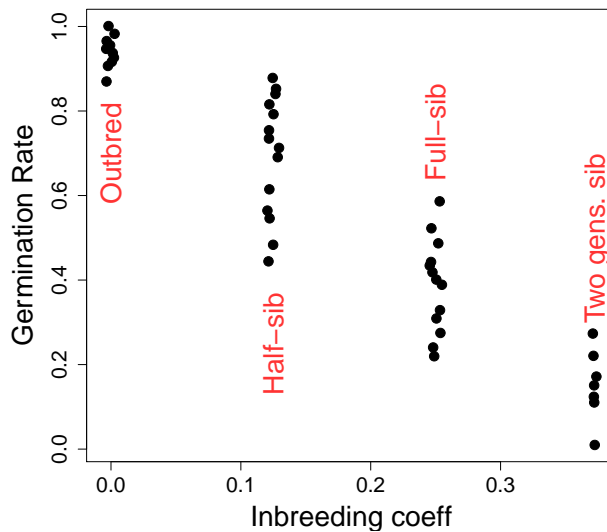


Figure 7.3: Data showing inbreeding depression over different degrees of inbreeding in *S. latifolia*. Each point is the mean seed germination rates for different family crosses. Data from RICHARDS. Code here.

4620 One consequence of segregating for low-frequency recessive deleterious alleles is that inbreeding can reduce fitness. In typically outbred populations, the mean fitness of individuals decreases with the inbreeding coefficient, i.e. so-called 'inbreeding depression' is a common observation. This wide-spread observation dates back to systematic surveys of inbreeding depression by DARWIN (1876). Inbreeding depression is likely primarily a consequence of being homozygous at many loci for alleles with recessive deleterious effects.

4628 One example of inbreeding depression is shown in Figure 7.3. White campion (*Silene latifolia*) is a dioecious flowering plant; dioecious means that the males and females are separate individuals. RICHARDS performed crosses to create offspring who were outbred, the offspring of half-sibs, full-sibs, and of two generations of full-sib mating. He measured their germination success, which is plotted in Figure 7.3. Note how the fitness of individuals declines with increased inbreeding.

4636 *Purging the inbreeding load.* Populations that regularly inbreed over sustained periods of time are expected to partially purge this load



Figure 7.4: White campion (*S. latifolia*).
Deutschlands Flora in Abbildungen (1796).
 Johann Georg Sturm (Painter: Jacob Sturm).
 Public Domain, wikipedia.

4638 of deleterious alleles. This is because such populations have exposed
 many of these alleles in a homozygous state, and so selection can more
 4640 readily remove these alleles from the population.

If the population has sustained inbreeding, such that individuals
 4642 in the population have an inbreeding coefficient F , deleterious alle-
 les at each locus will find a new equilibrium frequency. Assuming
 4644 the mutation-selection model, now with inbreeding, the equilibrium
 frequency is

$$q_e = \frac{\mu}{(h(1 - F) + F)s} \quad (7.9)$$

4646 The frequency of the deleterious allele is decreased due to the al-
 lele now being expressed in homozygotes, and therefore exposed to
 4648 selection, more often due to inbreeding. Thus, all else being equal,
 populations with a high degree of inbreeding will purge their load.

4650 7.0.3 Migration-selection balance

Another reason for the persistence of deleterious alleles in a population
 4652 is that there is a constant influx of maladaptive alleles from other pop-
 ulations where these alleles are locally adaptive. Migration-selection
 4654 balance seems unlikely to be as broad an explanation for the persis-
 tence of deleterious alleles genome-wide as mutation-selection balance.
 4656 However, a brief discussion of such alleles is worthwhile, as it helps to
 inform our ideas about local adaptation.

Local adaptation can occur over a range of geographic scales. Lo-
 cal adaptation is relatively unimpeded by migration at broad geo-
 4660 graphically scales, where selection pressures change more slowly than
 distances over which individuals typically migrate over a number of
 4662 generations. Adaptation can, however, potentially occur on much finer
 geographic scales, from kilometers down to meters in some species. On
 4664 such small scales, dispersal is surely rapidly moving alleles between
 environments, but local adaptation is maintained by the continued
 4666 action of selection. An example of adaptation at fine-scales is shown
 in Figure 7.6 . JAIN and BRADSHAW (1966) studied the patterns of
 4668 heavy-metal resistance in plants on mine tailings and in nearby mead-
 ows, a set of classic studies of population differences maintained by
 4670 local adaptation to different soils. Even at these very short geo-
 graphically scales, over which seed and pollen will definitely move, we see
 4672 strong local adaptation. Zinc-intolerant alleles are nearly absent from
 the mine tailings because they prevent plants from growing on these
 4674 zinc-heavy soils; conversely, zinc-tolerant alleles do not spread into
 the meadow populations, likely due to some trade-off or fitness cost of
 4676 zinc-tolerance.

As a first pass at developing a model of local adaptation, let's con-
 4678 sider a haploid two-allele model with two different populations, see



Figure 7.5: Sweet vernal grass (*Anthoxanthum odoratum*).

Billeder af nordens flora (1917). Mentz, A & Ostenfeld, C H. Image from the Biodiversity Heritage Library. Contributed by New York Botanical Garden. Not in copyright.

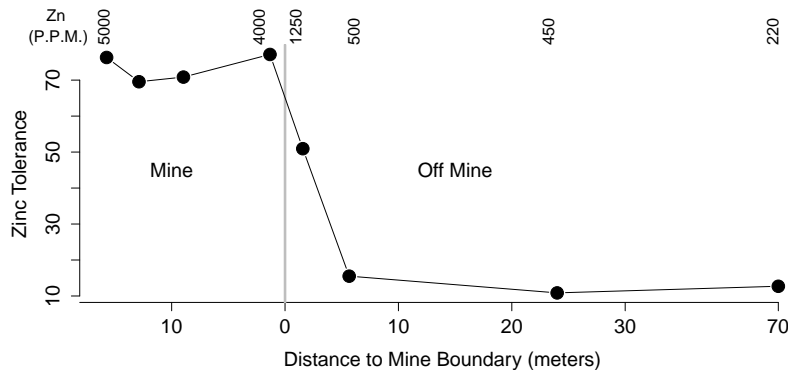


Figure 7.6: Data showing the Zinc tolerance of *Anthoxanthum odoratum* on and off of the Trelogan Mine, Flintshire, North Wales. The numbers along the top give the soil contamination of Zinc in parts per million. Data from JAIN and BRADSHAW (1966). Code here.

Figure 7.7, where the relative fitnesses of our alleles are as follows

allele	1	2
population 1	1	$1-s$
population 2	$1-s$	1

As a simple model of migration, let's suppose within a population a fraction of m individuals are migrants from the other population, and $1 - m$ individuals are from the same population.

To quickly sketch an equilibrium solution to this scenario, we'll take an approach analogous to our mutation-selection balance model. To do this, let's assume that selection is strong compared to migration ($s \gg m$), such that allele 1 will be almost fixed in population 1 and allele 2 will be almost fixed in population 2. If that is the case, migration changes the frequency of allele 2 in population 1 (q_1) by

$$\Delta_{Mig.} q_1 \approx m \quad (7.10)$$

while as noted above $\Delta_S q_1 = -sq_1$, so that migration and selection are at an equilibrium when $0 = \Delta_S q_1 + \Delta_{Mig.} q_1$, i.e. an equilibrium frequency of allele 2 in population 1 of

$$q_{e,1} = \frac{m}{s} \quad (7.11)$$

Here, migration is playing the role of mutation and so migration-selection balance (at least under strong selection) is analogous to mutation-selection balance.

We can use this same model by analogy for the case of migration-selection balance in a diploid model. For the diploid case, we replace our haploid s by the cost to heterozygotes hs from our directional selection model, resulting in a diploid migration-selection balance equilibrium frequency of

$$q_{e,1} = \frac{m}{hs} \quad (7.12)$$

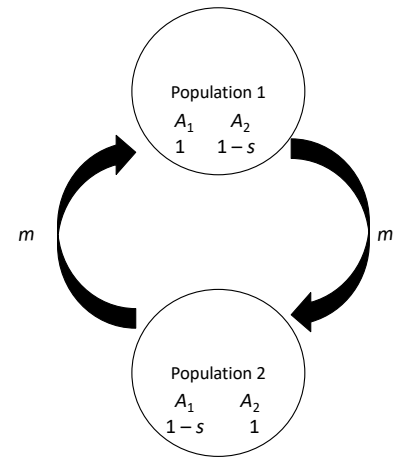


Figure 7.7: Setup of a two-population haploid model of local adaptation.

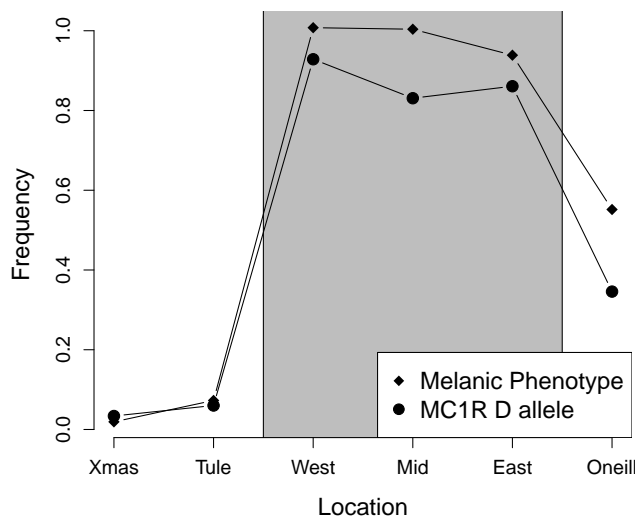


Figure 7.8: Frequency of melanic mice on the lava flow, and at nearby locations (diamonds). Frequency of MC1R melanic allele at same locations. Data from HOEKSTRA *et al.* (2004). Code here.

As an example of fine-scale local adaptation due to a single locus,

4702 consider the case of the rock pocket mice adapting to lava flows. Throughout the deserts of the American Southwest there are old lava 4704 flows, where the rocks and soils are much dark than the surrounding desert.

4706 Many populations of small animals that live on these flows have evolved darker pigmentation to be cryptic against this dark substrate 4708 and better avoid visual predators. One example of such a locally adapted population are the rock pocket mice (*Chaetodipus intermedius*) who live on the Pinacate lava flow on the Arizona-Mexico border, studied by HOEKSTRA *et al.* (2004). These mice have much 4710 darker, more melanic pelts than the mice who live on nearby rocky outcrops (see Figure 7.8). NACHMAN *et al.* (2003) determined that 4712 a dominant allele (*D*) at MC1R is the primary determinant of this melanistic phenotype. The frequency of this allele across study sites is 4714 shown in Figure 7.8. HOEKSTRA *et al.* (2004) found that other, unlinked markers showed little differentiation over these populations, 4716 suggesting that the migration rate is high.

4718 **Question 3.** HOEKSTRA *et al.* (2004) found that the dark *D* allele was at 3% frequency at the Tule Mountains study site. Using *F_{ST}*-based approaches, for unlinked markers, they estimated that the per individual migration rate was $m = 7.0 \times 10^{-4}$ per generation 4722 between this site and the Pinacate lava flow. What is the selection coefficient acting against the dark *D* allele at the Tule Mountains site?



Figure 7.9: Two species from the genus *Chaetodipus*, pocket mice, formally known as *Perognathus*. Wild animals of North America, intimate studies of big and little creatures of the mammal kingdom (1918), Nelson, E. W. Image from the Biodiversity Heritage Library. Contributed by American Museum of Natural History Library. Not in copyright.

⁴⁷²⁶ *The width of a genetic cline.* We can also extend these ideas beyond our discrete model to a model of a population spread out on a landscape where individuals migrate in a more continuous fashion. For simplicity, let's assume a one dimensional habitat, where the habitat makes a sharp transition in the middle of our region. You could imagine this to be a set of populations sampled along a transect through some environmental transition. Our individuals disperse to live on average σ miles away from where they were born (we can think of this as our individuals migrating a random distance drawn from a normal distribution, with mean zero, and σ being the standard deviation of this distribution). . We'll think of a bi-allelic model where the homozygotes for allele 1 have an additive selective advantage s over allele 2 homozygotes to the east of our habitat transition (left of zero in Figure 7.10). This flips to allele 2 having the same advantage s west of the transition (right of zero). If you've read this send Prof Coop a picture of the East and West Beast.

“Upon an island hard to reach, the East Beast sits upon his beach. Upon the west beach sits the West Beast. Each beach beast thinks he’s the best beast.” – Theodor Seuss Geisel

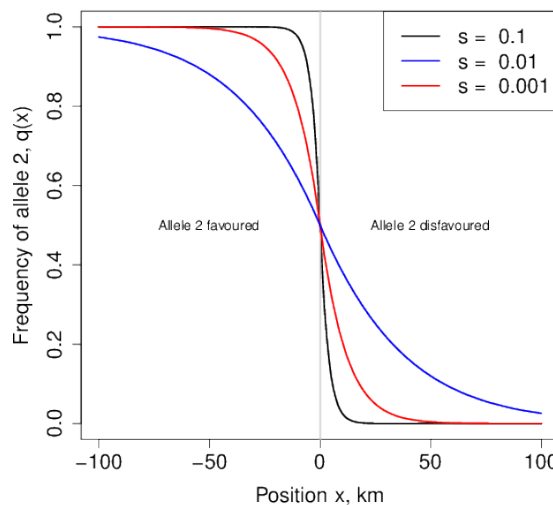


Figure 7.10: An equilibrium cline in allele frequency (the frequency of allele 2, $q(\cdot)$ is shown). Our individuals disperse an average distance of $\sigma = 1$ miles per generation, and our allele 2 has a relative fitness of $1 + s$ and $1 - s$ on either side of the environmental change at $x = 0$. Code here.

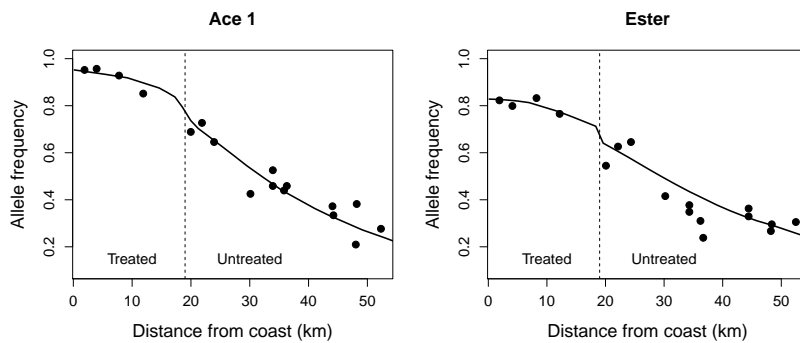
⁴⁷⁴² With this setup, we get an equilibrium distribution of our two alleles, where to the left of zero our allele 2 is at higher frequency, while ⁴⁷⁴⁴ to the right of zero allele 1 predominates. As we cross from the left to the right side of our range, the frequency of our allele 2 decreases in ⁴⁷⁴⁶ a smooth cline. The frequency of allele 2, $q(\cdot)$, is shown as a function of location along the cline for a variety of selection coefficients (s) in ⁴⁷⁴⁸ Figure 7.10. The width of this cline, i.e. the geographic distance over which the allele frequency changes, depends on the relative strengths

of dispersal and selection. If selection is strong compared to dispersal, then selection acts to remove maladaptive alleles much faster than migration acts to move alleles across the environmental transition. Thus the allele frequency transition would be very rapid, and the cline narrow, as we move across the environmental transition. In contrast, if individuals disperse long distances and selection is weak, many alleles are being moved back and forth over the environmental transition much faster than selection can act against these alleles and so the cline would be very wide.

The width of our cline, i.e. the distance over which we make this shift from allele 2 to allele 1 predominating, can be defined in a number of different ways. One way to define the cline width, which is simple to define but perhaps hard to measure accurately, is via the slope (i.e. the tangent) of $q(x)$ at $x = 0$. See Figure 7.11. Under this definition, the cline width is approximately

$$0.6\sigma/\sqrt{s} \text{ miles}, \quad (7.13)$$

note that the units are miles here just because we defined the average dispersal distance (σ) in miles above. Thus the cline will be wider if individuals disperse further, higher σ , and if selection is weaker, smaller s . The appendix below talks through the math underlying these ideas in more detail.



LENORMAND *et al.* (1999) collected mosquitoes (*Culex pipiens*) in a north-south transect moving away from the Southern French coast. Areas near the coast were treated with pesticides, and the mosquitos have evolved resistance, but areas just a few tens of kilometers from the coast were untreated. LENORMAND *et al.* estimated the frequency of two unlinked, pesticide-resistance alleles, and found them at high frequency near the coast but found that their frequencies declined rapidly moving inland. LENORMAND *et al.* fit migration-selection cline models to their data, similar to those in Figure 7.10,

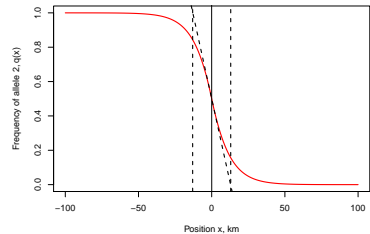


Figure 7.11: An equilibrium cline in allele frequency from Figure 7.10, $s = 0.01$. Vertical lines show the cline width. The diagonal line shows the tangent to the cline at its midpoint. [Code here](#).

Figure 7.12: Allele frequency clines of two pesticide resistance alleles, at the Ace 1 and Ester genes, in the mosquito *Culex pipiens*. The dotted line shows where we move from pesticide-treated to untreated areas as we move away from the French coast. The dots show observed allele frequencies, the solid lines clines fit under a migration-selection balance model of a cline. These allele frequencies represent collections over two summers, the frequencies of the alleles are substantially reduced in the winter due to the reduced use of pesticides. Data from LENORMAND *et al.* (1999). [Code here](#).

with the pesticide-resistance alleles having an selection advantage (s) in treated areas an a cost (c) in untreated areas (they didn't enforce the selective advantage and cost being symmetric).

They estimated that a higher selective advantage for the Ace 1 allele than Ester allele ($s = 0.33$ and $s = 0.19$ respectively) and a higher cost to the Ace 1 allele than Ester allele in untreated areas ($c = 0.11$ and $c = 0.07$ respectively) potentially explaining the less extreme cline for Ester allele than the Ace 1 allele. Despite these strong selection pressures we still see a cline over tens of kilometers because dispersal is relatively high ($\sigma = 6.6\text{km per generation}$).

Hybrid zones Local adaptation isn't the only way that selection can generate strong spatial patterns. We can also see strong selection-driven clines when partially-reproductively isolated species spread back in to secondary contact they can hybridize bringing alleles together that may not work well with each other. One simple model of is to think about an under-dominant polymorphism, i.e. where the heterozygote has lower fitness. The two ancestral populations are alternatively fixed for the two fitter homozygote states, e.g. ancestral population 1 fixed A_1A_1 and ancestral population two the A_2A_2 . The hybrid population forming at the mating edge between the two ancestral populations has a high frequency of the less fit heterozygotes. Thus hybrids are at a disadvantage, potentially acting to keep the two populations from collapsing into each other.

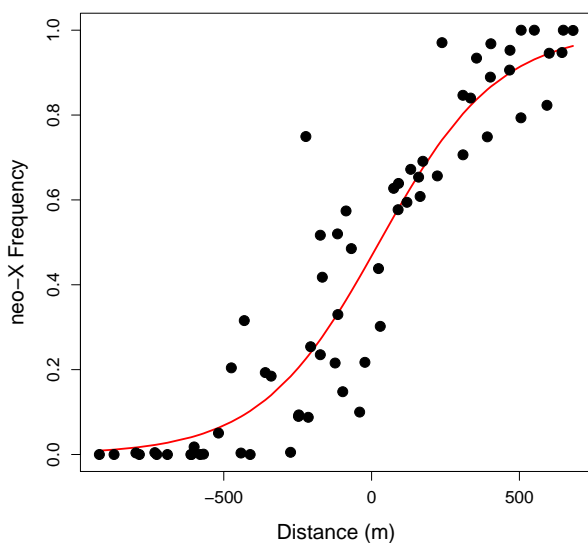


Figure 7.14: The frequency of the southern neo-X chromosome moving along a valley transect (more southern locations to the right of the graph). This represents data from four different valleys in the French Alps over less than a kilometer, each point represents a sample of 20 males. The red curve is the fitted cline under a model of heterozygote disadvantage (BAZYKIN, 1969). Data from BARTON and HEWITT (1981), Code here.

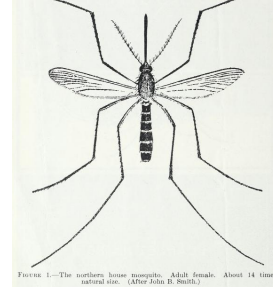
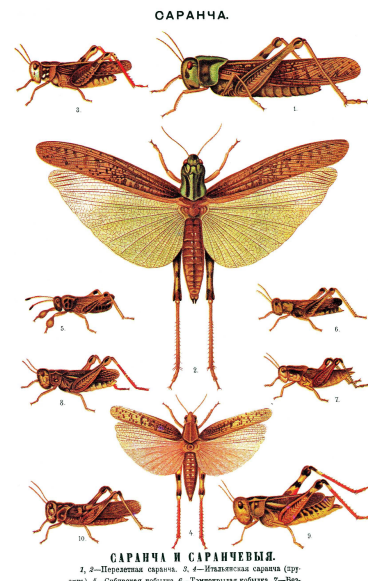


Figure 7.13: mosquito (*Culex pipiens*). Domestic mosquitoes (1939). Bishopp, F. C. Image from the Biodiversity Heritage Library. Contributed by U.S. Department of Agriculture, National Agricultural Library. Not in copyright.

Two previously isolated populations of the short-horned grasshopper *Podisma pedestris* have spread into secondary contact in the French Alps, probably after the last ice age. The population that has spread into the Alps from the south has a large section of novel X chromosome, due to a chromosomal fusion. This ‘neo-X’ is absent in the populations that spread from the North into the Alps. The two populations meet in many valleys running through the Alps, and repeated form a narrow hybrid zone, with the frequency of the neo-X chromosome forming a very steep cline transitioning in frequency over a few hundred meters (BARTON and HEWITT, 1981). One potential reason for this steep cline is that females who are heterozygous for the neo-X (neo-X/old-X) may have reduced fitness, consistent with an underdominant polymorphism. The neo-X allele cannot spread into the northern population as it cannot increase in frequency when rate. Conversely the northern population cannot displace the neo-X, as the old-X is at a disadvantage. This spatial distribution at this locus is a tension zone between the two populations, where neither population can make ground on the other due to the low fitness of the hybrid.

We can use our same continuous model of migration and selection to study this setup. Assuming that the homozygotes are equally fit, and that the heterozygotes relative fitness is reduced by a selection coefficient s_h , the width of the cline is

$$\frac{\sigma}{\sqrt{s_h}} \quad (7.14)$$

The stronger the selection the more abrupt the transition between the populations. These wingless grasshoppers move $\sigma \sim 20$ meters a generation. Thus a reduction in the relative fitness of the hybrid would be needed to explain this hybrid zone with a width of ~ 800 m.

More generally we can see tension zones arise when hybrids have reduced fitness compared to either species. For example, this can occur due to be due to bad epistatic interactions between alleles from each species. If selection is strong enough on hybrids, often because many loci are involved in incompatibilities between the species, the entire genome can be tied up in a tension zone between the two species.

Appendix: Some theory of the spatial distribution of allele frequencies under deterministic models of selection

Imagine a continuous haploid population spread out along a line. Each individual disperses a random distance Δx from its birthplace to the location where it reproduces, where Δx is drawn from the probability density $g()$. To make life simple, we will assume that $g(\Delta x)$ is normally distributed with mean zero and standard deviation σ , i.e. migration is unbiased and individuals migrate an average distance of

4842 σ .

The frequency of allele 2 at time t in the population at spatial location x is $q(x, t)$. Assuming that only dispersal occurs, how does our allele frequency change in the next generation? Our allele frequency in the next generation at location x reflects the migration from different locations in the proceeding generation. Our population at location x receives a contribution $g(\Delta x)q(x + \Delta x, t)$ of allele 2 from the population at location $x + \Delta x$, such that the frequency of our allele at x in the next generation is

$$q(x, t + 1) = \int_{-\infty}^{\infty} g(\Delta x)q(x + \Delta x, t)d\Delta x. \quad (7.15)$$

To obtain $q(x + \Delta x, t)$, let's take a Taylor series expansion of $q(x, t)$:

$$q(x + \Delta x, t) = q(x, t) + \Delta x \frac{dq(x, t)}{dx} + \frac{1}{2}(\Delta x)^2 \frac{d^2q(x, t)}{dx^2} + \dots \quad (7.16)$$

4852 then

$$q(x, t+1) = q(x, t) + \left(\int_{-\infty}^{\infty} \Delta x g(\Delta x) d\Delta x \right) \frac{dq(x, t)}{dx} + \frac{1}{2} \left(\int_{-\infty}^{\infty} (\Delta x)^2 g(\Delta x) d\Delta x \right) \frac{d^2q(x, t)}{dx^2} + \dots \quad (7.17)$$

Because $g(\)$ has a mean of zero, $\int_{-\infty}^{\infty} \Delta x g(\Delta x) d\Delta x = 0$, and has because $g(\)$ has variance σ^2 , $\int_{-\infty}^{\infty} (\Delta x)^2 g(\Delta x) d\Delta x = \sigma^2$. All higher order terms in our Taylor series expansion cancel out (as all high moments of the normal distribution are zero). Looking at the change in allele frequency, $\Delta q(x, t) = q(x, t + 1) - q(x, t)$, so

$$\Delta q(x, t) = \frac{\sigma^2}{2} \frac{d^2q(x, t)}{dx^2} \quad (7.18)$$

4858 This is a diffusion equation, so that migration is acting to smooth out allele frequency differences with a diffusion constant of $\frac{\sigma^2}{2}$. This is 4860 exactly analogous to the equation describing how a gas diffuses out to equal density, as both particles in a gas and our individuals of type 2 4862 are performing Brownian motion (blurring our eyes and seeing time as continuous).

4864 We will now introduce fitness differences into our model and set the relative fitnesses of allele 1 and 2 at location x to be 1 and $1 + s\gamma(x)$. 4866 To make progress in this model, we'll have to assume that selection isn't too strong, i.e. $s\gamma(x) \ll 1$ for all x . The change in frequency of 4868 allele 2 obtained within a generation due to selection is

$$q'(x, t) - q(x, t) \approx s\gamma(x)q(x, t)(1 - q(x, t)) \quad (7.19)$$

i.e. logistic growth of our favoured allele at location x . Putting our 4870 selection and migration terms together, we find the total change in

allele frequency at location x in one generation is

$$q(x, t+1) - q(x, t) = s\gamma(x)q(x, t)(1 - q(x, t)) + \frac{\sigma^2}{2} \frac{d^2q(x, t)}{dx^2} \quad (7.20)$$

- 4872 In deriving this result, we have essentially assumed that migration
acted upon our original allele frequencies before selection, and in doing
4874 so have ignored terms of the order of σs .

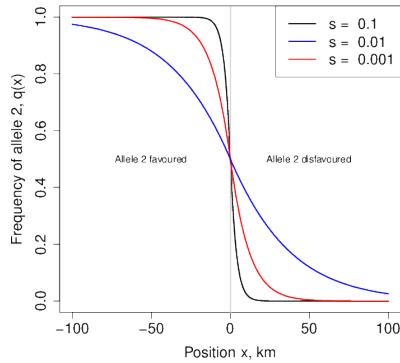


Figure 7.16: An equilibrium cline in allele frequency. Our individuals disperse an average distance of $\sigma = 1$ km per generation, and our allele 2 has a relative fitness of $1 + s$ and $1 - s$ on either side of the environmental change at $x = 0$.

The cline in allele frequency associated with a sharp environmental transition. To make progress, let's consider a simple model of local adaptation where the environment abruptly changes. Specifically, we assume that $\gamma(x) = 1$ for $x < 0$ and $\gamma(x) = -1$ for $x \geq 0$, i.e. our allele 2 has a selective advantage at locations to the left of zero, while this allele is at a disadvantage to the right of zero. In this case we can get an equilibrium distribution of our two alleles, where to the left of zero our allele 2 is at higher frequency, while to the right of zero allele 1 predominates. As we cross from the left to the right side of our range, the frequency of our allele 2 decreases in a smooth cline.

Our equilibrium spatial distribution of allele frequencies can be found by setting the left-hand side of eqn. (7.20) to zero to arrive at

$$s\gamma(x)q(x)(1 - q(x)) = -\frac{\sigma^2}{2} \frac{d^2q(x)}{dx^2} \quad (7.21)$$

We then could solve this differential equation with appropriate boundary conditions ($q(-\infty) = 1$ and $q(\infty) = 0$) to arrive at the appropriate functional form for our cline. While we won't go into the solution of this equation here, we can note that by dividing our distance x by $\ell = \sigma/\sqrt{s}$, we can remove the effect of our parameters from the above equation. This compound parameter ℓ is the characteristic length of our cline, and it is this parameter which determines over what geographic scale we change from allele 2 predominating to allele 1 predominating as we move across our environmental shift.

8

The Impact of Genetic Drift on Selected Alleles

4898 “Natural selection is a mechanism for generating an exceedingly high
4900 degree of improbability.” –R.A. Fisher

In the previous chapter we assumed that the selection acting on our
4902 alleles was strong enough that we could ignore the action of genetic
4904 drift in shaping allele frequencies. However, genetic drift affects all al-
4906 leles, and so in this chapter we explore the interaction of selection and
4908 drift. Strongly selected alleles can be lost from the population via drift
4910 when they are rare in the population, while both weakly beneficial and
4912 weakly deleterious alleles are subject to the random whims of genetic
drift throughout their entire time in the population. Understanding
the interaction of selection and genetic drift is key to understand-
ing the extent to which small populations may be mutation-limited
in their rates of adaptation, and how rates of molecular and genome
evolution may differ across taxa.

8.1 Stochastic loss of strongly selected alleles

4914 Even strongly beneficial alleles can be lost from the population when
they are sufficiently rare. This is because the number of offspring left
4916 by individuals to the next generation is fundamentally stochastic. A
selection coefficient of $s=1\%$ is a strong selection coefficient, which can
4918 drive an allele through the population in a few hundred generations
once the allele is established. However, if individuals have on average a
4920 small number of offspring per generation, the first individual to carry
our beneficial allele, who has on average 1% more children than their
4922 peers, could easily have zero offspring, leading to the loss of our allele
before it ever gets a chance to spread.

4924 To take a first stab at this problem, let’s think of a very large hap-
loid population in which a single individual starts with the selected
4926 allele, and ask about the probability of eventual loss of our selected
allele starting from this single copy. To derive this probability of loss
4928 (p_L), we’ll make use of a simple argument (derived from branching

processes FISHER, 1923; HALDANE, 1927). Our selected allele will be eventually lost from the population if every individual with the allele fails to leave descendants. Well we can think about different cases:

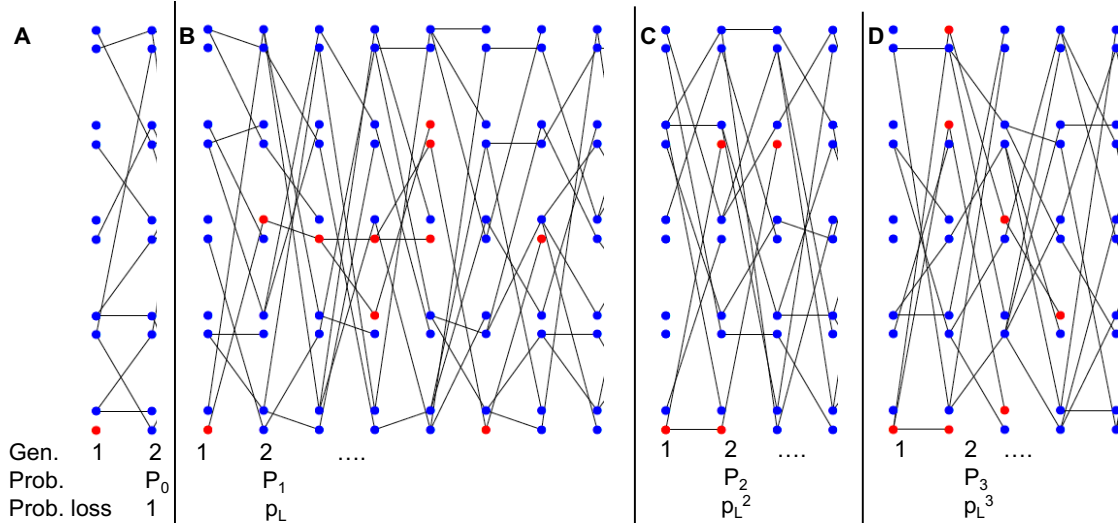


Figure 8.1: Four different outcomes of a selected allele present as a single copy in the population, leaving zero, one, two, three offspring in the next generation.

- 4932 1. In our first generation, with probability P_0 our individual allele leaves no copies of itself to the next generation, in which case our allele is lost (Figure 8.1A).
- 4934 2. Alternatively, our allele could leave one copy of itself to the next generation (with probability P_1), in which case with probability p_L this copy eventually goes extinct (Figure 8.1B).
- 4936 3. Our allele could leave two copies of itself to the next generation (with probability P_2), in which case with probability p_L^2 both of these copies eventually go extinct (Figure 8.1C).
- 4938 4. More generally, our allele could leave k copies ($k > 0$) of itself to the next generation (with probability P_k), in which case with probability p_L^k all of these copies eventually go extinct (e.g. Figure 8.1D).

Summing over these probabilities, we see that

$$p_L = \sum_{k=0}^{\infty} P_k p_L^k \quad (8.1)$$

- 4946 5. We'll now need to specify P_k , the probability that an individual carrying our selected allele has k offspring. In order for this population to stay constant in size, we'll assume that individuals without the selected mutation have on average one offspring per generation, while

4950 individuals with our selected allele have on average $1 + s$ offspring per generation. We'll assume that the number of offspring an individual has is Poisson distributed with mean given by 1 or $1 + s$, i.e. the probability that an individual with the selected allele has i children is

$$P_i = \frac{(1+s)^i e^{-(1+s)}}{i!} \quad (8.2)$$

Substituting P_k into the equation above, we see

$$\begin{aligned} p_L &= \sum_{k=0}^{\infty} \frac{(1+s)^k e^{-(1+s)}}{k!} p_L^k \\ &= e^{-(1+s)} \left(\sum_{k=0}^{\infty} \frac{(p_L(1+s))^k}{k!} \right) \end{aligned} \quad (8.3)$$

4954 The term in the brackets is itself an exponential expansion, so we can rewrite this equation as

$$p_L = e^{(1+s)(p_L - 1)} \quad (8.4)$$

4956 Solving for p_L would give us our probability of loss for any selection coefficient. Let's rewrite our result in terms of the probability of 4958 escaping loss, $p_F = 1 - p_L$. We can rewrite eqn. (8.4) as

$$1 - p_F = e^{-p_F(1+s)} \quad (8.5)$$

To gain an approximate solution for this result, let's consider a small 4960 selection coefficient $s \ll 1$ such that $p_F \ll 1$ and then use a Taylor series to expand out the exponential on the right hand side (ignoring 4962 terms of higher order than s^2 and p_F^2):

$$1 - p_F \approx 1 - p_F(1 + s) + p_F^2(1 + s)^2 / 2 \quad (8.6)$$

Solving this we find that

$$p_F = 2s. \quad (8.7)$$

4964 Thus even an allele with a 1% selection coefficient has a 98% probability of being lost when it is first introduced into the population by 4966 mutation.

If the mutation rate towards our advantageous allele is μ , and there 4968 are N individuals in our haploid population, then $N\mu$ advantageous mutations arise per generation. Each of these new beneficial mutations 4970 has a probability p_F of fixing. Thus the number of advantageous mutations arising per generation that will eventually fix in the population 4972 is $N\mu p_F$, and the waiting time for a mutation that will fix to arise is the reciprocal of this: $1/N\mu p_F$. Thus, in adapting to a novel selection 4974 pressure via new mutations, the population size, the mutational target size, and the selective advantage of new mutations all matter. One

4976 reason why combinations of drugs are used against viruses like HIV
 4977 and malaria is that, even if the viruses adapt to one of the drugs, the
 4978 viral load (N) of the patient is greatly reduced, making it very un-
 4979 likely that the population will manage to fix a second drug-resistant
 4980 allele.

4982 *Diploid model of stochastic loss of strongly selected alleles.* We can
 4983 also adapt this result to a diploid setting. Assuming that heterozy-
 4984 gotes for the 1 allele have on average $1 + hs$ children, the probability
 4985 allele 1 is not lost, starting from a single copy in the population, is

$$p_F = 2hs \quad (8.8)$$

4986 for $h > 0$. Note this is a slightly different parameterization from our
 4987 diploid model in the previous chapter; here h is the dominance of our
 4988 positively selected allele, with $h = 1$ corresponding to the full se-
 4989 lective advantage expressed in an individual with only a single copy.
 4990 Thus the probability that a beneficial allele is not lost depends just
 4991 on the relative fitness advantage of the heterozygote; this is because
 4992 when the allele is rare it is usually present in heterozygotes and so its
 4993 probability of escaping loss just depends on the fitness of these indi-
 4994 viduals compared to homozygotes for the ancestral allele (assuming an
 4995 outbred population).

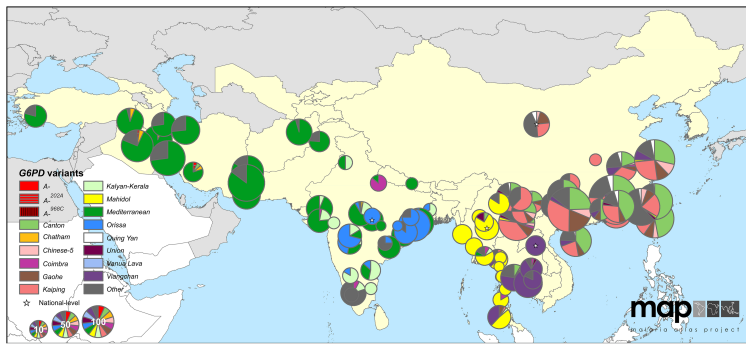


Figure 8.2: Map of G6PD-deficiency allele frequencies across Asia. The pie chart shows the frequency of G6PD-deficiency alleles. The size of the pie chart indicates the number of G6PD-deficient individuals sampled. Countries with endemic malaria are colored yellow. Figure from HOWES *et al.* (2013), licensed under CC BY 4.0.

4996 Over roughly the past ten thousand years, adaptive alleles con-
 4997 ferring resistance to malaria have arisen in a number of genes and
 4998 spread through human populations in areas where malaria is en-
 4999 demic (KWIATKOWSKI, 2005). One particularly impressive case of
 5000 convergent evolution in response to selection pressures imposed by
 5001 malaria are the numerous changes throughout the G6PD gene, which
 5002 include at least 15 common variants in Central and Eastern Asia
 5003 alone that lower the activity of the enzyme (HOWES *et al.*, 2013).
 5004 These alleles are now found at a combined frequency of around 8%
 5005 frequency in malaria endemic areas, rarely exceeding 20% (HOWES

et al., 2012). Whether these variants *all* confer resistance to malaria is unknown, but a number of these alleles have demonstrated effects against malaria and are thought to have a selective advantage to heterozygotes $sh > 5\%$ where malaria is endemic (RUWENDE *et al.*, 1995; TISHKOFF *et al.*, 2001; LOUICHAROEN *et al.*, 2009).

With a 5% advantage in heterozygotes, a G6PD allele present as a single copy would only have a 10% probability of fixing in the population. If that's so, how come malaria adaptation has repeatedly occurred via changes at G6PD? Well, maybe adaptation didn't start from a single copy of the selected allele. How many copies of the G6PD-deficiency alleles do we expect were segregating in the population before selection pressures changed?

In the absence of malaria, these G6PD alleles are deleterious with carriers suffering from G6PD deficiency, leading to hemolytic anemia when individuals are exposed to a variety of different compounds, notably those present in fava beans. There's upward of one hundred bases where G6PD-deficiency alleles can arise, so assuming a mutation rate of $\approx 10^{-8}$ per base pair per generation, we can roughly estimate the rate of mutations arising that affect the G6PD gene as $\mu \approx 10^{-6}$ per generation. In the absence of malaria, the selective cost of being a heterozygote carrier of a G6PD-deficient allele must have been on the order of 5% or more, and thus the frequency of the allele under mutation-selection balance would have been $\approx 10^{-6}/0.05 = 2 \times 10^{-5}$.

Assuming an effective population size of 2 – 20 million individuals, roughly five to ten thousand years ago that means that there would have been forty to four hundred copies of the G6PD-deficiency allele present in the population when selection pressures shifted at the introduction of malaria. The chance that one of these newly adaptive alleles is lost is 90% but the chance that they're all lost is $< (0.9)^{40} \approx 0.02$, i.e. there would have been a greater than 98% chance that adaptation would occur via one or more alleles at G6PD. How many alleles would escape drift? Well with 40 – 400 copies of the allele pre-malaria, and each of them having a 10% probability of escaping drift, we expect between 4 and 40 G6PD alleles to escape drift and contribute to adaptation. We see 15 common G6PD alleles in Eurasia, so our simple model of adaptation from mutation-selection balance seems reasonable.

Question 1. ‘Haldane’s sieve’ is the name for the idea that the mutations that contribute to adaptation are likely to be dominant or at least co-dominant.

A) Briefly explain this argument with a verbal model relating to the results we've developed in the last two chapters.

B) Haldane’s sieve is thought to be less important for adaptation from previously deleterious standing variation, than adaptation from



Figure 8.3: Pythagoras’s “just say no to fava beans” campaign. Pythagoras prohibited the consumption of fava beans by his followers; perhaps because favism, the anemia induced in G6PD-deficient individuals by fava beans, is relatively common in the Mediterranean due to adaptation to endemic malaria. French early 16th Century. Woodner Collection, National Gallery of Art. Public Domain, wikimedia.

A full analysis of this case requires modeling of G6PD’s X chromosome inheritance, and the randomness in the number of copies of the allele present at mutation-selection balance (RALPH and COOP, 2015).



Figure 8.4: Haldane’s sieve. To our knowledge Haldane never wore a sieve, but we assume he owned one. Sieve, Flickr licensed under CC BY 2.0. Haldane, Public Domain, wikimedia.

new mutation. Can you explain the intuition behind of this idea?

5050 **C)** Haldane's sieve is likely to be less important in inbred, e.g. selfing, populations. Why is this?

5052 **Question 2.** Melanic squirrels suffer a higher rate of predation (due to hawks) than normally pigmented squirrels. Melanism is due to 5054 a dominant, autosomal mutation. The frequency of melanic squirrels at birth is 4×10^{-5} .

5056 **A)** If the mutation rate to new melanic alleles is 10^{-6} , assuming 5058 the melanic allele is at mutation-selection equilibrium, what is the reduction in fitness of the heterozygote?

5060 Suddenly levels of pollution increase dramatically in our population, 5062 and predation by hawks now offers an equal (and opposite) advantage to the dark individuals as it once offered to the normally pigmented individuals.

5064 **B)** What is the probability that a single copy of this allele (present just once in the population) is lost?

5066 **C)** If the population size of our squirrels is a million individuals, 5068 and is at mutation-selection balance, what is the probability that the population adapts from one or more allele(s) from the standing pool of melanic alleles?

8.2 The interaction between genetic drift and weak selection.

5070 For strongly selected alleles, once the allele has escaped initial loss at low frequencies, its path will be determined deterministically by its 5072 selection coefficients. However, if selection is weak compared to genetic drift, the stochasticity of reproduction can play a role in the trajectory 5074 an allele takes even when it is common in the population. If selection is sufficiently weak compared to genetic drift, then genetic drift will 5076 dominate the dynamics of alleles and they will behave like they're effectively neutral. Thus, the extent to which selection can shape 5078 patterns of molecular evolution will depend on the relative strengths of selection and genetic drift. But how weak must selection on an 5080 allele be for drift to overpower selection? And do these interactions between selection and drift have longterm consequences for genome-wide patterns evolution?

To model selection and drift each generation, we can first calculate 5084 the deterministic change in our allele frequency due to selection using our deterministic formula. Then, using our newly calculated expected 5086 allele frequency, we can binomially sample two alleles for each of our offspring to construct the next generation. This approach to jointly 5088 modeling genetic drift and selection is called the Wright-Fisher model.

Under the Wright-Fisher model, we will calculate the expected



Figure 8.5: cress bug (*Asellus aquaticus*) in the isopod family *Asellidae*. Brehms Tierleben. Allgemeine kunde des Tierreichs (1911). Brehm A.E. Image from the Biodiversity Heritage Library. Contributed by Smithsonian Libraries. Not in copyright.

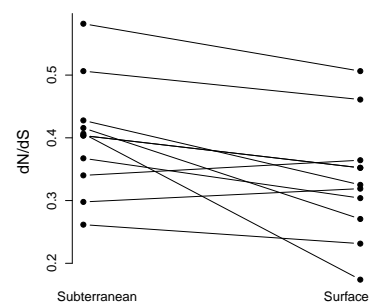


Figure 8.6: Asellid isopods have repeatedly invaded subterranean, ground-water habitats from surface-water habitats, and leading to a genome-wide increase in dN/dS and larger genomes (Data from LEFÉBURE *et al.*, 2017, comparing independent isopod species pairs). One possible explanation of this is that the longterm effective population sizes of the subterranean species are lower and so these species are less able to prevent mildly deleterious

5090 change in allele frequency due to selection and the variance around
this expectation due to drift. To make our calculations simpler, let's
5092 assume an additive model, i.e. $h = 1/2$, and that $s \ll 1$ so that $\bar{w} \approx 1$.
Using our directional selection deterministic model, from Chapter 6,
5094 and these approximations gives us our deterministic change due to
selection

$$\Delta_{SP} = \mathbb{E}(\Delta p) = \frac{s}{2}p(1-p) \quad (8.9)$$

5096 To obtain our new frequency in the next generation, p_1 , we binomially
sample from our new deterministic frequency $p' = p + \Delta_{SP}$, so the
5098 variance in our allele frequency change from one generation to the
next is given by

$$Var(\Delta p) = Var(p_1 - p) = Var(p_1) = \frac{p'(1-p')}{2N} \approx \frac{p(1-p)}{2N}. \quad (8.10)$$

5100 where the previous allele frequency p drops out because it is a con-
stant and the variance in our new allele frequency follows from the
5102 fact that we are binomially sampling $2N$ new alleles from a frequency
 p' to form the next generation.

5104 To get our first look at the relative effects of selection vs. drift we
can simply look at when our change in allele frequency caused by se-
5106 lection within a generation is reasonably faithfully passed down through
the generations. In particular, if our expected change in allele fre-
5108 quency is much greater than the variance around this change, genetic
drift will play little role in the fate of our selected allele (once the al-
5110 lele is not at low copy number within the population). When does se-
lection dominant genetic drift? This will happen if $\mathbb{E}(\Delta p) \gg Var(\Delta p)$,
5112 i.e. when $|Ns| \gg 1$. Conversely, any hope of our selected allele follow-
ing its deterministic path will be quickly undone if our change in allele
5114 frequencies due to selection is much less than the variance induced by
drift. So if the absolute value of our population-size-scaled selection
5116 coefficient $|Ns| \ll 1$, then drift will dominate the fate of our allele.

To make further progress on understanding the fate of alleles with
5118 selection coefficients of the order $1/N$ requires more careful modeling.
However, under our diploid model, with an additive selection coef-
5120 ficient s , we can obtain the probability that allele 1 fixes within the
population, starting from a frequency p :

$$p_F(p) = \frac{1 - e^{-2Ns}}{1 - e^{-2Ns}} \quad (8.11)$$

5122 The proof of this result is sketched out below (see Section 8.2.1). A
new allele that arrives in the population at frequency $p = 1/(2N)$ has
5124 a probability of reaching fixation of

$$p_F\left(\frac{1}{2N}\right) = \frac{1 - e^{-s}}{1 - e^{-2Ns}} \quad (8.12)$$

To see this denote our new count of
allele 1 by i , then

$$\begin{aligned} Var(p_1 - p) &= Var\left(\frac{i}{2N} - p\right) = Var\left(\frac{i}{2N}\right) \\ &= \frac{Var(i)}{(2N)^2} \end{aligned}$$

and from binomial sampling $Var(i) = 2Np'(1-p')$ and so we arrive at our
answer. Assuming that $s \ll 1$, $p' \approx p$, then in practice we can use

$$Var(\Delta p) = Var(p' - p) \approx p(1-p)/2N.$$

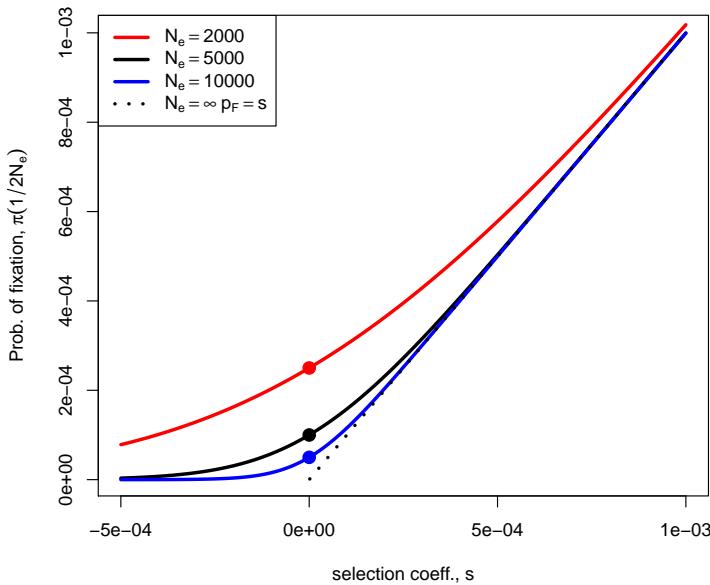


Figure 8.7: The probability of the fixation of a new mutation with selection coefficient s ($h = 1/2$) in a diploid population of effective size N_e . The dashed line gives the infinite population solution. The dots give the solution for $s \rightarrow 0$, i.e. the neutral case, where the probability of fixation is $1/(2N_e)$. Code here.

If $s \ll 1$ but $Ns \gg 1$ then $p_F(\frac{1}{2N}) \approx s$, which nicely gives us back the result that we obtained above for an allele under strong selection (eqn. (8.8)). Our probability of fixation (eqn. (8.12)) is plotted as a function of s and N in Figure 8.8. To recover our neutral result, we can take the limit $s \rightarrow 0$ to obtain our neutral fixation probability, $1/(2N)$.

In the case where Ns is close to 1, then

$$p_F\left(\frac{1}{2N}\right) \approx \frac{s}{1 - e^{-2Ns}} \quad (8.13)$$

This is greater than our earlier result $p_F = s$ from the branching process argument (using our additive model of $h = 1/2$), increasingly so for smaller N . Why is this? The reason why is that p_F is really the probability of "never being lost" in an infinitely large population. So to persist indefinitely, the allele has to escape loss permanently, by never being absorbed by the zero state. When the population size is finite, to fix we only need to reach a size $2N$ individuals. Weakly beneficial mutations ($Ns > 1$) are slightly more likely to fix than the s probability, as they only have to reach $2N$ to never be lost.

If, for selection to operate on an allele, we need the selection coefficient to satisfy $|Ns| \gg 1$, then that holds if $|s| \gg 1/N$. Well, effective population sizes are often reasonably large, on the order of hundreds of thousands or millions of individuals, thus selection coefficients on the order of 10^{-5} to 10^{-6} can be effectively selected upon, i.e. selection equivalent to individuals have incredibly slight advantages in

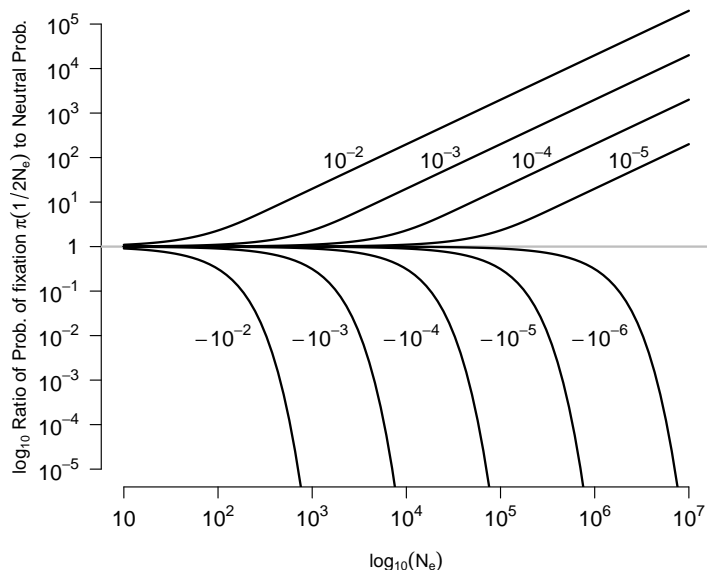


Figure 8.8: The probability of the fixation of a new mutation with selection coefficient s relative to the neutral fixation probability ($1/2N_e$) as a function of the effective size N_e . The selection coefficient is shown next to the line. Note how quickly the probabilities move away from the neutral expectation as $N_e s$ moves passed 1. Code here.

5146 terms of the number of offspring they leave to the next generation.
 While we are incapable of detecting measuring all but the large fitness
 5148 effect sizes, except in some elegant experiments (e.g. in microbes),
 such small effects are visible to selection in large populations. Thus, if
 5150 consistent selection pressures are exerted over long time periods, natural
 selection can potentially finely tune various aspects of an organism.

5152 As one example of this fine-tuning, consider how carefully crafted
 and optimized the sequence of codons is for translation. Due to the
 5154 degeneracy of the protein code, multiple codons code for the same
 amino-acid. For example, there are six different codons that can code
 5156 leucine. While these synonymous codons are equivalent at the protein
 level, cells do differ in the number of tRNA molecules that bind these
 5158 codons and so the efficacy and accuracy with which proteins can be
 formed through translation and folding. These slight differences in
 5160 translation rates likely often correspond to tiny differences in fitness,
 but do they matter?

5162 In many organisms there is a strong bias in the codons to encode
 particular amino-acids, see Figure 8.9, with the most abundant codon
 5164 matching the most abundant tRNA in cells. This 'codon bias' likely
 reflects the combined action of weak selection and mutational pressure,
 5166 pushing the codon composition of the genome and tRNA abundances
 towards an adaptive compromise. These selection pressures have acted
 5168 over long time periods, as codon usage patterns are often very simi-

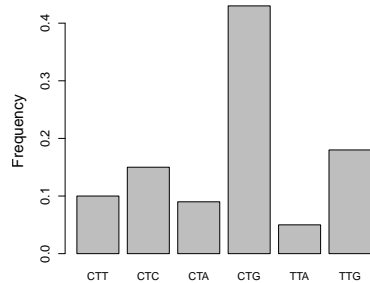


Figure 8.9: Data from *Drosophila melanogaster* on the frequency of different codons for Leucine. Data from Genscript. Code here.

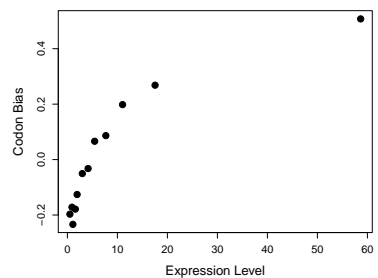


Figure 8.10: A measure of unequal codon frequencies (F) plotted in bins of gene expression (E) for genes across the *Drosophila melanogaster* genome. Data from HEY and KLIMAN (2002). Code here.

lar for species that diverged over many tens of millions of years ago.

5170 Compared to other genes, highly expressed genes show a strong bias towards using codons matching abundant tRNAs, consistent with the idea that the synonymous codon content of highly expressed genes

5172 is evolving to optimize their translation (see Figure 8.10 for an early example). These patterns likely represent the action of selection pressures that are incredibly weak on average, but that have played out

5174 over vast time-periods.

5176

The fixation of slightly deleterious alleles. From Figure 8.8 we can see that weakly deleterious alleles can also fix, especially in small populations. To understand how likely it is that deleterious alleles by chance reach fixation by genetic drift, let's assume a diploid model with additive selection (with a selection coefficient of $-s$ against our allele 2).

If $Ns \gg 1$ then our deleterious allele (allele 2) cannot possibly reach fixation. However, if Ns is not large, then the probability of fixation

$$p_F \left(\frac{1}{2N} \right) \approx \frac{s}{e^{2Ns} - 1} \quad (8.14)$$

for our single-copy deleterious allele. So deleterious alleles can fix within populations (albeit at a low rate) if Ns is not too large. As above, this is because while deleterious mutations will never escape loss in infinite populations, they can become fixed in finite population by reaching $2N$ copies.

Question 3. An additive mutation arises that lowers the relative fitness of heterozygotes by 10^{-5} . What is the probability that this mutation fixes in a diploid population with effective size of 10^4 ? What is the probability it fixes in a population of effective size 10^6 ? By comparing both to their neutral probability describe the intuition behind this result.

OHTA proposed the ‘nearly-neutral’ theory of molecular evolution in a series of papers¹. She suggested that a reasonable fraction of newly arising functional mutations may have very weak selection coefficients, such that species with smaller effective population sizes may have higher rates of fixation of these very weakly deleterious alleles. In effect, her suggestion is that the constraint parameter C of a functional region is not a fixed property, but rather depends on the ability of the population to resist the influx of very weakly deleterious mutations.

¹ OHTA, T., 1972 Population size and rate of evolution. *Journal of Molecular Evolution* 1(4): 305–314; OHTA, T., 1973 Slightly deleterious mutant substitutions in evolution. *Nature* 246(5428): 96; and OHTA, T., 1987 Very slightly deleterious mutations and the molecular clock. *Journal of Molecular Evolution* 26(1-2): 1–6

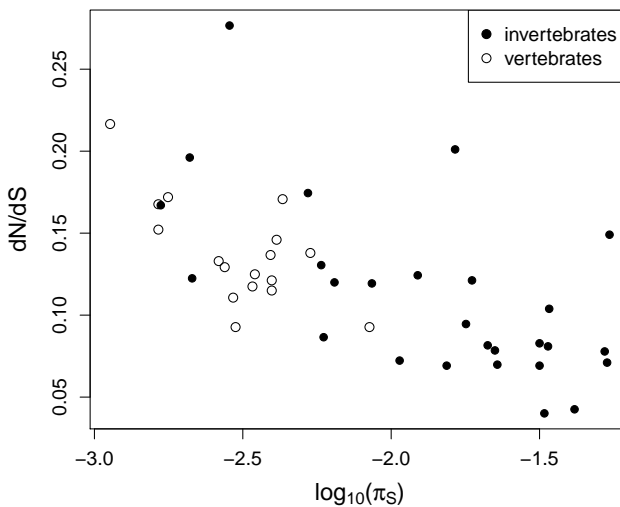


Figure 8.11: Data from 44 metazoan species from Cuttlefish to Sifakas. Each dot represents the average of over many genes plotting d_N/d_S against synonymous diversity (π_S). Data from GALTIER (2016). Code here.

Across species, genome-wide averages of d_N/d_S do seem to be correlated with measures of the effective population size (such as synonymous diversity), see Figure 8.11. This evidence supports the idea that in species with smaller effective population sizes (lower π_S), proteins may be subject to lower degrees of constraint, as very weakly deleterious mutations are able to fix. Thus, some reasonable proportion of functional substitutions in populations with small effective population sizes, such as humans, may be mildly deleterious.

8.2.1 Appendix: The fixation probability of weakly selected alleles

What is the probability a weakly beneficial or deleterious additive allele fixes in our population? We'll let $P(\Delta p)$ be the probability that our allele frequency shifts by Δp in the next generation. Using this, we can write our probability $p_F(p)$ in terms of the probability of achieving fixation averaged over the frequency in the next generation

$$p_F(p) = \int p_F(p + \Delta p)P(\Delta p)d(\Delta p) \quad (8.15)$$

This is very similar to the technique that we used when deriving our probability of escaping loss in a very large population above.

So we need an expression for $p_F(p + \Delta p)$. To obtain this, we'll do a Taylor series expansion of $p_F(p)$, assuming that Δp is small:

$$p_F(p + \Delta p) \approx p_F(p) + \Delta p \frac{dp_F(p)}{dp} + (\Delta p)^2 \frac{d^2 p_F(p)}{dp^2}(p) \quad (8.16)$$



Figure 8.12: Common Cuttlefish (*Sepia officinalis*). Cefalopodi viventi nel Golfo di Napoli (1896). Jatta G. Image from the Biodiversity Heritage Library. Contributed by Smithsonian Libraries. Licensed under CC BY-2.0.

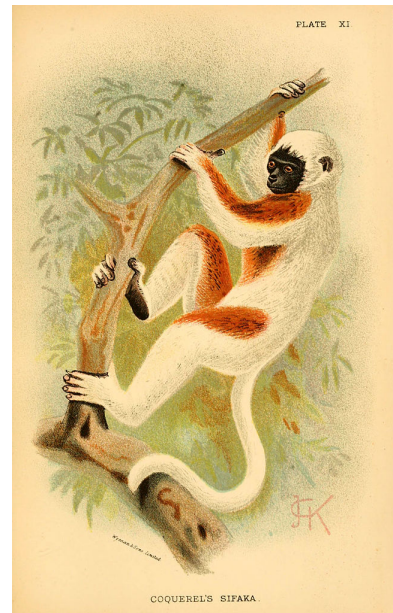


Figure 8.13: Coquerel's Sifaka (*Propithecus coquereli*). A hand-book to the primates (1894). Forbes, H. O. Image from the Biodiversity Heritage Library. Contributed by Smithsonian Libraries. Licensed under CC BY-2.0.

ignoring higher order terms.

⁵²²⁴ Taking the expectation over Δp on both sides, as in eqn. 8.15, we obtain

$$p_F(p) = p_F(p) + \mathbb{E}(\Delta p) \frac{dp_F(p)}{dp} + \mathbb{E}((\Delta p)^2) \frac{d^2 p_F(p)}{dp^2} \quad (8.17)$$

⁵²²⁶ Well, $\mathbb{E}(\Delta p) = \frac{s}{2}p(1-p)$ and $Var(\Delta p) = \mathbb{E}((\Delta p)^2) - \mathbb{E}^2(\Delta p)$, so if $s \ll 1$ then $\mathbb{E}^2(\Delta p) \approx 0$, and $\mathbb{E}(\Delta p)^2 = \frac{p(1-p)}{2N}$. Substituting in these values and subtracting p from both sides of our equation, this leaves us with

$$0 = \frac{s}{2}p(1-p) \frac{dp_F(p)}{dp} + \frac{p(1-p)}{2N} \frac{d^2 p_F(p)}{dp^2} \quad (8.18)$$

⁵²³⁰ and we can specify the boundary conditions to be $p_F(1) = 1$ and $p_F(0) = 0$. Solving this differential equation is a somewhat involved process, but in doing so we find that

$$p_F(p) = \frac{1 - e^{-2Ns p}}{1 - e^{-2Ns}} \quad (8.19)$$

This proof can be extended to alleles with arbitrary dominance, however, this does not lead to a analytically tractable expression so we do not pursue this here.

The Effects of Linked Selection.

5238 GENETIC DRIFT IS NOT THE ONLY SOURCE OF RANDOMNESS
in the dynamics of alleles. Alleles also experience random fluctua-
5240 tions in frequency due to the fact that they present on a set of random
genetic backgrounds with different fitnesses. For example, when a
5242 beneficial allele arises via a single mutation, it arises on a particular
genetic background, i.e. a particular haplotype (Figure 9.1A). Imagine
5244 this mutation arising in a region with no recombination, or in an or-
ganism where genetic exchange is rare. If our beneficial allele becomes
5246 established in the population, i.e. escapes loss by genetic drift in those
first few generations, it will start to increase in frequency rapidly. As
5248 it rises in frequency, so will the alleles that happened to be present
on the haplotype that the mutation arose on (if those other alleles are
5250 neutral or at least not too deleterious). These other alleles are get-
ting to 'hitchhiking' along. The alleles that are not on that particular
5252 background are swept out of the population, so the net effect of this
selective sweep is to remove genetic diversity from the population. Di-
5254 versity will eventually recover, as new mutations arise and some slowly
drift up in frequency. But in the short-term, selective sweeps remove
5256 genetic variation from populations.

WILLIAMS and PENNINGS (2019) have visualized selective
5258 sweeps in HIV. In Figure 9.1B) we see a set of HIV haplotypes sam-
pled from a patient before and after of a selective sweep of a drug-
5260 resistant mutation. The patient is taking a retrotransposase inhibitor
(Efavirenz), but sadly within 161 days a drug-resistant mutation that
5262 changes the HIV retrotransposase protein has arisen and spread. Note
how a particular haplotype is now fixed in the sample, and little ge-
5264 netic diversity remains, due to the hitchhiking effect of the strong
selective sweep of this allele.

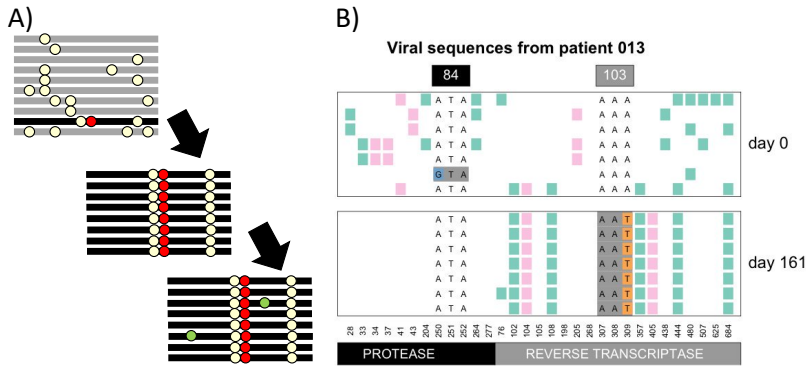


Figure 9.1: **A)** In the top panel, a selected mutation (red dot) arises on a particular haplotype in the population. It sweeps to fixation, carrying with it the haplotype on which it arose, middle panel, erasing the standing genetic diversity in the region. The bottom panel is some time after the selective sweep when some new neutral alleles (green dots) have started to drift up in frequency. **B)** Top panel: HIV sequences from a patient at the start of drug treatment in the protease and retrotransposase coding regions. Bottom panel: A sample 161 days later, after a drug resistant mutation has spread, the $A \rightarrow T$ in the 103rd codon of retrotransposase. Each row is a haplotype, with the alleles present shown as coloured blocks. Figure B from WILLIAMS and PENNINGS (2019), licensed under CC BY 4.0.

To better understand hitchhiking, first let's imagine examining variation at a locus fully linked to our selected locus, just after our sweep reached fixation. Neutral alleles sampled at this locus must trace their ancestral lineages back to the neutral allele on whose background the selected allele initially arose (Figure 9.6). This is because that background neutral allele, which existed τ generations ago, is the ancestor of the entire population at this fully linked locus. Our individuals who carry the beneficial allele are, from the perspective of these alleles, experiencing a rapidly expanding population. Therefore, a pair of neutral alleles sampled at our linked neutral locus will be forced to coalesce $\approx \tau$ generations ago. A newly derived allele with an additive selection coefficient s will take a time $\tau = 4 \log(2N)/s$ generations to reach fixation within our population (see eqn. (6.39)). This is a very short-time scale compared to the average neutral coalescent time of $2N$ generations for a pair of alleles. Thus we expect little variation, as few mutations will have arisen on these very short branches, and those that have done will likely be singletons in our sample.

Now let's think about a sweep in a recombining region. Again the selected mutation arises on a particular haplotype, and it and its haplotype starts to increase in frequency in the population. However, now recombination events can occur between haplotypes carrying and not carrying the selected allele, in individuals who are heterozygote for the selected allele. These recombination events allow alleles that were not present on the original selected haplotype to avoid being swept out of the population, and also decouple the selected allele somewhat from hitchhiking alleles, preventing many of them from hitchhiking all the way to fixation. Far out from the selected site, the recombination rate is high enough that alleles that were present on the original background barely get to hitchhike along at all, as recombination breaks up their association with the selected allele very

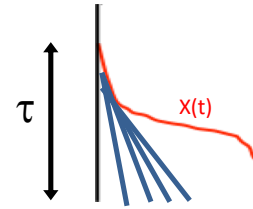


Figure 9.2: The coalescent of 4 lineages, marked in blue, at a locus completed linked to our selected allele. The frequency trajectory of the selected allele $X(t)$ is shown in red.

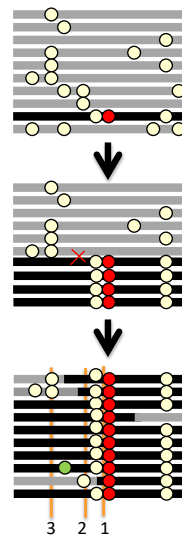


Figure 9.3: A cartoon depiction of a sweep of a red beneficial allele over three time points. The haplotype that the beneficial arose on by mutation is shown in black. The three vertical orange lines mark the loci shown in Figure 9.4. Neutral alleles segregating prior to the sweep appear as white circles, new mutations after the sweep as green circles.

5296 rapidly.

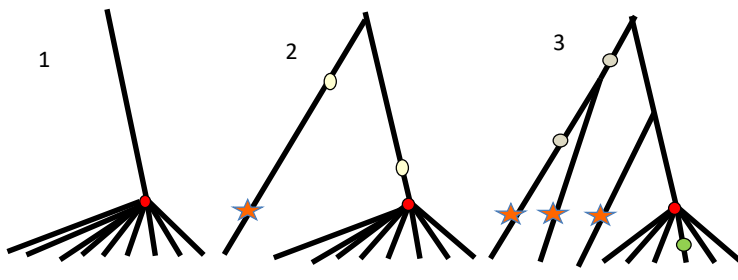


Figure 9.4: Coalescent genealogies at three loci different distances along the genome from a selective sweep. The locations of these three loci along the genome are marked in Figure 9.3. The selected mutation is shown in red. Lineages descended from recombination events during the sweep are marked in stars. Neutral mutations close to each of the loci are shown on the genealogy.

What do the coalescent genealogies look like at loci various distances away from the selected site? Well, close to the selected site all our alleles in the present day trace back to a most recent common ancestral allele present on that selected haplotype, and so are all forced to coalesce around τ generations ago (locus 1). Slightly further out from the selected site (locus 2), we have lineages that don't trace their ancestry back to the original selected haplotype, but instead are descended from recombinant haplotypes that recombined onto the sweep (the haplotype 2 from the bottom). These lineages can coalesce neutrally with the other ancestral lineages over far deeper time scales and mutations on these deeper lineages correspond to the standing diversity present in our population prior to the sweep. As we move even further out from the selected site (locus 3), we encounter more and more lineages descended from recombinant haplotypes that coalesce neutrally much deeper in time than τ , allowing diversity to recover to background levels as we move away from the selected site.

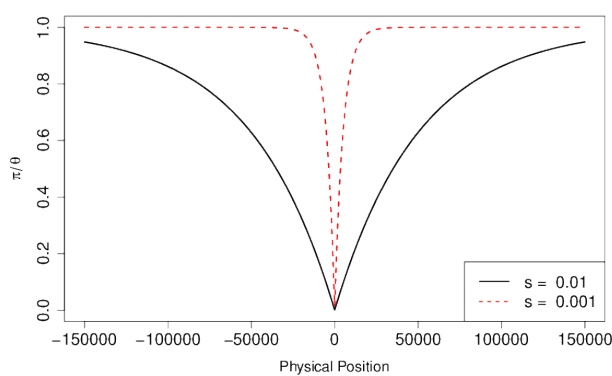


Figure 9.5: The expected reduction in diversity compared to its neutral expectation as a function of the distance away from a site where a selected allele has just gone to fixation. The sweeps associated with two different strengths of selection are shown, corresponding to a short timescale (τ) for the sweep and long one. The recombination rate is $r_{BP} = 1 \times 10^{-8}$. Code here.

To model the expected pattern of diversity surrounding a selected site, we can think about a pair of alleles sampled at a neutral locus a recombination distance r away from our selected site. Our pair of

5316 alleles will be forced to coalesce $\approx \tau$ generations if neither of them of
are descended from recombinant haplotypes.

5318 We know that in the present day our neutral lineage is linked to the
selected allele. The probability that our lineage, in some generation
5320 t back in time, is in a heterozygote is $1 - X(t)$, and the probability
that a recombination occurs in that individual is r . So the probability
5322 that our neutral lineage is descended from a recombinant haplotype t
generations back is

$$r(1 - X(t)) \quad (9.1)$$

5324 So the probability (p_{NR}) that our lineage is not descended from a re-
combinant haplotype from a recombination event in the τ generations
5326 it takes our selected allele to move through the population is

$$p_{NR} = \prod_{t=1}^{\tau} (1 - r(1 - X(t))) \quad (9.2)$$

Assuming that r is small, then $(1 - r(1 - X(t))) \approx e^{-r(1-X(t))}$, such
5328 that

$$p_{NR} = \prod_{t=1}^{\tau} (1 - r(1 - X(t))) \approx \exp\left(-r \sum_{t=1}^{\tau} 1 - X(t)\right) = \exp\left(-r\tau(1 - \hat{X})\right) \quad (9.3)$$

where \hat{X} is the average frequency of the derived beneficial allele across
5330 its trajectory as it sweeps up in frequency, $\hat{X} = \frac{1}{\tau} \sum_{t=1}^{\tau} X(t)$. As
our allele is additive, its trajectory for frequencies < 0.5 is the mirror
5332 image of its trajectory for frequencies > 0.5 , therefore its average
frequency $\hat{X} = 0.5$. This simplifies our expression to

$$p_{NR} = e^{-r\tau/2}. \quad (9.4)$$

5334 The probability that neither of our lineages is descended from a re-
combinant haplotype, and hence are forced to coalesce, is p_{NR}^2 (as-
5336 suming that they coalesce at a time close to τ so that they recombine
independently of each other for times $< \tau$).

5338 If one or other of our lineages is descended from a recombinant
haplotype, it will take them on average $\approx 2N$ generations to find a
5340 common ancestor, as we are back to our neutral coalescent probabil-
ities. Thus, the expected time till our pair of lineages find a common
5342 ancestor is

$$\mathbb{E}(T_2) = \tau \times p_{NR}^2 + (1 - p_{NR}^2)(\tau + 2N) \approx (1 - p_{NR}^2) 2N \quad (9.5)$$

where this last approximation assumes that $\tau \ll 2N$. So the expected
5344 pairwise diversity for neutral alleles at a recombination distance r
away from the selected sweep (π_r) is

$$\mathbb{E}(\pi_r) = 2\mu\mathbb{E}(T_2) \approx \pi_0 (1 - e^{-r\tau}) \quad (9.6)$$

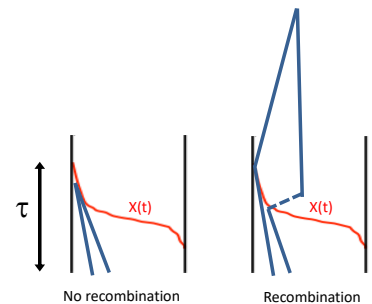
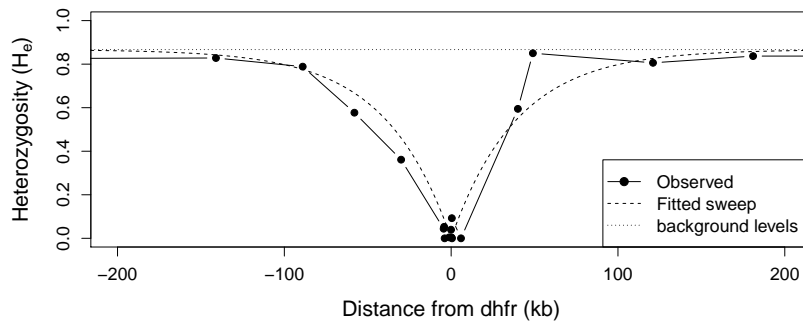


Figure 9.6:

5346 So diversity increases as we move away from the selected site, slowly
and exponentially plateauing to its neutral expectation π_0 .

5348 The malaria pathogen (*Plasmodium falciparum*) has evolved drug
resistance to anti-malaria drugs, often by changes at the dhfr gene.

5350 Figure 9.8 shows levels of genetic diversity (heterozygosity) at a set
of markers moving out from the dhfr gene in a set of drug resistant
5352 malaria sequences collected in Thailand (NASH *et al.*, 2005). We see
the characteristic dip in diversity around the gene, with zero diversity
5354 at a number of the loci very close to the gene, suggesting a strong
selective sweep. Fitting our simple model of a sweep to this data, we
5356 estimate that $\tau \approx 40$ generations, corresponding to the drug-resistance
allele fixing in very short time period.



5358 To get a sense of the physical scale over which diversity is reduced,
consider a region where recombination occurs at a rate r_{BP} per base
5360 pair per generation, and a locus ℓ base pairs away from the selected
site, such that $r = r_{BP}\ell$ (where $r_{BP}\ell \ll 1$ so we don't need to worry
5362 about more than one recombination event occurring per generation).
Typical recombination rates are on the order of $r_{BP} = 10^{-8}$. In Figure
5364 9.5 we show the reduction in diversity, given by eqn. (9.6), for two
different selection coefficients.

5366 For our expected diversity level to recover to 50% of its neutral
expectation $\mathbb{E}(\pi_r)/\theta = 0.5$, requires a physical distance ℓ^* such that
5368 $\log(0.5) = -r_{BP}\ell^*\tau$, and by re-arrangement,

$$\ell^* = \frac{-\log(0.5)}{r_{BP}\tau}. \quad (9.7)$$

As τ depends inversely on the selection s (eqn. (6.39)), the width
5370 of our trough of reduced diversity depends on s/r_{BP} . All else being
equal, we expect stronger sweeps or sweeps in regions of low recombi-
5372 nation to have a larger hitchhiking effect. For example, in a genomic
region with a recombination rate $r_{BP} = 10^{-8}\text{bp}^{-1}$ a selection coeffi-
5374 cient of $s = 0.1\%$ would reduce diversity over 10's of kb, while a sweep
of $s = 1\%$ would affect $\sim 100\text{kb}$.

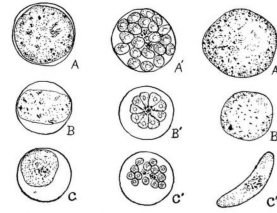


FIG. 47. Comparison of three species of malaria parasites $\times 2000$ (figures selected largely from Manson). A, A' and A'', *Plasmodium vivax*; B, B' and B'', *Plasmodium vivax*; C and C', *Plasmodium falciparum*. A, B and C, mature parasites in red corpuscles. A', B' and C', segmented parasites ready to leave corpuscles. A'', B'' and C'', mature gametocytes.

Figure 9.7: Three species of malaria parasites (*Plasmodium*) in red blood cells.
Animal parasites and human disease (1918). Chandler, A.C. Image from the Biodiversity Heritage Library. Contributed by Cornell University Library. Not in copyright.

Figure 9.8: Levels of heterozygosity at a set of microsatellite markers surrounding the dhfr gene in samples of drug-resistant malaria (*Plasmodium falciparum*) from Thailand. The dotted horizontal line gives the average level of heterozygosity found at these markers in a set of drug-resistant malaria; we take this background as our π_0 . The dashed line shows our fitted hitchhiking model from equation 9.6 with $\tau \approx 40$, fitted by non-linear least squares. The recombination rate in *P. falciparum* is $r_{BP} \approx 10^{-6}\text{bp}^{-1}$. Data from NASH *et al.* (2005). Code here.

5376 Question 1. VAN'T HOF *et al.* (2011) identified the genetic
5378 basis of melanism in the peppered moth (*Biston betularia*). This al-
5380 lele swept to fixation in northern parts of the UK; a classic case of
5382 adaptation to industrial pollution (made famous by the work of KET-
5384 TLEWELL, see MAJERUS (2009) and COOK *et al.* (2012)). The
5386 genetic basis of melanism is a transposable element (TE) inserted
5388 into a pigmentation gene. VAN'T HOF *et al.* found that diversity
5390 is suppressed in a broad region around the TE. Specifically, on the
5392 background of the TE, it takes roughly 200 kb in either direction for
5394 diversity levels to recover to 50% of genome-wide levels.

5396 Random facts: In all moths and butterflies only males recombine;
5398 chromosomes are transmitted without recombination in females. The
5400 recombination rate in males is 2.9 cM/Mb. Peppered moths have an
5402 effective population size of roughly a hundred thousand individuals.
5404 Kettlewell used to eat moths when out collecting them in the field
5406 (personal communication, Art. Shapiro).

A) Briefly explain how this pattern offers further evidence that the
5392 melanic allele was favoured by selection.

B) Using this information, and assuming the allele's effects on
5394 fitness are additive, what is your estimate of the age of the allele?

C) What is your estimate of the selection coefficient favouring this
5396 melanic allele?

5398 Other signals of selective sweeps The primary signal of a recently completed selective sweep is the characteristic reduction in diversity surrounding the selected site. However, sweeps do leave other signals and these have also often been used to identify loci undergoing selection. For example, neutral alleles further away from the selected site may hitchhiking only part of the way to fixation if recombination occurs during the sweep, which can lead to an excess of high-frequency derived alleles at intermediate distances away from the selected site, a pattern lasting for a short time after a sweep (FAY and WU, 2000; PRZEWORSKI, 2002; KIM, 2006). Also, as neutral diversity levels slowly recover through an influx of new mutations after a sweep, there is a strong skew towards low frequency derived alleles, a pattern that persists for many generations (BRAVERMAN *et al.*, 1995; PRZEWORSKI, 2002; KIM, 2006). The excess of rare alleles, compared to a neutral model, can be captured by statistics such as Tajima's D (which we encountered back in our discussion of the neutral site frequency eqn 3.42). Thus one way to look for loci that have undergone selective sweeps is to calculate Tajima's D from data in windows along the genome and look for strong departures from the null distribution.



Figure 9.9: peppered moth (*Biston betularia*), non-melanic morph
Les papillons dans la nature (1934). Robert, P.-A. Image from the Biodiversity Heritage Library. Contributed by University of Illinois Urbana-Champaign. Not in copyright.

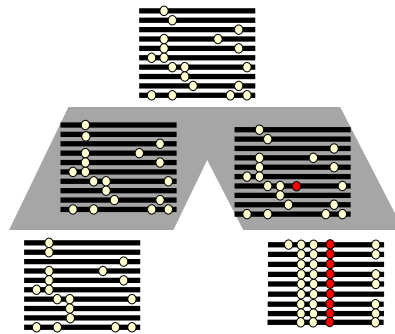


Figure 9.10: Two populations descended from a common ancestral population. A beneficial mutation has occurred in population and swept to fixation.

We can also use comparisons among multiple populations to look

5418 for evidence of sweeps occurring in one of the populations, for example
to identify alleles involved in local adaptation (see 9.11). A selective
5420 sweep will decrease the within-population diversity (H_S) surrounding
the selected site, without affecting the diversity between different
5422 populations. Thus local sweeps create peaks of F_{ST} between weakly
differentiated populations.

5424 HOHENLOHE *et al.* (2010) studied genome-wide patterns of F_{ST}
between marine and freshwater populations of threespine stickleback
5426 (*Gasterosteus aculeatus*). Between different marine populations, they
found no strong peaks of F_{ST} ; however, between the marine and fresh-
5428 water comparisons they found a number of high F_{ST} peaks that were
replicated over a number of freshwater-marine comparisons. They
5430 identified a number of novel regions responsible for the adaptation
of sticklebacks to freshwater environments and also a number of loci
5432 previously identified in crosses between marine and freshwater pop-
ulations. For example, the first peak of Linkage Group IV includes
5434 Ectodysplasin A (Eda), a gene involved in the adaptive loss of armour
plating in freshwater environments.

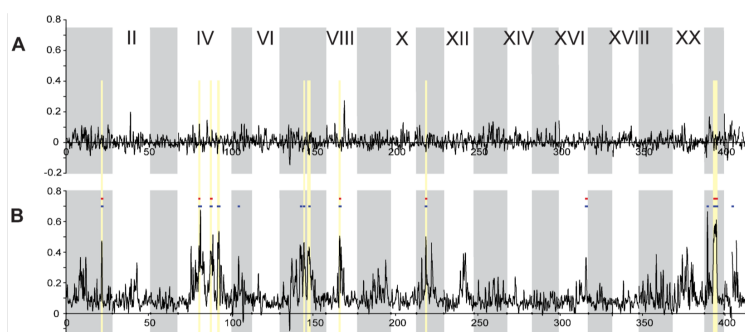


Figure 9.11: F_{ST} across the stickleback genome, with colored bars indicating significantly elevated ($p \leq 10^{-5}$, blue; $p \leq 10^{-7}$, red) and reduced ($p \leq 10^{-5}$, green) values. The alternating white and grey panels indicate different linkage groups. **A)** F_{ST} between two oceanic populations **B)** Average F_{ST} between a freshwater population and the two marine populations. Figure and caption text from HOHENLOHE *et al.* (2010), licensed under CC BY 4.0.

5436 *Soft Sweeps from multiple mutations and standing variation.* In our
 sweep model above, we assumed that selection favoured a beneficial
 5438 allele from the moment it entered the population as a single copy
 mutation (left panel, Figure 9.12). However, when a novel selection
 5440 pressure switches on, multiple mutations at the same gene may start
 to sweep, such that no one of these alleles sweeps to fixation (middle
 5442 panel, Figure 9.12). These sweeps involving multiple mutations signif-
 icantly soften the impact of selection on genomic diversity, and so are
 5444 called 'soft sweeps'.

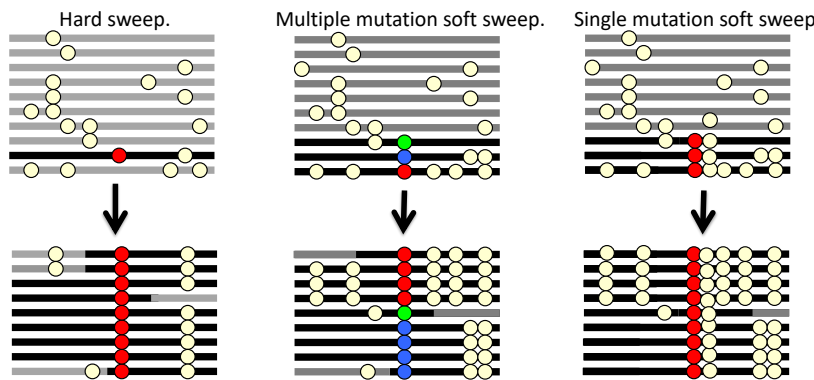


Figure 9.12: Three types of sweeps.

Another way that the impact of a sweep can be softened is if our
 5446 allele was segregating in the population for some time before it became
 beneficial. That additional time means that our allele can have recom-
 5448 bined onto various haplotype backgrounds, such that when selection
 pressures switch, the selected allele sweeps up in frequency on multiple
 5450 different haplotypes (right panel, Figure 9.12). Detecting and differ-
 entiating these different types of sweeps is an active area of empirical
 5452 research and theory in population genomics (see HERMISSON and
 PENNINGS (2017) for an overview of developments in this area).

5454 9.1 The genome-wide effects of linked selection.

To what extent are patterns of variation along the genome and among
 5456 species shaped by linked selection, such as selective sweeps? We can
 hope to identify individual cases of strong selective sweeps along the
 5458 genome, but how do they contribute to broader patterns of variation?

Two observations have puzzled population geneticists since the in-
 5460 ception of molecular population genetics. The first is the relatively
 high level of genetic variation observed in most obligately sexual
 5462 species. The neutral theory of molecular evolution was developed in
 part to explain these high levels of diversity. As we saw in Chapter
 5464 3, under a simple neutral model, with constant population size, we

should expect the amount of neutral genetic diversity to scale with the product of the population size and mutation rate. The second observation, however, is the relatively narrow range of polymorphism across species with vastly different census sizes (see Figure 2.2 and LEFFLER *et al.* (2012) for a recent review). As highlighted by LEWONTIN (1974) in his discussion of the paradox of variation, this observation seemingly contradicts the prediction of the neutral theory that genetic diversity should scale with the census population size. There are a number of explanations for the discrepancy between genetic diversity levels and census population sizes. The first is that the effective size of the population (N_e) is often much lower than the census size, due to high variance in reproductive success and frequent bottlenecks (as discussed in Chapter 3). The second major explanation, put forward by MAYNARD SMITH and HAIGH (1974), is that neutral levels of diversity are also systematically reduced by the effects of linked selection. In large populations, selective sweeps and other forms of linked selection may come to dominate over genetic drift as a source of stochasticity in allele frequencies, potentially establishing an upper limit to levels of diversity (KAPLAN *et al.*, 1989; GILLESPIE, 2000).

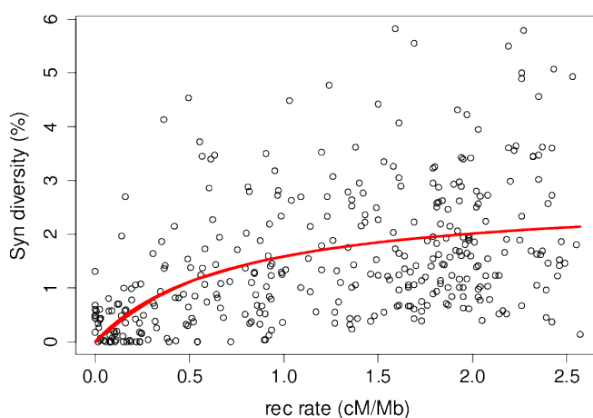


Figure 9.13: The relationship between (sex-averaged) recombination rate and synonymous site pairwise diversity (π) in *Drosophila melanogaster*. The curve is the predicted relationship between π and recombination rate, obtained by fitting the recurrent hitchhiking equation (9.13) to this data using non-linear least squares via the `nls()` function in R. Data from (SHAPIRO *et al.*, 2007), kindly provided by Peter Andolfatto, see SELLA *et al.* (2009) for details. Code here.

One strong line of evidence for the action of linked selection in reducing levels of polymorphism is the positive correlation between putatively neutral diversity and recombination seen in a number of species, as, all else being equal, linked selection should remove diversity more quickly in regions of low recombination (AGUADÉ *et al.*, 1989; BEGUN and AQUADRO, 1992; WIEHE and STEPHAN, 1993b; CUTTER and CHOI, 2010; CAI *et al.*, 2009). For example, *Drosophila melanogaster* diversity levels are much lower in genomic regions of low recombination (see Figure 9.13). This pattern can not

be explained by differences in mutation rate between low and high recombination regions as this pattern is not seen strongly in divergence data among species.

These patterns could reflect the action of selective sweeps happening recurrently along the genome. In the next section we'll present a model for how levels of genetic diversity should depend on recombination and the density of functional sites under a model of recurrent selective sweeps. However, other forms of linked selection can impact genetic diversity in similar ways. For example, linked genetic diversity is continuously lost from natural populations due to the removal of haplotypes that carry deleterious alleles (CHARLESWORTH *et al.*, 1995; HUDSON and KAPLAN, 1995b); this is called the 'background selection' model. Below we'll discuss the background selection model and its basic predictions.

More generally, a wide range of models of selection predict the removal of neutral diversity linked to selected sites. This is because the diversity-reducing effects of high variance in reproductive success are compounded over the generations when there is heritable variance in fitness (ROBERTSON, 1961; SANTIAGO and CABALLERO, 1995, 1998; BARTON, 2000). Many different modes of linked selection likely contribute to these genome-wide patterns of diversity; the present challenge is how to differentiate among these different modes.

9.1.1 A simple recurrent model of selective sweeps

To explain how a constant influx of sweeps could impact levels of diversity, here we will develop a model of recurrent selective sweeps.

Imagine we sample a pair of neutral alleles at a locus a genetic distance r away from a locus where sweeps are initiated within the population at some very low rate ν per generation. The waiting time between sweeps at our locus is exponentially distributed $\sim \text{Exp}(\nu)$. Each sweep rapidly transits through the population in τ generations, such that each sweep is finished long before the next sweep ($\tau \ll 1/\nu$).

As before, the chance that our neutral lineage fails to recombine off the sweep is p_{NR} , such that the probability that our pair of lineages are forced to coalesce by a sweep is $e^{-r\tau}$. Our lineages therefore have a very low probability

$$\nu e^{-r\tau} \tag{9.8}$$

of being forced to coalesce by a sweep per generation. If our lineages do not coalesce due to a sweep, they coalesce at a neutral rate of $1/2N$ per generation. Thus the average waiting time till a coalescent event between our neutral pair of lineages due to either a sweep or a neutral coalescent event is

$$\mathbb{E}(T_2) = \frac{1}{\nu e^{-r\tau} + 1/2N} \tag{9.9}$$

Now imagine that the sweeps don't occur at a fixed location with respect to our locus of interest, but now occur uniformly at random across our genome. The sweeps are initiated at a very low rate of ν_{BP} per basepair per generation. The rate of coalescence due to sweeps at a locus ℓ basepairs away from our neutral loci is $\nu_{BP}e^{-r_{BP}\ell\tau}$. If our neutral locus is in the middle of a chromosome that stretches L basepairs in either direction, the total rate of sweeps per generation that could force our pair of lineages to coalesce is

$$2 \int_0^L \nu_{BP} e^{-r_{BP}\ell\tau} d\ell = \frac{2\nu_{BP}}{r_{BP}\tau} (1 - e^{-r_{BP}\tau L}) \quad (9.10)$$

so that if L is very large ($r_{BP}\tau L \gg 1$), the rate of coalescence per generation due to sweeps is $2\nu_{BP}/r_{BP}\tau$. The total rate of coalescence for a pair of lineages per generation is then

$$\frac{2\nu_{BP}}{r_{BP}\tau} + \frac{1}{2N} \quad (9.11)$$

So our average time till a pair of lineages coalesce is

$$\mathbb{E}(T_2) = \frac{1}{\frac{2\nu_{BP}}{r_{BP}\tau} + 1/2N} = \frac{r_{BP}2N}{4N\nu_{BP}/\tau + r_{BP}} \quad (9.12)$$

such that our expected pairwise diversity ($\pi = 2\mu\mathbb{E}(T_2)$) in a region with recombination rate r_{BP} that experiences sweeps at rate ν_{BP} is

$$\mathbb{E}(\pi) = \pi_0 \frac{r_{BP}}{\frac{4N\nu_{BP}}{\tau} + r_{BP}} \quad (9.13)$$

where π_0 is our expected diversity without any selective sweeps, ($p_{i0} = \theta = 4N\mu$). The expected diversity increases with r_{BP} , as higher recombination rates decrease the likelihood a neutral allele hitchhikes along with a sweep and is thus forced to coalesce by the sweep. Expected diversity decreases with ν_{BP} , as a greater density of functional sites experiencing sweeps increases the chance of being linked to a nearby sweep. As we move to high r_{BP} , assuming that ν_{BP} doesn't increase with r_{BP} , our level of diversity should plateau to θ , the level of genetic diversity of a neutral site completely unlinked to any selected loci. If we assume that our genome experiences a constant rate of sweeps of a given strength, i.e. that $4N\nu_{BP}/\tau$ is a constant, we can fit the variation in π across regions that vary in their recombination rate (r_{BP}) to estimate a population's rate of recurrent sweeps per basepair. An example of fitting this curve to data from *Drosophila melanogaster* is shown in Figure 9.13; see WIEHE and STEPHAN (1993a) for an early example of fitting a similar recurrent hitchhiking model to such data. The parameter giving us this best-fitting curve is $4N\nu_{BP}/\tau \approx 7 \times 10^{-9}$. With an effect population size of a million and assuming that the sweeps take a thousand generations to reach fixation,

5566 we find this implies $\nu_{BP} \approx 10^{-12}$. Thus, a really low rate of moderately strong sweeps, roughly one every megabase every million generations, is all we need to explain the profound dip in diversity seen in regions of the genome with low recombination. However, sweeps from 5570 positively selected alleles are not the only cause of genome-wide signals of linked selection. Selection against deleterious alleles can also drive 5572 these patterns.

9.1.2 Background selection

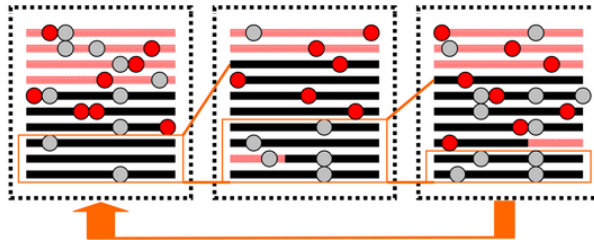
5574 Populations experience a constant influx of deleterious mutations at functional loci while selection acts to purge them from the population, 5576 thus preventing deleterious substitutions and maintaining function at these loci. As we discussed in Chapter 6, this balance between mutation 5578 and selection results in a constant level of deleterious variation in the population. The constant selection against this deleterious variation has effects on diversity at linked sites. Each deleterious mutation 5580 arises at random on a haplotype in the population, and as selection purges this mutation, it removes with it any neutral alleles that were 5582 also on this haplotype. This constant removal of linked alleles from the 5584 population acts to reduce diversity in regions surrounding functional loci (HUDSON and KAPLAN, 1995a; NORDBORG *et al.*, 1996), an 5586 effect known as background selection (BGS).

What proportion of our haplotypes are free of deleterious mutations 5588 in any given generation, and so free to contribute to future generations? Well, under mutation-selection balance, a constrained locus 5590 with a mutation rate μ towards deleterious alleles that experience a selection coefficient sh against them in heterozygotes, will result in 5592 μ/sh chromosomes carrying the deleterious allele. Some of these haplotypes may be passed on to the next generation, but if they are fully 5594 linked to the deleterious locus they will all eventually be lost because they carry a deleterious mutation at a site under constraint. Thus, for 5596 a neutral polymorphism completely linked to a constrained locus, only $2N(1 - \mu/sh)$ alleles get to contribute to future generations. Therefore, 5598 the level of pairwise diversity in a constant population due to BGS at such a locus will be

$$\mathbb{E}[\pi] = 2\mu \times 2N(1 - \mu/sh) = \pi_0(1 - \mu/sh) \quad (9.14)$$

5600 where $\pi_0 = 4N\mu$, the level of neutral pairwise diversity in the absence 5602 of linked selection.

The effects of background selection are more pronounced in regions 5604 of low recombination, where neutral alleles are less able to recombine off the background of deleterious alleles. Thus, under background 5606 selection, we also expect to see reduced diversity in regions of lower recombination.



For a neutral locus that is a recombination fraction r away from a
5608 locus subject to constraint, the level of diversity is

$$\mathbb{E}[\pi] = \pi_0 \left(1 - \frac{\mu sh}{2(r+sh)^2}\right) \quad (9.15)$$

As we move away from a locus experiencing purifying selection, we
5610 increase r , and diversity should recover. For example, moving away
from genic regions in the maize genome we see the average level of
5612 diversity recover. This occurs in both maize and teosinte, the wild
progenitor of maize. The dip in diversity around non-synonymous sites
5614 is stronger in teosinte, perhaps because the accelerated drift due to
the bottleneck in maize may have somewhat released constraint on
5616 sites where very weakly deleterious alleles segregated previously at
mutation-selection balance.

More generally, if a neutral locus is surrounded by L loci experiencing
5618 purifying selection at recombination distances r_1, \dots, r_L , then
compounding equation (9.16) across these loci, the expected reduced
5620 diversity is approximately

$$\mathbb{E}[\pi] = \pi_0 \prod_{i=1}^L \left(1 - \frac{\mu sh}{2(r_i+sh)^2}\right) \approx \exp\left(\sum_{i=1}^L \frac{\mu sh}{2(r_i+sh)^2}\right) \quad (9.16)$$

To model an average neutral locus in a genomic region with a given
5622 recombination rate, we can imagine that our neutral locus is situated
in the center of a large region with total recombination rate R and
5624 total deleterious mutation rate U , where $U = \mu L$. Then our expression
for diversity, equation (9.16), simplifies to

$$\mathbb{E}[\pi] \approx \pi_0 \exp(-U/(sh+R)) \approx \pi_0 \exp(-U/R). \quad (9.17)$$

In this last approximation, we assume that we're looking at a large
5628 region, with $R \gg sh$. Note that much like genetic load, equation
(7.8), this expression depends only on the total deleterious mutation
5630 rate. Any dependence on the selection coefficient drops out, as weakly
selected mutations segregate in the population at higher frequencies,
5632 but are also removed from the population more slowly, allowing more
of the genome to recombine off the deleterious background.

Figure 9.14: A cartoon depiction of a region for 10 haplotypes experiencing background selection. Neutral mutations are shown as gray circles, and deleterious mutations in red. Over time, chromosomes carrying deleterious mutations are removed from the population, such that most individuals are descended from a subset of chromosomes free of deleterious alleles (highlighted here by orange boxes). Mutation is constantly generating new deleterious alleles on the background of chromosomes previously free of deleterious alleles. Figure modified from SELLA *et al.* (2009), licensed under CC BY 4.0.

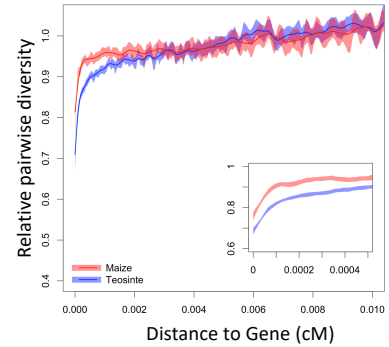


Figure 9.15: Relative diversity compared to the mean diversity in windows ≥ 0.01 cM as a function of the distance to the nearest gene. See (BEISSINGER *et al.*, 2016) for details. Figure licensed under CC BY 4.0 by Jeff Ross-Ibarra.

5634 For a first go at fitting this to genome-wide data, we could look
 5635 at diversity in windows of length W bp (as in Figure 9.16). If we
 5636 assume that there is a constant rate of deleterious mutation per base
 5637 pair, μ_{BP} , then $U = \mu_{BP}W$. Furthermore, if our genomic window
 5638 has a recombination rate r_{BP} per base-pair, our total genetic length
 5639 is $R = r_{BP}W$. Making these substitutions in equation (9.17), our
 5640 window size cancels out to give

$$\mathbb{E}[\pi] \approx \pi_0 \exp(-\mu_{BP}/r_{bp}) \quad (9.18)$$

5641 Looking across windows that vary in their recombination rate, i.e.
 5642 r_{BP} , we can fit equation (9.18) to data to estimate μ_{BP} . An example
 5643 of doing this to data from *D. melanogaster* is shown in Figure 9.16,
 5644 yielding an estimate of the deleterious mutation rate of $\mu_{BP} \approx 3.2 \times$
 10^{-9} . This is roughly on the same order as the mutation rate per
 5645 base pair in *D. melanogaster*, and so this deleterious mutation rate
 5646 estimate is somewhat high as it would require most of the genome to
 5647 be constrained, but as a first approximation it's not terrible. Note
 5648 how similar the fit is to a model of hitchhiking, suggesting that both
 5649 BGS and hitchhiking are capable of explaining the broad relationship
 5650 between diversity and recombination seen in *D. melanogaster* and
 5651 other species.

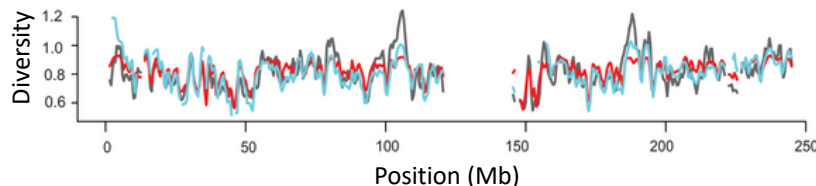


Figure 9.16: The relationship between recombination rate and synonymous site pairwise diversity (π) in *D. melanogaster*, as in Figure 9.13. The red curve is the predicted relationship between π and recombination rate, obtained by fitting the BGS equation (9.17) to this data using non-linear least squares via the `nls()` function in R. The blue line is the recurrent hitchhiking equation line from Figure 9.13. Code here.

5652 As our annotations of functional regions of the genome have im-
 5653 proved, so have our methods to infer background selection. A more
 5654 rigorous version of this analysis today would incorporate variation in
 5655 coding density among windows into the parameter μ_{BP} . With de-
 5656 tailed genomic annotations showing coding regions and constrained
 5657 non-coding regions, we can also move beyond just analyzing broad-
 5658 scale patterns. For example, MCVICKER *et al.* (2009) fit a model
 5659 of background selection to putatively neutral pairwise diversity along
 5660 the human genome, using equation 9.16 to estimate the effect of BGS
 5661 at each locus, weighing the genetic distance to all of the surround-
 5662 ing coding regions and constrained non-coding sites. This allowed
 5663 MCVICKER *et al.* (2009) to estimate mutation rates and average
 5664 selection coefficients acting against deleterious alleles in these regions
 5665 of the genome. This best fitting model also allowed them to predict

Figure 9.17: Observed (black line) and predicted pairwise diversity across chromosome 1, from a background selection model that assumes a uniform mutation rate (red line) or a mutation rate that varies with local human/dog divergence (blue line). Figure from (MCVICKER *et al.*, 2009), licensed under CC BY 4.0.

diversity levels along the genome, a section of which is shown in figure 5668 9.17. Thus, broad-scale features of polymorphism along the genome are well described by background selection (or by linked selection more 5670 generally).

The deleterious mutation rates estimated by MC VICKER *et al.* 5672 (2009) from fitting a model of BGS were again too high, as in the *Drosophila* example above, suggesting the BGS alone is not sufficient 5674 to explain all of the effect of linked selection. But how then do we go about distinguishing the impact of BGS from hitchhiking?

5676 *Distinguishing the impact of hitchhiking from background selection in genome-wide data* A variety of approaches have been taken to 5678 start to separate the effects of hitchhiking from background selection. Much of the strongest evidence showing the effects of both comes from 5680 *Drosophila melanogaster* and we review some of that evidence here. Hitchhiking is expected to have systematic effects on the neutral site 5682 frequency spectrum, distorting it towards rare minor alleles, (reflecting the slow recovery of diversity following a sweep). Therefore, we should 5684 expect a distortion of summary statistics such as Tajima's D in regions of low recombination if hitchhiking is contributing to the reduction in 5686 diversity in these regions (BRAVERMAN *et al.*, 1995; PRZEWORSKI, 2002; KIM, 2006). In *D. melanogaster*, there is a greater skew towards 5688 rare alleles at putatively neutral sites in regions of low recombination (ANDOLFATTO and PRZEWORSKI, 2001; SHAPIRO *et al.*, 2007), 5690 see left panel of Figure 9.18. However, while this skew isn't expected under simple models of strong background selection, other models of 5692 background selection can lead to such patterns.

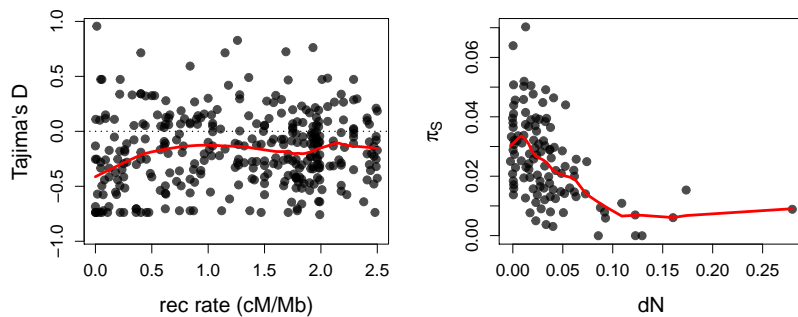


Figure 9.18: **Left)** Average Tajima's D in genomic windows plotted against their recombination rate in *D. melanogaster*. Data from SHAPIRO *et al.* (2007). **Right)** Synonymous pairwise diversity in genomic windows as a function of the density of non-synonymous substitutions in the window. Data from ANDOLFATTO (2007). Code here.

Another prediction of the hitchhiking model, where an allele sweeps 5694 to fixation, is that there should be a functional substitution associated 5696 with each sweep. Or, to flip that around, we might expect to see a greater impact of hitchhiking where there are more functional

5698 substitutions. For example, regions surrounding non-synonymous sub-
 5700 stitutions should have lower levels of diversity, if a high fraction of
 non-synonymous substitutions are adaptive. Again, this pattern is
 seen in *D. melanogaster* (ANDOLFATTO, 2007; MACPHERSON *et al.*,
 2007; SATTATH *et al.*, 2011b), right side of Figure 9.18.

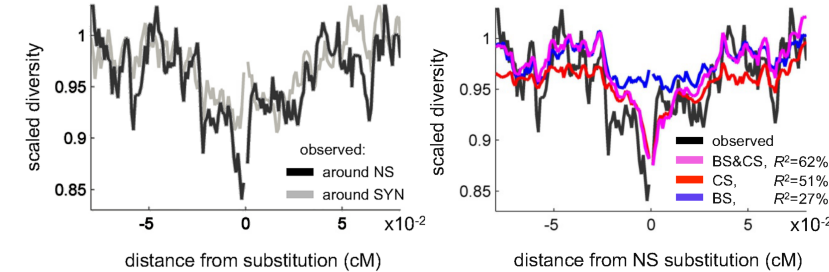


Figure 9.19: **Left)** Scaled synonymous pairwise diversity levels around non-synonymous (NS) and synonymous (SYN) substitutions in *D. melanogaster*. **Right)** Predicted scaled diversity levels around non-synonymous substitutions based on models including background selection (BS), classic sweeps (CS) and both (BS & CS). Figure from ELYASHIV *et al.* (2016), licensed under CC BY 4.0.

5702 Pushing this idea further, we can look at the dip in diversity sur-
 5704 rounding a non-synonymous substitution averaged across all the sub-
 5706 stitutions in the genome. ELYASHIV *et al.* (2016) found a stronger
 5708 dip in diversity around non-synonymous substitutions than synony-
 5710 mous substitutions (see also SATTATH *et al.*, 2011a). Extending the
 5712 model of MCVICKER *et al.* (2009) to fit a model of background se-
 5714 lection and hitchhiking to putative neutral diversity along the genome,
 they found that the dip in diversity around synonymous substi-
 5716 tutions comes mostly from BGS. But to fully explain the dip in diversity
 around non-synonymous substitutions, a reasonable proportion of
 5718 these non-synonymous substitutions have to have been accompanied
 by a classic (hard) sweep. The majority of these sweeps are estimated
 to be due to very weak selection, with selection coefficients $< 10^{-4}$.
 Furthermore, ELYASHIV *et al.* (2016) estimated a 77 - 89% reduc-
 5716 tion in neutral diversity due to selection on linked sites, and concluded
 that no genomic window was entirely free of the effects of selection.
 Thus linked selection has a profound effect in some species such as
Drosophila melanogaster.

Interaction of Multiple Selected Loci

- 5722 Consider two biallelic loci segregating for A/a and B/b . There are four
 5723 haplotypes, AB , Ab , aB , ab , which for simplicity we label 1-4. The
 5724 frequency of our four haplotypes are x_1 , x_2 , x_3 , and x_4 . Each indi-
 5725 vidual has a genotype consisting of two haplotypes; we label w_{ij} the
 5726 fitness of an individual with the genotype made up of haplotype i and
 5727 j (we assume that $w_{ij} = w_{ji}$, i.e. there are no parent of origin effects).
 5728 Assuming that these fitnesses reflect differences due to viability selec-
 5729 tion, and that individuals mate at random, we can write the following
 5730 table of our genotype proportions after selection:

	AB	Ab	aB	ab
AB	$w_{11}x_1^2$	$w_{12}2x_1x_2$	$w_{13}2x_1x_3$	$w_{14}2x_1x_4$
Ab	•	$w_{22}x_2^2$	$w_{23}2x_2x_3$	$w_{24}2x_2x_4$
aB	•	•	$w_{33}x_3^2$	$w_{34}2x_3x_4$
ab	•	•	•	$w_{44}x_4^2$

- 5731 This follows from assuming that our haplotypes are brought together
 5732 at random (HWE), then discounted by their fitnesses. Our mean
 5733 fitness \bar{w} is the sum of all the entries in the table, so dividing by \bar{w}
 5734 normalizes the complete table to sum to one. The frequency of the AB
 5735 haplotype (1) in the next generation of gametes is

$$x'_1 = \frac{(w_{11}x_1^2 + \frac{1}{2}w_{12}2x_1x_2 + \frac{1}{2}w_{13}2x_1x_3 + \frac{1}{2}(1-r)w_{14}2x_1x_4 + \frac{1}{2}rw_{23}2x_2x_3)}{\bar{w}} \quad (10.1)$$

- 5736 This is a bit of a mouthful, but each of the terms is easy to under-
 5737 stand. Each of the HWE genotype frequencies (e.g. $2x_1x_2$) is weighted
 5738 by its fitness relative to the mean fitness (w_{ij}/\bar{w}), and by its proba-
 5739 bility of transmitting the AB haplotype to the next generation. For
 5740 example, AB/Ab individuals (1/2) transmit the AB haplotype only
 5741 half the time. The final two terms include the recombination fraction
 5742 (r). The first term involving recombination refers to the AB/ab geno-
 5743 type (1/4), who with probability $(1-r)/2$ transmits a non-recombinant
 5744 AB haplotype to the gamete. Similarly, the second term refers to the

5746 Ab/aB genotype; a proportion $r/2$ of its gametes carry the recombinant AB haplotype.

5748 In the single locus case, we defined the marginal fitness of an allele. Here it will help us to define the marginal fitness of the i^{th} haplotype:

$$\bar{w}_i = \sum_{j=1}^4 w_{ij} x_j \quad (10.2)$$

5750 This is the fitness of the i^{th} haplotype averaged over all of the *diploid* genotypes it could occur in, weighted by their probability under random mating. Using this notation, and with some rearrangement of equation (10.1), we obtain

$$x'_1 = \frac{x_1 \bar{w}_1 - w_{14} r D}{\bar{w}} \quad (10.3)$$

5754 Here we have assumed that $w_{23} = w_{14}$, i.e. that the fitness of AB/ab individuals is the same as Ab/aB individuals (i.e. that fitness depends only on the alleles carried by an individual, and not on which chromosome they are carried; this assumption is sometimes called no 5756 *cis*-epistasis).

5758 We can then write the change in the frequency of our 1 haplotype as

$$\Delta x_1 = \frac{x_1 (\bar{w}_1 - \bar{w}) - r w_{14} D}{\bar{w}} \quad (10.4)$$

5760 Generalizing this result, we write the change in *any haplotype i from* our set of four haplotypes as

$$\Delta x_i = \frac{x_i (\bar{w}_i - \bar{w}) \pm r w_{14} D}{\bar{w}} \quad (10.5)$$

5764 where the coupling haplotypes 1 and 4 use $+D$ and repulsion haplotypes 2 and 3 use $-D$. Note that the sum of these four Δx_i is zero, as our haplotype frequencies sum to one.

5766 So the change in the frequency of a haplotype (e.g. AB, haplotype 1) is determined by the interplay of two factors: First, the extent 5768 to which the marginal fitness of our haplotype is higher (or lower) than the mean fitness of the population (the magnitude and sign of 5770 $(\bar{w}_1 - \bar{w})/\bar{w}$). Second, whether there is a deficit or any excess of our 5772 haplotype compared to linkage equilibrium (the magnitude and sign of D), modified by the strength of recombination. This tension between selection promoting particular haplotypic combinations, and recombination breaking up overly common haplotypes is the key to a lot of 5774 interesting dynamics and evolutionary processes.

5776 10.1 Types of interaction between selection and recombination

To illustrate these ideas we make use of Muller diagrams (MULLER, 5778 1932), where we visualize the allele dynamics in terms of a plot of the stack frequencies over time.

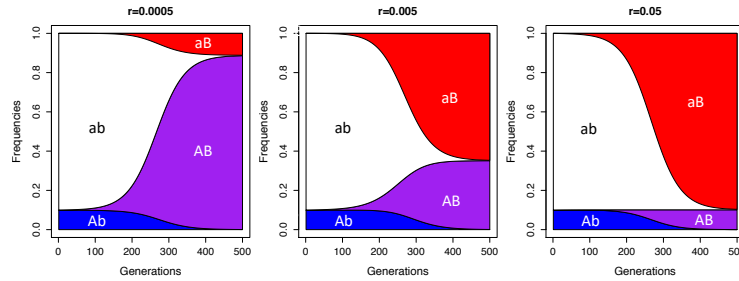


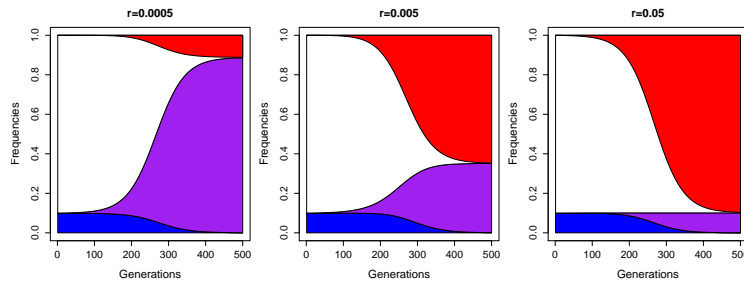
Figure 10.1: A beneficial mutation B arises on the background of a neutral allele whose initial frequency is $p_A = 10\%$. The beneficial allele has a strong, additive selection coefficient of $hs = 0.05$.

5780 *The hitchhiking of deleterious alleles* Let's start by revisiting our
 5781 neutral hitchhiking in this two locus setting in the previous chapter
 5782 we saw that neutral alleles can hitchhike along with our selected allele
 5783 if they are tightly linked enough. Figure 10.1 shows the frequency
 5784 trajectories of the various haplotypes for neutral allele (A) that is
 5785 present at 10% frequency in the population when our beneficial allele
 5786 (B) arises on its background. When the recombination rate (r) is low
 5787 between the loci, A gets to hitchhike to high frequency, but for higher
 5788 recombination rates it only gets dragged to intermediate frequencies.
 5789 For the highest recombination rate shown ($r \approx s$) the neutral allele's
 5790 dynamics ($p_{Ab} + p_{AB}$) are barely changed at all, as it recombines
 5791 on and off the sweeping allele frequently and so barely perceives the
 5792 sweep.

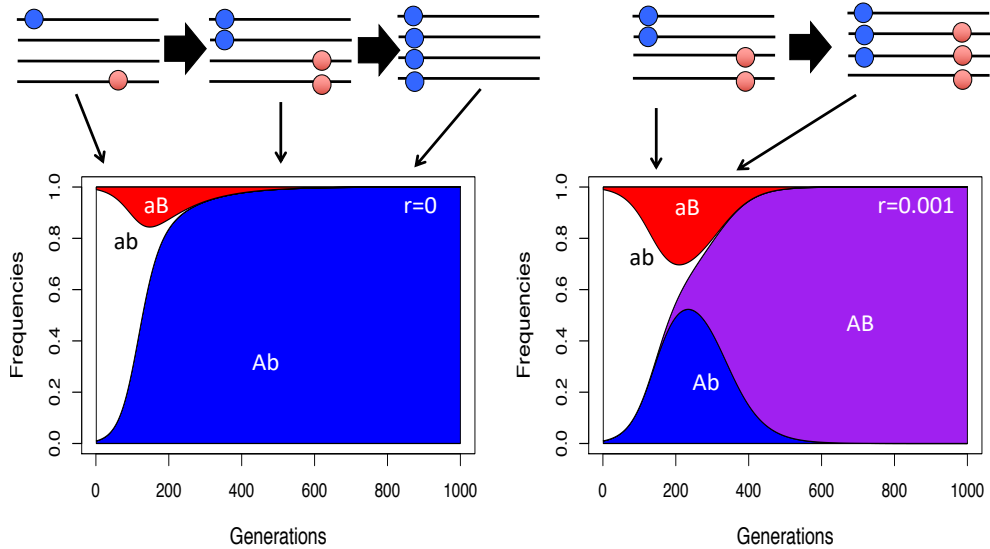
5793 *The hitchhiking of deleterious alleles* Deleterious alleles can also
 5794 hitchhike along with beneficial mutations if they are not too deleterious
 5795 compared to the benefits offered by the selected allele. Again our allele
 5796 A is at 10% frequency in the population in Figure ??, but this time it
 5797 is deleterious and so initially decreasing in frequency across the gener-
 5798 ations when the beneficial mutation (B) arises on its background. If
 5799 the loci are tightly linked, and A were too deleterious, B would never
 5800 get to take off in the population. However, if the benefits of B out-
 5801 weighs the cost of A , even in the case of no recombination between our
 5802 loci, allele A gets to hitchhike to fixation and merely slows down B 's
 5803 rate of increase and their combined fitness is reduced. With moderate
 5804 amounts of recombination between the loci, our deleterious starts to
 5805 hitchhike but before it can get to fixation the beneficial allele man-
 5806 ages to recombine off its background. This recombinant aB haplotype,
 5807 which has higher fitness as it lacks the deleterious allele, now sweeps
 5808 through the population displacing the AB haplotype. For higher re-
 5809 combination events we have to wait less long for a recombination to
 5810 breakup the hitchhiking deleterious allele, so the adaptive allele easily
 5811 escapes its background. For the purposes of illustration here we've
 5812 used a relatively common deleterious allele, but in reality these alleles

will likely be often be rare in the population and at mutation selection balance. If they are rare it is likely that a beneficial mutation arises on a specific deleterious allele's background, but as we have seen there 5814 are likely going to be many rare deleterious alleles in the population so it is likely that a beneficial mutations may often have to contend with deleterious hitchhikers.

5816



5818



Clonal interference between favourable alleles. When rates of sex 5820 and recombination are zero, or very low, positively selected alleles can prevent each other reach fixation and so the rate of adaptation can be slowed. In the absence of sex and recombination, when two positively selected alleles arise on different genetic backgrounds in the 5822 population they cannot both fix (left side of Figure 10.2). They can initially increase in frequency, but necessarily compete with each 5824 other when they become common. This is called selective interference, or sometime clonal interference. If one of the alleles has a much larger 5826

Figure 10.2: Interference between two positively selected alleles. **Left)** the red and blue (A and B) beneficial alleles arise on different haplotypes. They rise in frequency, but in the absence of recombination only one can fix. This is shown in a Muller diagram, where p_{AB} is initially set to zero. **Right)** In the presence of recombination the population can generate the recombinant (AB) haplotype, which can subsequently fix.

selection coefficient it will fix, forcing the other allele from the population, but when they are relatively equally matched it may take some time for this situation to resolve itself resulting in a traffic jam in the population. Thus in an asexual adaptive alleles necessarily have to fix sequentially. However, with even a small amount of recombination beneficial alleles can recombine on to each others background, allowing them to fix in parallel (right side of Figure 10.2).

Given the rapid evolution of HIV we can see interference taking place over very short time periods indeed. HIV uses its reverse transcriptase (RT) gene to write itself from an RNA virus into its host's DNA, allowing HIV to hijack the hosts regulatory machinery, a critical part of its life cycle. One of the early HIV drugs was Efavirenz, which inhibits HIV's RT protein. Sadly, mutations are common in the RT HIV gene, and these mutations, in the presence of the drug, confer a profound fitness advantage, allowing them to spread through the HIV population in patients undergoing anti-HIV treatment. In Figure 10.3 we see that by day 224 after the start of drug treatment two different drug-resistance amino-acid changes beginning to spread within a patient (also shown as a Muller diagram in Figure 10.4). Because these alleles occur on different genetic backgrounds, with little chance for genetic exchange between them, they interfere in each other progress as they compete to fix within the population. Eventually the amino acid change at site 188 wins out.

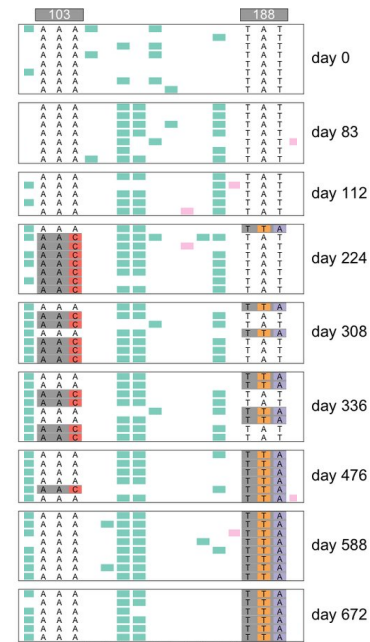


Figure 10.3: HIV sequences from a patient over the course of drug treatment in the retrotransposase coding region. Figure cropped from WILLIAMS and PENNINGS (2019), licensed under CC BY 4.0.

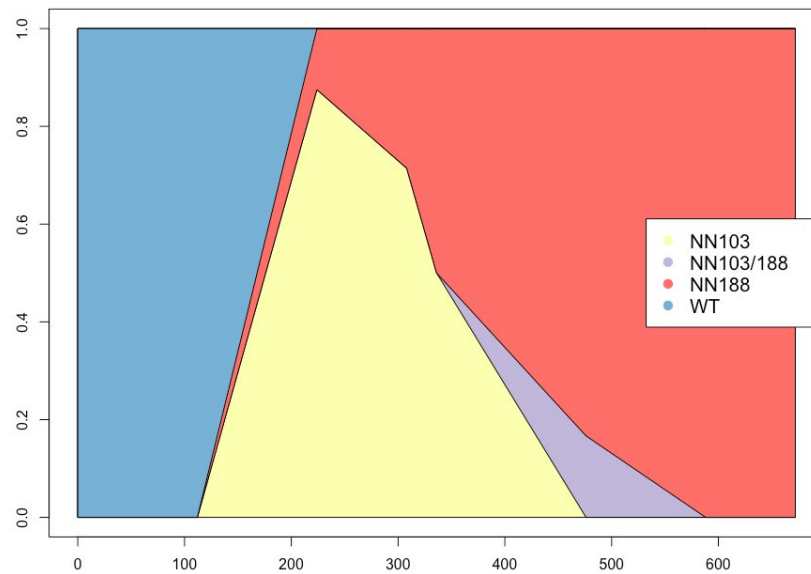


Figure 10.4: Muller plot of the drug resistance interference dynamics from Figure 10.3. Figure from WILLIAMS and PENNINGS (2019), licensed under CC BY 4.0.

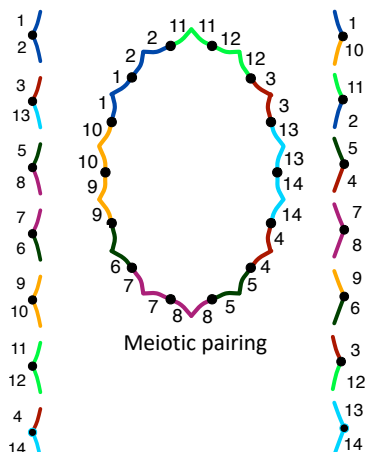


Figure 10.5: A schematic diagram of the karyotype of an evening primrose. The two columns show a heterozygote individual's diploid chromosomal complement. Each chromosome is heterozygote for two different translocations. For example both the top-most chromosomes has one arm from chromosome 1, but the other arm is heterozygote for a large translocation from the ancestral chromosome 2 and 10. Due to these translocations the meiotic pairing form a complete ring of chromosomes.

An example of the costs of asexuality. In the Evening primrose genus (*Oenothera*), there are a number of young, independently-derived, asexual species. In each species this asexuality is due to a complicated series of reciprocal translocations which prevent recombination and segregation and ensure that every plant is permanently-heterozygote for these rearrangements due to lethality. This system is quite complicated, and super cool. We don't need to worry about the details but importantly each species is functionally asexual. HOLLISTER *et al.* (2014) sampled transcriptome data from across the Evening primrose clade, and took advantage of 7 independent, asexual-sexual sister pairs of species to examine the impact of the evolution of asexuality for molecular evolution.

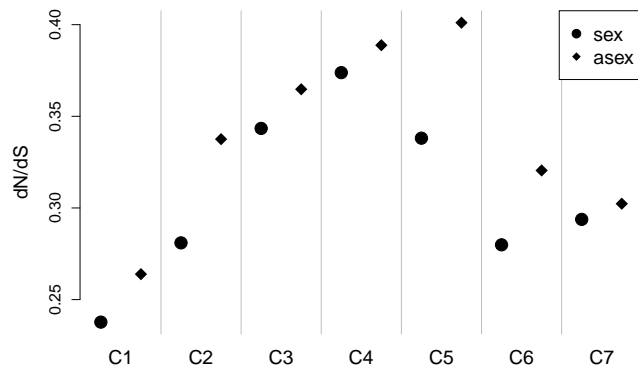


Figure 10.6: d_N/d_S calculated on sexual (circles) and asexual (diamonds)



Figure 10.7: Showy evening primrose (*Oenothera speciosa*), the sexual species in the clade C2 from Figure 10.6.

Favourite flowers of garden and greenhouse (1896). Step, E. Image from the Biodiversity Heritage Library. Contributed by Missouri Botanical Garden. Licensed under CC BY-2.0.

The d_N/d_S for the sexual and asexual species for each of the seven pairs (C1-C7) is shown in Figure 10.6. In every pair d_N/d_S is higher in the asexual species. The genomes of the asexual species are evolving in a less constrained fashion, likely due to weakly deleterious mutations accumulating due to hitchhiking with beneficial alleles and the slow crank of Muller's ratchet.

The maintainance of combinations of alleles in the face of recombination. In some cases balancing selection may be attempting to maintain multiple combinations of alleles in the population that work well together. However, recombination may be constantly ripping those alleles away from each other making it difficult to maintain these alleles. This can select for the suppression of recombination. Some of the most dramatic demonstrations of this tension involve the evolution of so-called super genes. We'll first consider the evolution of a mimicry supergene in *Heliconius numata* as an example of this.

Some of the most spectacular examples of Müllerian mimicry in

the world are found in *Heliconius* butterflies. These butterflies are
 5880 unpalatable to predators, and different species mimic each other so
 benefiting from not being eaten by predators, which rapidly learn to
 5882 avoid all these species). In many of these species multiple mimicry
 morphs are found as we move across geographic space. In *Heliconius*
 5884 *numata* a number of different morphs mimic morphs from a distantly
 related *Melinaea* species.

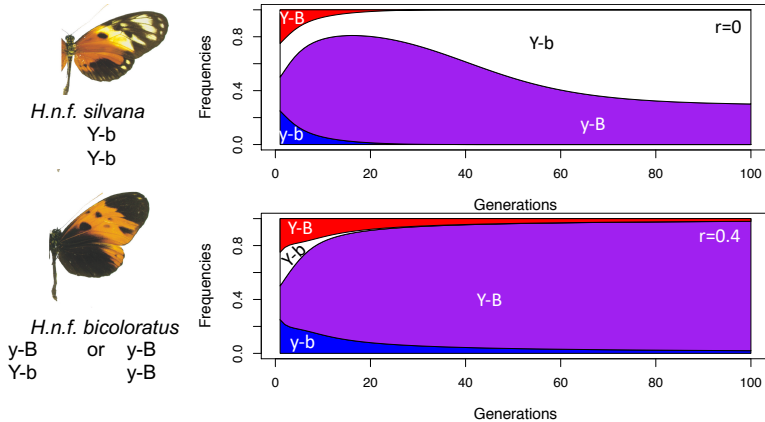


Figure 10.8: Five sympatric forms of *H. numata* from northern Peru, and their distantly related mimetic *Melinaea* species. First row: *M. menophilus* ssp. nov., *M. ludovica ludovica*, *M. marsaeus rileyi*, *M. marsaeus mothone*, and *M. marsaeus phasiana*. Second row, *H. n. f. tarapotensis*, *H. n. f. silvana*, *H. n. f. aurora*, *H. n. f. bicoloratus*, and *H. n. f. arcuella*. Figure and caption from JORON et al. (2006) cropped, licensed under CC BY 4.0.

5886 To keep things relatively simple lets focus on two differences between *silvana* and *bicoloratus*, the yellow stripe on the top wing of
 5888 *silvana* and the black bottom wing of *bicoloratus*. Lets imagine that
 5890 these two differences are due to a simple two locus system. The first
 5892 locus segregates for Y/y, where the Y allele encodes for a top-wing
 yellow band, and y encodes for the absence of the yellow band. The
 5894 second locus segregates for B/b where B encodes for the bottom-wing
 being black, and b for the absence of black on the bottom wing. If Y
 5896 is recessive and B is dominant, then the *silvana* phenotype corresponds
 to a YY bb genotype. Due to the dominance of the y and B alleles the
 5898 *bicoloratus* phenotype can be achieved by various genotypes (Yy Bb,
 yy BB, Yy BB, yy Bb). Both of these phenotypes offer an advantage
 5900 as they mimic a *M. menophilus* model. But there are also genotypes
 that don't do as well; YY BB individuals have a yellow band and a
 5902 black bottom and so don't do a great job mimicing anything and so
 will be eaten. Thinking about the four possible haplotypes, y-B has
 5904 high marginal fitness as due to its combo of dominant alleles it'll always
 produce a *bicoloratus* phenotype. Likewise the Y-b haplotype
 5906 has high marginal fitness, as it does well in the homozygous state (*silvana* phenotype), and when it is paired with the y-B allele. However,
 5908 the Y-B and y-b haplotypes fair less well as they carry two alleles that
 don't work well with each other and so are often individuals who suffer
 high rates of predation.

If no recombination occurs between these loci ($r = 0$, Figure 10.9),

Figure 10.9:



5910 then the Y-B and y-b are selected out of the population, and the y-B
 5911 and Y-b can be stably maintained. However, when there's too
 5912 much recombination between our loci (e.g. $r = 0.4$, Figure 10.9) the
 5913 high-fitness haplotypes keep getting ripped apart by recombination
 5914 and the Y-b is lost from the population as it's recessive advantage is
 5915 lost as it's too often being broken up by recombination in heterozy-
 5916 gotes.

5918 *Supergenes to the rescue!* So our polymorphisms can only be main-
 5919 tained if they are tightly linked, i.e. if these alleles arose at loci that are
 5920 genetically close to each other. But how is it possible that these alleles
 5921 arose close to each other? Well the trick is that they don't necessarily
 5922 have to arise very close to each other. If such a system is polymor-
 5923 phic but being regularly broken up by recombination, a chromosomal
 5924 inversion—the flipping around of a whole section of chromosome—can
 5925 arise and will suppress recombination. Imagine that our two loci are
 5926 far apart genetically, and a chromosomal inversion arises on the Y-b
 5927 background forming the b-Y haplotype. This inverted haplotype will
 5928 not recombine with the y-B haplotype when it is present in a het-
 5929 erozygote, thus it is not broken down by recombination. This inverted
 5930 haplotype, which enjoys the fitness benefits of the Y-b, can therefore
 5931 replace the Y-b haplotype in the population. The two other low fitness
 5932 haplotypes will disappear as they are no longer being generated by re-
 combination, leaving just the y-B and b-Y. The polymorphism system

“coadapted combinations
 of several or many genes
 locked in inverted sections of
 chromosomes and therefore
 inherited as single units.”
 DOBZHANSKY (1970) on
 supergenes.

now behaves like alleles at a single locus, a super gene (e.g. like $r = 0$ in Figure 10.9).

Now the *H. numata* system is vastly more complicated than our toy two locus system, presumably involving many changes and refinements, but the same principle holds (JORON *et al.*, 2011). The differences between the different *H. numata* mimmy morphs is found on a single chromosome, and the inheritance behaves as if controlled by a single locus (albeit with many alleles). The *H. n. f. silvana* individuals carry a recessive haplotype of alleles that which is known to be locked together by a $\sim 400\text{kb}$ inversion, that is a different chromosomal orientation from the *bicoloratus* allele (haplotype) which acts as a dominant allele. Other alleles at this same chromosomal region provide the genetic basis of the other morphs, and sometimes correspond to further inversions with a range of dominance relationships.

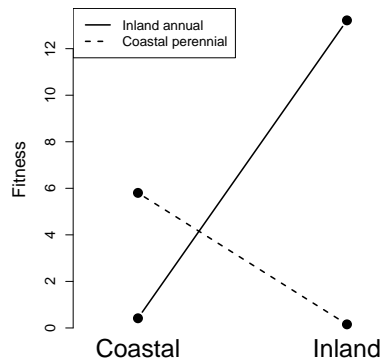


Figure 10.10: **Left**) A coastal perennial and an Inland annuals *Mimulus guttatus* LOWRY and WILLIS (2010), image from LOWRY and WILLIS (2010) licensed under CC BY 4.0.

Right) A reciprocal transplant experiment showing that coastal perennial and an Inland annuals are locally adapted to their respective habitats. Data from LOWRY and WILLIS (2010), Code here..

Local Adaptation, Speciation, and Inversions. Inversions have long been thought to play an important role in local adaptation and speciation. One example of an inversion underlying local adaptation occurs in *Mimulus guttatus*, in Western North America, where there are annual and perennial ecomorphs. The perennial form grows in many places along the Pacific coast, and in other places with year around moisture; it invests a lot of resources in achieving large size and laying down resources for the next year, and as a result flowers late. The annual form grows inland, e.g. the California central valley, where it has to invest all its effort in flowering rapidly before the long, hot, dry summer. Neither ecomorph does well in the other's environment. The perennials get crisped before they have a chance to flower, while the annuals suffer from high rates of herbivory and cannot tolerate the salt spray. LOWRY and WILLIS (2010) found that large inversion controled a lot of of the phenotypic variation in flowering time and a range of other morphological differences between these two morphs.

They also showed that the inversion controlled a reasonable proportion
 5964 of the differences in fitness in the field, consistent with it underlying
 the fitness tradeoffs involved in local adaptation.

5966 Why would an inversion be involved in locking together local
 adapted alleles? The basic idea, like above, is an inversion can be
 5968 selected for we have two (or more) loci segregating for locally adapted
 alleles. Locally advantageous haplotypes are in danger of being broken
 5970 up by recombination with maladapted haplotypes, which are con-
 stantly being introduced into each population by migration from the
 5972 other. If an inversion arises that locks these alleles together in one
 population, it can be selected for as does not suffer the ill effects from
 5974 recombination with migrating maladaptive haplotype.

10.1.1 Sex Chromosomes and the dynamics of selection and recom- 5976 bination.

The production of different sized gametes (anisogamy) has arisen a
 5978 number of times in multi-cellular life, with male and female gametes
 are defined by their relative sizes. The smaller, and often more mobile,
 5980 gametes are defined male gametes (e.g. sperm), while the larger, well
 provisioned, and often less mobile are defined as female gametes (e.g.
 5982 egg cell). The evolution of anisogamy is thought to be due to disruptive
 selection due to a tradeoff pulling in opposite directions towards
 5984 mobile gametes able to move further and in the opposite direction
 towards better provisioned gametes better able to build larger zygotes.
 5986 In many organisms individuals can produce both male and female ga-
 metes, while some species have evolved separate sexes, likely in part
 5988 as an inbreeding avoidance mechanism. There is huge diversity in sex
 determination mechanisms across the eukaryotic tree (Figure 10.13).

5990 This is all to say, that biology is wonderfully complicated.

In mammals, and many other systems with genetic sex determi-
 5992 nation, the genes responsible for sex determination lie on a pair of
 heteromorphic sex chromosomes, i.e. pair of chromosomes that are
 5994 quite different in size. In mammals it is the male determining Y chro-
 mosome that has a very small gene content compared to the X chro-
 5996 mosome (Figure 10.14). But in other groups such as birds, and some
 snakes, females carry a gene poor W with males being the homoga-
 5998 metic sex, carrying two Zs. If you are still reading send Graham a
 picture of Nettie Stevens, she discovered sex chromosomes in 1905
 6000 (STEVENS, 1905). These examples of heteromorphic sex chromo-
 somes, and many others like them, are thought to have arisen from an
 6002 ancestral pair of autosomes? What then explains their evolution?

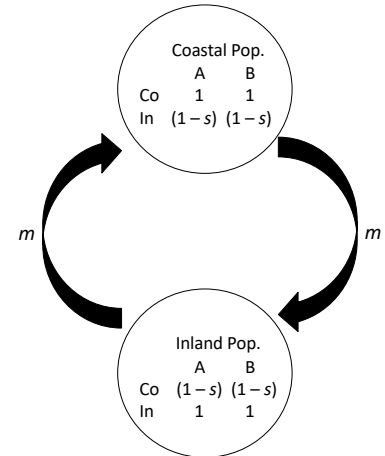


Figure 10.11: A two locus, two population migration-selection balance system. Two loci A and B segregate for an Inland and Coastal adapted alleles.

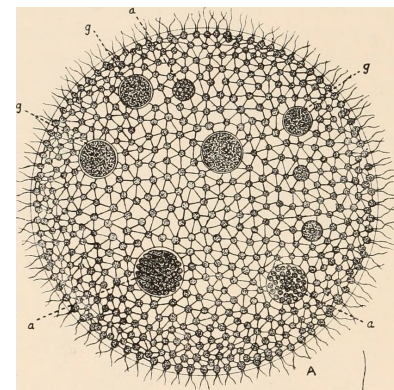


Figure 10.12: *Volvox aureus*, Volvox are spherical, multicellular green algae. The surface is made up of a single layer of somatic cells (up to 50k cells) beating their flagella. Some species of Volvox have male and female gametes, being made in the germ cells (a and g respectively) in the middle of the sphere. Some Volvox have separate sexes, where different individuals produce male and female gametes.

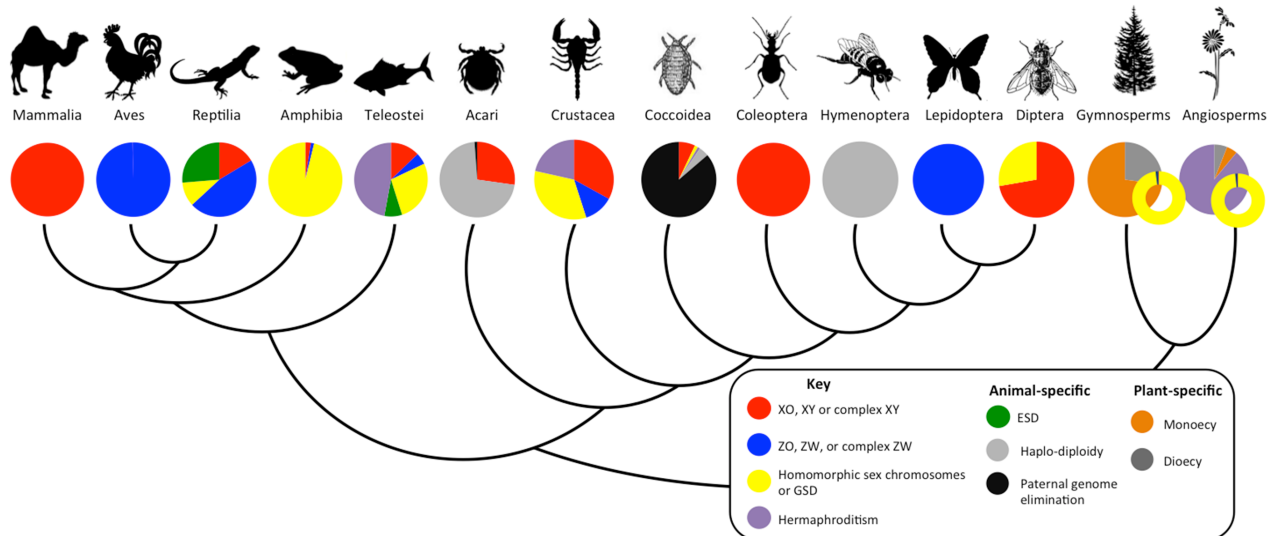


Figure 10.13: Diversity of sex determination systems for representative plant and animal clades. Figure

A broad explanation for the evolution of sex chromosome goes as follows:

In lake Malawi there are many very closely related cichlids species. In many of these species the males are brightly coloured to attract females, while the females are often brown to help them avoid predators. In some of these species there is an alternative orange morph, called the marmalade cat morph, which are cryptic against the rocky bottom of the lake. This morph is due to a dominant (?) mutation called OB at the *pax7* (?), and the allele appears to be shared across many of these species. This OB allele works well in females, however, in the males the OB allele disrupts their bright colouration. Thus the OB polymorphism is sexually antagonistic, i.e. it works well in females and poorly in males.

Males carrying the male-deleterious OB allele are rarely found, despite the allele being common in females. Why is that? Well because the OB allele is tightly linked to a newly emerged female-determining allele (W), with males carrying two copies of the Z allele. Males usually are homozygous for the ob-Z haplotype, while females can be either orange (OB-W/ob-Z) or brown (ob-W/ob-Z). Recombination between these two loci seems to be very rare, and so the sexually antagonistic allele OB appears to be mainly female specific. An inversion on the Z background would lock together the

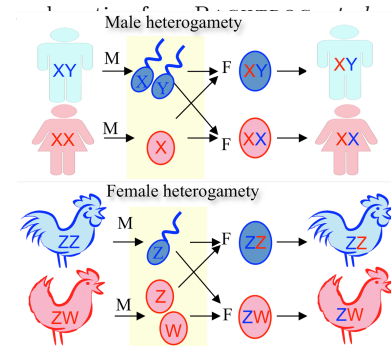


Figure 10.14: Figure from BACHTROG et al. (2014), licensed under CC BY 4.0cropped from original.



Figure 10.15:

Image credits: Blue mbuna Male *L. fuelleborni* by Chmee2; OB Male *L. fuelleborni* by Dorenko; Brown ob *Tropheops* female by Alexandra Tyers; Female *L. fuelleborni* orange morph, by Mikko Stenberg

6026 *Bibliography*

- 6028 AGUADÉ, M., N. MIYASHITA, and C. H. LANGLEY, 1989 Reduced variation in the yellow-achaete-scute region in natural populations of *Drosophila melanogaster*. *Genetics* **122**: 607–615.
- 6030 AGUILLO, S. M., J. W. FITZPATRICK, R. BOWMAN, S. J. SCHOECH, A. G. CLARK, G. COOP, and N. CHEN, 2017, 08) Deconstructing isolation-by-distance: The genomic consequences of limited dispersal. *PLOS Genetics* **13**(8): 1–27.
- 6034 AKÇAY, E. and J. VAN CLEVE, 2016 There is no fitness but fitness, and the lineage is its bearer. *Phil. Trans. R. Soc. B* **371**(1687): 6036 20150085.
- 6038 ALCAIDE, M., E. S. SCORDATO, T. D. PRICE, and D. E. IRWIN, 2014 Genomic divergence in a ring species complex. *Nature* **511**(7507): 83.
- 6040 ALEXANDER, D. H., J. NOVEMBRE, and K. LANGE, 2009 Fast model-based estimation of ancestry in unrelated individuals. 6042 *Genome research* **19**(9): 1655–1664.
- 6044 ALGEE-HEWITT, B. F., M. D. EDGE, J. KIM, J. Z. LI, and N. A. ROSENBERG, 2016 Individual identifiability predicts population identifiability in forensic microsatellite markers. *Current Biology* **26**(7): 935–942.
- 6048 ALLENDORF, F. W. and J. J. HARD, 2009 Human-induced evolution caused by unnatural selection through harvest of wild animals. *Proceedings of the National Academy of Sciences* **106**(Supplement 1): 9987–9994.
- 6052 ALVAREZ, G., F. C. CEBALLOS, and C. QUINTEIRO, 2009 The role of inbreeding in the extinction of a European royal dynasty. *PLoS One* **4**(4): e5174.

- 6054 ANDOLFATTO, P., 2007 Hitchhiking effects of recurrent beneficial
amino acid substitutions in the *Drosophila melanogaster* genome.
6056 *Genome Res.* **17**: 1755–1762.
- 6058 ANDOLFATTO, P. and M. PRZEWORSKI, 2001 Regions of lower
crossing over harbor more rare variants in African populations of
Drosophila melanogaster. *Genetics* **158**: 657–665.
- 6060 AYLLON, F., E. KJÆRNER-SEMB, T. FURMANEK, V. WEN-
NEVIK, M. F. SOLBERG, G. DAHLE, G. L. TARANGER,
6062 K. A. GLOVER, M. S. ALMÉN, C. J. RUBIN, and OTHERS,
2015 The vgl3 locus controls age at maturity in wild and domesti-
6064 cated Atlantic salmon (*Salmo salar* L.) males. *PLoS genetics* **11**(11):
e1005628.
- 6066 BACHTROG, D., J. E. MANK, C. L. PEICHEL, M. KIRK-
PATRICK, S. P. OTTO, T.-L. ASHMAN, M. W. HAHN,
6068 J. KITANO, I. MAYROSE, R. MING, and OTHERS, 2014 Sex
determination: why so many ways of doing it? *PLoS biology* **12**(7):
6070 e1001899.
- 6072 BARRETT, R. D. H., S. M. ROGERS, and D. SCHLUTER,
2008 Natural Selection on a Major Armor Gene in Threespine
Stickleback. *Science* **322**(5899): 255–257.
- 6074 BARSON, N. J., T. AYKANAT, K. HINDAR, M. BARANSKI,
G. H. BOLSTAD, P. FISKE, C. JACQ, A. J. JENSEN, S. E.
6076 JOHNSTON, S. KARLSSON, and OTHERS, 2015 Sex-dependent
dominance at a single locus maintains variation in age at maturity
6078 in salmon. *Nature* **528**(7582): 405.
- 6080 BARTON, N. and G. HEWITT, 1981 A chromosomal cline in the
grasshopper *Podisma pedestris*. *Evolution*: 1008–1018.
- 6082 BARTON, N. H., 2000 Genetic hitchhiking. *Philos. Trans. R. Soc.
Lond., B, Biol. Sci.* **355**: 1553–1562.
- 6084 BASOLO, A. L., 1994 The dynamics of Fisherian sex-ratio evolu-
tion: theoretical and experimental investigations. *The American
Naturalist* **144**(3): 473–490.
- 6086 BAZYKIN, A., 1969 Hypothetical mechanism of speciation. *Evolu-
tion* **23**(4): 685–687.
- 6088 BECQUET, C., N. PATTERSON, A. C. STONE, M. PRZE-
WORSKI, and D. REICH, 2007 Genetic structure of chimpanzee
6090 populations. *PLoS genetics* **3**(4): e66.

- BEGUN, D. J. and C. F. AQUADRO, 1992 Levels of naturally occurring DNA polymorphism correlate with recombination rates in *D. melanogaster*. *Nature* **356**: 519–520.
- BEISSINGER, T. M., L. WANG, K. CROSBY, A. DURVA-SULA, M. B. HUFFORD, and J. ROSS-IBARRA, 2016 Recent demography drives changes in linked selection across the maize genome. *Nature plants* **2**(7): 16084.
- BELL, M. A., M. P. TRAVIS, and D. M. BLOUW, 2006 Inferring natural selection in a fossil threespine stickleback. *Paleobiology* **32**(4): 562–577.
- Box, G. E., 1979 Robustness in the strategy of scientific model building. In *Robustness in statistics*, pp. 201–236. Elsevier.
- BRADBURY, G. S., P. L. RALPH, and G. M. COOP, 2016 A spatial framework for understanding population structure and admixture. *PLoS genetics* **12**(1): e1005703.
- BRANDVAIN, Y., A. M. KENNEY, L. FLAGEL, G. COOP, and A. L. SWEIGART, 2014 Speciation and introgression between *Mimulus nasutus* and *Mimulus guttatus*. *PLoS Genetics* **10**(6): e1004410.
- BRAVERMAN, J. M., R. R. HUDSON, N. L. KAPLAN, C. H. LANGLEY, and W. STEPHAN, 1995 The hitchhiking effect on the site frequency spectrum of DNA polymorphisms. *Genetics* **140**: 783–796.
- BRODIE III, E. D., 1992 Correlational selection for color pattern and antipredator behavior in the garter snake *Thamnophis ordinoides*. *Evolution* **46**(5): 1284–1298.
- CAI, J. J., J. M. MACPHERSON, G. SELLA, and D. A. PETROV, 2009 Pervasive hitchhiking at coding and regulatory sites in humans. *PLoS Genet.* **5**: e1000336.
- CASSA, C. A., D. WEGHORN, D. J. BALICK, D. M. JORDAN, D. NUSINOW, K. E. SAMOCHA, A. O'DONNELL-LURIA, D. G. MACARTHUR, M. J. DALY, D. R. BEIER, and OTHERS, 2017 Estimating the selective effects of heterozygous protein-truncating variants from human exome data. *Nature genetics* **49**(5): 806.
- CHARLESWORTH, B., 2009 Effective population size and patterns of molecular evolution and variation. *Nature Reviews Genetics* **10**(3): 195.

- CHARLESWORTH, D., B. CHARLESWORTH, and M. T. MOR-
6130 GAN, 1995 The pattern of neutral molecular variation under the
background selection model. *Genetics* **141**: 1619–1632.
- CHARLESWORTH, D. and V. LAPORTE, 1998 The male-sterility
polymorphism of *Silene vulgaris*: analysis of genetic data from two
6134 populations and comparison with *Thymus vulgaris*. *Genetics* **150**(3):
1267–1282.
- 6136 CHEN, N., E. J. COSGROVE, R. BOWMAN, J. W. FITZ-
PATRICK, and A. G. CLARK, 2016 Genomic Consequences of
6138 Population Decline in the Endangered Florida Scrub-Jay. *Current
Biology* **26**(21): 2974 – 2979.
- 6140 COHEN, D., 1966 Optimizing reproduction in a randomly varying
environment. *Journal of theoretical biology* **12**(1): 119–129.
- 6142 COOK, L. M., B. S. GRANT, I. J. SACCHERI, and J. MAL-
LET, 2012 Selective bird predation on the peppered moth: the last
6144 experiment of Michael Majerus. *Biology Letters* **8**(4): 609–612.
- COTTERMAN, C. W., 1940 A calculus for statistico-genetics. Ph.
6146 D. thesis, The Ohio State University.
- COUSMINER, D. L., D. J. BERRY, N. J. TIMPSON, W. ANG,
6148 E. THIERING, E. M. BYRNE, H. R. TAAL, V. HUIKARI,
J. P. BRADFIELD, M. KERKHOF, and OTHERS, 2013
6150 Genome-wide association and longitudinal analyses reveal genetic
loci linking pubertal height growth, pubertal timing and childhood
6152 adiposity. *Human molecular genetics* **22**(13): 2735–2747.
- CUTTER, A. D. and J. Y. CHOI, 2010 Natural selection shapes
6154 nucleotide polymorphism across the genome of the nematode
Caenorhabditis briggsae. *Genome Res.* **20**: 1103–1111.
- 6156 DARWIN, C., 1859 *On the Origin of Species by Means of Natural
Selection*. London: Murray. or the Preservation of Favored Races in
6158 the Struggle for Life.
- DARWIN, C., 1876 The effect of cross and self fertilization in the
6160 vegetable kingdom: Murray. London, UK.
- 6162 DARWIN, C., 1888 *The descent of man and selection in relation to
sex*, Volume 1. Murray.
- DEMPSTER, E., 1955 Maintenance of genetic heterogeneity. *Cold
6164 Spring Harb Symp Quant Biol* **20**: 25–32.

- 6166 DICKERSON, R. E., 1971 The structure of cytochrome c and the
rates of molecular evolution. *Journal of Molecular Evolution* 1(1):
26–45.
- 6168 DOBZHANSKY, T., 1943 Genetics of natural populations IX. Tem-
poral changes in the composition of populations of *Drosophila pseu-*
6170 *doobscura*. *Genetics* 28(2): 162.
- 6172 DOBZHANSKY, T., 1951 *Genetics and the Origin of Species* (3rd
Ed. ed.), pp. 16.
- 6174 DOBZHANSKY, T., 1970 *Genetics of the evolutionary process*, Vol-
ume 139. Columbia University Press.
- 6176 EDWARDS, A., 1961 The population genetics of “sex-ratio” in
Drosophila pseudoobscura. *Heredity* 16(3): 291.
- 6178 EDWARDS, A. W., 1998 Natural selection and the sex ratio:
Fisher’s sources. *The American Naturalist* 151(6): 564–569.
- 6180 ELTON, C., 1942 *Voles, mice and lemmings. Problems in population
dynamics*. Oxford: Clarendon Press.
- 6182 ELYASHIV, E., S. SATTATH, T. T. HU, A. STRUTSOVSKY,
G. MCVICKER, P. ANDOLFATTO, G. COOP, and G. SELLA,
2016 A genomic map of the effects of linked selection in *Drosophila*.
6184 *PLoS genetics* 12(8): e1006130.
- 6186 EWENS, W. J., 2010 What is the gene trying to do? *British Jour-
nal for the Philosophy of Science* 62(1): 155–176.
- 6188 EWENS, W. J., 2016 Motoo Kimura and James Crow on the In-
finitely Many Alleles Model. *Genetics* 202(4): 1243–1245.
- 6190 FAY, J. C. and C. I. WU, 2000 Hitchhiking under positive Dar-
winian selection. *Genetics* 155: 1405–1413.
- 6192 FEDER, A. F., C. KLINE, P. POLACINO, M. COTTRELL,
A. D. KASHUBA, B. F. KEELE, S.-L. HU, D. A. PETROV,
6194 P. S. PENNINGS, and Z. AMBROSE, 2017 A spatio-temporal
assessment of simian/human immunodeficiency virus (SHIV) evo-
lution reveals a highly dynamic process within the host. *PLoS
pathogens* 13(5): e1006358.
- 6198 FERREE, P. M. and D. A. BARBASH, 2007 Distorted sex ratios:
a window into RNAi-mediated silencing. *PLoS biology* 5(11): e303.
- 6200 FISHER, R. A., 1915 The evolution of sexual preference. *The
Eugenics Review* 7(3): 184.

- FISHER, R. A., 1923 XXI.—on the dominance ratio. Proceedings of
6202 the royal society of Edinburgh **42**: 321–341.
- FISHER, R. A., 1930 *The genetical theory of natural selection: a
6204 complete variorum edition*. Oxford University Press.
- FRANCIOLI, L. C., A. MENELAOU, S. L. PULIT,
6206 F. VAN DIJK, P. F. PALAMARA, C. C. ELBERS, P. B.
NEERINCX, K. YE, V. GURYEV, W. P. KLOOSTERMAN,
6208 and OTHERS, 2014 Whole-genome sequence variation, population
structure and demographic history of the Dutch population. *Nature
6210 genetics* **46**(8): 818.
- FRENTIU, F. D., G. D. BERNARD, C. I. CUEVAS, M. P.
6212 SISON-MANGUS, K. L. PRUDIC, and A. D. BRISCOE, 2007
Adaptive evolution of color vision as seen through the eyes of but-
6214 terflies. *Proceedings of the National Academy of Sciences* **104**(suppl
1): 8634–8640.
- GALEN, C., 1996 Rates of floral evolution: adaptation to bumblebee
6216 pollination in an alpine wildflower, *Polemonium viscosum*. *Evolu-*
6218 *tion* **50**(1): 120–125.
- GALTIER, N., 2016 Adaptive protein evolution in animals and the
6220 effective population size hypothesis. *PLoS genetics* **12**(1): e1005774.
- GIGORD, L. D., M. R. MACNAIR, and A. SMITHSON, 2001
6222 Negative frequency-dependent selection maintains a dramatic
flower color polymorphism in the rewardless orchid *Dactylorhiza
6224 sambucina* (L.) Soo. *Proceedings of the National Academy of Sci-
ences* **98**(11): 6253–6255.
- GILLESPIE, J. H., 1973 Natural selection with varying selection
6226 coefficients—a haploid model. *Genetics Research* **21**(2): 115–120.
- GILLESPIE, J. H., 1977 Natural selection for variances in offspring
6228 numbers: a new evolutionary principle. *The American Natural-
ist* **111**(981): 1010–1014.
- GILLESPIE, J. H., 2000 Genetic drift in an infinite population. The
6232 pseudohitchhiking model. *Genetics* **155**: 909–919.
- GREMER, J. R. and D. L. VENABLE, 2014 Bet hedging in
6234 desert winter annual plants: optimal germination strategies in a
variable environment. *Ecology Letters* **17**(3): 380–387.
- HALDANE, J., 1942 The selective elimination of silver foxes in east-
6236 ern Canada. *Journal of Genetics* **44**(2-3): 296–304.

- 6238 HALDANE, J. and S. JAYAKAR, 1963 Polymorphism due to selection of varying direction. *Journal of Genetics* 58(2): 237–242.
- 6240 HALDANE, J. B. S., 1927 A mathematical theory of natural and artificial selection, part V: selection and mutation. In *Mathematical Proceedings of the Cambridge Philosophical Society*, Volume 23, pp. 6242 838–844. Cambridge University Press.
- 6244 HALDANE, J. B. S., 1937 The Effect of Variation of Fitness. *The American Naturalist* 71(735): 337–349.
- 6246 HAMILTON, W. D., 1964a The genetical evolution of social behaviour. II. *Journal of theoretical biology* 7(1): 17–52.
- 6248 HAMILTON, W. D., 1964b The genetical evolution of social behaviour. II. *Journal of theoretical biology* 7(1): 17–52.
- 6250 HERMISSON, J. and P. S. PENNINGS, 2017 Soft sweeps and beyond: understanding the patterns and probabilities of selection 6252 footprints under rapid adaptation. *Methods in Ecology and Evolution* 8(6): 700–716.
- 6254 HEY, J. and R. M. KLIMAN, 2002 Interactions between natural selection, recombination and gene density in the genes of 6256 *Drosophila*. *Genetics* 160(2): 595–608.
- 6258 HOEKSTRA, H. E., K. E. DRUMM, and M. W. NACHMAN, 2004 Ecological genetics of adaptive color polymorphism in pocket mice: geographic variation in selected and neutral genes. *Evolution* 6260 58(6): 1329–1341.
- 6262 HOHENLOHE, P. A., S. BASSHAM, P. D. ETTER, N. STIFFLER, E. A. JOHNSON, and W. A. CRESKO, 2010 Population genomics of parallel adaptation in threespine stickleback 6264 using sequenced RAD tags. *PLoS genetics* 6(2): e1000862.
- 6266 HOLLISTER, J. D., S. GREINER, W. WANG, J. WANG, Y. ZHANG, G. K.-S. WONG, S. I. WRIGHT, and M. T. JOHNSON, 2014 Recurrent loss of sex is associated with accumulation 6268 of deleterious mutations in *Oenothera*. *Molecular biology and evolution* 32(4): 896–905.
- 6270 HOPKINS, J., G. BAUDRY, U. CANDOLIN, and A. KAITALA, 2015 I'm sexy and I glow it: female ornamentation in a nocturnal capital breeder. *Biology letters* 11(10): 20150599.
- 6272 HOUDE, A. E., 1994 Effect of artificial selection on male colour 6274 patterns on mating preference of female guppies. *Proc. R. Soc. Lond. B* 256(1346): 125–130.

- 6276 HOWES, R. E., M. DEWI, F. B. PIEL, W. M. MONTEIRO,
 K. E. BATTLE, J. P. MESSINA, A. SAKUNTABHAI, A. W.
 6278 SATYAGRAHA, T. N. WILLIAMS, J. K. BAIRD, and S. I.
 HAY, 2013 Spatial distribution of G6PD deficiency variants across
 6280 malaria-endemic regions. *Malar. J.* **12**: 418.
- HOWES, R. E., F. B. PIEL, A. P. PATIL, O. A. NYANGIRI,
 6282 P. W. GETHING, M. DEWI, M. M. HOGG, K. E. BAT-
 TLE, C. D. PADILLA, J. K. BAIRD, and S. I. HAY, 2012
 6284 G6PD deficiency prevalence and estimates of affected populations in
 malaria endemic countries: a geostatistical model-based map. *PLoS*
 6286 Medicine
- HUDSON, R. R., 2015, 07)A New Proof of the Expected Frequency
 6288 Spectrum under the Standard Neutral Model. *PLOS ONE* **10**(7):
 1–5.
- 6290 HUDSON, R. R. and N. L. KAPLAN, 1995a Deleterious back-
 ground selection with recombination. *Genetics* **141**: 1605–1617.
- 6292 HUDSON, R. R. and N. L. KAPLAN, 1995b The coalescent pro-
 cess and background selection. *Philos. Trans. R. Soc. Lond., B, Biol.*
 6294 *Sci.* **349**: 19–23.
- 6296 HUDSON, R. R., M. KREITMAN, and M. AGUADÉ, 1987 A test
 of neutral molecular evolution based on nucleotide data. *Genet-*
ics **116**(1): 153–159.
- 6298 HUNT, G., M. A. BELL, and M. P. TRAVIS, 2008 Evolution
 toward a new adaptive optimum: phenotypic evolution in a fossil
 6300 stickleback lineage. *Evolution* **62**(3): 700–710.
- 6302 JAIN, S. and A. D. BRADSHAW, 1966 Evolutionary divergence
 among adjacent plant populations I. The evidence and its theoreti-
 cal analysis. *Heredity* **21**(3): 407.
- 6304 JANICKE, T., I. K. HÄDERER, M. J. LAJEUNESSE, and
 N. ANTHES, 2016 Darwinian sex roles confirmed across the an-
 6306 imal kingdom. *Science advances* **2**(2): e1500983.
- 6308 JENNINGS, W. B. and S. V. EDWARDS, 2005 Speciational his-
 tory of Australian grass finches (*Poephila*) inferred from thirty gene
 trees. *Evolution* **59**(9): 2033–2047.
- 6310 JOHANNSEN, W., 1911 The Genotype Conception of Heredity. *The*
American Naturalist **45**(531): 129–159.
- 6312 JOHNSTON, S. E., J. GRATTON, C. BERENOS, J. G. PILK-
 INGTON, T. H. CLUTTON-BROCK, J. M. PEMBERTON, and

- 6314 J. SLATE, 2013 Life history trade-offs at a single locus maintain
sexually selected genetic variation. *Nature* **502**(7469): 93.
- 6316 JORON, M., L. FREZAL, R. T. JONES, N. L. CHAMBER-
LAIN, S. F. LEE, C. R. HAAG, A. WHIBLEY, M. BECUWE,
6318 S. W. BAXTER, L. FERGUSON, and OTHERS, 2011 Chromo-
somal rearrangements maintain a polymorphic supergene controlling
6320 butterfly mimicry. *Nature* **477**(7363): 203.
- 6322 JORON, M., R. PAPA, M. BELTRÁN, N. CHAMBERLAIN,
J. MAVÁREZ, S. BAXTER, M. ABANTO, E. BERMING-
HAM, S. J. HUMPHRAY, J. ROGERS, and OTHERS, 2006 A
6324 conserved supergene locus controls colour pattern diversity in *Heli-*
conius butterflies. *PLoS biology* **4**(10): e303.
- 6326 JUKEMA, J. and T. PIERSMA, 2006 Permanent female mimics in
a lekking shorebird. *Biology letters* **2**(2): 161–164.
- 6328 KAPLAN, N. L., R. R. HUDSON, and C. H. Langley, 1989
The hitchhiking effect revisited. *Genetics* **123**: 887–899.
- 6330 KARN, M. N. and L. PENROSE, 1951 Birth weight and gestation
time in relation to maternal age, parity and infant survival. *Annals*
6332 of eugenics **16**(1): 147–164.
- 6334 KETTLEWELL, H. B. D., 1955 Selection experiments on industrial
melanism in the Lepidoptera. *Heredity* **9**(3): 323.
- 6336 KIM, Y., 2006 Allele frequency distribution under recurrent selective
sweeps. *Genetics* **172**: 1967–1978.
- 6338 KIMURA, M., 1968 Evolutionary rate at the molecular level. *Na-*
ture **217**(5129): 624–626.
- 6340 KIMURA, M., 1983 *The neutral theory of molecular evolution*. Cam-
bridge University Press.
- 6342 KIMURA, M. and J. F. CROW, 1964 The number of alleles that
can be maintained in a finite population. *Genetics* **49**(4): 725.
- 6344 KIMURA, M. and T. OHTA, 1974 On some principles govern-
ing molecular evolution. *Proceedings of the National Academy of*
Sciences **71**(7): 2848–2852.
- 6346 KING, J. L. and T. H. JUKES, 1969 Non-darwinian evolution.
Science **164**(3881): 788–798.
- 6348 KORNEGAY, J. R., J. W. SCHILLING, and A. C. WILSON,
1994 Molecular adaptation of a leaf-eating bird: stomach lysozyme
6350 of the hoatzin. *Molecular Biology and Evolution* **11**(6): 921–928.

- KRAKAUER, A. H., 2005 Kin selection and cooperative courtship in
6352 wild turkeys. *Nature* 434(7029): 69.
- KRUUK, L. E., J. SLATE, J. M. PEMBERTON, S. BROTH-
6354 ERSTONE, F. GUINNESS, and T. CLUTTON-BROCK, 2002
Antler size in red deer: heritability and selection but no evolution.
6356 *Evolution* 56(8): 1683–1695.
- KÜPPER, C., M. STOCKS, J. E. RISSE, N. DOS REMEDIOS,
6358 L. L. FARRELL, S. B. MCRAE, T. C. MORGAN, N. KAR-
LIONOVA, P. PINCHUK, Y. I. VERKUIL, and OTHERS, 2016
6360 A supergene determines highly divergent male reproductive morphs
in the ruff. *Nature Genetics* 48(1): 79.
- KWIATKOWSKI, D. P., 2005, August)How malaria has affected
the human genome and what human genetics can teach us about
6362 malaria. *Am. J. Hum. Genet.* 77(2): 171–192.
- LABERGE, A.-M., M. JOMPHE, L. HOUDE, H. VÉZINA,
6366 M. TREMBLAY, B. DESJARDINS, D. LABUDA, M. ST-HI-
LAIRE, C. MACMILLAN, E. A. SHOUBRIDGE, and OTHERS,
6368 2005 A “Fille du Roy” introduced the T14484C Leber hereditary
optic neuropathy mutation in French Canadians. *The American
6370 Journal of Human Genetics* 77(2): 313–317.
- LAMICHHANEY, S., G. FAN, F. WIDEMO, U. GUNNARS-
6372 SON, D. S. THALMANN, M. P. HOEPPNER, S. KERJE,
U. GUSTAFSON, C. SHI, H. ZHANG, and OTHERS, 2016
6374 Structural genomic changes underlie alternative reproductive strate-
gies in the ruff (*Philomachus pugnax*). *Nature Genetics* 48(1): 84.
- LANDE, R., 1976 Natural selection and random genetic drift in
phenotypic evolution. *Evolution* 30(2): 314–334.
6376
- LANDE, R., 1979 Quantitative genetic analysis of multivariate evo-
lution, applied to brain: body size allometry. *Evolution* 33(1Part2):
6378 402–416.
- LAURIE, C. C., D. A. NICKERSON, A. D. ANDERSON, B. S.
6382 WEIR, R. J. LIVINGSTON, M. D. DEAN, K. L. SMITH,
E. E. SCHADT, and M. W. NACHMAN, 2007, 08)Linkage Dise-
6384 quilibrium in Wild Mice. *PLOS Genetics* 3(8): 1–9.
- LAWSON, D. J., L. VAN DORP, and D. FALUSH, 2018 A tuto-
6386 rial on how not to over-interpret STRUCTURE and ADMIXTURE
bar plots. *Nature communications* 9(1): 3258.
- LEFÉBURE, T., C. MORVAN, F. MALARD, C. FRANÇOIS,
6388 L. KONECNY-DUPRÉ, L. GUÉGUEN, M. WEISS-GAYET,

- 6390 A. SEGUIN-ORLANDO, L. ERMINI, C. DER SARKISSIAN,
and OTHERS, 2017 Less effective selection leads to larger genomes.
6392 Genome research: gr-212589.
- 6394 LEFFLER, E. M., K. BULLAUGHEY, D. R. MATUTE, W. K.
MEYER, L. SEGUREL, A. VENKAT, P. ANDOLFATTO, and
M. PRZEWORSKI, 2012 Revisiting an old riddle: what deter-
6396 mines genetic diversity levels within species? PLoS biology 10(9):
e1001388.
- 6398 LEK, M., K. J. KARCZEWSKI, E. V. MINIKEL, K. E.
SAMOCHA, E. BANKS, T. FENNELL, A. H. O'DONNELL-
6400 LURIA, J. S. WARE, A. J. HILL, B. B. CUMMINGS, and
OTHERS, 2016 Analysis of protein-coding genetic variation in
6402 60,706 humans. Nature 536(7616): 285.
- 6404 LENORMAND, T., D. BOURGUET, T. GUILLEMAUD, and
M. RAYMOND, 1999 Tracking the evolution of insecticide resis-
tance in the mosquito *Culex pipiens*. Nature 400(6747): 861.
- 6406 LEWONTIN, R. C., 1970 The units of selection. Annual review of
ecology and systematics 1(1): 1–18.
- 6408 LEWONTIN, R. C., 1974 *The Genetic Basis of Evolutionary
Change*. Columbia University Press, New York.
- 6410 LEWONTIN, R. C., 1994, 05)[DNA Fingerprinting: A Review of
the Controversy]: Comment: The Use of DNA Profiles in Forensic
6412 Contexts. Statist. Sci. 9(2): 259–262.
- 6414 LEWONTIN, R. C., 2001 *Thinking about evolution: historical, philo-
sophical, and political perspectives*, Chapter Natural History and
Formalism in Evolutionary Genetics, pp. 7–20. Cambridge Univer-
6416 sity Press.
- 6418 LI, J. Z., D. M. ABSHER, H. TANG, A. M. SOUTHWICK,
A. M. CASTO, S. RAMACHANDRAN, H. M. CANN, G. S.
BARSH, M. FELDMAN, L. L. CAVALLI-SFORZA, and OTH-
6420 ERS, 2008 Worldwide human relationships inferred from genome-
wide patterns of variation. science 319(5866): 1100–1104.
- 6422 LIN, C.-J., F. HU, R. DUBRUILLE, J. VEDANAYAGAM,
J. WEN, P. SMIBERT, B. LOPPIN, and E. C. LAI, 2018 The
6424 hpRNA/RNAi pathway is essential to resolve intragenomic conflict
in the Drosophila male germline. Developmental cell 46(3): 316–326.
- 6426 LISTER, A., 1989 Rapid dwarfing of red deer on Jersey in the last
interglacial. Nature 342(6249): 539.

- 6428 LOCKE, D. P., L. W. HILLIER, W. C. WARREN, K. C.
 WORLEY, L. V. NAZARETH, D. M. MUZNY, S.-P. YANG,
 6430 Z. WANG, A. T. CHINWALLA, P. MINX, and OTHERS, 2011
 Comparative and demographic analysis of orang-utan genomes.
 6432 *Nature* 469(7331): 529.
- 6434 LOSOS, J. B., S. J. ARNOLD, G. BEJERANO, E. BRODIE III,
 D. HIBBETT, H. E. HOEKSTRA, D. P. MINDELL, A. MON-
 TEIRO, C. MORITZ, H. A. ORR, and OTHERS, 2013 Evolution-
 6436 ary biology for the 21st century. *PLoS Biology* 11(1): e1001466.
- 6438 LOUICHAROEN, C., E. PATIN, R. PAUL, I. NUCHPRAY-
 OON, B. WITOONPANICH, C. PEERAPITTAYAMONGKOL,
 I. CASADEMONT, T. SURA, N. M. LAIRD, P. SINGHASI-
 6440 VANON, L. QUINTANA-MURCI, and A. SAKUNTABHAI, 2009,
 December)Positively selected G6PD-Mahidol mutation reduces *Plas-*
 6442 *modium vivax* density in Southeast Asians. *Science* 326(5959):
 1546–1549.
- 6444 LOWRY, D. B. and J. H. WILLIS, 2010 A widespread chromo-
 somal inversion polymorphism contributes to a major life-history
 6446 transition, local adaptation, and reproductive isolation. *PLoS biol-*
 ogy 8(9): e1000500.
- 6448 MACARTHUR, D. G., S. BALASUBRAMANIAN, A. FRANK-
 ISH, N. HUANG, J. MORRIS, K. WALTER, L. JOSTINS,
 6450 L. HABEGGER, J. K. PICKRELL, S. B. MONTGOMERY, and
 OTHERS, 2012 A systematic survey of loss-of-function variants in
 6452 human protein-coding genes. *Science* 335(6070): 823–828.
- 6454 MACPHERSON, J. M., G. SELLA, J. C. DAVIS, and D. A.
 PETROV, 2007 Genomewide spatial correspondence between non-
 synonymous divergence and neutral polymorphism reveals extensive
 6456 adaptation in *Drosophila*. *Genetics* 177: 2083–2099.
- 6458 MAJERUS, M. E., 2009 Industrial melanism in the peppered moth,
Biston betularia: an excellent teaching example of Darwinian evolu-
 tion in action. *Evolution: Education and Outreach* 2(1): 63.
- 6460 MALÉCOT, G., 1948 Les mathématiques de l'hérédité.
- 6462 MALÉCOT, G., 1969 The Mathematics of Heredity (Revised, edited
 and translated by Yermanos, DM).
- 6464 MARCINIAK, S. and G. H. PERRY, 2017 Harnessing ancient
 genomes to study the history of human adaptation. *Nature Reviews
 Genetics* 18(11): 659.

- 6466 MAYNARD SMITH, J., 1964 Group selection and kin selection.
Nature 201(4924): 1145.
- 6468 MAYNARD SMITH, J. and J. HAIGH, 1974 The hitch-hiking
effect of a favourable gene. *Genet. Res.* 23: 23–35.
- 6470 McDONALD, J. H. and M. KREITMAN, 1991 Adaptive protein
evolution at the Adh locus in Drosophila. *Nature* 351(6328): 652.
- 6472 MCVICKER, G., D. GORDON, C. DAVIS, and P. GREEN, 2009
Widespread genomic signatures of natural selection in hominid
evolution. *PLoS Genet.* 5: e1000471.
- MENOZZI, P., A. PIAZZA, and L. CAVALLI-SFORZA, 1978
6476 Synthetic maps of human gene frequencies in Europeans. *Sci-
ence* 201(4358): 786–792.
- 6478 MEREDITH, R. W., J. GATESY, W. J. MURPHY, O. A. RY-
DER, and M. S. SPRINGER, 2009, 09)Molecular Decay of the
6480 Tooth Gene Enamelin (ENAM) Mirrors the Loss of Enamel in the
Fossil Record of Placental Mammals. *PLOS Genetics* 5(9): 1–12.
- 6482 MESSIER, W. and C.-B. STEWART, 1997 Episodic adaptive
evolution of primate lysozymes. *Nature* 385(6612): 151.
- 6484 MILOT, E., C. MOREAU, A. GAGNON, A. A. COHEN,
B. BRAIS, and D. LABUDA, 2017 Mother's curse neutralizes
6486 natural selection against a human genetic disease over three cen-
turies. *Nature ecology & evolution* 1(9): 1400.
- 6488 MULLER, H. J., 1932 Some genetic aspects of sex. *The American
Naturalist* 66(703): 118–138.
- 6490 NACHMAN, M. W., H. E. HOEKSTRA, and S. L.
D'AGOSTINO, 2003 The genetic basis of adaptive melanism
6492 in pocket mice. *Proceedings of the National Academy of Sci-
ences* 100(9): 5268–5273.
- 6494 NASH, D., S. NAIR, M. MAYXAY, P. N. NEWTON, J.-P.
GUTHMANN, F. NOSTEN, and T. J. ANDERSON, 2005 Selec-
6496 tion strength and hitchhiking around two anti-malarial resistance
genes. *Proceedings of the Royal Society of London B: Biological
Sciences* 272(1568): 1153–1161.
- NELSON, M. R., D. WEGMANN, M. G. EHM, D. KESSNER,
6500 P. S. JEAN, C. VERZILLI, J. SHEN, Z. TANG, S.-A. BA-
CANU, D. FRASER, and OTHERS, 2012 An abundance of rare
6502 functional variants in 202 drug target genes sequenced in 14,002
people. *Science*: 1217876.

- 6504 NORDBORG, M., B. CHARLESWORTH, and
 D. CHARLESWORTH, 1996 The effect of recombination on back-
 ground selection. *Genet. Res.* **67**: 159–174.
- 6508 NOVEMBRE, J. and M. STEPHENS, 2008 Interpreting principal
 component analyses of spatial population genetic variation. *Nature
 genetics* **40**(5): 646.
- 6510 OHTA, T., 1972 Population size and rate of evolution. *Journal of
 Molecular Evolution* **1**(4): 305–314.
- 6512 OHTA, T., 1973 Slightly deleterious mutant substitutions in evolu-
 tion. *Nature* **246**(5428): 96.
- 6514 OHTA, T., 1987 Very slightly deleterious mutations and the molecu-
 lar clock. *Journal of Molecular Evolution* **26**(1-2): 1–6.
- 6516 OHTA, T. and J. H. GILLESPIE, 1996 Development of neutral
 and nearly neutral theories. *Theoretical population biology* **49**(2):
 6518 128–142.
- 6520 OWEN, D. and D. CHANTER, 1972 Polymorphic mimicry in a
 population of the African butterfly, *Pseudacraea eurytus* (L.) (Lep.
 Nymphalidae). *Insect Systematics & Evolution* **3**(4): 258–266.
- 6522 PAABY, A. B., A. O. BERGLAND, E. L. BEHRMAN, and
 P. S. SCHMIDT, 2014 A highly pleiotropic amino acid polymor-
 phism in the *Drosophila* insulin receptor contributes to life-history
 6524 adaptation. *Evolution* **68**(12): 3395–3409.
- 6526 PATTERSON, N., A. L. PRICE, and D. REICH, 2006 Population
 structure and eigenanalysis. *PLoS genetics* **2**(12): e190.
- 6528 PICKRELL, J. K., T. BERISA, J. Z. LIU, L. SÉGUREL, J. Y.
 TUNG, and D. A. HINDS, 2016 Detection and interpretation of
 6530 shared genetic influences on 42 human traits. *Nature genetics* **48**(7):
 709.
- 6532 POTTI, J. and D. CANAL, 2011 Heritability and genetic corre-
 lation between the sexes in a songbird sexual ornament. *Hered-
 ity* **106**(6): 945.
- 6534 PRITCHARD, J. K., M. STEPHENS, and P. DONNELLY, 2000
 Inference of population structure using multilocus genotype data.
Genetics **155**(2): 945–959.
- 6538 PROVINE, W. B., 2001 *The origins of theoretical population genet-
 ics: with a new afterword*. University of Chicago Press.

- 6540 PRZEWORSKI, M., 2002 The signature of positive selection at ran-
domly chosen loci. *Genetics* **160**: 1179–1189.
- 6542 PTAK, S. E., A. D. ROEDER, M. STEPHENS, Y. GILAD,
S. PÄÄBO, and M. PRZEWORSKI, 2004 Absence of the TAP2
6544 human recombination hotspot in chimpanzees. *PLoS biology* **2**(6):
e155.
- 6546 QUELLER, D. C., 1992 Quantitative genetics, inclusive fitness, and
group selection. *The American Naturalist* **139**(3): 540–558.
- 6548 R, 2018 R: A Language and Environment for Statistical Computing.
RALPH, P. L. and G. COOP, 2015 The role of standing varia-
6550 tion in geographic convergent adaptation. *The American Natural-
ist* **186**(S1): S5–S23.
- 6552 RANDS, C. M., S. MEADER, C. P. PONTING, and
G. LUNTER, 2014 8.2% of the human genome is constrained:
6554 variation in rates of turnover across functional element classes in the
human lineage. *PLoS genetics* **10**(7): e1004525.
- 6556 RICHARDS, C. M., 2000 Inbreeding depression and genetic rescue
in a plant metapopulation. *The American Naturalist* **155**(3): 383–
6558 394.
- 6560 RITLAND, K., C. NEWTON, and H. MARSHALL, 2001 Inher-
itance and population structure of the white-phased “Kermode”
black bear. *Current Biology* **11**(18): 1468 – 1472.
- 6562 ROBERTSON, A., 1961 Inbreeding in artificial selection programmes.
Genet. Res. **2**: 189—194.
- 6564 ROBINSON, J. A., D. ORTEGA-DEL VECCHYO, Z. FAN,
B. Y. KIM, C. D. MARSDEN, K. E. LOHMUELLER, R. K.
6566 WAYNE, and OTHERS, 2016 Genomic flatlining in the endangered
island fox. *Current Biology* **26**(9): 1183–1189.
- 6568 ROBINSON, L. M., J. R. BOLAND, and J. M. BRAVERMAN,
2016 Revisiting a Classic Study of the Molecular Clock. *Journal of
6570 molecular evolution* **82**(2-3): 110–116.
- 6572 ROSENBERG, N. A., J. K. PRITCHARD, J. L. WEBER,
H. M. CANN, K. K. KIDD, L. A. ZHIVOTOVSKY, and
M. W. FELDMAN, 2002 Genetic structure of human populations.
6574 *science* **298**(5602): 2381–2385.
- RUWENDE, C., S. C. KHOO, R. W. SNOW, S. N. YATES,
6576 D. KWIATKOWSKI, S. GUPTA, P. WARN, C. E. ALLSOPP,

- 6578 S. C. GILBERT, and N. PESCHU, 1995, July)Natural selection of
hemi- and heterozygotes for G6PD deficiency in Africa by resistance
to severe malaria. *Nature* **376**(6537): 246–249.
- 6580 SAMS, A. J. and A. R. BOYKO, 2018a Fine-scale resolution and
analysis of runs of homozygosity in domestic dogs. *bioRxiv*.
- 6582 SAMS, A. J. and A. R. BOYKO, 2018b Fine-Scale Resolution of
Runs of Homozygosity Reveal Patterns of Inbreeding and Substan-
6584 tial Overlap with Recessive Disease Genotypes in Domestic Dogs.
G3: Genes, Genomes, Genetics: g3–200836.
- 6586 SANKARARAMAN, S., N. PATTERSON, H. LI, S. PÄÄBO, and
D. REICH, 2012, 10)The Date of Interbreeding between Neander-
6588 tals and Modern Humans. *PLOS Genetics* **8**(10): 1–9.
- SANTIAGO, E. and A. CABALLERO, 1995 Effective size of popu-
6590 lations under selection. *Genetics* **139**: 1013–1030.
- SANTIAGO, E. and A. CABALLERO, 1998 Effective size and
6592 polymorphism of linked neutral loci in populations under directional
selection. *Genetics* **149**: 2105–2117.
- 6594 SATTATH, S., E. ELYASHIV, O. KOLODNY, Y. RINOTT, and
G. SELLA, 2011a Pervasive adaptive protein evolution apparent
6596 in diversity patterns around amino acid substitutions in *Drosophila*
simulans. *PLoS genetics* **7**(2): e1001302.
- 6598 SATTATH, S., E. ELYASHIV, O. KOLODNY, Y. RINOTT, and
G. SELLA, 2011b Pervasive adaptive protein evolution apparent
6600 in diversity patterns around amino acid substitutions in *Drosophila*
simulans. *PLoS Genet.* **7**: e1001302.
- 6602 SCHEMSKE, D. W. and P. BIERZYCHUDEK, 2001 Perspective:
evolution of flower color in the desert annual *Linanthus parryae*:
6604 Wright revisited. *Evolution* **55**(7): 1269–1282.
- SEGER, J. and H. BROCKMANN, 1987 *Oxford Surveys in Evo-*
6606 *lutionary Biology*, Volume 4, Chapter What is bet-hedging, pp.
182–211. Oxford University Press.
- SELLA, G., D. A. PETROV, M. PRZEWORSKI, and P. AN-
6608 DOLFATTO, 2009 Pervasive natural selection in the *Drosophila*
genome? *PLoS genetics* **5**(6): e1000495.
- SHAPIRO, J. A., W. HUANG, C. ZHANG, M. J. HUBISZ,
6612 J. LU, D. A. TURISSINI, S. FANG, H. Y. WANG, R. R.
HUDSON, R. NIELSEN, Z. CHEN, and C. I. WU, 2007 Adap-
6614 tive genic evolution in the *Drosophila* genomes. *Proc. Natl. Acad.
Sci. U.S.A.* **104**: 2271–2276.

- 6616 SMITH, J. M., 1982 *Evolution and the Theory of Games*. Cambridge university press.
- 6618 SMITH, T. B., 1993 Disruptive selection and the genetic basis of bill size polymorphism in the African finch Pyrenestes. Nature 363(6430): 618.
- 6622 SMITHSON, A. and M. R. MACNAIR, 1997 Negative frequency-dependent selection by pollinators on artificial flowers without rewards. Evolution 51(3): 715–723.
- 6624 STEVENS, N. M., 1905 *Studies in Spermatogenesis: With especial reference to the "accessory chromosome"*, Volume 36. Carnegie Institution of Washington.
- 6628 STUMPF, M. P., Z. LAIDLAW, and V. A. JANSEN, 2002 Herpes viruses hedge their bets. Proceedings of the National Academy of Sciences 99(23): 15234–15237.
- 6630 STURTEVANT, A. H., 1915 The behavior of the chromosomes as studied through linkage. Zeitschrift für induktive Abstammungs- und Vererbungslehre 13(1): 234–287.
- 6634 TAJIMA, F., 1989 Statistical method for testing the neutral mutation hypothesis by DNA polymorphism. Genetics 123(3): 585–595.
- 6636 TAO, Y., L. ARARIPE, S. B. KINGAN, Y. KE, H. XIAO, and D. L. HARTL, 2007 A sex-ratio meiotic drive system in Drosophila simulans. II: an X-linked distorter. PLoS biology 5(11): e293.
- 6640 TAO, Y., J. P. MASLY, L. ARARIPE, Y. KE, and D. L. HARTL, 2007 A sex-ratio meiotic drive system in Drosophila simulans. I: an autosomal suppressor. PLoS biology 5(11): e292.
- 6642 TISHKOFF, S. A., R. VARKONYI, N. CAHINHINAN, S. ABBES, G. ARGYROPOULOS, G. DESTRO-BISOL, A. DROUSSIOTOU, B. DANGERFIELD, G. LEFRANC, J. LOISELET, A. PIRO, M. STONEKING, A. TAGARELLI, G. TAGARELLI, E. H. TOUMA, S. M. WILLIAMS, and A. G. CLARK, 2001 Haplotype Diversity and Linkage Disequilibrium at Human G6PD: Recent Origin of Alleles That Confer Malarial Resistance. Science 293(5529): 455–462.
- 6650 TOEWS, D. P., S. A. TAYLOR, R. VALLENDER, A. BRELSFORD, B. G. BUTCHER, P. W. MESSEY, and I. J. LOVETTE, 2016 Plumage Genes and Little Else Distinguish the Genomes of Hybridizing Warblers. Current Biology 26(17): 2313 – 2318.
- 6654

- TURELLI, M., D. W. SCHEMSKE, and P. BIERZYCHUDEK,
 6656 2001 Stable two-allele polymorphisms maintained by fluctuating
 fitnesses and seed banks: protecting the blues in *Linanthus parryae*.
 6658 *Evolution* 55(7): 1283–1298.
- ULIZZI, L. and L. TERRENATO, 1992 Natural selection associated
 6660 with birth weight. VI. Towards the end of the stabilizing compo-
 nent. *Annals of human genetics* 56(2): 113–118.
- VAN'T HOF, A. E., N. EDMONDS, M. DALÍKOVÁ, F. MAREC,
 6662 and I. J. SACCHERI, 2011 Industrial melanism in British pep-
 6664 pered moths has a singular and recent mutational origin. *Sci-
 ence* 332(6032): 958–960.
- VOIGHT, B. F., A. M. ADAMS, L. A. FRISSE, Y. QIAN,
 6666 R. R. HUDSON, and A. DI RIENZO, 2005 Interrogating mul-
 6668 tiple aspects of variation in a full resequencing data set to infer hu-
 man population size changes. *Proceedings of the National Academy
 of Sciences* 102(51): 18508–18513.
- VONHOLDT, B. M., J. P. POLLINGER, D. A. EARL,
 6672 J. C. KNOWLES, A. R. BOYKO, H. PARKER, E. GEF-
 FEN, M. PILOT, W. JEDRZEJEWSKI, B. JEDRZEJEJEW-
 6674 SKA, V. SIDOROVICH, C. GRECO, E. RANDI, M. MU-
 SIANI, R. KAYS, C. D. BUSTAMANTE, E. A. OSTRANDER,
 6676 J. NOVEMBRE, and R. K. WAYNE, 2011 A genome-wide per-
 spective on the evolutionary history of enigmatic wolf-like canids.
 6678 *Genome Research*.
- WANG, J., J. DING, B. TAN, K. M. ROBINSON, I. H.
 6680 MICHELSON, A. JOHANSSON, B. NYSTEDT, D. G.
 SCOFIELD, O. NILSSON, S. JANSSON, and OTHERS, 2018
 6682 A major locus controls local adaptation and adaptive life history
 variation in a perennial plant. *Genome biology* 19(1): 72.
- WATTERSON, G., 1975 On the number of segregating sites in ge-
 6684 netical models without recombination. *Theoretical population
 biology* 7(2): 256–276.
- WEIS, A. E. and W. L. GORMAN, 1990 Measuring selection
 6688 on reaction norms: an exploration of the *Eurosta-Solidago* system.
 Evolution 44(4): 820–831.
- WHEELER, W. M., 1907 Pink Insect Mutants. *The American
 6690 Naturalist* 41(492): 773–780.
- WIDEMO, F., 1998 Alternative reproductive strategies in the ruff,
 6692 *Philomachus pugnax*: a mixed ESS? *Animal Behaviour* 56(2): 329–
 6694 336.

- WIEHE, T. and W. STEPHAN, 1993a Analysis of a genetic hitch-
6696 hiker model, and its application to DNA polymorphism data from
Drosophila melanogaster. *Molecular Biology and Evolution* **10**(4):
6698 842–854.
- WIEHE, T. H. and W. STEPHAN, 1993b Analysis of a genetic
6700 hitchhiker model, and its application to DNA polymorphism data
from *Drosophila melanogaster*. *Mol. Biol. Evol.* **10**: 842–854.
- 6702 WILKINSON, G. S., 1993 Artificial sexual selection alters allometry
in the stalk-eyed fly Cyrtodiopsis dalmanni (Diptera: Diopsidae).
6704 *Genetics Research* **62**(3): 213–222.
- 6706 WILLIAMS, G. C., 1966 *Adaptation and Natural Selection*. Princeton.
WILLIAMS, K.-A. and P. S. PENNINGS, 2019 Drug resistance
6708 evolution in HIV in the late 1990s: hard sweeps, soft sweeps, clonal
interference and the accumulation of drug resistance mutations.
6710 bioRxiv.
- 6712 WISELY, S. M., S. W. BUSKIRK, M. A. FLEMING, D. B.
MCDONALD, and E. A. OSTRANDER, 2002 Genetic Diversity
and Fitness in Black-Footed Ferrets Before and During a Bottle-
6714 neck. *Journal of Heredity* **93**(4): 231–237.
- 6716 WRIGHT, K. M., U. HELLSTEN, C. XU, A. L. JEONG,
A. SREEDASYAM, J. A. CHAPMAN, J. SCHMUTZ, G. COOP,
D. S. ROKHSAR, and J. H. WILLIS, 2015 Adaptation to
6718 heavy-metal contaminated environments proceeds via selection
on pre-existing genetic variation. bioRxiv: 029900.
- 6720 WRIGHT, S., 1932 *The roles of mutation, inbreeding, crossbreeding,
and selection in evolution*, Volume 1. na.
- 6722 WRIGHT, S., 1943 Isolation by Distance. *Genetics* **28**(2): 114–138.
- 6724 WRIGHT, S., 1949 The Genetical Structure of Populations. *Annals
of Eugenics* **15**(1): 323–354.
- 6726 WRIGHT, S. and T. DOBZHANSKY, 1946 Genetics of natural
populations. XII. Experimental reproduction of some of the changes
caused by natural selection in certain populations of *Drosophila*
6728 *pseudoobscura*. *Genetics* **31**(2): 125.
- 6730 WRIGHT, S. I., I. V. BI, S. G. SCHROEDER, M. YAMASAKI,
J. F. DOEBLEY, M. D. McMULLEN, and B. S. GAUT,
2005 The Effects of Artificial Selection on the Maize Genome.
6732 *Science* **308**(5726): 1310–1314.

- YANG, Z., 1998 Likelihood ratio tests for detecting positive selection
6734 and application to primate lysozyme evolution. *Molecular Biology*
and *Evolution* 15(5): 568–573.
- ZUCKERKANDL, E. and L. PAULING, 1965 Evolutionary diver-
gence and convergence in proteins. In *Evolving genes and proteins*,
6736 pp. 97–166. Elsevier.
- 6738